

UNIVERSITE DE YAOUNDE I

\*\*\*\*\*

CENTRE DE RECHERCHE ET DE  
FORMATION DOCTORALE EN  
SCIENCES, TECHNOLOGIE ET  
GEOSCIENCES

\*\*\*\*\*

UNITE DE RECHERCHE ET DE  
FORMATION DOCTORALE CHIMIE  
ET APPLICATIONS

\*\*\*\*\*

LABORATORY OF APPLIED INORGANIC CHEMISTRY  
LABORATOIRE DE CHIMIE INORGANIQUE APPLIQUEE

UNIVERSITY OF YAOUNDE I

\*\*\*\*\*

POSTGRADUATE SCHOOL OF  
SCIENCES, TECHNOLOGY  
AND GEOSCIENCES

\*\*\*\*\*

RESEARCH AND POSTGRADUATE  
TRAINING UNIT IN CHEMISTRY AND  
APPLICATIONS

\*\*\*\*\*



**USE OF  $K_2O$  -  $CaO$  BASED COMPOUNDS TO IMPROVE THE  
SINTERING BEHAVIOUR AND PROPERTIES OF  
SUSTAINABLE SEMI-VITRIFIED PRODUCTS**

A thesis submitted in total fulfillment of the requirements for the degree of Doctor of  
Philosophy in Chemistry

By

**TCHAKOUTEU MBAKOP Theophile**

**(Mat. 02Z261)..**

*M.Sc/DESS in Inorganic Chemistry*

**Jury**



**President :** KETCHA MBADCAM Joseph, *Professor - University of Yaounde I*

**Reporters**

- Uphie CHINJE MELO, *Professor - University of Yaounde I*
- Elie KAMSEU, *Chief Research Officer - MINRESI/MIPROMALO*

**Examiners**

- ELIMBI Antoine, *Professor - University of Yaounde I*
- NGOUNE Jean, *Professor - University of DSCHANG*
- ACAYANKA Elie, *Associate Professor - university of Yaounde I*

*Year 2021*

UNIVERSITE DE YAOUNDE I

\*\*\*\*\*

CENTRE DE RECHERCHE ET DE  
FORMATION DOCTORALE EN  
SCIENCES, TECHNOLOGIE ET  
GEOSCIENCES

\*\*\*\*\*

UNITE DE RECHERCHE ET DE  
FORMATION DOCTORALE CHIMIE ET  
APPLICATIONS

FACULTE DES SCIENCES  
DEPARTEMENT DE CHIMIE  
INORGANIQUE

\*\*\*\*\*



UNIVERSITY OF YAOUNDE I

\*\*\*\*\*

POSTGRADUATE SCHOOL OF  
SCIENCES, TECHNOLOGY  
AND GEOSCIENCES

\*\*\*\*\*

RESEARCH AND POSTGRADUATE  
TRAINING UNIT IN CHEMISTRY AND  
APPLICATIONS

FACULTY OF SCIENCE  
DEPARTMENT OF INORGANIC  
CHEMISTRY

\*\*\*\*\*

## ATTESTATION DE CORRECTION

Nous soussignés, les membres du jury, reconnaissons que **M. TCHAKOUTEU MBAKOP Theophile**, Matricule **02Z261** a pris en compte toutes les observations relevées lors de la soutenance publique de sa thèse de Doctorat/ PhD du Département de Chimie Inorganique, le **Lundi 13 Septembre 2021** à **11 heures** précise dans la **Salle 01** de la Faculté des Sciences sur le sujet intitulé :

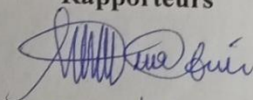
«Use of  $K_2O/CaO$  based compounds to improve the sintering behavior and properties of sustainable semi-vitrified products»

En foi de quoi, nous attestons que toutes les observations ont été prises en compte pour l'amélioration de la qualité du document.

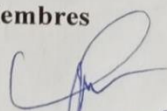
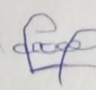
Fait à Yaoundé, le 21/10/2021

Le jury

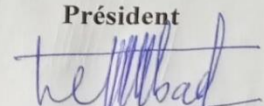
Rapporteurs

  
Elie Kamseu, PhD

Membres

  
RAYANNA elir  
  
A. ELIMBI

Président

  
KETCHA J. M.

# TABLE OF CONTENTS

List of figure.....	vi
List of tables.....	ix
List of abbreviations.....	x
List of symbols.....	xii
Dedication.....	xiv
Acknowledgment.....	xv
Résumé.....	1
Abstract.....	3
GENERAL INTRODUCTION.....	5

## CHAPTER I: LITERATURE REVIEW

I-1: CERAMICS.....	10
I-1-1: Generalities.....	10
I-1-2: Types of Ceramics.....	10
I-2: GENERALITIES ON CERAMICS RAW MATERIALS.....	11
I-2-1: Plastics raw materials : clays.....	11
I-2-2: Non plastics raw materials : degreasing materials.....	18
I-2-3: <i>Fluxing materials : feldspar, limestones, micas, nepheline syenite</i> .....	22
I-3: GENERAL PROPERTIES OF CERAMICS.....	33
I-3-1: Physical properties.....	33
I-3-2: Chemical properties.....	33
I-3-3: Mechanical properties.....	34
I-3-4: Electrical properties... ..	34
I-3-5: Thermal properties.....	34
I-4: SHAPING OF CERAMICS.....	34
I-5: DRYING OF CERAMICS.....	34
I-5-1: Air drying.....	35

<b>I-5-2: Air drying in closed room.....</b>	<b>35</b>
<b>I-5-3: Drying in conventional dryer.....</b>	<b>35</b>
<b>I-5-4: Microwave and radio frequency drying.....</b>	<b>35</b>
<b>I-6: CERAMICS SHRINKAGE.....</b>	<b>35</b>
<b>I-7: SINTERING OF CERAMICS.....</b>	<b>36</b>
<b>I-8: SEMI-VITRIFIED CERAMICS.....</b>	<b>40</b>
<b>I-8-1: Generalities.....</b>	<b>40</b>
<b>I-8-2: Classification : porcelain whiteware, vitreous, porcelain stoneware, sanitary ware, stoneware.....</b>	<b>41</b>
<b>I-9: FIRING PROCESS AND STRENGTH OF VITRIFIED AND SEMI-VITRIFIED CERAMICS.....</b>	<b>45</b>
<b>I-10: ADVANCEMENT OF RESEARCH IN THE FIELD OF VITRIFIED AND SEMI-VITRIFIED CERAMICS.....</b>	<b>47</b>
<b>I-10-1: Decrease of sintering temperature.....</b>	<b>47</b>
<b>I- 10-2: Investigation on alternative raw material for semi-vitrified ceramics.....</b>	<b>50</b>

## **CHAPTER II: MATERIALS AND EXPERIMENTAL PROCEDURES**

<b>II-1: MATERIALS.....</b>	<b>53</b>
<b>II-1-1: Clay material.....</b>	<b>53</b>
<b>II-1-2: Feldspar materials.....</b>	<b>54</b>
<b>II-1-3: Nepheline syenite.....</b>	<b>55</b>
<b>II-1-4: Limestone of Figuil.....</b>	<b>55</b>
<b>II-1-4: Quartz.....</b>	<b>55</b>
<b>II-2: RAW MATERIALS PREPARATION AND SAMPLE ELABORATIONS.....</b>	<b>56</b>
<b>II-2-1: Raw materials preparation.....</b>	<b>56</b>
<b>II-2-2: Samples preparation.....</b>	<b>57</b>
<b>II-3: METHODS OF CHARACTERIZATION.....</b>	<b>57</b>
<b>II-3-1: Granulometry Test.....</b>	<b>57</b>
<b>II-3-2: Chemical analysis.....</b>	<b>57</b>

<b>II-3-3: Mineralogical analysis by X-ray diffraction.....</b>	<b>58</b>
<b>II-3-4: Thermal analysis.....</b>	<b>62</b>
<b>II-3-5: Method of physical analysis (Water Absorption, Bulk Density, Apparent Porosity, Apparent Specific Gravity.....</b>	<b>65</b>
<b>II-3-6: Resistance of ceramic tile to chemical substances.....</b>	<b>66</b>
<b>CHAPTER III- RESULTS AND DISCUSSION.....</b>	<b>70</b>
<b>III-1: PHASE EVOLUTION AND THERMAL BEHAVIOR OF RAW MATERIALS..</b>	<b>71</b>
<b>III-1-1: Mineral phase.....</b>	<b>71</b>
<b>III-1-2: Phase evolution of raw materials.....</b>	<b>71</b>
<b>III-1-3: Chemical composition of raw materials.....</b>	<b>72</b>
<b>III-1-4: Thermal behavior of raw materials.....</b>	<b>73</b>
<b>III-1-5: Physical properties of kaolinitic clay of Mankon.....</b>	<b>75</b>
<b>III-2: INVESTIGATION OF THE PHYSICO-CHEMICAL PROPERTIES OF TWO PORCELAIN STONEWARE COMPOSITION BASED ON NEPHELINE SYENITE (G) AND BOBOYO PEGMATITE 1 (B).....</b>	<b>78</b>
<b>III-2-1: Thermal behavior of the two porcelain stoneware compositions based on Nepheline syenite and Boboyo pegmatite1.....</b>	<b>78</b>
<b>III-2-2: Sintering behavior of the two porcelain stoneware compositions based on nepheline syenite and Boboyo pegmatite 1.....</b>	<b>78</b>
<b>III-2-3: Variation of the physico-mechanical properties with firing temperature and rate .....</b>	<b>82</b>
<b>III-2-4: XRD patterns of the fired samples as function of temperature and soaking time .....</b>	<b>84</b>
<b>III-2-5: Water absorption and density of the fired specimen.....</b>	<b>85</b>
<b>III-2-6: Tortuosity.....</b>	<b>86</b>
<b>II-2-7: Cumulative pore volume and pore size distribution.....</b>	<b>87</b>

<b>III-3: PARTIAL CONCLUSION.....</b>	<b>94</b>
<b>III-4: INVESTIGATION ON THE ROLE AND PROPER PORTION OF LIMESTONE IN ENHANCING THE CRYSTALLIZATION PHENOMENA AND STRENGTH OF PORCELAIN STONEWARE.....</b>	<b>96</b>
<b>III-4-1: Thermal behavior and phase evolution in formulations.....</b>	<b>96</b>
<b>III-4-2: Physical and mechanical properties: linear shrinkage, water absorption, density, flexural strength and hardness.....</b>	<b>102</b>
<b>III-5: Study of the correlation between physical properties.....</b>	<b>114</b>
<b>III-5-1: Study of the correlation between flexural strength and density.....</b>	<b>114</b>
<b>III-4-4: Study of the correlation between the evolution of water absorption and the volume of open pores.....</b>	<b>117</b>
<b>III-6: Hardness of samples.....</b>	<b>119</b>
<b>III-7: DESCRIPTIVE MICROSTRUCTURE .....</b>	<b>121</b>
<b>III-7-1: Descriptive microstructure of two porcelain stoneware based on nepheline syenite (G) and Boboyo’s Pegmatite1 (B).....</b>	<b>121</b>
<b>III-7-2: Descriptive microstructure of two porcelain stoneware based on Manjo (P) and Boboyo’s Pegmatite2 (B).....</b>	<b>125</b>
<b>GENERAL CONCLUSION.....</b>	<b>131</b>
<b>RECOMMENDATIONS AND PROSPECT.....</b>	<b>134</b>
<b>REFERENCES.....</b>	<b>135</b>
<b>ANNEXES.....</b>	<b>I - XII</b>

## LIST OF FIGURES

<b>Figure 1:</b> Location of different ceramics materials in the feldspar-quartz-clay triaxial diagram...	11
<b>Figure 2:</b> Water fixing mechanism on clay micelles.....	12
<b>Figure 3:</b> Structure of kaolinite.....	15
<b>Figure 4:</b> montmorillonite structure.....	16
<b>Figure 5:</b> Crystal structure of illite.....	17
<b>Figure 6:</b> Crystal structure of chlorite.....	18
<b>Figure 7:</b> Crystal structure of (a) $\alpha$ -quartz and (b) $\beta$ -quartz .....	20
<b>Figure 8:</b> Phase diagram of the different minerals of feldspar solid solution.....	26
<b>Figure 9:</b> Crystal structure of calcite.....	29
<b>Figure 10:</b> Crystal structure of muscovite.....	30
<b>Figure 11:</b> Perspective view of the crystal structure of nepheline syenite.....	32
<b>Figure 12:</b> Schematic microstructures of the different sintering stages.....	39
<b>Figure 13:</b> The initial stage of solid phase sintering (evolution over time) .....	39
<b>Figure 14:</b> Liquid phase sintering in an eutectic point system.....	40
<b>Figure 15 :</b> different categories of sintering in a schematic phase diagram .....	40
<b>Figure 16:</b> Geological map of the North-West Region including the study area.....	54
<b>Figure 17:</b> XRD of raw materials kaolin (KM), Boboyo pegmatite 2 (FBb2), Manjo pegmatite (FMj), limestone (Lst) and quartz.....	72
<b>Figure 18:</b> Thermo-chemical transformation of raw materials (Q, Lst, $K_M$ ) under (a) DTA and (b) TG.....	74

<b>Figure 19:</b> Thermo-chemical transformation of raw Boboyo feldspar and nepheline syenite under DTA/TG.....	76
<b>Figure 20:</b> Particle size analysis of the Mankon clay sample (KM).....	77
<b>Figure 21:</b> DTA/TG curves of pegmatite (B) and nepheline syenite (G)-based porcelain stoneware composition.....	78
<b>Figure 22a:</b> Variation of the volumes of the two compositions of porcelain stoneware with the temperature development.....	80
<b>Figure 22b:</b> Important steps of the sintering.....	81
<b>Figure 23:</b> Variation of the flexural strength (MPa) of the two porcelain stonewares with temperature and soaking time.....	83
<b>Figure 24:</b> XRD patterns of the fired specimens of (a) B at 1,200 C (2 h) and 1,225 C (1 h) and (b) G at 1,200 C (2 h) and 1,225 C (1 h).....	84 - 85
<b>Figure 25:</b> Water absorption as function of the variation of apparent density.....	86
<b>Figure 26:</b> Variation of the tortuosity with temperature and soaking time for samples B and G...87	
<b>Figure 27 (a, b):</b> Variation of the cumulative pores volume (mL/g) with pores sizes ( $\mu\text{m}$ ) for sample B with 1h (a) soaking time and (b) 2h soaking time.....	88
<b>Figure 27 (c, d) :</b> Variation of the cumulative pores volume (mL/g) with pores sizes ( $\mu\text{m}$ ) for sample G with 1h (c) and 2h (d) soaking time.....	89
<b>Figure 28:</b> Pore size distribution of sample (B) as function of temperature and soaking time (c) for 1h and (d) for 2h soaking time	
<b>Figure 28:</b> Pore size distribution of sample (G) as function of temperature and soaking time (c) for 1h and (d) for 2h soaking time	
<b>Figure 29 (a, b):</b> DTA (a) and TG (b) curves of formulations (C0, C10, P0, P10).....	98
<b>Figure 29(c):</b> Thermal expansion of formulation (C0, C10, P0, P10).....	99
<b>Figure 30:</b> XRD pattern of fired samples.....	101
<b>Figure 31:</b> Linear shrinkage true sintering at various temperature of C series (a) and P series (b).....	103
<b>Figure 32:</b> Water Absorption true sintering at various temperature of C series (a) and P series (b).....	105
<b>Figure 33:</b> Bulk density of sintered samples for C Series (a) and P series (b).....	107



<b>Figure 34:</b> Open pores volume of sintered samples for C series (a) and P series (b).....	108
<b>Figure 35:</b> Apparent porosity of sintered samples (a) for C series and (b) for P series.....	110
<b>Figure 36:</b> Cumulative pore volume of samples (a) for C series and (b) for P series as function of radius.....	111
<b>Figure 37:</b> Flexural strength of sintered samples (a) for C series and (b) for P series.....	113
<b>Figure 39:</b> Correlation between flexural strength and density for C serie at 1175°C.....	117
<b>Figure 40:</b> Hardness of samples (a) for C and (b) for P at various temperatures.....	119
<b>Figure 41:</b> Micrographs of porcelain stoneware showing the semi-vitreous structure of B (a) and G (b) together with the interfaces matrix-crystalline phases for B (c) and G (d).....	122
<b>Figure 42:</b> Micrographs of porcelain stoneware showing the optimum densification for B at 1200°C (a and c) and G at 1225°C (b and d).....	123
<b>Figure 43:</b> Inhomogeny of crystallization (a and b) and difference in pores shape in porcelain stoneware (c and d).....	124
<b>Figure 44:</b> Phases distribution in the full dense (a and c) and relative porous (b and d) porcelain stoneware.....	125
<b>Figure 45 a:</b> Comparative microstructure of reference sample C0 at different temperature.....	126
<b>Figure 45 b:</b> Comparative microstructure of reference sample P0 at different temperature.....	127
<b>Figure 45 c:</b> Comparative microstructure of sample C10 at different temperature.....	127
<b>Figure 45 d:</b> Comparative microstructure of sample P10 at different temperature.....	128
<b>Figure 46 a:</b> Comparative microstructures of etching surface of reference samples at 1175 and 1200°C.....	129
<b>Figure 46 b :</b> Comparative microstructures of etching surface of samples C7 and P7 at 1175 and 1200°C.....	130

---

## LIST OF TABLES

---

<b>Table 1:</b> Physical properties of quartz.....	20
<b>Table 2:</b> Classification of materials according to the plasticity index (NF P 94-051, 1993).....	60
<b>Table 3:</b> Mineral phases in the two minerals materials (pegmatite of Boboyo and nepheline syenite).....	71
<b>Table 4:</b> Chemical composition of raw materials (Boboyo feldspar (FBb), Manjo feldspar (FM) and Ntamuka kaolin (KNt), quartz (Q) and limestone (Lst)).....	72
<b>Table 5:</b> Particle size distribution of the sample KM.....	76
<b>Table 6:</b> Plasticity test results.....	77
<b>Table 7:</b> Porcelain stoneware formulation.....	96
<b>Table 8:</b> Physical properties values of C series (a) and P series (b).....	101-102

## LIST OF ABBREVIATIONS

**ASTM:** American Standard for Testing Materials

**ISO:** international Standard Organization

**DTA:** Differential Thermal Analysis

**DTG:** Thermal Gravimetry Analysis

**DSC :** Differential Scanning Calorimetry

**XRD:** X-Ray diffraction Test

**EDS:** Energy Dispersion X-ray Spectrometry

**SEM:** Scanning Electron Microscopy

**XRF:** X-ray fluorescence

**SEI:** Secondary Electron Images

**MIP:** Mercury Intrusion Porosimeter

**WL:** Liquidity Limit

**WP:** Plasticity limit

**IP:** Index of plasticity

**SEI:** Secondary Electron Images

**Rpm:** Rotation Per Minute

**CEC:** Cation Exchange Capacity

**IUGS:** International Union of Geological Sciences

**HK:** Knoop Hardness

**FMj:** Pegmatite from Manjo

**FBb:** Pegmatite from Boboyo,

**KM:** Kaolin from Mankon

**Lst:** Limestone from Figuil

**Q:** Quartz

**NPH:** Nepheline Syenite

**B:** Porcelain stoneware composition based on pegmatite of Boboyo 1

**G:** Porcelain stoneware composition based on nepheline syenite

**C:** Porcelain stoneware composition based on pegmatite of Boboyo 2

**P:** Porcelain stoneware composition based on pegmatite of Manjo

**t:** Thickness, **a:** Radius of the circle of the support points **b:** Radius of the region of uniform loading at the centre,

**Y<sub>s</sub>** = density of the grains

**Y<sub>w</sub>** = density of the water

**r** = density of the suspension

**Φ** = diameter of grains still in solution

**η** = dynamic viscosity

**H** = depth of grain drop

## LIST OF SYMBOLS

$\alpha$ : Alpha

$\beta$ : Beta

$\gamma$  : gamma

%: Pourcentage

$\mu\text{m}$ : Micro-meter

**Cu**: Cupper

**Kv**: Kilo volt

**mA**: Mico amper

**ml**: Milliliter

**mm**: Millimeter

**cm**: Centimeter

$^{\circ}\text{C}$ : Celsius degree

**T**: Temperature

**s**: Second

**min**: Minute

**N**: Newton

**MPa**: Mega Pascal

GPa : Giga Pascal

**%w**: weight percent

**P** : Load

**R**: Radius

**v**: Poisson's ratio

**$\sigma_{\text{max}}$** : Bi – axial Strength

**l**: Liter

**g**: Gramme

**g/l**: Gramme per liter

Ca :

K : Potash

$\text{Al}_2\text{O}_3$  : Alumina

$\text{CaCO}_3$  : Calcium carbonate

$\text{Al}_2\text{O}_3 \cdot 2\text{SiO}_2 \cdot 2\text{H}_2\text{O}$  : Kaolinite

$\text{CaO} \cdot \text{Al}_2\text{O}_3 \cdot 2\text{SiO}_2$  : Anorthite

$\text{NaAlSi}_3\text{O}_8$  : Albite

$\text{KAlSi}_3\text{O}_8$  : orthoclase

## DEDICATION

### I DEDICATE THIS THESIS:

*In memory of my late sweet wife Mme TCHAKOUTEU Born BAGOU P CHOU MI  
Lyne Valerie*

To my loving wife MAGOMOU Edith

To my Parents Mr. MBAKOP Jean and Mrs. MBAKOP Sephora

TO MY CHILDREN: Sephora, Naomie, Raphaelie, Lyne G., KENAN, Stella

To my brothers and sisters especially Etienne NANA and Leopold KETCHIAMEN

AS A TESTIMONY TO THEIR AFFECTION

## ACKNOWLEDGMENTS

I would like to thank a number of individuals, without their unique insights and wisdom, I would have struggled to find the motivation, enthusiasm, inspiration, support, and guidance to complete this work.

First of all, I wish to express my deepest gratitude to my advisors, Professor Uphie CHINJE MELO and Doctor KAMSEU Elie for their inspiration, continued encouragement, priceless suggestions, and support. Their mentorship has helped me become a better scientific writer and critical thinker about science.

I would like to express my profound appreciation to Professor Vincenzo SGLAVO who graciously welcomed me to his laboratory in 2018 and then provided me with the incredible opportunity to complete my Ph.D. at the University of Trento in Italy. There is no doubt without his continued encouragement, invaluable suggestions, invaluable mentorship, exceptional support and keen insights, patient guidance, I would not have made it to this stage of success. I would also like to thank the staff members of the laboratory of Ceramic and Glass of the University of Trento specially Mme Alexia CONCI for the support and assistance in different analysis and characterisations and training in equipments manipulations. My deep gratitude to Professor Cristina Leoneli of University of Modena in Italy for her orientation and support for the characterization of samples in the first part of this thesis.

Additionally, I would like to thank Professor Daniel NJOPWOUO and Professor Antoine ELIMBI who encouraged me to continue with research and for their help and kind suggestions related to my research.

I would like to thank all the lecturers of The Faculty of Science, University of Yaounde I in general and those of the Department of Inorganic Chemistry in particular for their availability, devotedness and encouragement..

I would like to express my gratitude to the jury which examined this work for the quality of their remarks with a view to improving the quality of this document ; i also thank them for their disponibility.



I would also like to thank and to express deep appreciation to my colleagues and friends at the Local Material Promotion Authority and University of Yaounde I; all of their support and encouragements helped me significantly toward the completion of my studies. The following is a list of my colleagues who helped me carry out the different research projects. I was fortunate to work within this environment. In particular, i would like to thank my friends and colleagues Dr TCHAMBA, Dr DEUTOU Juvenal, Dr TCHOUNANG Serge, Mr NJINYA Yannick, Mr SUILABAYU LOWEH, Mme TCHAMAKO and Mme AWA MOHAMED for their encouragement and support. I thank my current and formers fellow labmates from Ceramics Group, specially, Mr KAZE Rodrigue, Mr NGOUNOUE KAMGA Francis, Mr TIFFO Emmanuel and Mlle NYONDA Gaëlle.

I gratefully acknowledge the funding sources that funded my Ph.D. work. First I thank the Local Material Promotion Authority and his General Manager, Dr Likiby BOUBAKAR. This financial support has enabled me to focus on my professional and scientific development. It is my hope that our efforts in this thesis can add to a better quality of life in Cameroon.

I would like to thank my entire family and long-time friends for their love, support and encouragement. I would like to express profound gratitude and deeply appreciation to my parents (Mr and Mrs MBAKOP) and all siblings from whom i got unconditional love and inspiration that shaped my actions and morals. A special thanks to my brothers and sisters, Etienne NANA, Leopold KETCHIAMEN, Virginie NJINKE, Rose KUIKEU and Brigitte NANA.

Last and not least, I am greatly indebted to my beautiful wife, Mme TCHAKOUTEU Edith. None of this could have happened without her patience and sacrifices. I am thankful for her endless love and encouragement. Edith, you are always there cheering me up, supporting me spiritually throughout the good and bad times of our life. I thank my lovely children: Sephora, Naomie, Raphaeli, Lyne Geovanella, Kenan, Jennifer and Stella; you are a blessing in my life. Thank God!!

To you all, without you this thesis would not have been possible. I thank you.



---

---

## RESUME

---

---

Des matières premières locales dont une argile kaolinitique ( $K_M$ ) provenant de la Région du Nord-ouest, des matériaux feldspathiques (FBb1, FBb2, FMj) provenant de Boboyo (FBb) dans l'Extrême-Nord Cameroun et de Manjo (FMj) dans le littoral ; une syénite néphéline (NPH) provenant d'Eboundja dans la Région du Sud et un matériau calcaire (du marbre) provenant de Figuil dans le Nord ont fait l'objet d'une étude en vue de l'élaboration des matériaux semi-vitrifiés de Hautes Performances à des températures relativement basses. Des analyses chimiques, minéralogiques, thermiques et microstructurales ont été réalisées sur ces matériaux.

L'argile kaolinitique de Mankon utilisées allie à la fois les propriétés d'un bon kaolin avec la kaolinite comme phase majeure et d'une ball clay avec un indice de plasticité de 27,69 %. Les matériaux feldspathiques ont été choisis pour leur teneur en oxyde de potassium ( $K_2O$ ) variant entre 4-6% en masse. Le marbre titrant 95% de carbonate de calcium et 5% de dolomite a été utilisé pour ajuster la fraction fondante et favoriser la formation des eutectiques en vue d'abaisser la température de frittage des céramiques élaborées.

Dans la première phase du travail, le marbre a été ajouté en pourcentage fixe (5%) dans deux compositions dont l'une à base de feldspath de Boboyo 1 (P) et l'autre à base de syénite néphéline (G) ; La vitrification du matériau à base de syénite néphéline (G) a été retardée par rapport au matériau à base de pegmatite (P). La cristallisation de la leucite qui est apparue dans la courbe d'Analyse Thermique Différentielle (ATD) de la pegmatite n'a pas été trouvée dans la courbe d'ATD du grès cérame (B). Ces différences ont été attribuées à l'influence du CaO dans l'amélioration de la vitrification et la réduction de la viscosité du fluide formé dans les systèmes à base d'orthose par rapport aux systèmes à base d'albite. La composition (P) a montré une résistance en flexion élevée et une porosité relativement faible à une température de 1175°C avec moins de 0,4% d'absorption d'eau à 1200°C. (G) est resté poreux jusqu'à 1225°C (avec 2,5% d'absorption d'eau) et a atteint la résistance à la flexion de la composition (P) uniquement à 1225°C.

Dans la deuxième partie du travail, nous avons éliminé la syénite nephelinite et intégré deux matériaux riches en  $K_2O$ : un deuxième échantillon de pegmatite de Boboyo ainsi qu'une pegmatite prélevée à Manjo. Les pourcentages d'ajout du marbre ont été variés entre 0 – 10% et les matériaux élaborés ont été traités thermiquement entre 1150°C – 1225°C pour les compositions avec ajout et jusqu'à 1300°C pour les compositions de référence (sans ajout).

L'ajout de calcaire au mélange a amélioré de manière significative les propriétés physiques et mécaniques des matériaux élaborés et a diminué remarquablement la température de frittage.

La mullite s'est avérée être la phase principale des échantillons de référence, tandis que la mullite et l'anorthite ont été présentées comme phases principales des échantillons basés sur l'ajout de calcaire de 3 à 7%.

Les échantillons avec addition de calcaire ont montré un phénomène d'expansion contrôlée après le retrait maximum entre 1175 et 1200 ° C; cela a contribué à réduire le retrait linéaire des matériaux obtenus.

À partir de 1175 °C, certains échantillons additionnés de calcaire ont présenté une résistance à la flexion très élevée (jusqu'à 138 MPa), une bonne densité (jusqu'à 3,2), une faible absorption d'eau (proche de zéro) et de faibles pourcentages de pores ouverts.

Les céramiques à base de mullite et d'anorthite simultanément comme phases principales ont développé une vitrification précoce, une résistance à la flexion élevée, une faible porosité et une bonne densité à une température relativement basse.

À partir de 1225 °C, les échantillons avec ajout de calcaire (à partir de 3%) ont montré une diminution des performances mécaniques, indiquant que ces formulations n'ont pas besoin de températures supérieures à 1200 °C pour obtenir des matériaux de qualité optimale. Cela signifie un gain en température de près de 150 °C par l'addition contrôlée du calcaire à la composition et l'application d'un bon process de production.

**Mots clés:** Céramique, semi-vitrifiés, calcaire, haute résistance, carreaux de grès cérame, frittage, cristallisation, économie d'énergie, matières premières locales.

## ABSTRACT

Local raw materials including kaolinitic clay (KNt) from the North West Region, feldspathics materials (FBb1, FBb2, FMj) from Boboyo (FBb) in far North Cameroon and Manjo in the coast; a nepheline syenite from Eboundja in the South Region and a limestone material (marble) from Figuil in the North were used as raw materials for the development of high performance semi-vitrified products at relatively low temperature. Chemical, mineralogical, thermal and microstructural analyzes were carried out on these materials. The Mankon kaolinitic clay used, combines the characteristic of a good kaolin with kaolinite as the major phase and ball clay with a high plasticity index (27.69%). The feldspar materials were chosen for their potash ( $K_2O$ ) content varying between 4-6% by mass. Limestone containing 95% calcium carbonate and 5% dolomite was used to adjust the melting fraction and promote the formation of eutectics in order to lower the maturation temperature of elaborated ceramics.

In the first part of the work, limestone was added in a fixed percentage (5%) in two compositions, one based on pegmatite from Boboyo 1 (B) and the other based on nepheline syenite (G) from Eboundja. The vitrification of the nepheline syenite (G) was delayed with respect to the pegmatite-based material (B). The crystallization of leucite that appeared in DTA curve of pegmatite was not found in the DTA curve of the porcelain stoneware (B). These differences were ascribed to the influence of CaO in enhancing the crystallisation and reducing the viscosity of the fluid formed in orthose-based systems compared with albite-based systems. The composition (B) showed high strength and relatively low porosity at temperatures range from 1175 °C (with less than 0.4 % of water absorption) to 1200 °C. The composition (G) remained porous up to 1225°C (with 2.5 % of water absorption) and reached the flexural strength developed by (B) at 1175°C only at 1250 °C.

The addition of limestone to the mixture enhanced conveniently the physical and mechanical properties of porcelain stoneware tiles and decreased significantly the sintering temperature. Mullite was found to be the main phase on reference samples, while mullite and anorthite were observed as main phases of samples based on limestone addition from 3 to 7%. From 1175 °C, some samples with limestone addition exhibited very high flexural strength (up to 138 MPa), with good density (up to 3.2), low water absorption (close to zero) and low open pores.

Samples with addition of limestone exhibited a controlled expansion phenomenon after the maximum shrinkage between 1175°C and 1200°C; this contributed to reduce the firing shrinkage of the porcelain stoneware obtained.

The ceramics bodies based on mullite and anorthite, simultaneously, as main phases developed early vitrification, high flexural strength, low porosity and good density at relatively low temperature.

As from 1225 °C, specimens with limestone addition (from 3%) showed a decrease in mechanical performance, indicating that these formulations do not need firing temperature above 1200 °C to achieve optimum porcelain stoneware tiles. This signifies an energy saving of almost 150 °C by the limestone addition to the bulk composition and an optimum processing.

**Key Words:** Ceramics, semi-vitreous, limestone, high strength, porcelain stoneware tiles, sintering, crystallization, energy saving, local raw materials.

## GENERAL INTRODUCTION

The high strength, greater chemical stability, lower water absorption and the durability of semi-vitrified ceramics make them one of the prominent structural materials. The above mentioned properties have as origin the ability of the triaxial clay-feldspar-quartz paste compositions to develop crystalline phases upon firing, that remain embedded together with high viscous liquid phase generated from the fluxing agent (feldspars and others) (Sane et al, 1951; Kingery WD, 1993; Reed JS, 1993; Maity et al, 1996 ; Carty et al, 1998). Originally, the history of porcelain reveals a soft type thermally treated for a complete translucence at 1250°C using albite ( $6\text{SiO}_2\text{Al}_2\text{O}_3\text{Na}_2\text{O}$ ) feldspar for its relative low temperature of congruent fusion at 1118°C. The hard type of porcelain is produced above the temperature of 1300°C using potash feldspar, essentially orthose or microcline ( $6\text{SiO}_2\text{Al}_2\text{O}_3\text{K}_2\text{O}$ ) which presents an incongruent fusion at 1150°C. While a viscous glass appears at this temperature, a stable crystalline phase is formed: Leucite. The orthose melt completely only at 1510°C. To remain competitive while keeping the high quality, the porcelain industry has known great evolution and innovations which has required changes in raw materials, sintering time and energy consumption (Carty et al, 1998; Schulle W, 2003 ; Kivitz et al, 2009). Much attention has been paid to the development of low energy consuming technology. In this connection, the fluxing fraction (feldspars) has been the most affected by changes and innovations. It is also the component that governs the sintering and the grade of porcelain. The mix of albite-orthose, the use of nepheline syenite and the increase in fluxing content together with processing technology have conducted in the recent years to the so called porcelain stoneware (Koenig CJ, 1942 ; Oberschmidt LE, 1957 ; Lundin ST, 1959 ; Esposito et al, 2005).

Despite the fact that ceramics are produced in many countries around the world, developping countries are facing many difficulties in the appropriation an application of these technologies unless their annual consumption of these materials are increasing more and more over the years; for example, the data collected in the National Institute of Statistic in Cameroon shows that, the country has imported 6189.7 tons of tiles in 2010; 8148 tons in 2011; 96908 tons in 2012; 111737.75 tons in 2013 and 103218 tons in 2014 for a total of hundreds of billions of CFA francs.

In Cameroon, a good number of kaolin and kaolinitic clayey deposits have been investigated for their suitability to be used as plastic materials in the triaxial ceramic compositions (Njoya et al, 2006; Leonelli, 2008 ; Nkoumbou et al, 2009; Kamseu et al, 2010). Geological investigations have identified various grade of feldspars suitable for the development of porcelain, porcelain stoneware, stoneware, vitreous, etc... Granites with high alkali content and

good fusibility behavior are described in the West Region of Cameroon. Njoya et al (2010) found that the feldspathic materials of this region present 43 wt% of albite, 26 to 41 wt% of microcline, about 15 wt% of quartz and very low plagioclase and biotite. In the South Region, a very important deposit of nepheline syenite exists with 15.69 wt% of alkalis (Melo et al, 2004 ; Elimbi et al, 2005). The deposit is essentially nepheline syenite with about 15 wt% of alkali in addition to some inclusions of lime-rich feldspars. (Elimbi et al, 2005) described the pegmatite minerals at Penja in the Littoral Region with 14.62 wt% of alkalis. The pegmatites have larger size of grains that can reach 5cm. The nepheline syenite from Kribi has been studied in details by (Melo et al, 2004) which described the good fusibility and some variations of compositions. (Tchakounte et al, 2013) studied pegmatite from Boboyo in the far Nord Cameroon and found that it contains 55% of microcline and 15% of albite. Conversely to potash and soda feldspars, the nepheline syenite and pegmatite are composites in their natural state. In the  $\text{NaAlSi}_3\text{O}_8$ - $\text{KAlSi}_3\text{O}_8$  of feldspathic solid solutions, nepheline syenite is one of the probable crystalline phase when  $\text{Na}_2\text{O}/\text{K}_2\text{O}$  molar ratio is  $\geq 3$  ; the solid solution will have eutectic points at temperatures under  $1118^\circ\text{C}$  (Tchakounte et al, 2013). When the orthoclase or microcline is the major phase in the solid solution, the molecules of  $\text{NaAlSi}_3\text{O}_8$  and  $\text{KAlSi}_3\text{O}_8$  form a continuous series of solid solutions at high temperatures from  $990^\circ\text{C}$ , but at temperatures below  $600^\circ\text{C}$ , there is a gap in the isomorph series: solid solutions between potash and soda feldspars are metastable and under conditions of slow cooling show alterations into oriented growth of sub-parallel lamellae which are alternatively rich in potash feldspar. Such intergrowths are present in pegmatite as perthites in which soda feldspar occurring as uniformly-oriented films. The mineral nature of phases in the solid solutions is therefore dependent upon the temperatures of the magma from which the feldspar crystallized (Tchakounte et al, 2013). This mineral nature directly affects the thermal behavior of the solid solution.

In this work, the chemical approach was used to integrate locally available raw feldspars, clays and quartz for the design of fine ceramics as porcelain, stoneware, etc...

Limestone is use to modify the sintering behavior of fluxing fraction in forming new eutectics in other to produce sustainable semi-vitrified ceramics. The compositions were design through chemical approach (Kamseu et al, 2007); the use of locally available raw materials and milling to put in place sustainable bulk compositions of porcelain stoneware. By designing the fine ceramic pastes with particles size under  $45\ \mu\text{m}$  was found to insure to the materials a controlled range of porosity and pores size (Amoros et al, 2007 ; Alves et al, 2012). However, the milling time is considered as a parameter that can affect the apparent density, pores sizes and the degree of densification. (Amoros et al, 2007 ; Alves et al, 2012). The fineness of the particles also governs the firing shrinkage, strength, thermal expansion and the warpage.



The microstructure of porcelain stoneware is governed by the amount and viscosity of the vitreous phase formed during sintering and the interactions between this major phase and the dispersed crystalline ones (mullite, anorthite, etc.) or remaining as non-transformed raw materials (quartz, etc.). When an equilibrium is reached between the viscosity of the vitreous phase and the size of newly formed crystalline phases, optimum compaction is achieved associated to minimum pore size to insure the maximum mechanical strength of the matrix. The sintering involves both densification and grains growth which occur basically through atomic movements in bulk or at the liquid–solid interfaces. The grains growth conducts to trapped pores within the larger grains. The equilibrium is generally difficult to achieve due to the spontaneous closed pores that evolve with the liquid formation while this liquid is significant on reducing the open porosity. With the raw materials selection and the processing optimized, the final microstructure and the pore size distribution are functions of the contribution of the amount and characteristics of the liquid phase capable on eliminating porosity through a suitable thermal cycle. Focusing on the relation between the sintering process and the microstructure, a recent study has demonstrated that the granulometric distribution of spray-dried material does not interfere significantly in its pore size distribution after sintering since the distinct granulometric composition led to the same porosity in the sintered product (Amoro et al, 2007). The granulometric distribution with  $\phi < 45 \mu\text{m}$  and a maximum green compact of different pastes of porcelain stoneware will reduce the dependence of final microstructure to the capacity of the thermal cycle applied to promote quality of fluid for maximum densification. In these conditions, the nature of the kaolin used, the quality of silica and more important the nature of the fluxing agents are significant (Martin-Marques et al, 2008 ; Alves et al, 2010 ; Alves et al, 2011). The microstructure of the standard commercial porcelain consists of  $\beta$ -quartz grains held in a complex matrix, surrounded by vitreous silica-rich phase. The matrix contains clay relics, primary mullite crystals, secondary mullite and feldspar relics (Yaseen Iqbal et al, 1999). The crystalline texture of the porcelain bodies receiving a long, low-temperature firing shows more quartz solution and more mullite development than the bodies which have received a short, high temperature firing. During the long firing, some sort of slow diffusion goes on which makes the feldspar glass sufficiently rich in alumina so that secondary mullite crystallizes (Yaseen Iqbal et al, 1999). The relationship between viscosity of alkali-feldspar glass and temperature is approximately logarithmic between 1000°C and 1200°C. The presence of silica increases the viscosity and more rapidly with larger quantities. The eutectic temperature for potash feldspar with silica starts at around 990°C and that of soda feldspar at 1050°C (William Carty et al, 1998). The lower liquid formation temperature in the potash feldspar is beneficial for reducing the porcelain firing temperature. The presence of albite in potash feldspar can reduce the liquid formation temperature by as much as 60°C (Leven et al, 1964 ; William Carty et al, 1998;). More than albite, CaO reduces the range of fusibility as well

as the viscosity allowing complete wrapping at relative low temperature. The reduction of the firing time of porcelain to the minimum (60–90 min) is particularly applied to porcelain stoneware with the changes in the bulk chemical composition and improvement of the processing for the considerable decreases of the firing temperature which nowadays is  $\leq 1200^{\circ}\text{C}$  (Schulle, 2003 ; Bartush, 2004 ; Tucci et al, 2007 ; Kivitz et al, 2009 ; Martin marquez et al, 2010). The basic component that is able to decrease the firing temperature while maintaining the physical properties of the material is the fluxing agent. More than a single mineral of albite or orthose, solid solution promote ideal flux for semi-vitreous bodies. The use of solid solutions have been demonstrated to be the ideal route. Moreover, addition of mineralizers is projected to enhance the action of the solution and increase the spectra of the potential solid solutions that can be used. The changes described above contribute to decrease the energy consumption implying a decline of energy cost and a lower environmental pollution because of less  $\text{CO}_2$  emission. The formation of the vitreous phase by the progressive melting of fluxing agent is a fast phenomenon, starting from  $990^{\circ}\text{C}$  in the orthoclase based flux; that is mostly accomplished before viscous flow begins densification. Densification goes on involving a slow-rate quartz dissolution. The viscosity and surface tension of the liquid phase will play major role in sintering kinetics. The fast formation of liquid phase in porcelain stoneware hinder the formation of enough mullite (<15 vol.%) as in conventional porcelain, the amount of liquid phase is high (>60 vol.%) and the strengthening mechanism is mostly linked to the matrix reinforcement and dispersion-strengthening theories (Amores et al, 2007). Plagioclase is formed instead of anorthite and crystals dissolution at high temperatures are commonly observed (Martz, 1933). It is apparent that open porosity decreases with the increase of firing temperature due to the formation of a glassy phase that is mainly originates from the feldspar. As the melting temperature of the flux system is reached, the amount of liquid phase increase with the decrease in viscosity.

Therefore, the present study investigated the thermo-mechanical properties of ceramics designed by addition of limestone on potash pegmatite materials in order to help towards sustaining the natural resources, reduce the environmental hazards caused by the high firing temperature of ceramics and promote the local production of ceramics materials.

### **Objectives of the study**

The aim of the research was to study the effects of the addition of various portion of calcium oxide on potash feldspars and investigated their influence on the properties of semi-vitrified ceramics. In order to achieve that, three objectives were designed as follows:

- (i) To compare the effect of CaCO<sub>3</sub> addition on two compositions based on a potash feldspar and a nepheline syenite
- (ii) To determine and optimize the effects of limestone addition on the mechanical and physical properties of porcelain ceramics based on two different potash feldspars:
  - (a) Mechanical properties which include, bending strength and Vickers hardness.
  - (b) Physical properties, which include linear shrinkage, percentage of porosity (apparent porosity and open pores volume), bulk density and microstructure.
  - (c) Thermal properties including Differential Thermal Analysis (DTA), Differential Thermal Gravimetry (TG) and Differential Thermal Calorimetry (DSC) of raw materials and porcelain formulations
- (iii) To determine the optimum parameters such as sintering temperature, sintering rate, soaking time with respect to the physical and mechanical properties.

### **Scope of the study**

In order to realize the objectives of the study to be successfully and reasonably implemented, the following scope of works have been derived.

- (i) The chemical approach was used to integrate the locally available raw feldspars, clays, and quartz for the design of fine ceramics;
- (ii) Two porcelain stoneware formulations, one with pegmatite minerals and the second with nepheline syenite was first elaborated and studied with fixed portion of limestone;
- (iii) Standard porcelain ceramic composition was adopted and limestone was progressively and proportionally introduced in compositions based on two potash feldspars;
- (iv) In order to determine the optimum temperature, 1150°C, 1175°C, 1200°C, 1225°C and 1250°C, 1300 °C for reference samples were investigated; the soaking time was varied from 1 hour to 2 hours in order to determine the best soaking time with sintering rate of 20°C/min and 5°C/min were applied.



# **CHAPTER I: LITERATURE REVIEW**

### **I-1: CERAMICS**

#### **I-1-1: Generalities**

The word “ceramic” comes from the Greek word “keramikos”, which means “of pottery”. While the earliest ceramics were pottery, the term encompasses a large group of materials, including some pure products. A ceramic is an inorganic, nonmetallic solid made of oxides, nitride, boride or carbide that is fired at a high temperature (A. Helmenstine, 2019). Ceramics may be glazed prior to firing to produce a coating that reduce porosity and gives a smooth, often colored surface. Many ceramics contain a mixture of ionics and covalent bonds between atoms. The resulting material may be crystalline, semi-crystalline or vitreous.

#### **I-1-2: Types of Ceramics:**

Ceramics can be classified on four main classes which are: white wares, structural ceramics, technical ceramics and refractories.

White wares include cookware, pottery and wall tiles. Structural ceramics include bricks, pipes, roofing tiles and floor tiles. Technical ceramics are also known as special, fine, advanced or engineering ceramics; this class include: bearings, special tiles (eg. Spacecraft heat shielding), biomedical implants, ceramic brakes, nuclear fuels, ceramics engines and ceramic coatings. Refractories are very high temperature ceramics; these classes include bricks, crucibles, line kilns and radiate heat in gas fireplaces.

Figure below illustrate the location of ceramics materials in the feldspar-quartz-clay triaxial diagram (Romero & Pérez, 2015)

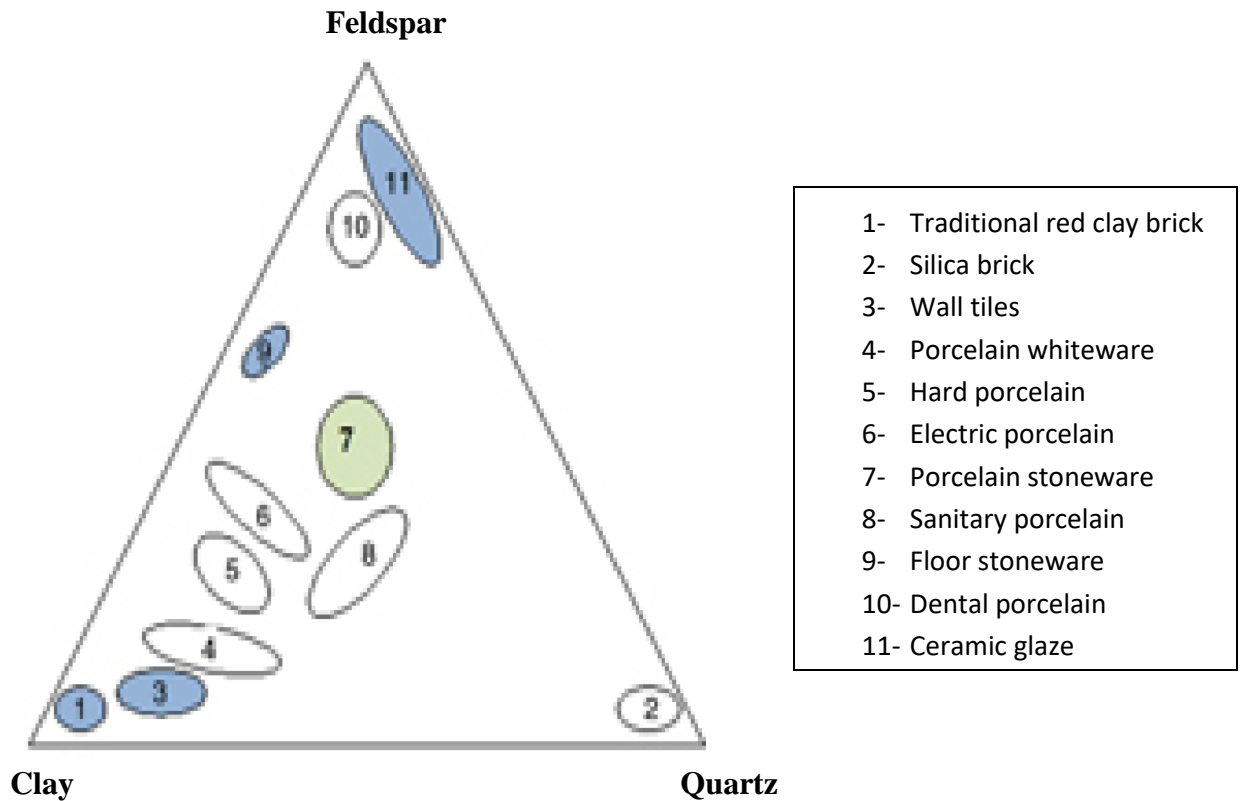


**Figure 1:** Location of different ceramics materials in the feldspar-quartz-clay triaxial diagram (M. Romero & J. Pérez, 2015)

## I-2: GENERALITIES ON CERAMICS RAW MATERIALS

The bodies of ceramic materials are composed of various typologies of raw materials in amounts characteristic of the desired product. The composition of the body and the treatment conditions determine the transformation that involve the raw material and mainly define the final characteristics and field of employment of finished product. These raw materials are divided into two groups: plastic raw materials and non-plastic raw materials.

### I-2-1: Plastic raw materials: Clays

These are the most important raw materials for the manufacture of ceramic products. The plastic raw materials that are found in their natural state are alumino-silicates, whose two dimensional structure justifies the designation of phylitic minerals. This particular morphology gives the clay paste, properties of plasticity, swelling with water, formation of colloids, etc. The mechanism of fixing water on elementary particles, called micelles, explains the swelling phenomenon of clays soaked in water, as well as the reverse phenomenon called shrinkage when the materials lose water during drying.

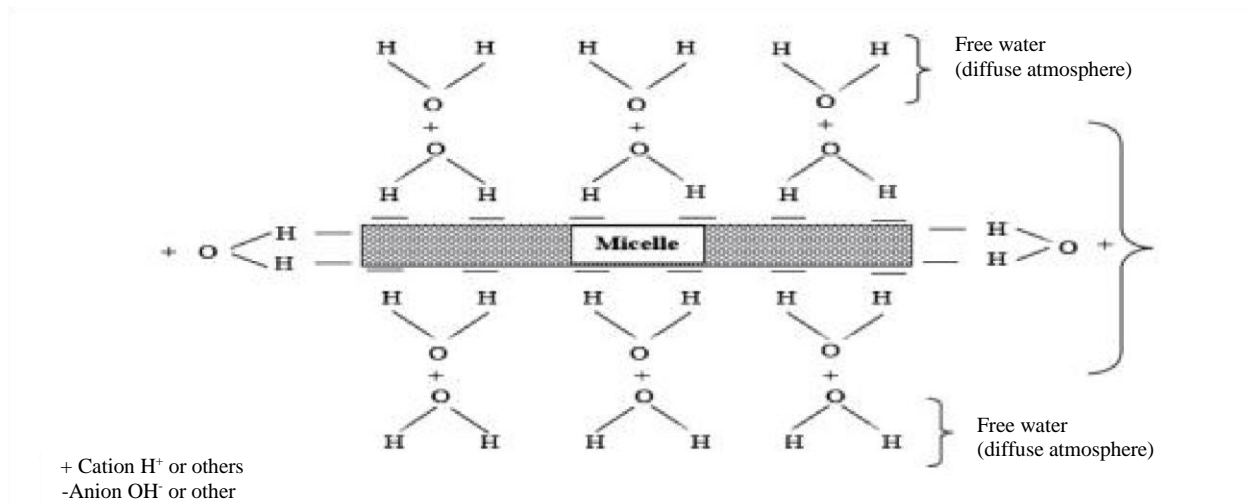


**Figure 2:** Water fixing mechanism on clay micelles (Kerboul & Bossler, 1990)

Clay based minerals are the main constituent of ceramic bodies; their amount generally ranges from 40 to 60 wt %. They confer plasticity and workability in the green state and gives the main oxides involved, with fluxes and sintering aids, in the consolidation mechanism of the body during firing (Manfredini et al, 2012). These changes convert the clay into a ceramic material; because of these properties, clay is used for making utilitarian and decorative pottery as well as construction material such as bricks, wall and floor tiles. Different types of clay with associated minerals and firing conditions are used to produce earthenware, stoneware and porcelain.

### a) *Definition*

According to the International Association of Clays Studies (IACS), clay indicated any natural material with fine grains (< 2 $\mu$ m) which become plastic with suitable water content and became hard when dried or sintered (Guggenheim et al, 1995).

Clay is an earth material of very fine particle size which results from the weathering or by hydrothermal action inducing a sedimentary deposit. Clay is cohesive and usually plastic when wet. It serves as a primary binder and fires in different colors depending on the type and compositions. It shrinks when dry and expands when wet. It is a poor conductor thus, clay materials are used as thermal insulators. Clay materials are usually stable at high temperatures and this makes them have good thermal shock, i.e. ability to retain their original forms without cracking, spalling or flaking under sudden thermal changes and to have good resistance to environmental attack. It has appreciable amounts of organic matter (Ajakor et al, 2015).



Clay can also be defined as a finely-grained natural rock or soil material that combines one or more clay minerals with traces of metal oxides and organic matter. The materials are plastic due to their water content and become hard, brittle and non-plastic upon drying or firing (Saleh Ahdiri et al, 2016). Clays exhibit plasticity when mixed with water in certain proportions. However, when dry, clay becomes firm and when fired in a kiln, permanent physical and chemical changes occur, converting clay into a ceramic material. Because of these properties and depending on the soil's content in which it is found, clay can appear in various colors from white to dull grey or brown to deep orange-red. Although many naturally occurring deposits include both silts and clay, clays are distinguished from other fine-grained soils by differences in size and mineralogy. Silts, which are fine-grained soils that do not include clay minerals, tend to have larger particle sizes than clays. There is, however, some overlap in particle size and other physical properties. The distinction between silt and clay varies by discipline. Geologist and soil scientists usually consider the separation to occur at a particle size of 2 $\mu\text{m}$  (clays being finer than silts), sedimentologist often use 4–5 $\mu\text{m}$ , and colloid chemist use 1 $\mu\text{m}$ ; Geotechnical engineers distinguish between silts and clays based on the plasticity properties of the soil, as measured by Atterberg limit. Clay minerals typically form over long periods of time as a result of the gradual chemical weathering of rocks, usually silicate-bearing, by low concentrations of carbonic acid and other diluted solvents. These solvents, usually acidic, migrate through the weathering rock after leaching through upper weathered layers. In addition to the weathering process, some clay minerals are formed by the hydrothermal activity.

### **b) *Classification of Clays***

According to the deposit mode, there are two types of clay deposits: primary and secondary.

1) Primary clays form as residual deposits in soil and remain at the site of formation, these type of clay are called 'kaolin'; they are mainly found on the tops and interflaves of hills (Nzeukou, 2014); residual clays are most commonly formed by surface weathering, which gives rise to clay in three ways (Encyclopedia Britannica, 2016):

- i) Chemical decomposition of rocks, such as granite, containing silica and alumina
- ii) Solution of rocks, such as limestone, containing clayey impurities;
- iii) Disintegration and solution of shale.

2) Secondary clay also known as alluvial clay are removed from the place of origin by erosion agents and deposited in a new and possibly distant position (Nzeukou, 2014); they are generally found along the terraces and banks of the water ways. The transport and deposition of clays and clay minerals produced by eroding older continental and marine rocks and soils are important parts of the cycle that forms sedimentary rocks. The ancient sedimentary rock record is composed of

about 70 percent mudstones which contain about 50 percent clay-sized fragments and shales which are coarser than mudstones but which may contain clay-sized particles. (Blatt et al, 1980).

Depending on the academic source, there are three or four main groups of clays minerals: kaolinite, montmorillonite – smectite, illite, and chlorite.

### **i) Kaolinite**

Kaolinite, of structural formula  $\text{Si}_2\text{Al}_2\text{O}_5(\text{OH})_4$ , is in the form of hexagonal lamellar particles formed by the stack of sheets. The elementary sheet is formed by a layer of tetrahedra silica resting on a layer of octahedra aluminum linked by common edges. These polyhedra are formed by the superposition of three layers of oxygen and hydroxide (see Figure 3). The sheets are more or less fixed relative to each other and cannot fix either water or cation in their intervals; the possibilities of swelling, the absorbency of bases are therefore reduced. Kaolinites are very resistant to heat. No substitution in the layers, the sheet is neutral. Kaolinite is formed in well-drained soils with acid pH. Its crystals are often large (up to  $15\mu\text{m}$ ). Kaolinite is snow white, oily to the touch, soapy and plastic (H. Boussak, 2010).

Among all the minerals of clayey materials, kaolinite remains one of the most frequently used and desired for the manufacture of widely used ceramics, it is for this reason that clays mainly made up of kaolinite are called kaolinitic clays. In industry, the term "kaolin" being reserved for the product resulting from the purification of these clays, and in which the proportion of kaolinite exceeds 80wt% (N. Koumtoudji, 2004).

At the microscopic level, kaolinite is composed of crystals which have a flaky shape, this type of crystalline structure is at the origin of the properties of kaolin, which make it a useful material for multiple uses: manufacture of porcelain, thermal insulator, layer pigment in paper, filler and coating for cardboard articles and inks (H. Boussak, 2010).

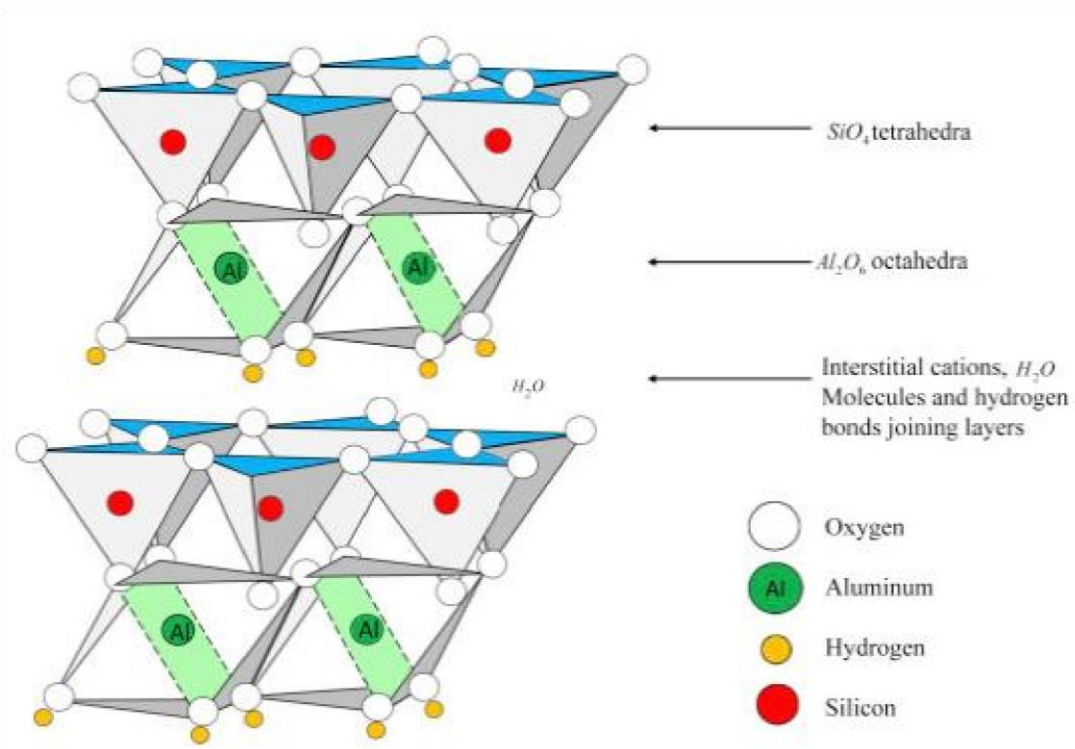


**Figure 3:** Structure of kaolinite (Kotal et al, 2015)

## ii) Montmorillonite

Montmorillonite was first described in 1847 for an occurrence in Montmorillon in the Department of Vienne, France; it is a very soft phyllosilicate group of mineral with basis formula  $4\text{SiO}_2\text{Al}_2\text{O}_3 \cdot 2\text{H}_2\text{O}$  that's form when they precipitated from water solution as microscopic crystals known as clay. Montmorillonite is a 2:1 clay, member of smectite group with two tetraedral sheets sandwiching a central octaedral sheet of alumina of thickness  $10 \text{ \AA}$ . It has high cation exchange capacity (CEC) varies from 100 to 130 meq / 100g of clay calcined at  $900^\circ\text{C}$  (H. Boussak, 2010).

Montmorillonite can be concentrated and transformed within cave environments. The natural weathering of the cave can leave behind concentrations of aluminosilicate which were contained within the bedrock. Montmorillonite can form slowly in solutions of aluminosilicates. High  $\text{HCO}_3^-$  concentrations and long periods of time can aid in its formation. Montmorillonite can then transform to palygoskite under dry conditions and to halloysite- $10\text{\AA}$  (endelite) in acidic conditions (pH 5 or lower). Halloysite- $10\text{\AA}$  can further transform into halloysite - $7\text{\AA}$  by drying (Hill Carol et al, 1997).

Montmorillonite is used in the oil drilling industry as a component of drilling mud, It is also used as a component of foundry sand and as a dessicant to remove moisture from air and gases; Montmorillonite is effective as an adsorptive of heavy metals.

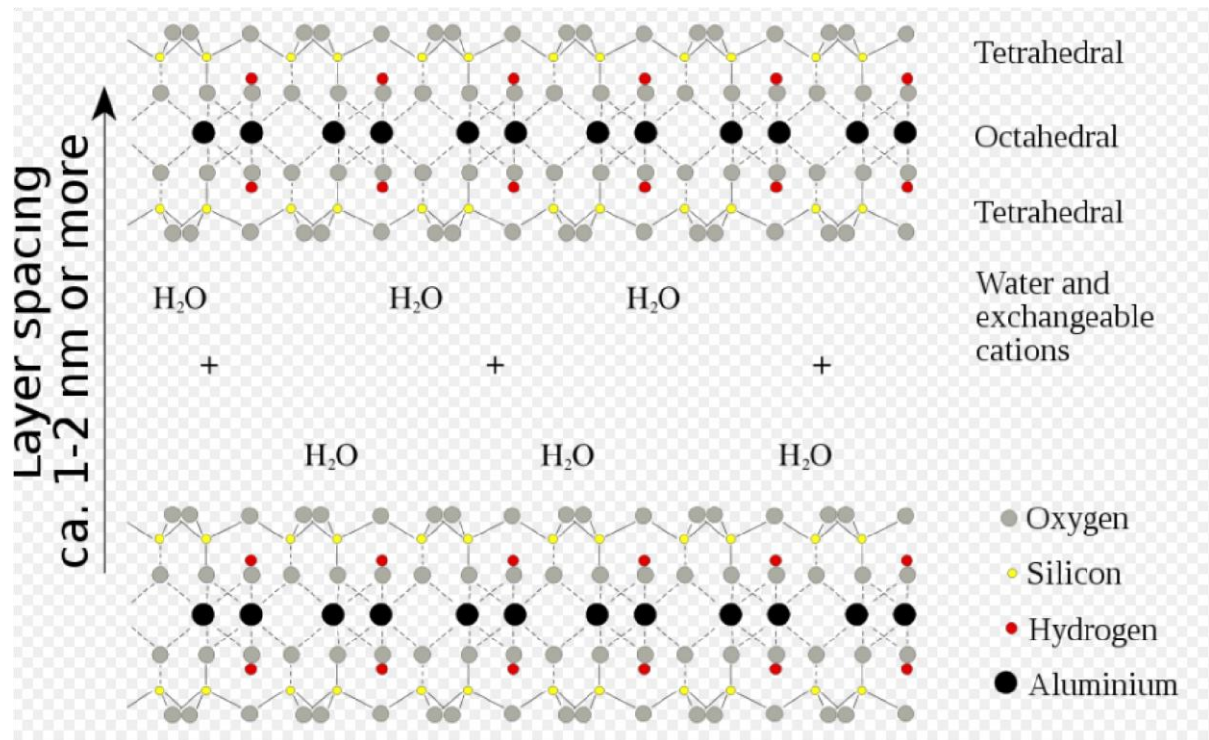


**Figure 4:** montmorillonite structure (Anthony John et al, 1995)

### iii) Illites

Illite is a group of closely related non-expanding clay minerals. Illite is a secondary mineral precipitate and an example of a phyllosilicate, or layered alumino-silicate. Its structure is a 2:1 sandwich of silica tetrahedron (T) – alumina octahedron (O) – silica tetrahedron (T) layers (Blum A. E., 1994). The space between this T-O-T sequences of layers is occupied by poorly hydrated potassium cations which are responsible for the absence of swelling. The chemical formula is given as  $(K,H_3O)(Al,Mg,Fe)_2(Si,Al)_4O_{10}[(OH)_2,(H_2O)]$  (Dana 8, 1997). The name ‘Illite’ was derived from the location of Illinois where the mineral was first described for occurrence in 1937 (Grim Ralph et al, 1937)

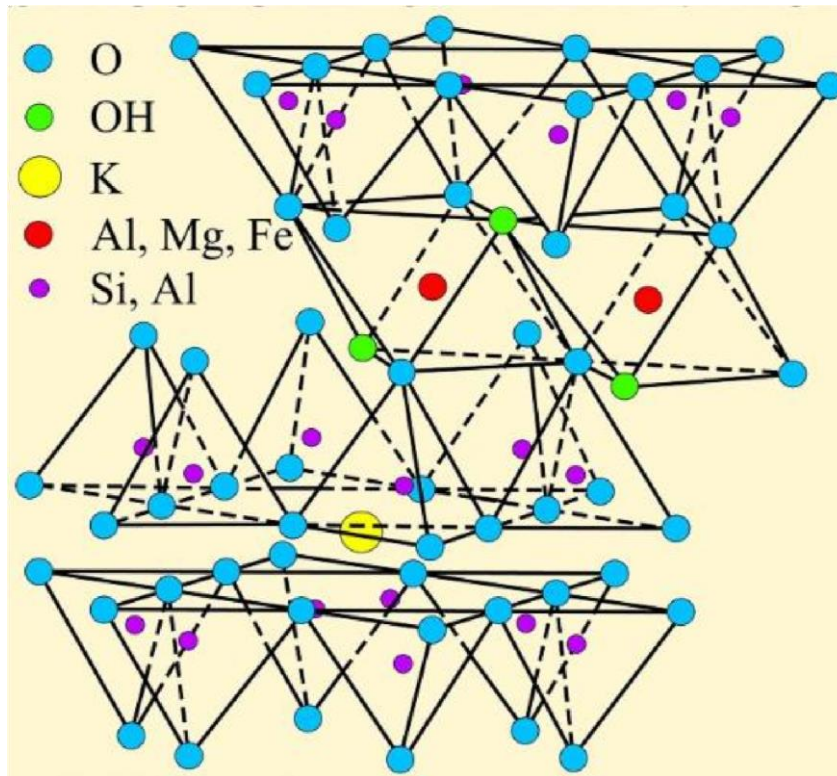


**Figure 5:** Crystal structure of illite (Brindley et al, 1980) modified from (GRIM, 1962)

**Characteristics of illites:**

- Density: 2.66 to 2.72 (g / cm<sup>2</sup>)
- Fusibility: 1350 ° C
- Hardness: 2 (Mohs)
- Solidity: the illites is attackable by acids

**iv) Chlorites**

Chlorites are iron or magnesium aluminosilicates, generally greenish in color, commonly found in igneous rock as an alteration product of mafic minerals such as pyroxene, amphibole, and biotite. In this environment, chlorite may be a retrograde metamorphic alteration mineral of existing ferromagnesian minerals, or it may be present as a metasomatism product via insertion of Fe, Mg, or other metals into the rock mass (Hurlbut et al, 1985). Chlorite is a common mineral associated with hydrothermal ore deposits and commonly occurs with sericite, epidote, adularia and sulfide minerals; it is also a common metamorphic mineral, usually indicative of low-grade metamorphism. It is the diagnostic species of the zeolite facies and of lower greenschist facies.

Chlorite is so soft that it can be scratched by a finger nail. The powder generated by scratching is green. It feels oily when rubbed between the fingers.

The plates are flexible, but not elastic like mica. Various types of chlorite stone have been used as raw material for carving into sculptures and vessels since prehistoric times.

The chemical formula is  $(\text{Mg, Fe})_3(\text{Si, Al})_4\text{O}_{10}(\text{OH})_2 \cdot (\text{Mg, Fe})_3(\text{OH})_6$ .

The crystal structure of Chlorite is indicated in figure 6 below:

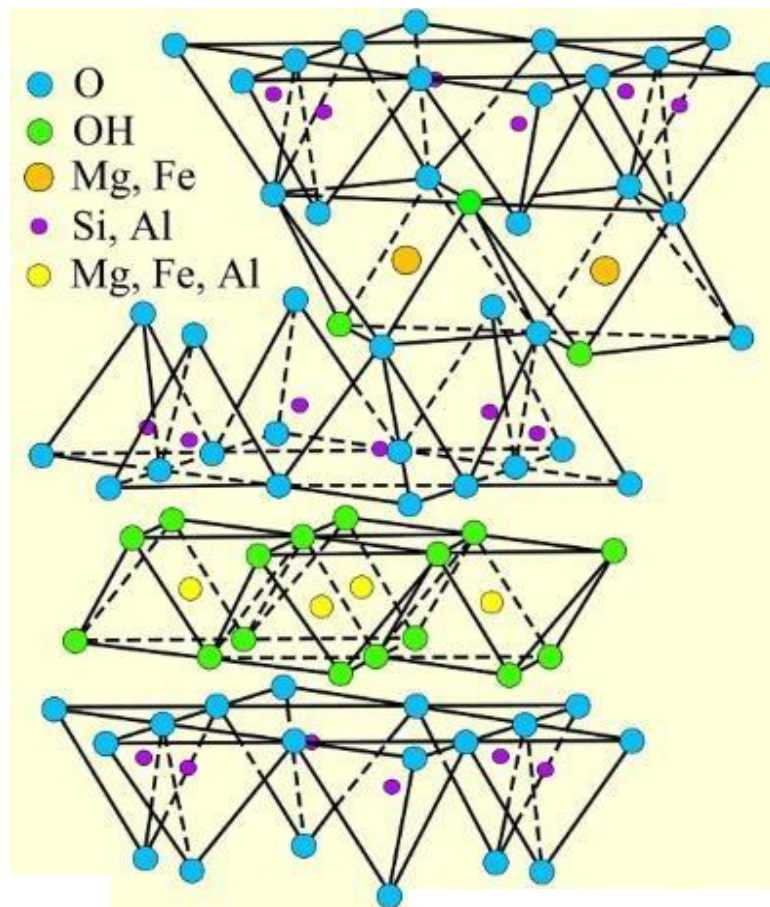


**Figure 6:** Crystal structure of Chlorite (Deer et al, 1975), modified from (GRIM, 1962)

## I-2-2: Non plastic raw materials

### a) *The degreasing materials*

These materials have the role of reducing the shrinkage due to the plasticity of the clay. They are distinguished by the term degreaser. Additions of degreaser to clays generally have the effect of improving the property of the raw paste, facilitating the drying of the products by the diffusion of water during drying and giving a skeleton to the raw paste and the fired product (H. Hurray, 2000). The main degreasers used are fine grain of quartz (sand) and grog

## 1) Quartz

### i) Generalities

The word “quartz” is derived from German word “Quarz” which comes from the Polish dialect “kwardy” meaning “hard” (Tomkeieff, 1942). The ancient Greek referred to quartz as “krustallos” or “kruos” meaning “icy cold” because, some philosophers as Theophrastus believed that the mineral is a form of super cooled ice (Tomkeieff, 1942).

Quartz is a mineral composed of silicon and oxygen atoms in a continuous framework of SiO<sub>4</sub> silicon-oxygen tetrahedral, with each oxygen being shared between two tetrahedra giving an overall chemical formula of SiO<sub>2</sub>. Quartz is the second most abundant mineral in the Earth’s continental crust behind feldspars (Robert et al, 2010)

Quartz crystals are chiral and exist in two forms: the normal  $\alpha$ -quartz and the high temperature  $\beta$ -quartz. The  $\alpha \rightarrow \beta$  phase transformation of quartz crystals takes place at  $\sim 573$  °C during the heating-cooling process and to the relaxation of micro-stresses originated between quartz grains and the surrounding glassy phase by the differences in their thermal expansion coefficients (Singer and Singer, 1971). Since the transformation is accompanied by a significant change in volume, it can easily induce fracturing in ceramics or rocks passing through this temperature limit; similarly, cristobalite inversion occurs.

Quartz is among the most common rock forming minerals and is found in many metamorphic rocks, sedimentary rocks and those igneous rocks that are high in silica content such as granites and rhyolites. It is estimated that about 12% of the mass of the earth’s crust is made of quartz (Hurlbut Cornelius et al, 1985). Under conditions at or near the surface, quartz is more stable than most other minerals and assumes a mostly passive role in the geological environment; this is the reason why billion years ago, the old quartz from Brazil look just as fresh and new as Alpine rock crystals that formed just 10 million years ago. At higher temperature and pressure, quartz becomes very active and participates in many complex reactions during rock forming and mineral formation. Under optimized conditions of firing and for a particle size of 10 – 30  $\mu\text{m}$  (Norton, 1970; Ece and Nakagawa, 2002; Bragança and Bergmann, 2003), quartz has a beneficial effect on the strength of porcelain, in conformity with the pre-stressing theory.

## ii) Crystal structure of Quartz

Quartz belongs to the trigonal crystal system. The ideal crystal shape is a six-sided prism terminating with six-sided pyramids at each end. In nature quartz crystals are often twinned (with twin right-handed and left-handed quartz crystals), distorted, or so inter grown with adjacent crystals of quartz or other minerals as to only show part of this shape, or to lack obvious crystal faces all together and appear massive. Well-ordered crystals typically form in a 'bed' that has unconstrained growth into a void; usually the crystals are attached at the other end to a matrix and only one termination pyramid is present. However, doubly terminated crystals do occur where they develop freely without attachment, for instance within gypsum (Wyckoff, 1963).  $\alpha$ -quartz crystallizes in trigonal crystal system while  $\beta$ -quartz belong to the hexagonal system. Both  $\alpha$  and  $\beta$ -quartz are example of chiral crystal structures composed of a chiral building tetrahedral blocks  $\text{SiO}_4$ . The transformation between  $\alpha$ - and  $\beta$ -quartz only involves a comparatively minor rotation of the tetrahedra with respect to one another, without change in the way they are linked (Wyckoff, 1963)

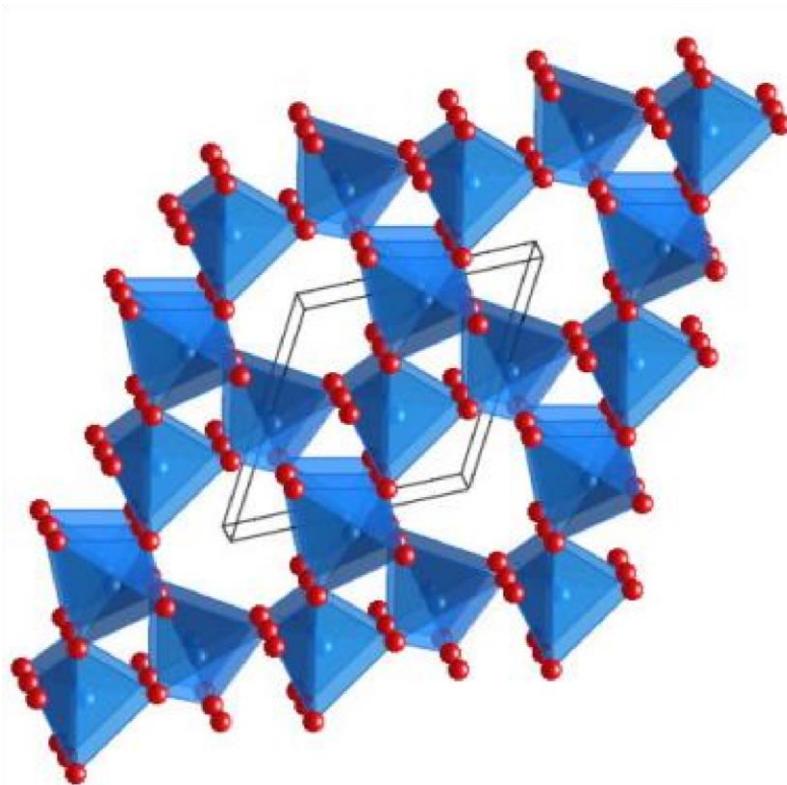


**Figure 7a:** Crystal structure of  $\alpha$ -quartz (Crystal Data, Determinative Tables, ACA Monograph N° 5, American Crystallographic Association, 1963)



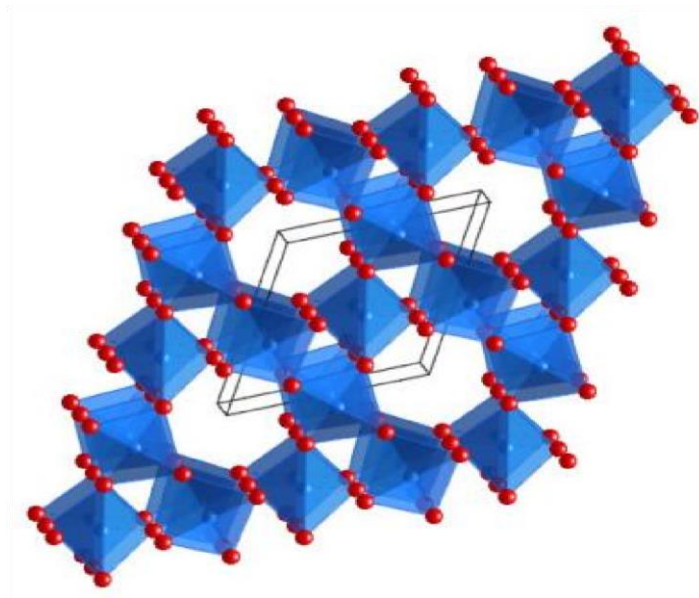


**Figure 7b:** Crystal structure of  $\beta$ -quartz (Crystal Data, Determinative Tables, ACA Monograph N° 5, American Crystallographic Association, 1963)

### iii) Properties of quartz

**Table 1: Physical properties of Quartz**

<b>Chemical classification</b>	Silicate
<b>Color</b>	Quartz occurs in virtually every color, common colors are : clear, white, gray, purple, yellow, brown, black, pink, green, red.
<b>Streak</b>	Colorless (harder than the streak plate)
<b>Luster</b>	Vitreous
<b>Diaphaneity</b>	Transparent to translucent
<b>Cleavage</b>	None - typically breaks with conchoidal fracture
<b>Mohs Hardness</b>	7
<b>Specific Gravity</b>	2.6 to 2.7
<b>Diagnostics properties</b>	Conchoidal fracture, glassy luster, hardness
<b>Chemical composition</b>	SiO <sub>2</sub>
<b>Crystal system</b>	Hexagonal

### iv) Uses of Quartz

Quartz is one of the most useful natural materials. Its usefulness can be linked to its physical and chemical properties. It has a hardness of seven on the Mohs scale which makes it very durable. It is chemically inert in contact with most substances. It has electrical properties and heat resistance that make it valuable in electronic products. Its luster, color, and diaphaneity make

it useful as a gemstone and also in the making of glass (G. Kunz, 1971). Quartz has a beneficial effect on the strength of vitrified ceramics, in conformity with the pre-stressing theory. However, the  $\alpha \rightarrow \beta$  phase transformation of quartz crystals takes place at  $\sim 573^\circ\text{C}$  during the heating-cooling process and to the relaxation of micro-stresses originated between quartz grains and the surrounding glassy phase by the differences in their thermal expansion coefficients (Singer and Singer, 1971). Similarly,  $\beta \rightarrow \alpha$  cristobalite inversion occurs at a temperature of  $225^\circ\text{C} - 250^\circ\text{C}$  similar to the quartz inversion, but produces larger volumetric change of approximately 5%. For small particle sizes, the dissolution is more rapid leaving less quartz crystals in the glass and hence yielding a low pre-stress and low strength of the material. For large particle sizes, an interconnected matrix with favorable crack path is formed leading to low strength (Carty and Senapati, 1998). Hence, quartz grain size affects bending strength in two ways, that is, directly through the induction of compressive stresses to the vitreous phase and indirectly through the development of a favorable microstructure (Stathis et al, 2004).

Quartz is a material of primary importance ; its action in ceramic pastes can be summarized as follows : its corrects the plasticity, being a non-plastic material ; it increases the whiteness of the finished product given that it normally contain only small quantities of iron and/or titanium ; it helps to vary the body's expansion coefficient ; it increases the body's vitrification temperature ; by its combinaison, in part with feldspathic glass, mullite is formed that, together with residual quartz, makes up the framework of the ceramic body that restrict its deformation during firing (E. Martini, 2017).

#### **b) Grog**

The grog is a material resulting from the high temperature heat treatment of clays ( $1000 - 1400^\circ\text{C}$ ) or from the recycling of a ceramic material already heat treated. The grog is ground and sieved according to different granular sizes of its components. It is added to clay with a well-defined percentage to give the following characteristics to the fired products (H. Boussak, 2015):

- From shaping to firing: formal stability, limitation of shrinkage, improvement of drying - During the firing process: stability

#### **I-2-3 : Fluxing materials**

These materials in general ensure the increase of the sintering interval and the decrease of the firing temperature. The main function of the flux is to form a glassy phase; then, the densification are facilitated and the firing temperature reduced. The best fluxing agent are those which allow to lower the vitrification point without lowering the melting point (H. Boussak, 2015). Among the fluxing materials, we can cite:

## a) Feldspars

### 1) Generalities

The name feldspar derives from the German Feldspat, a compound of words Feld, 'field' and Spat, "a rock that does not contain ore" (J. David, 2007). According to the Oxford English Dictionary, the change from Spat to spar was influenced by the English word spar, meaning a non-opaque mineral with good cleavage. Feldspathic refers to materials that contain feldspar, a group of closely related rock forming aluminosilicate minerals which contain varying proportions of potassium, sodium, barium and calcium. The term silicate stands for a combination of silicon and oxygen. This mineral is commonly found in igneous, sedimentary and metamorphic rocks. It is extracted from large granite formations. In geology, these formations are called plutons. Besides plutons, it is also extracted from sands and pegmatites. (Kyonka et al, 2007). Feldspar is found in different colors such as white, pink, brown, or gray. This mineral belongs to the tectosilicate group; in case of a pure mineral, each of the crystal has an uneven pattern and are found grouped together. They are opaque and have glassy luster. Some of the rocks are categorized based on their feldspar content; this fact demonstrates the significance of this mineral. The mineral feldspar can be subdivided into different classes, depending on the proportion of sodium, calcium or potassium. The color of the resulting mineral depends on its composition. The higher the sodium content, the lighter the color of the mineral; alternatively, the higher the calcium content, the more colored the mineral is.

### 2) Types of feldspar

Feldspars are basically classified into two groups by the International Union of Geological Sciences (IUGS). These two types include plagioclase and alkali. (K. Krishnan, 2018)

#### i) Plagioclase feldspar

These minerals have a triclinic structure; this classification includes: anorthite, bytownite, labradorite, andesine, oligoclase.

**Anorthite:** It is mostly found in igneous rocks and used in making ceramics and cement; it has the formula  $\text{CaAl}_2\text{Si}_2\text{O}_8$ .

**Bytownite:** This mineral is one of the rarest types of feldspar; its chemical formula is  $(\text{NaSi,CaAl})\text{AlSi}_2\text{O}_8$ .

**Labradorite:** This mineral is used in tiling, making kitchen counters and ornaments; it is represented by the chemical formula  $(Ca,Na)Al(Al,Si)Si_2O_8$ .

**Andesine:** It is used in the production of gemstones or semi-precious stones; its chemical composition can be represented by  $NaAlSi_3O_8 - CaAl_2Si_2O_8$ .

**Oligoclase:** This feldspar is used in tiling and making semi-precious stones; its chemical formula is  $(Na,Ca)(Al,Si)AlSi_2O_8$ .

### ii) Alkali feldspar

These minerals have monoclinic or a triclinic structures. They are further classified into four groups: microcline, anorthoclase, orthoclase and sanidine.

**Microcline:** these minerals have a triclinic arrangement with colors vary from mild-pink to salmon. Some of its varieties such as amazonite can be used as gemstones. The chemical formula  $KAlSi_3O_8$  represent this class of feldspar.

**Anorthoclase:** It has a triclinic formation. The general chemical formula for this class of feldspars is  $(Na,K)AlSi_3O_8$ . It is found in various colors such as yellow, green, or grayish pink.

**Orthoclase:** It has a monoclinic structure with the formula  $KAlSi_3O_8$ , these minerals are used in the manufacture of polymers, to make gemstones, and for fashion jewelry.

**Sanidine:** It has a monoclinic arrangement. This mineral is known to be stable at high temperatures. Its yellow colored variant is used to make gemstones.

### 3) Chemical Structure

The formula representing feldspar structure is  $XAl_{(1-2)} Si_{(3-2)} O_8$ . The letter 'X' represents cations elements such as calcium, sodium, or potassium. If the charge of X is +1, then the corresponding number of aluminum and silicon atoms will change to 'one' and 'three', respectively. If the charge of X is +2, then the corresponding number of aluminum and silicon atoms will change to '2' each. The mineral is said to have a tetrahedral structure, with the aluminum and silicon atoms located at the center of the tetrahedron (Krishnan, 2018).

#### 4) Properties of feldspar

##### i) Chemical Properties

Each type of feldspar has a different chemical formula, depending on its composition. The specific chemical formula for this group of compounds is **KAlSi<sub>3</sub>O<sub>8</sub> - NaAlSi<sub>3</sub>O<sub>8</sub>-CaAl<sub>2</sub>Si<sub>2</sub>O<sub>8</sub>**; these minerals are chemically inert, and have a stable value of pH.

##### ii) Physical Properties

- Feldspars have monoclinic or triclinic crystal system.
- The refractive index of this mineral is in the range 1.518 - 1.526.
- The cleavage of feldspar is two. It has two planes intersecting each other at an angle of 90°.
- The hardness of this mineral is 6 - 6.5 on the Mohs hardness scale.
- The density of this compound is 2.56 g/cm<sup>3</sup>.
- Its birefringence or double refraction is of the first order.
- They have a conchoidal or a brittle fracture.
- Its fracture can be noticed along the cleavage planes.
- These minerals have a vitreous or a pearly luster, and a white streak.
- They are not known to have any optical phenomenon.
- The specific gravity of feldspar is in the range of 2.55 to 2.76.

#### 5) Uses of feldspar

Feldspar contains alumina, which results in an increase in the strength of the manufactured product. Therefore, this mineral is used: in glass-making, as a filler agent for plastic, rubber, and paint. It is also used to make porcelain, sanitary ware, and tableware as well as making mild abrasives, latex foam, and urethane.

6) Phase diagram of the different minerals that constitute the feldspar solid solution.

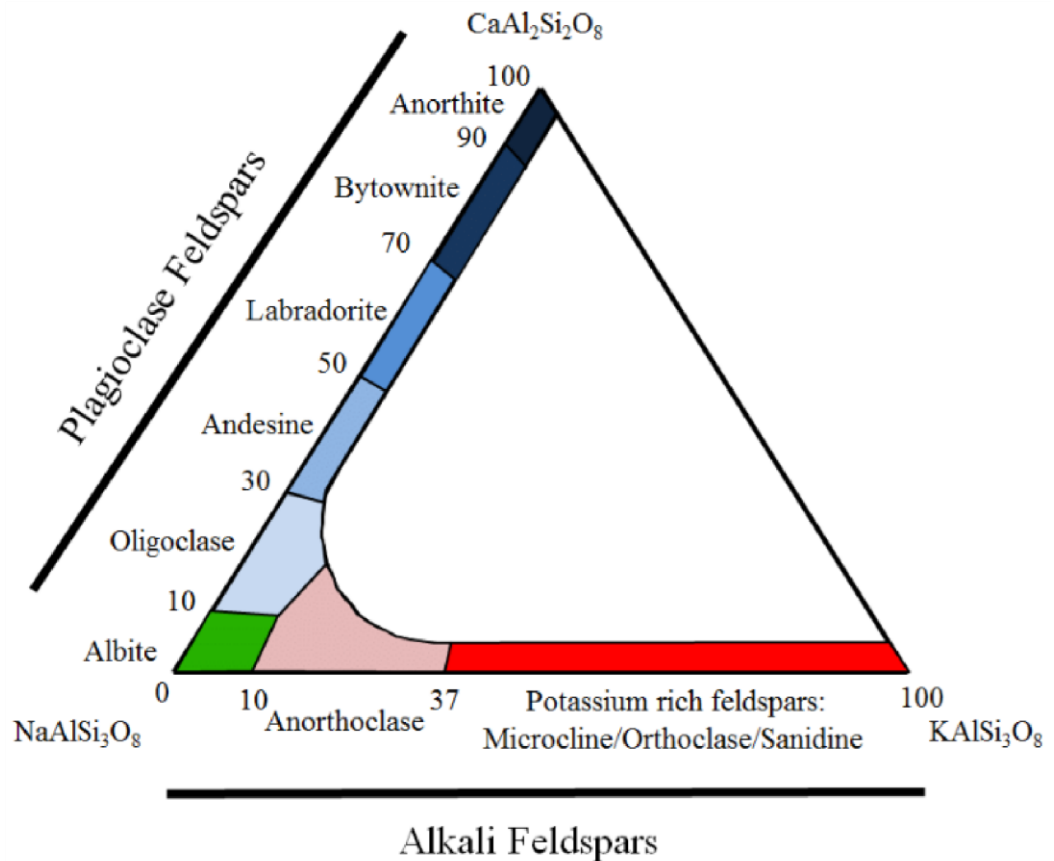


Figure 8: Phase diagram of the different minerals of feldspar solid solution (Harrison et al, 2016)

c) Limestone

i) Definition

Limestone is a sedimentary rock composed primarily of calcium carbonate ( $\text{CaCO}_3$ ) in the form of the mineral calcite. It most commonly forms in clear, warm, shallow marine waters. It is usually an organic sedimentary rock that forms from the accumulation of shell, coral, algal, and fecal debris. It can also be a chemical sedimentary rock formed by the precipitation of calcium carbonate from lake or ocean water (Folk, 1974).

Limestone is by definition a rock that contains at least 50% calcium carbonate in the form of calcite by weight. All limestone contain at least a few percent other materials as quartz, feldspar, clay minerals, pyrite, siderite and others.

ii) Limestone forming environment

Most limestone form in shallow, calm, warm marine waters. This type of environment is where organisms capable of forming calcium carbonate shells and skeletons can easily extract

the needed ingredients from ocean water. When these animals die, their shell and skeletal debris accumulate as a sediment that might be lithified into limestone. Their waste products can also contribute to the sediment mass. Limestones formed from this type of sediment are biological sedimentary rock (Trewin & Davidson, 1999). Their biological origin is often revealed in the rock by the presence of fossils.

Some limestones can form by direct precipitation of calcium carbonate from marine or fresh water. Limestones formed this way are chemical sedimentary rocks. They are thought to be less abundant than biological limestones.

Limestone can also form in cave through evaporation; droplets of water seeping down from above enter the cave through fractures or other pore spaces in the cave ceiling. Therefore, they might evaporate before falling to the cave floor. When the water evaporates, any calcium carbonate that was dissolved in the water will be deposited on the cave ceiling. Over time, this evaporative process can result in an accumulation of icicle-shaped calcium carbonate on the cave ceiling. These deposits are known as stalactites. If the droplet falls to the floor and evaporates there, a stalagmite could grow upwards from the cave floor (Patricia et al, 1996).

### iii) **Type of limestone**

There are many types of limestone based on the mode of formation, the appearance, the composition and other factors; according to Dunham, (1962). Here are some of the more commonly used varieties:

- **Chalk:** It is a soft limestone with a very fine texture that is usually white or light gray in color. It is formed mainly from the calcareous shell remains of microscopic types of marine organisms such as algae.
- **Coquina:** It is a poorly-cemented limestone that is composed mainly of broken shell debris. It often forms on beaches where wave action segregates shell fragments of similar size.
- **Fossiliferous limestone:** It is a limestone that contains obvious and abundant fossils; these are normally shell and skeletal fossils of the organisms that produced the limestone.
- **Lithographic limestone:** It is a dense limestone with a very fine and very uniform grain size that occurs in thin beds which separate easily to form a very smooth surface.
- **Oolitic limestone:** A limestone composed mainly of calcium carbonate "oolites," small spheres formed by the concentric precipitation of calcium carbonate on a sand grain or shell fragment.

- **Travertine:** is a limestone that forms by evaporative precipitation, often in a cave to produce formations such as stalactites, stalagmites and flowstone.
- **Tufa:** A limestone produced by precipitation of calcium-laden waters at a hot spring, lake shore, or other location.

#### iv) Use of limestone

Limestone is a rock with an enormous diversity of uses. It could be the one rock that is used in more ways than any other. Most limestone can be made into crushed stone and used as a construction material. It is used as a crushed stone for road base and railroad ballast. It is used as an aggregate in concrete. It is fired in a kiln with crushed shale to make cement (Kogel, 2006)

Some varieties of limestone perform well in these uses because they are strong, dense rocks with few pore spaces. These properties enable them to stand up well to abrasion and freezethaw. Although limestone does not perform as well in these uses as some of the harder silicate rocks, it is much easier to mine and does not exert the same level of wear on mining equipment, crushers, screens, and the beds of the vehicles that transport it.

Some additional but also important uses of limestone include:

- **Dimension stone:** Limestone is often cut into blocks and slabs of specific dimensions for use in construction and in architecture. It is used for facing stone, floor tiles, stair treads, window sills, and many other purposes.
- **Roofing granules:** Crushed to a fine particle size, crushed limestone is used as a weather and heat-resistant coating on asphalt-impregnated shingles and roofing. It is also used as a top coat on built-up roofs.
- **Flux stone:** Crushed limestone is used in smelting and other metal refining processes. In the heat of smelting, limestone combines with impurities and can be removed from the process as a slag.
- **Portland cement:** Limestone is heated in a kiln with shale, sand, and other materials and ground to a powder that will harden after being mixed with water.
- **Aglime:** Calcium carbonate is one of the most cost-effective acid-neutralizing agents. When crushed to sand-size or smaller particles, limestone becomes an effective material for treating acidic soils. It is widely used on farms throughout the world.



- **Lime:** If calcium carbonate ( $\text{CaCO}_3$ ) is heated at high temperature in a kiln, the products will be a release of carbon dioxide gas ( $\text{CO}_2$ ) and calcium oxide ( $\text{CaO}$ ). The calcium oxide is a powerful acid-neutralization agent. It is widely used as a soil treatment agent (faster acting than aglime) in agriculture and as an acid-neutralization agent by the chemical industry.

**Other uses of limestone:** powdered limestone is used as a filler in paper, paint, rubber, and plastics. Crushed limestone is used as a filter stone in on-site sewage disposal systems. Powdered limestone is also used as a sorbent (a substance that absorbs pollutants) at many coal-burning facilities.

v) **Crystal structure of limestone**

The principal mineral component of limestone is a crystalline form of calcium carbonate ( $\text{CaCO}_3$ ) known as calcite which belong to the trigonal crystal system as shown in figure 9 below.

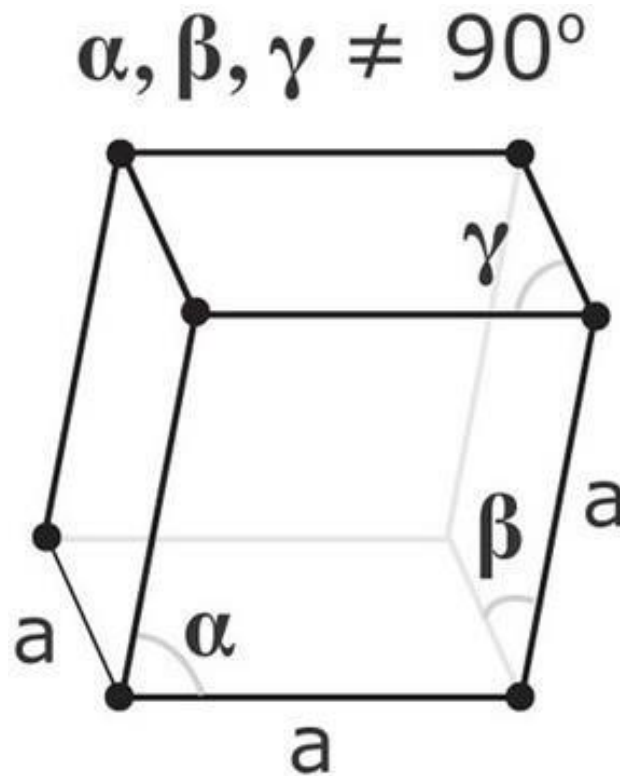


**Figure 9:** Crystal structure of calcite (Anthony et al, 2003)

#### d) Micas

##### i) Definition :

Mica is a collection of hydrous potassium, aluminium silicate minerals ; it is a kind of phyllosilicate showing a dimensional sheet or layer structure located in all three rock types : igneous, sedimentary and metamorphic (R. Dietrich, 2020).

##### ii) Chemical formula

The general formula for minerals of the mica group is  $XY_{2-3}Z_4O_{10}(OH, F)_2$  with  $X = K, Na, Ba, Ca, Cs, (H_3O), (NH_4)$ ;  $Y = Al, Mg, Fe^{2+}, Li, Cr, Mn, V, Zn$ ; and  $Z = Si, Al, Fe^{3+}, Be, Ti$ .

##### iii) Crystal structure

Micas have sheet structures whose basic units consist of two polymerized sheets of silica ( $SiO_4$ ) tetrahedrons juxtaposed with the vertices of their tetrahedrons pointing toward each other; the sheets are cross-linked with cations; for example, aluminum in muscovite and hydroxyl pairs complete the coordination of these cations. Muscovite sheets contain octahedral layers sandwiched between tetrahedral layers. Also, there are some substitutions of aluminum for silicon in the tetrahedral layers. Muscovite sheets contain octahedral layers sandwiched between tetrahedral layers; there are also some substitutions of aluminum for silicon in the tetrahedral layer. A striking difference between montmorillonite and muscovite is the absence of water molecules between layers in the mica. Instead, the space between the sheets is occupied only by potassium ions (Rickwood, 1982).

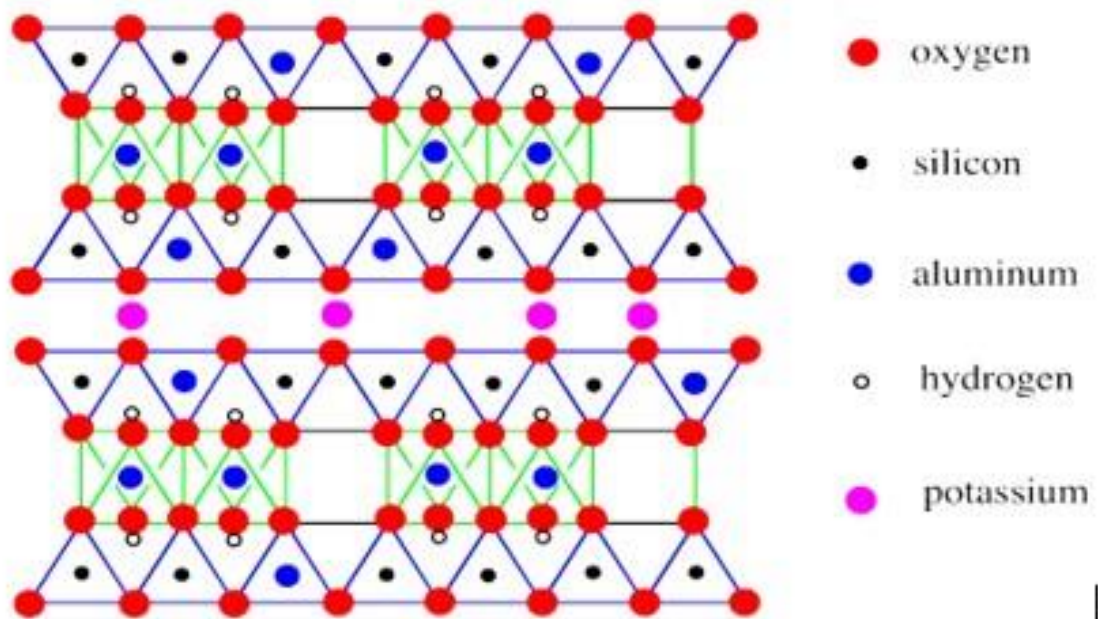


Figure 10: Crystal structure of muscovite (Anthony John et al, 1995)

#### **iv) Properties of mica group minerals**

The rock forming micas can be divided into two groups (Deer et al, 1966) :

- Those that are light coloured (muscovite, paragonite, lepidolite) and
- Those that are dark-coloured (biotite and phlogopite)

Most of the properties of the mica group with minerals other than those of glauconite can be described together as pertaining simply to micas; the main properties are:

- Perfect cleavage into thin elastic sheets
- Luster cleavage faces for most micas and pearly cleavage face for few
- The overall specific gravity for micas varies from 2.76 for muscovite to 3.2 for iron rich biotite
- Mohs hardness of the micas is approximately  $2^{1/2}$  on cleavage flakes and 4 across cleavage

#### **v) Uses of mica group minerals**

Mica is used in a variety of products ranging from drywalls, paints, fillers, especially in parts for automobiles, roofing and shingles, electronics etc (R. Dietrich, 2020).

#### **e) Nepheline syenite**

##### **i) Definition**

Nepheline syenite is a silica undersaturated igneous rock (halocrystalline rock) that consist largely on nepheline and an alkali feldspar. Nepheline syenite is a feldspathoid, a solid solution mineral that does not coexist with quartz, rather nepheline will react with quartz to produce alkali feldspar (H. Sorensen, 1974).

Silica undersaturated rocks are typically formed by low degree of partial melting in the earth's mantle. Carbon dioxide may dominate over water in source regions. Magmas of such rocks are formed in a variety of environments including continental rifts, ocean islands and supra-subduction position in subduction zones (Motoki et al, 2011). Nepheline syenite and phonolite may be derived by crystal fractionation from more mafic silica undersaturated mantle derived melts or as partial associated with igneous rocks such as carbonatite (Motoki et al, 2011).

## ii) Chemical and mineral composition

Nepheline syenite is characterized by high ratio of  $(\text{Na}_2\text{O}+\text{K}_2\text{O})/\text{SiO}_2$  and  $(\text{Na}_2\text{O}+\text{K}_2\text{O})/\text{Al}_2\text{O}_3$ , which are represented respectively by the existence of nepheline and alkaline mafic minerals. Therefore, it is geochemically classified as alkaline rock (Motoki et al, 2010). This rock has low Fe and Mg contents; its chemical formula is  $(\text{Na},\text{K})\text{AlSiO}_4$ . The main minerals of nepheline syenite are: alkali feldspar, nepheline and  $(\pm)$  clinopyroxene, amphibole and biotite. The alkaline feldspar is not potassic, but generally sodic-potassic, which is characterized by interlocking anorthoclase, called perthite.

## iii) Uses of nepheline syenite

The industrial use of nepheline syenite includes refractories, glass making, ceramics, pigments and fillers. In these applications the nepheline syenite is ground and dark minerals are carefully separated leaving a mixture of primarily feldspar and nepheline. This mixture contain higher alkali, aluminum and typically lower control in iron.

## iv) Crystal structure

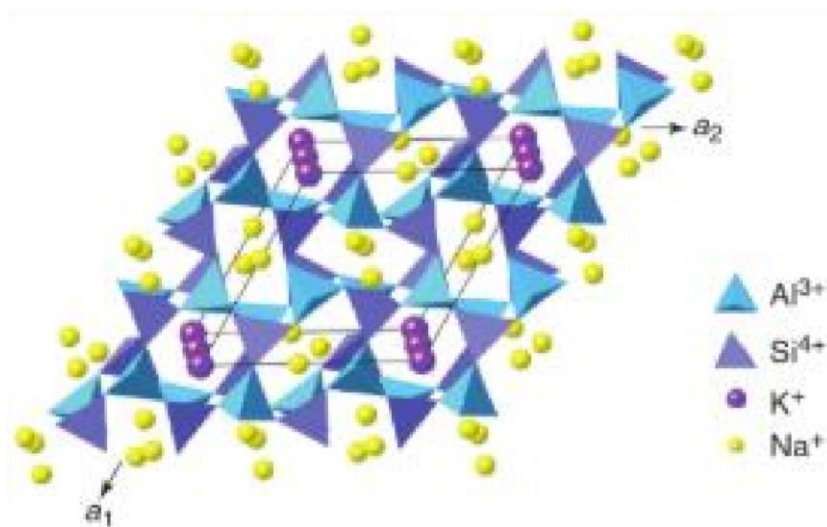


**Figure 11:** Perspective view of the Crystal structure of nepheline syenite (Cornelis et al, 2017)

NB: A primitive hexagonal unit cell is outlined. The sites in which K<sup>+</sup> are housed are nearly hexagonal in symmetry, the Na<sup>+</sup> are in more irregular sites

### **I-3: GENERAL PROPERTIES OF CERAMICS**

The properties of a material determine the field of its application; the properties of ceramic materials are dictated by the types of atoms present, the types of bonding between atoms and the atomic scale structure. In ceramic, the atoms are held together by a chemical bond; the two most common chemical bond for ceramics are covalent and ionic. Generally, materials properties are divided into physical and mechanical properties, chemical and environmental properties, thermal properties and electrical properties.

#### **I-3-1: Physical properties**

Physical properties of ceramics characterize the inalterability and the longevity of a material; they include: weight, density, permeability to liquids, gases, heat and radioactive emanation, resistance to aggressive action of the environment (A. Michot, 2008). Ceramics usually exhibit very good physical properties.

#### **I-3-2: The chemical properties**

Chemical properties of ceramics are evaluated according to the ability of the material to resist to acid, base and salts solution which can cause exchange reactions and lead to the destruction of the matter.

Ceramics generally have a very high chemical inertness and resist well to attacks by aggressive substances, to oxidation and to climatic aggressions. This character of neutral and inert materials means that they do not present a danger to man and to the nature. They are also widely used for sanitary, medical or food equipments. The ability to resist to chemical attack is called chemical inertness. Since oxide ceramics are oxidized, they are much more resistant to corrosive environments than certain metals.

#### **I-3-3: Mechanical properties**

Mechanical properties of ceramics characterize the power of the materials to resist to compression, traction, impact, penetration of foreign bodies as well as anything resulting from the application of force (F. Andreola et al, 2009). Ceramics have very high elasticity modulus and extremely limited elastic deformations. As the ceramic densities are low, their high specific moduli make them very attractive

### **I-3-4: Electrical properties:**

Ceramics are excellent electrical insulators and can be used as support elements of electric circuits. They constitute in particular insulators of high-voltage lines. Under certain conditions, such as extremely low temperatures, certain ceramics become superconductors.

### **I-3-5: Thermal properties**

When ceramics are heat treated, the clay transforms and, after cooling, it is then consists only of an amorphous phase or a mixture of an amorphous phase and crystallized phases. The often empirical choice of raw materials and the firing cycle depends on the desired use properties of the end products ; for example : low thermal conductivity, strong mechanical resistance or even certain aesthetic aspects (color). The firing of ceramic products in an industrial oven is long and requires several stages. However, since the 1970s, the reduction of firing time was a great challenge, not only for sustainability reason (reduction in storage, reduction of personnel charges, ...), but also to reduce the amount of energy used; it is then important to know the structural and microstructural transformations of raw materials during a thermal treatment, because they induce an evolution of their thermo-physical properties. However, the heat capacity determines the energy requirement for a firing process. In addition the temperature distribution in a room in steady state is controlled by thermal conductivity and in transition state by thermal diffusivity.

## **I-4: SHAPING OF CERAMICS**

Raw materials for ceramics include clay, kaolinite, aluminum oxide, silicon oxide, silicon carbide, tungsten carbide and certain pure elements. The raw materials are combined with water to form a mix that can be shaped or molded. Ceramics are difficult to work after they are made, so, usually they are shaped into their final desired forms. The form is allowed to dry and is fired in an oven called kiln. The firing process supplies the energy to form new chemical bonds in the material (vitrification) and sometime, new minerals (e.g. mullite forms from kaolin in the firing of porcelain). The first firing of a ceramic yield a product called “the bisque”; the first firing burns off organics and other volatile impurities. The second or third firing may be called glazing. Shaping of ceramics usually included: molding, pressing, extrusion, atomization.

## **I-5: DRYING OF CERAMICS**

Drying of a ceramic is the process of removing water from the ware without causing any damage; the process must be of course done efficiently and economically. There are four basic drying methods used in the ceramic industry.

### **I-5-1: Air drying or open drying**

Air drying or open drying of ceramics is a process in which, drying products are placed on shelves or on the ground outside and allow to dry on air and sun. This drying process requires a great length of time and many products are often damaged due to the inability to control drying conditions.

### **I-5-2: Air drying in a closed room**

It is a drying process which consist of confining the products in one indoor room; this process provides slightly more control over the climate conditions but still largely unregulated and numerous losses still result.

### **I-5-3: Drying in a conventional dryer.**

A conventional dryer provides sufficient speed and control to ensure efficient drying. It is either a stationary enclosed room or a continuously moving platform through an enclosed room, in which the speed and direction of the air can be controlled. In some cases, the dryer is a series heaters placed so that the product passes by them. In other cases, the dryer provides very large movements of air with a series of increasing temperatures. New dryer's models offer programmable control over both the temperature and relative air humidity.

### **I-5-4: Microwave and radio frequency drying.**

These dryers work by sending electromagnetic energy to the water molecules inside the ceramics wares which are transparent to these waves of energy; all the water inside the piece is affected. Radio frequency dryer operate on a different frequency than microwave dryers and are able to evenly excite all the water molecules throughout the ceramic so that the water migrates from the inside to the outside at a more uniform rate.

At a given air velocity and a given temperature, only so many pounds of water can be removed per hour for each square foot of exposed surface area; no matter what we change inside the piece, the water can still only leave the surface at some fixed rate. At high temperatures or high air velocities, this rate can be quite high. In fact, even in an open manufacturing room with low humidity, the speed of surface drying is so fast that even a gentle air movement is enough to cause pieces to warp before they are put into a dryer; for this reason, many manufacturers cover their ware with plastic immediately after forming to avoid the fast drying in one surface. Understanding the drying process can help manufacturers to solve drying problems and develop faster drying schedules; since each ceramic body dries differently gaining a real understanding

of drying requires both observations and measurement of the drying process on a given ceramic body.

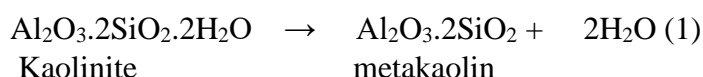
## **I-6: CERAMICS SHRINKAGE**

The study of drying must include insights into how the water leaves the compacted mass of ceramics as well as the individual clay grains. When any ceramic is wet, with or without the presence of clay, the water leaves the surface very easily; as the ceramic becomes drier, the grains of material shrink together to fill the space occupied by water. It is this shrinkage which brings the danger of damage to the ware during drying; if one side dries more than the other, pieces of ceramics will either warp or crack. As the ceramic continues to dry, it finally stops shrinking; once the shrinkage has stopped, the temperature can be increased to speed the remaining drying.

## **I-7: SINTERING OF CERAMICS**

Sintering is known as a process of creating objects from powders or particles. Ceramic sintering is a processing technique used to produce density-controlled components from ceramic powders by applying thermal energy. The basic mechanism is atomic diffusion which occurs much faster at higher temperature. Few parameters are known to affect sintering such as type of materials, particle sizes, sintering atmosphere, temperature, time and heating rate (Rahaman, 2003). During firing process, sequence of inter-crystalline (regarding a single crystalline/amorphous phase) and extra crystalline (interaction of a crystalline/amorphous phase with one another) take place. Temperature, time and atmosphere in the furnace affect chemical reactions and microstructural development of the ceramic and consequently, are important in the fired properties of the final product. The basic reaction steps can be outlined as follows:

(i) The loss of weight when kaolin is fired to temperatures exceeding about 450°C to 550°C under normal atmospheric conditions is commonly ascribed to “dehydration” and the water involved in the reaction is designated “structural water”. Neither term is correct, as the crystal lattice loses hydroxyl groups. The process is better described as “dehydroxylation” and it can be represented chemically by the equation (1).



(ii) The mechanism is most probably one of proton migration so that if two protons momentarily find themselves associated with the same oxygen ion, there is a probability that a water molecule will be formed and will detach itself. The temperature of occurrence and the



exhibition of thermal events of kaolinite generally depend upon number of variables; for example,

(a) Origin of kaolinite and its level of crystallinity, size distribution and impurities content.

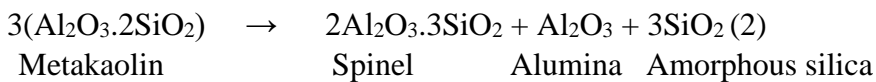
(b) DTA equipment and its sample holder, thermocouple, sensitivity, furnace and its atmosphere.

(c) Operating conditions, heating rate, sample size, packing, etc (Tarvornpanich et al, 2008).

The  $\alpha \rightarrow \beta$  phase transformation of quartz crystals takes place at  $\sim 573^\circ\text{C}$  during the heating-cooling process and to the relaxation of micro-stresses originated between quartz grains and the surrounding glassy phase by the differences in their thermal expansion coefficients ( $\alpha \sim 23 \times 10^{-6} \text{ }^\circ\text{C}^{-1}$  for quartz and  $\alpha \sim 3 \times 10^{-6} \text{ }^\circ\text{C}^{-1}$  for the glassy phases) in the  $20^\circ\text{C} - 750^\circ\text{C}$  temperature interval (Tarvornpanich et al., 2008).

(iii) The homogeneous high-temperature, mixed-alkali feldspar (sanidine) forms within  $700^\circ\text{C} - 1000^\circ\text{C}$  (Martín-Márquez et al, 2010). The formation temperature apparently is dependent on the sodium/potassium ratio.

(iv) Metakaolin transforms to a spinel-type structure and amorphous free silica at the temperature range of  $950^\circ\text{C} - 1000^\circ\text{C}$  (Sonuparlak, 1987). !!10



(v) The amorphous silica liberated during the metakaolin decomposition is highly reactive, possibly assisting eutectic melt formation at  $990^\circ\text{C}$ , as suggested by Ece and Nakagawa (2002). Carty and Senapati (1998) suggested instead that amorphous silica transforms directly to cristoballite at  $1050^\circ\text{C}$ , but the general lack of cristoballite in modern commercial porcelain ceramics suggests that the former scenario is more plausible.

(vi) Potash feldspar has been established as melting incongruently at  $1150 \pm 20^\circ\text{C}$  to form crystals of leucite ( $\text{K}_2\text{O} \cdot \text{Al}_2\text{O}_3 \cdot 4\text{SiO}_2$ ) and a viscous liquid; there is a long temperature interval during which leucite and the liquid may coexist at equilibrium (Morey and Bowen, 1922); above temperatures of  $1530^\circ\text{C}$ , the leucite crystals disappear. As a compound in the system  $\text{K}_2\text{O} - \text{Al}_2\text{O}_3 \cdot 2\text{SiO}_2$ , potash feldspar theoretically forms a binary eutectic with silica at  $990 \pm 20^\circ\text{C}$ . Soda feldspar has been found to melt congruently to a very viscous liquid at a temperature of  $1118 \pm 3^\circ\text{C}$  (Greig et al, 1937; Shairer et al, 1947). The lower liquid formation is beneficial to the

reduction of the porcelain firing temperature. The presence of feldspar can reduce the liquid formation by as around 60°C (Pérez et al, 2012).

(vii) Primary and secondary mullite formation takes place at temperature of 1075°C (Carty et al, 1998). Some studies however, indicate that the stable form of alumino-silicates is formed at a higher temperature (Carty et al, 1998).

(viii) At temperature of 1200°C, SiO<sub>2</sub>-quartz dissolution ends, and the melt becomes saturated with the silica; quartz to cristoballite transformation begins.

(ix) At 1230 °C feldspar has totally decomposed and the body is just comprised simply of mullite crystals, quartz grains and a glassy phase (Rincón, 1992).

(x) Pyroplastic deformation begins to take place as the porcelain body begins to cool, relaxation also starts within the glass phase to prevent the development of residual stresses until glass transition temperature is reached. As the body cools below the glass transition temperature, residual stresses are developed because of thermal expansion mismatch between the glass and the included crystalline phases (i.e., mullite and quartz, and in some cases, alumina and cristoballite).

(xi) On cooling, quartz inversion takes place at temperature of 573°C these results in a decrease of volume by around 2 % (Carty and Senapati, 1998).

(xii) cristoballite inversion occurs at a temperature of 225°C -250°C similar to the quartz inversion, but produces larger volumetric change of approximately 5 % (Carty and Senapati, 1998).

The figure bellow show the schematic microstructure of different sintering stages

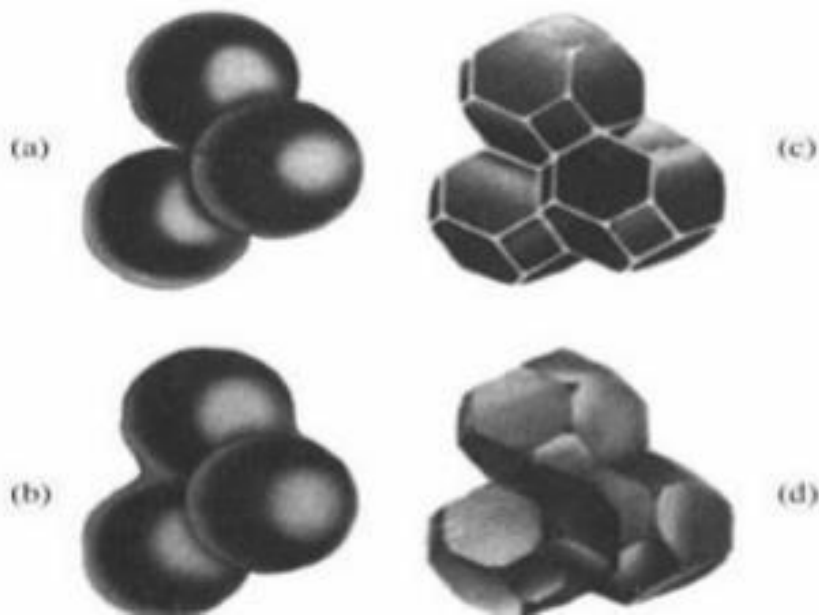


**Figure 12:** Schematic microstructures of the different sintering stages (Tulyaganov, 2005)

- (a) : formation of necks at the contact points of the powder grains
- (b) : initial stage, growth of bridges between particles
- (c) : intermediate stage, grains of polyhedral form and open porosity
- (d) : final stage, closure of porosity and grain coarsening

From physico-chemical point of view, there are three types of sintering according to the reaction which take place inside the compound (R. Calvet, 1982).

### 1- Solid phase sintering

In solid phase sintering, all the constituents remain solid during heat treatment; densification is produced by soldering and changing the shape of the grains. This sintering can therefore be single-phase to a constituent or multi-phase. From time to time, additives can be added which accelerate densification without creating a liquid phase.

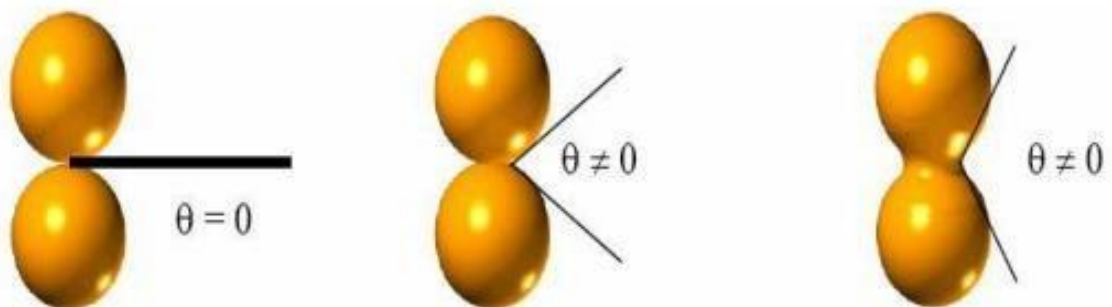


**Figure 13:** The initial stage of solid phase sintering (evolution over time) (D. Grossin, 2006)

## 2- vitrification

Vitrification corresponds to the appearance of a significant vitreous phase during firing; the quantity is then sufficient to fill the porosity. This process is widely used to densify traditional ceramics such as porcelain.

## 3- Liquid phase sintering

In liquid phase sintering, the quantity of liquid which appears is just sufficient to allow the rearrangement of the particles, to form liquid bridges between the grains and thus bring them into contact with one another. This type of sintering is also polyphase; it calls for the reaction between several chemical constituents.

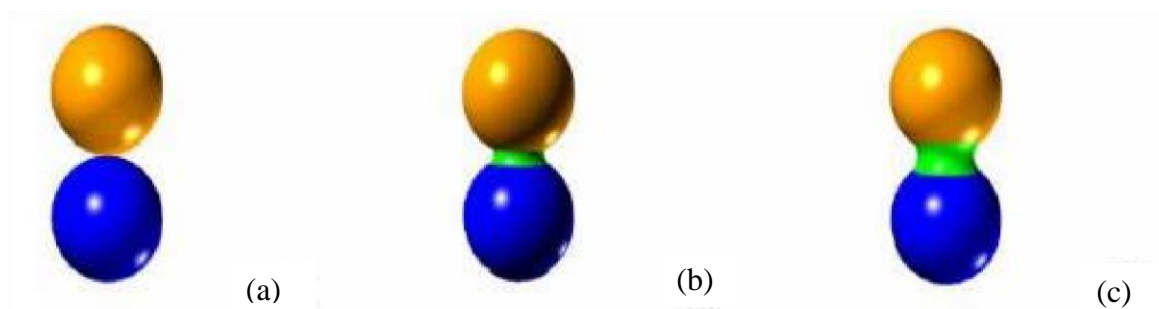


**Figure 14** : Liquid phase sintering in a eutectic point system. (D. Grossin, 2006)

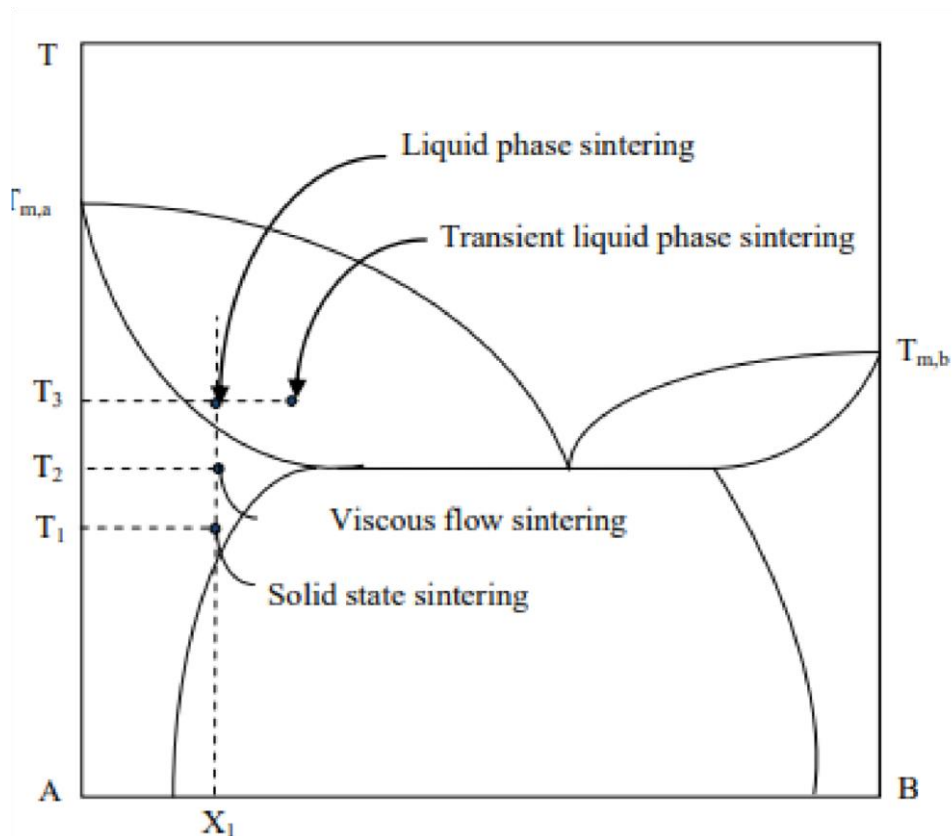


**Figure 15** : different categories of sintering in a schematic phase diagram (Hassanin, 2010)

## **I-8: SEMI-VITRIFIED CERAMICS**

### **I-8-1: Generalities**

Semi-vitrified ceramics are ceramics in which the degree of vitrification is indicated by moderate water absorption of 0.3 to 3.0 %.

Vitrification is the transformation of a substance into a glass, that is a non-crystalline amorphous solid ; vitrification is usually achieved by heating materials until they liquidize, then cooling the liquid often rapidly, so that it passes through the glass transition to form a vitrified solid. Certain chemical reactions also result in glasses. In a wider sense, the embedding of a material in a glassy matrix is also called vitrification.

In ceramics, vitrification is the progressive partial fusion of a clay or of a body as a result of a firing process. As the vitrification proceeds, the proportion of glassy bond increases and the apparent porosity of the fired product becomes progressively lower. Vitreous bodies have open porosity and may be either opaque or translucent.

### **I-8-2: Classification**

Semi-vitrified ceramics include: porcelain whiteware (hard porcelain, soft porcelain, bone china), electric porcelain, vitreous, porcelain stoneware and stoneware.

#### **a) Porcelain whiteware**

Porcelain or China is a glazed or unglazed vitreous ceramic whiteware generally made up of kaolin clay, quartz and feldspar; but can also contain ball clay, calcium carbonate, alumina, bone ash, steatites, etc, with water absorption rate less than or equal to 0.5%. Porcelain are naturally white but artificially coloured and are translucent through 4 mm thickness with glaze removed, when viewed against a 7W light. Their firing temperature are generally between 1200 and 1400° C. Structures of porcelain are great particles of stuffing (usually quartz), grain, and bond kind grasped completely by a delicate matrix, which is entirely compact, collected by the glassy phase and crystals of mullite (Andreola et al, 2002). Due to the multifaceted between raw materials, routes of processing, and the firing procedure, kinetics of the porcelains signify particular of the most ceramic systems complicate (Claussen et al, 2011). Porcelain are describe as completely vitrified, hard, impermeable (even before glazing) white or artificially colored, translucence (except considerable thickness), and resonant (Hildyard Robin, 1999). Porcelain can be divided into three main categories: hard porcelain, soft paste porcelain and bone china.

**i) Hard porcelain**

Hard-paste porcelain or true Porcelain is a ceramic material that was originally made from compound of a feldspathic rock and kaolin fired at very high temperature, usually at 1400°C (Fleming John & Hugh Honour, 1997). It was first made in China around the 7<sup>th</sup> or 8<sup>th</sup> Century. Hard porcelain are translucent and bright white ceramics; they are less likely to crack when exposed to hot liquids.

**ii) Soft paste porcelain**

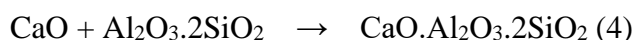
Soft paste porcelain is a type of ceramic material in pottery which does not require either high firing temperature or special mineral ingredients ; soft paste formulation containing little clay are not very plastic and shaping it on the potter's wheel is difficult. Paste with more clays are extremely plastic and can be shaped easily by method such as jollying and turning. The feldspathic formulation more resilient and suffer less pyroplastic deformation. Soft paste is fired at lower temperature than hard paste porcelain, typically around 1100°C for frit based compositions and 1200 to 1250°C for those based on feldspars or nepheline syenite as the primary flux (Queiroz & Agatholous, 2005).

**iii) Bone china**

Bone China traditional recipe is made of 50% of bone ash, 25% of kaolin and 25% of potash feldspar (Franklin, 1975). The main role of bone ash is to form crystalline phases. Its main constituent is hydroxyapatite ( $\text{Ca}(\text{OH})_2 \cdot 3\text{Ca}_2(\text{PO}_4)_2$ ) which decomposes forming calcium oxide (CaO) and  $\beta$ -tricalcium phosphate ( $\beta\text{-Ca}_3(\text{PO}_4)_2$ ) according to the following equation :



Lime released during the process rapidly reacts with dehydrated kaolinite to form anorthite according to the following equation:



Part of the phosphoric acid is consumed in the formation of  $\beta$  -tricalcium phosphate and another part acts in the formation of glass. Bone china has about 70% of crystalline phase and 30% of glass. Main qualities of bone china are whiteness, translucency, brightness, glassy quality, high flexural strength compared to other kind of porcelain (C. Portillo, 1998). Firing of bone china

demands strict process parameters control since vitrification occurs within a narrow range, about 15 to 25°C. Maximum firing temperature is critical and it lies usually between 1200 and 1250°C.

### **b) Electric Porcelain**

Electrical insulator is a material in which the electron does not flow freely or the atom of the insulator have tightly bound electrons whose internal electric charge do not flow freely; very little electric current will flow through it under the influence of an electric field. The electric insulators are used in transmission lines to support the cables and isolating them of the ground (Nzenwa et al, 2020).

Insulator used for high-voltage power transmission are made from glass, porcelain or composite polymer materials. Porcelain insulators are made from clay, quartz or alumina and feldspar and covered with a smooth glaze to shed water. Porcelain has a dielectric strength of about 4-10 kV/mm.

Nwachukwu and Lawa (2018) Investigated the Production Quality of Electrical Porcelain Insulators from Local Materials and found that, samples based on kaolin, 28%; ball clay, 10%; feldspar, 35% and quartz, 25% developed suitable insulation properties as follow : electrical resistance between  $3.52 \times 10^8 \Omega$  and  $2.05 \times 10^9 \Omega$ , dielectric constant between 8.7 and 11.4, an insulation resistance of 1.15 Giga ohms at injection of 5,000 volts, low water absorption and may be employed for usage at high frequencies

Anih (2005) elaborated and characterized electric porcelain insulator based on Nigerian raw materials: Oji River Kaolin, Abekuta feldspar and Igokoda sand; he found that electrical porcelain with good dielectric properties can be produced using locally available raw materials since it has dielectric constant below 12 and volume resistivity greater than  $10^6$  ohm cm; those insulators might be more efficient at high frequencies where the dissipation factor is correspondingly lower.

### **c) Vitreous**

Vitreous China is a vitrified or opaque ceramic, composed of a mixture of kaolin clay, ball clay, quartz and feldspar; white or naturally colored grey or brownish because of impurities in the clay used for its manufacture; normally glazed. Its water absorption rate is less than or equal to 0.5%. Vitreous are normally white or off-white and opaque through 4 mm thickness with glaze removed, when viewed against a 7W light ; their firing temperature are generally between 1150

- 1315° C. The term vitreous generally signifies less than 0.5% absorption except for floor tiles and low-voltage electrical insulators which are considered vitreous up to 3% water absorption.

#### **d) Porcelain stoneware**

The derivative of porcelain stoneware tile is a building material characterized by extraordinary technical appearances and dense microstructure (Varshneya, 2013). The main variance between porcelain stoneware and porcelain is on firing platform; therefore, extended time (some hours) procedure of firing porcelain stimulate the formation of extraordinary mullite while fired in a quicker firing progression (60-90 min) to cooling in porcelain tile associated to 24 h or further in porcelain stoneware tile, in the tiles which are into the kiln no extended than 60-90 min (Lee et al., 2011). The dissimilar process of firing indications to immense variances in the crystal-like phases percentage in the finale output and while glass and mullite comprise chief porcelain parts, which too comprises certain cristobalite, quartz, and tridymite. In porcelain tile quartz is additional rich than mullite. Greatest of the reactions happening throughout ruled kinetically firing procedures (Carty et al, 2009) which do not touch equipoise thermodynamic production of porcelain stoneware, then the series of industrial are littler than 1 hour.

#### **j) Sanitary ware**

Sanitaryware is a division of ceramic wares, made using clay, quartz and feldspar. Sanitarywares are non-porous ceramic materials fired at temperatures ranging from 1200 - 1350°C and its technology is well known and described in different textbooks and papers. However, the optimization of the sanitaryware porcelain production is still ongoing and many new works; discussing the ceramic structure or the improvement of its properties, are published every year.

Nazim Kunduraci et al, (2015) studied the effect of nepheline syenite addition on the sintering and properties of santaryware body. They found that the addition of 40% of nepheline syenite provided decreasing total shrinkage, water absorption, decrease the sintering temperature (1190°C) and helped to obtain better mechanical properties (dry and firing strength).

#### **k) Stoneware**

Stoneware is a vitreous or semi-vitreous ceramic, usually naturally colored grey or brownish because of impurities in the clay used for its manufacture; normally glazed, made from non-refractory fireclay or a combination of clays, fluxes and silica. Its water absorption rate is less than or equal to 3%. Stoneware is opaque through 4 mm thickness with glaze removed, when viewed against a 7W light. Their firing temperature are generally between 1150 and 1315° C.



## **I-9: FIRING PROCESS AND STRENGTH OF VITRIFIED AND SEMI-VITRIFIED CERAMICS**

Firing of silicate ceramics which are made of clay with high content of kaolin transforms a green body into a ceramic product; the green body exhibits significant changes of its properties resulting from dehydration, high-temperature reactions and densification during sintering (Advances in Ceramics, 2011). All these changes significantly influence mechanical properties of the fired body as well as its other physical properties. In this process, the kinetic limitations, the development of phases and the complexities of the microstructure must be considered. Generally, all the steps from raw material preparation, drying conditions and firing cycle are going to have a strong influence in the product qualities. The firing cycle influence is related to the kind of furnace, firing atmosphere, maximum temperature mould pressure and soaking time. All these parameters are related to quality and cost of the products. The work of Mattyasovszky-Zsonay (1957) is very conclusive with respect to porcelain mechanical strength; he recommended a particle diameter of quartz of 10–30  $\mu\text{m}$  and shown the influence of quartz. He disregarded the effect of mullite and explained the prestress theory. Schuller (1979) has made an analogy between quartz content and particle size explaining mechanical strength as a consequence of radial and tangential stress. Schuller found that a variation in strength occurred with a variation in quartz content. He also highlighted that the best diameter of quartz is between 15 and 30  $\mu\text{m}$ . Carty et al, (1998) examined three hypothesis: (1) mullite, (2) matrix reinforcement and (3) dispersion strengthening mechanism. They concluded that these three factors have an influence but the principal factor depends on the microstructure. The intrinsic flaw can be either a simple pore in a sample containing a glassy phase or a preexisting crack in a sample that does not contain a glassy phase. This is due to the presence of quartz and cristobalite. Kobayashi et al. (1992) found a high bending strength body containing a large amount of porosity. This body presented small pores distributed uniformly within the microstructure; the apparent porosity was zero although a high relative density was not obtained.

The influence of the flux used in the fast firing of porcelain was investigated by Mortel and Pham-Gia (1981). The author compared the properties obtained in porcelains composed of K-feldspar or Na-feldspar and concluded that they are strongly influenced by the viscosity of the glass phase during firing. The glass phase depends on the kind of flux used in the batch; Lee and Iqbal (2001), discovered different forms of mullite in typical porcelain. They are: (1) Primary mullite from decomposition of pure clay; (2) Secondary mullite from reaction of feldspar and clay, clay and quartz; (3) Tertiary mullite that may have been precipitated from alumina-rich liquid obtained by dissolution of alumina filler. They stressed the size and shape of mullite crystals is to a large extent controlled by the fluidity of the local liquid matrix from which they

precipitate, and in which they grow, which itself is a function of its temperature and composition. The composition of this local liquid was determined by the extent of mixing of the porcelain raw materials and the role of the flux is critical. Braganca et al. (2004) investigated the mechanical properties of porcelain. They reported the optimum sintering temperature for the porcelain studied was 1340°C using a heating rate of 150 °C/h and a 30 min soaking time. At this temperature the modulus of rupture and bulk density were at a maximum. The authors recorded the technical parameters summarized as: water absorption: 0.34%; apparent porosity: 0.84%, bulk density: 2.48 g/cm<sup>3</sup>; linear shrinkage: 12.2% modulus of rupture: 46 MPa. Their analysis of the technical data showed that the modulus of rupture and the bulk density were related. The authors added that the maximum strength is a result of decrease in porosity and internal flaws. Samples fired at temperatures below the ideal (1340°C) showed open porosity. According to them, above this temperature, an increasing in closed porosity occurred due to oxygen releasing and bloating. They further explained that two types of porosity caused a decrease in sample strength. For the ideal firing temperature (1340°C) they found out that the fracture toughness is  $K_{IC}=1.6 \text{ MPa m}^{1/2}$ ; the fracture energy =16.4 J/m<sup>2</sup> and crack length  $c=200 \text{ mm}$ . These parameters are good values for a fine ceramic. On the microstructural analysis Braganca et al. (2004) revealed that the ideal firing temperature occurs when the glassy phase covers the entire sample surface with sufficient time to react with crystalline phases. Higher temperatures were limited by the porosity increase. This porosity is a result of oxygen released from Fe<sub>2</sub>O<sub>3</sub> decomposition and gas expansion in the pores. Stathis (2004) asserts that filler grain size has severe impact on the mechanical and physical properties of porcelain compared to the impact of the other three factors, namely quartz content in the filler, firing temperature and soaking time that were tested. Thus, optimization efforts should be focused on this factor. According to Stathis (2004), bending strength is affected by quartz grain size in two ways, directly through the induction of compressive stresses to the vitreous phase and indirectly through the development of a favorable microstructure. He stressed that both parameters depend strongly on the particle distribution of quartz grains. He recorded the optimum quartz grain size is 5–20 µm which gives the maximum bending strength. However, he noticed that the use of coarser grain sizes results in reduced bending strength due to the development of a detrimental microstructure for the mechanical properties.

#### **I-10: Advancement of research in the field of vitrified and semi-vitrified ceramics**

Vitrified and semi-vitrified ceramics field of research has enjoyed an authentic revival due to the introduction of new technologies as: fast firing, wet grinding with spray drying, shaping with ever more powerful presses capable of producing large sizes, 3D printing (Dondi et al, 2009).

They are characterized by high technological properties such as low water absorption (<0.5%), high bending strength, resistance to chemical substances and cleaning agent (ISO/FDIS 13006, 1998) as well as exceptional aesthetics appearance. The concern regarding the reduction of energy required for the production of ceramics, the respect of the environment together with the CO<sub>2</sub> emission have stimulated research into new concept of porcelain stoneware. Following this tendency, the research carried out in ceramic materials in the last decade can be distinguished in two lines notably, the synthesis of ceramics from new raw materials and the decrease of sintering temperature (Akpınar et al, 2017); in order to fulfill the requirements, many investigations have been made on alternative raw materials and/o combination of raw materials (Editz et al, 2009).

#### **I-10-1: Decrease of sintering temperature of vitrified and semi-vitrified ceramics**

Yürüyen and Toplan (2009) studied the effect of waste glass additions on the sintering properties of fly ash in porcelain bodies between 1100 °C and 1200 °C in air. In their study, they selected a basic porcelain composition consisting of 50% kaolin, 30% potassium-feldspar and 25% quartz, and fly ash was used instead of quartz at the selected porcelain composition. This composition was very similar to the basic porcelain composition. The authors found out that, the activation energy value of the porcelain was 145 kJ/mol for a composition of 10 wt.% waste glass addition which was very close to the value of 137.618 kJ/mol as reported by Demirkiran et al. (2002). Replacement of potassium-feldspar with waste glass resulted in a reduction of the activation energy required to initiate sintering in porcelain samples. Therefore, they concluded that the densification rate could be increased; as consequence of the lower activation energy, according to them it may be possible to produce the porcelain at 1200 °C instead of 1300–1350 °C. Moreover, they noted that it may be possible to use waste glass and fly ash instead of quartz and potassium-feldspar as raw materials in porcelain compositions.

Martín-Márquez et al. (2010) studied a mixture of 50% kaolinitic clay, 40% feldspar and 10% quartz as a representative composition of commercial porcelain stoneware (PSW) tiles produced via a fast-firing process. PSW samples fired in the 500–1000 °C interval show a typical under fired ceramic microstructure comprised of clay agglomerates, feldspar particles, quartz grains and a fine matrix of clay-feldspar.

Boussak et al. (2015) characterized different formulations of porcelain tableware with (0, 5, 10 and 15 wt. % of bentonite and concluded that, the incorporation of small quantities of bentonite (10%) in raw materials represents a great potential in industrial porcelain. The bentonite plays an important role in the mechanism of various steps of firing.

The influence of bentonite increases the thermal resistance, densification and improves thermal firing cycle of the porcelain tableware. Densification was perfect and the firing cycle was short compared to the porcelain without bentonite.

Dondi et al. (1999) studied the chemical composition of porcelain stoneware tiles and its influence on microstructure and mechanical properties and found a positive correlation between mechanical strength and the alumina and mullite content of the body; another correlation was found between the bulk density, Young modulus and modulus of rupture: the higher the bulk density, the greater the value of Young modulus and modulus rupture. They also noticed that the variability of the chemical composition of porcelain stoneware reflects the different formulations of raw materials which correspond to different technology pursued by various manufactures to achieve the product requirement.

Leonelli et al. (2001) investigated on the microstructure and phase development of porcelain stoneware to determine if the addition of low cost minerals (quartz, mullite and kyanite) would improve mechanicals properties. They found that, the addition of mullite and kyanite favour the increase of flexural strength of the porcelain stoneware. Their study suggests the possibility of designing compositional variation to enhance control mechanical and properties of porcelain stoneware.

Akpinar et al.(2017) studied the effect of calcined colemanite additions on properties of hard porcelain body and found that, incorporation with 3 wt% of calcined colemanite to the hard porcelain formulations by replacing with an equivalent amount of potash feldspar and after firing at 1300 °C, resulted in improvement of mechanical strength and a gradual reduction of porosity and water absorption; furthermore, the results indicated that firing temperature giving rise to porcelain with similar technological properties decreased of about 50 °C by addition 1 wt% of calcined colemanite.

Yahya et al (2018) have designed anorthite based porcelain using Malaysian mineral resource such as ball clay, quartz, feldspar and dolomite. They reached into conclusion that the addition of dolomite into the porcelain bodies lowered the sintering temperatures; the samples containing dolomite easily formed substantial glassy phase due to the existence of magnesium element in the material used. The maximum flexural strength achieved was ~73 MPa when dolomite used was less than 10 wt. %. They meets the strength and appearance quality specifications of commercial porcelains that are available in the market.

Karamanov et al. (2005) studied the effect of fired porcelain scrap addition on the sintering behavior of hard porcelain and found that, the addition of 15% porcelain scrap reduces

the sintering interval, decreases the sintering temperature and helps to obtain better mechanical properties.

Das and Dana (2003) investigated the differences in densification behavior of K- and Na-Feldspar containing porcelain bodies. They reported that the sequence of chemical reactions during thermal heating of potash and soda-feldspar-containing triaxial porcelain compositions using DTA–TGA technique. The authors observed that both the compositions followed similar reaction steps up to 1000 °C, beyond which feldspar forms eutectic melt and starts reacting. The difference in their densification behavior has been studied using high temperature dilatometer. The soda-feldspar-containing composition exhibits maximum densification rate of 1171 °C compared to 1195 °C for the potash-feldspar-containing composition. A separate set of pressed samples heated in an electric furnace to temperatures of 1160–1200 °C showed almost similar densification behavior. The soda-feldspar containing composition achieved higher bulk density (2.43 g/cm<sup>3</sup>), lower %WA (0.07%) and highest flexural strength (53.14 MPa) at 1200°C compared to potash-feldspar-containing composition. The whiteness of potash-feldspar-containing body is poorer than soda- feldspar containing body due to increased amount of Fe<sub>2</sub>O<sub>3</sub> and TiO<sub>2</sub> impurities present in it.

Kamseu et al. (2007) have produced and characterized soft and hard porcelain with excellent technical properties from two different clays from Cameroon. From their results, they concluded that, the two clays from Cameroon are suitable as clay for porcelain bodies; according to the authors, the properties of the final products show that: Soft porcelain with low clay content and higher proportion of fluxing agent can be produced in the range of temperature of 1200–1225°C with average density of 2.4 g/cm<sup>3</sup>, water absorption less than 0.1% and flexural strength of 149 MPa. Hard porcelain bodies with higher clay content and relatively low proportion of fluxing agent can be produced in the range of temperature of 1325°C –1350°C and flexural strength of 167 MPa. They concluded that, the use of China clays with TiO<sub>2</sub> and FeO<sub>2</sub> content permits a decrease of 25°C in firing temperature. This should reduce production costs which makes its utilization very attractive, especially for tiles where the white color is not required.

Braganc et al. (2002) produced porcelain with excellent technical characteristic which had similar properties as traditional porcelain by substituting quartz with glass powder. From the results they obtained, they concluded that the use of recycled soda–lime glass powder as a fluxing agent to replace feldspar in porcelain was viable. The appropriate firing temperature for glass powder porcelain was 1240 °C and for traditional porcelain was 1340°C. Therefore they asserted, that the use of glass powder permitted a decrease of 100°C in firing temperature which means a reduction of production costs. They found out that the firing curve (water absorption, linear

shrinkage and firing temperature) shows that glass powder porcelain has a behavior typical of a strong flux. Glass powder porcelain has an advantageously low firing temperature, but a shorter sintering range compared to traditional porcelain. The authors also reported that, after firing at the appropriate temperature, the modulus of rupture and bulk density were related. They however, noted that because of a high modulus of rupture (38 MPa) and low water absorption (0.39%) glass powder porcelain attained the technical specifications of a porcelain stoneware. Similarly, the authors observed that the microstructural analysis revealed that the ideal firing temperature occurred when the glassy phase covered the entire sample surface and had sufficient time to react with the crystalline phases. They however stressed that higher temperatures were deleterious to the properties of porcelain due to an increase in porosity. The porosity was due to the release of oxygen from the decomposition of  $\text{Fe}_2\text{O}_3$  and gas expansion within the pores. The higher amount of closed porosity in glass powder porcelain explains why this porcelain did not attain a higher bulk density.

Kuzmickas et al. (2013) studied the influence of partial substitution of potash feldspar by diopside in the production of white ceramics. They investigated ceramic reactions assessed by quantitative phase analysis (X-ray diffraction - Rietveld method) and found that, the addition of only 5% of diopside by replacement of the potash feldspar permitted to obtain porcelain at lower temperatures than those used in the ceramic industry, resulting in the reduction of energy consumption. The addition of diopside partially replacing potash feldspar, reduces water absorption and porosity of the ceramic bodies, and provides higher values of flexural resistance. Diopside favors anorthite formation. Potassium feldspar favors glass and mullite formation in the ceramic bodies. Cordierite could be favored by increased MgO content of the system.

#### **I-10-2: Investigation on alternative raw material for semi-vitrified ceramics**

Taskirana et al, (2004) formulated a new ceramic composition based on anorthite ( $\text{CaO}\cdot\text{Al}_2\text{O}_3\cdot 2\text{SiO}_2$ ) crystal formation, with a mixture of wollastonite, alumina, quartz, magnesia and Ukrainian ball clay as raw materials. They found that, all the technological properties of the porcelain material such as whiteness, water absorption ( $\sim 0\%$ ), bulk density ( $2.40 \text{ g/cm}^3$ ), thermal expansion coefficient ( $\sim 5.1 \times 10^{-6} \text{ }^\circ\text{C}^{-1}$ ) and the flexural strength (110 Mpa) of the designed material are significantly better than the properties of the conventional porcelain stoneware.

Mukhopadhyay et al. (2003) studied the effect of a talc addition on the thermo mechanical properties and microstructure of stoneware and found that, the addition of 3% talc resulted in an increase in flexural strength and relative density, and a decrease in water absorption value.

Galán-Arboledas and Bueno (2015) have used a selection of inorganic industrial waste (screen glass, steelworks ashes, coal power plant ashes, biomass power plant ash and sludge from cutting marble industry) and a waste with organic fraction (diatomaceous earth from oil filtration) to produce ceramics. The ternary phase equilibrium diagram  $\text{SiO}_2\text{-Al}_2\text{O}_3\text{CaO}$  was used to formulate mixtures with a chemical composition similar to that of ceramic building materials used by the ceramic industry of Bailén to manufacture structural bricks. Technological properties of the some elaborated materials as: Bulk density ( $1.75\text{-}1.90\text{ g/cm}^3$ ), water absorption (12-18%) and bending strength ( $50\text{-}150\text{ kg/cm}^2$ ) are within the range of normal values for ceramic construction materials.

Cicek et al, (2018) valorized boron mining waste in the production of floor and wall tiles. In floor tiles production, developed compositions containing 5.66 wt% waste showed  $65^\circ\text{C}$  lower sintering temperature than the standard production. The corresponding sintering shrinkage (6.8%), colour values (L: 57.00, a: 2.52b: 11.02) and water absorption values (0.49%) were within acceptable industrial standards. In wall tile compositions containing 5.64 wt% of boron waste, the sintering temperature was decreased by  $70^\circ\text{C}$ . Further, samples had acceptable sintering shrinkage (0.6%), colour values (L: 77.00, a: 7.7b: 17.57), water absorption (19.39%) and strength ( $20.46\text{ N/mm}^2$ ) properties, meeting the requirements of the ceramic tile industry. The fluxing effect of  $\text{B}_2\text{O}_3$  current in wastes provide liquid phase at lower temperatures, thus promoting viscous sintering below the industrial sintering temperatures, providing the expected final characteristics.

Chitwaree et al, (2018) made a study that aimed to compare the energy consumption during sintering process of the porcelain stoneware tile in which recycled glass and pottery stone were used in substitution of clay, feldspar and quartz. The vitrified tiles with 50% pottery stone and 50% recycled glass have been used to produce low temperature vitrified ceramic tiles at sintering temperature of  $1050^\circ\text{C}$ . The properties are in compliance with the standards. However, whiteness and strength are little inferior when compared with the high quality commercial vitrified tiles. The merits of the low sintering temperature are thermal energy saving of 30% and the lower  $\text{CO}_2$  emission of about  $0.0350\text{ kg CO}_2\text{eq/kg product}$ .

## **CHAPTER II: MATERIALS AND METHODS**



The methodology is fundamental for any scientific study. It provides a brief presentation of materials used and information on the equipments, the method that was necessary for the completion of the work ‘Use of  $K_2O/CaO$  based compound to improve the sintering behavior and properties of sustainable semi-vitrified products’.

### II-1: MATERIALS

The porcelain stoneware composition took as reference (Table 2) was considered as aggregates of oxides and we used pegmatite from Manjo (FMj), the kaolinitic clay from Mankon (Mile 9) and quartz to introduce the various oxides required in the compositions P ; in the same way, Pegmatite from Boboyo (Fb), the kaolinitic clay from Mankon, quartz were used to introduce the required oxides for the composition C; Nepheline syenite as fluxing agent combine with former mention materials are used to build the composition G. Limestone was used in all compositions to adjust the CaO content.

#### II-1-1: Clay material

The clay material was collected from Mile 9, Mankon Sub-Division in the Nord-West Region of Cameroon; it lies on the central part of the Cameroon Volcanic Line, between Bamboutos Mountain to the south and the Adamawa plateau to the North East (Nzeukou et al, 2018). A high relief, cool temperature, heavy rainfall and savannah vegetation characterize this area. The geomorphological features range from mountain terraces, vertically rising volcanic plugs with steep slopes, straight and rectilinear crests of multiple forms, broad-bottomed valleys, straights and elongated and round hills (Hawkins & Brunt, 1965; Afungang, 2015).

The sampling area is located at  $N6^{\circ}1'45.1''$  and  $E10^{\circ}7'17.04''$ . Sample collected is a kaolin which outcrop along road side on the hill trench; its colors vary from light grey (7, 5R 8/0) to white (10YR 8/2).

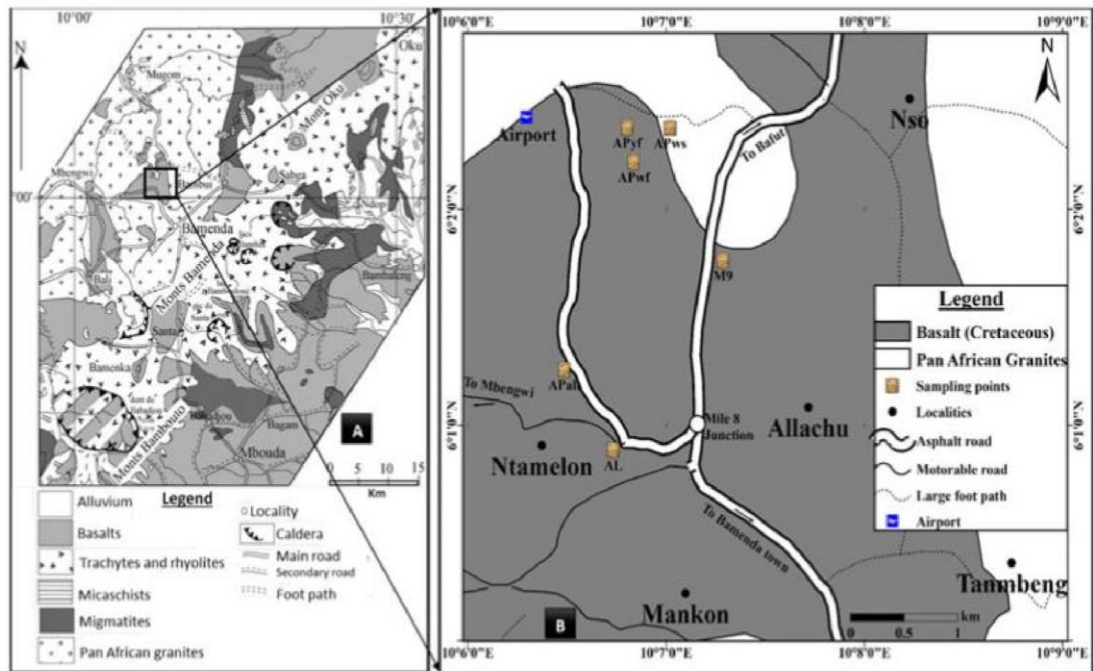


**Figure 16:** Geological map of the North-West Region including the study area. (modified from Nzeukou et al, 2018 which is a modification of Kamgang et al, 2008).

## II-1-2: Feldspar materials

In this research work, we have used three feldspar materials which are all pegmatites; two samples have been collected in Boboyo (FBb1 and FBb2), another one in Manjo (FMj) and the nepheline syenite (NPH) have been collected in Eboundja.

Boboyo is located in the Far-North Region of Cameroon, in Kaele sub-division. It belongs to the vast sedimentary basin of the end tertiary area to the quaternary of the basin of Chad. Two geological formations occupy most of the area: the granito-gneissic base and the alluvia; elsewhere, we observed various formations dispersed in the base area: sedimentary basins, metamorphic series, basics rocks and recent alluvia covering a surface lower than 20% (Ngounou Ngatcha et al, 2006). The granite-gneissic base occurs from the North Region in the line linking Kaele to Mora and was highlighted by geophysists. Samples were collected in an old carrier that was used for civil engineering work. Samples are pink in color characteristic of orthoclase feldspars.

Manjo is located in the Littoral Region of Cameroon, in Mounjo subdivision; it is located in the extension of the mountain ranges of West Cameroon. The sample describe is a pegmatite. The term pegmatite is used to identify coarse plutonics rocks with irregularity of grains. It is defined as an intrusive halocrystalline rock composed essentially of rock-making minerals which

are developed mostly with larger grains than the same minerals occurring in the normal plutonic condition: aggregation of perthite, albite, muscovite and quartz. The perthite is essentially orthoclase and the muscovite has potassium as the alkali cation. Pegmatite is a solid solution with the composition near to the system  $\text{KAlSi}_3\text{O}_8\text{-NaAlSi}_3\text{O}_8\text{-SiO}_2\text{-H}_2\text{O}$ . The sample under study presented a  $\text{K}_2\text{O}/\text{Na}_2\text{O}$  molar ratio of 3.54 largely above many of the pegmatite minerals described in Cameroon (Elimbi et al, 2005, Njoya et al, 2010).

### **II-1-3: Nepheline syenite of Eboudja**

The sampling area is located at Eboudja in South Region of Cameroon; this is a part of a geological Unit called 'Nyong Unit' that has been restructured by a metamorphic event. This restructuration was accompanied by the formation of magmatic rocks from which charnockites and an assembly of basics and ultrabasic rocks were derived (Koumetio et al, 2012); among these basic rocks is nepheline syenite.

Nepheline syenite is a silica undersaturated igneous rock (halocrystalline rock) that consist largely on nepheline and an alkali feldspar. Nepheline is a feldspathoid, a solid solution mineral that does not coexist with quartz, rather nepheline would react with quartz to produce alkali-feldspar. The microscopic color of nepheline syenite is grey being little darker than granite. The rock is generally equigranular, equidirectionnal and gross with grain size of 2 cm to 5 cm length and 5 mm to 2 cm thickness.

### **II-1-4: Limestone of Figuil**

Limestone is a sedimentary rock formed predominantly on the sea floor where material rich in calcium carbonate (calcareous materials) accumulates; its major materials are the minerals calcite and aragonite which are different crystal forms of calcium carbonate ( $\text{CaCO}_3$ ). Most limestones are composed of grains as many other sedimentary rocks; most of those grains are skeletal fragments of marine organism which secrete shells made of aragonite or calcite (Dunham, 1962). Some limestones do not consist of grain at all, and are formed completely by chemical precipitation of calcite or aragonite; this secondary calcite may be deposited by super saturated meteoric water (groundwater that saturated material in caves). This is probably the case of Figuil's limestone deposit that has been used in this research work. Figuil limestone deposit is an old sedimentary basin dating from at least 700 million years and was metamorphosed in the amphibolite facies with green schist towards 620 million years during the panafrican orogenesis. Two main companies are exploiting the carrier: CIMENCAM for the manufacturing of Portland cement and Roccario for the fabrication of tiles (marble's tiles) and lime. The sample collected

are solid wastes of these exploitations. Figuil is located in the Mayo-Louti division of the North Region of Cameroon.

### **II-1-5: Quartz**

Quartz is a mineral composed of silicon and oxygen atom in a continuous framework of SiO<sub>4</sub> silicon–oxygen tetrahedra with each oxygen being shared between two tetrahedral, giving an overall chemical formula of SiO<sub>2</sub>. Quartz is among the most common mineral in many rocks; it is found in many metamorphic, sedimentary and igneous rocks that have high silica content. Quartz is a chemically an almost inert and passive substance at the surface. Quartz is a very active agent under conditions deep within the earth's crust. At higher temperatures and pressures, it participates in many complex chemical reactions during rock and mineral formation. In ceramics, it is used as a network former compound and a flux agent at high temperature. In this work, we have used quartz mineral collected in some fine sand deposit in Yaounde main area.

## **II-2: RAW MATERIALS PREPARATION AND SAMPLES ELABORATION**

### **II-2-1: Raw materials preparation**

Clay as collected in the field was air dried for few days and then dried inside an oven at 105°C for 24 hours ; it was then ground inside a ball mill and sieved at 125µm. Hard materials as feldspar, quartz and limestone are first of all crushed, washed, dried inside a laboratory oven for 24h and then ground and sieved at 125µm.

### **II-2-2: Sample elaboration**

Various proportions of materials for different formulations (B, G and P, C) were weighed on a precise electronic scale. The mixes were dry milled for about 30 minutes and then wet milled with 85 mass percent of water for 3 hours with a fast rotating ball mill (1500 rpm). With these conditions, all the particles had sizes lower than 45 µm. The milled slurries were dried at room temperature down to 15 wt. % water. The granules were uni-axially pressed at 5 tons with a standard laboratory hydraulic press (SPECAC, 0-25 tons). Molded samples were in the form of cylinder having an average thickness of  $6.8 \pm 0.05$  mm and  $30 \pm 0.10$  mm of diameter. The various samples were fired in an electric furnace at 1125, 1150, 1175, 1200 and 1225°C. Temperatures of 1250 and 1300°C were applied for reference samples.

Investigation in order to determine the best soaking time combining with better sintering rate.

## **II-3: METHOD OF CHARACTERIZATION**

When used materials, characterization refers to the broad and general process by which a material's structure and properties are probed and measured. It is a fundamental process in the field of materials science without which, no scientific understanding engineering material could be ascertained (J. Kepler, 1611)

### **II-3-1: Chemical analysis**

The chemical analysis of materials were performed by XRF. The use of primary X-Ray beam to excite fluorescent radiation from sample was first proposed by Glocker and Schreiber in 1928 (Buhrke et al, 1998). Today, the method is used as a non-destructive analytical technique and as a process control tool in many extractive processing industries. X-ray fluorescence (XRF) is the emission of characteristic 'secondary' (or fluorescence) X-ray from materials that has been excited by bombarded with high-energy X-Ray. The phenomenon is widely used for elemental analysis and chemical analysis particularly in the investigation of metals, glass, ceramics, building materials and for research in geochemistry, forensic science, archaeology and art objects such as painting and murals (E. Bertin, 1996). The chemical analysis of raw materials and selected samples have been performed with X sequential XRF equipment (ARL) in the laboratory of Petrology, geochemistry and petro physics of Liege's University, Belgium.

### **II-3-2: Structural characterization methods**

The structural characterization method used was the mineralogical analysis by X-ray diffraction. X-Ray diffraction is a non-destructive analytical technique which reveal information on the crystal structure, the mineralogical composition and the properties of materials. This technique is based on observing the scattered density of an X-ray beam hitting a sample as function of incident and scattered angle, polarization and wavelength or energy.

The mineralogical compositions of raw materials and semi-vitrified ceramics were analyzed by XRD using a Rigaku DMAX III 4057A2 diffractometer, working at 40 kV and 30mA (Cu K $\alpha$ : 1.542 Å). All data were collected in the 2 $\theta$  range 10–60°, with a step size of 0.03° and a dwell time of 10s step 1.

### **II-3-3: Microstructural analytical methods**

#### ***a) Granulometry test***

This test was performed on the kaolinitic clay of Mankon, mile 9. It makes it possible to determine the respective weight percentages of the different families of particles constituting the

kaolin. In the laboratory, two tests make it possible to establish the granulometry of clay materials: wet sieving granulometry and sedimentometry (Chamayou et al, 1989).

**(i) The particle size test by sieving:**

It consists in separating the different fractions and evaluating them in weight percent of the whole sample according to the following protocol: each clay material is first dried in the open air, then dried at 105 ° C for twenty-four hours (24h). Subsequently, four hundred grams (400g) of material are weighed, soaked in water for twenty-four hours and then passed through a sieve column: 2 and 1.6 mm, thereafter 500, 400, 100 and 80µm. After several washes, the sieves containing the refusals are dried in an oven for twenty-four hours at 105 °C; the different fractions are calculated by weighing. Finally, the proportion of particles smaller than 80µm is used to perform particle size analysis by sedimentometry

**(ii) Particle size analysis by sedimentometry**

Sedimentometry is applied as a result of the dry particle analysis. A test sample of 40 g of fine fraction (less than or equal to 0.08 mm) is first subjected to deflocculation (10 g of deflocculant) in a solution of 440 ml of distilled water and 60 ml of a solution of 5% deflocculating sodium hexametaphosphate for about 15 hours. The mixture is then stirred for at least 3 minutes for complete deflocculation. Then, it is poured into a glass test tube. The adjustment to 1 liter is done with the rinse water. The whole rigorously undergoes homogenization using the manual stirrer for a few minutes. The solution is then subjected to settle the test tube during which it decants according to the Stokes law. The values of the densimeter and the thermometer are read after 30s, 1mn, 2mn, 10mn, 20mn, 40mn, 80mn, 2h, 4h, 24h and carried on a card designed for this purpose. These values make it possible to calculate the equivalent diameter of the grains remaining in solution at each instant and their percentage in order to construct the corresponding sedimentometric curves. Equations 4 and 5 of Costet and Sanglerat (1969) make it possible to calculate the diameters and these percentages.

$$Q(\%) = \frac{V.Y_s.Y_w}{p(Y_s - Y_w)} (r - 1) \quad (4) \qquad \phi = \sqrt{\frac{18\eta H}{(Y_s - Y_w)t}} \quad (5)$$

Q = weight percentage of grains remaining in solution at time t

- V = suspension volume

- t = time in second

**(iii) Atterberg limits**

The Atterberg limits are summarized in the determination of the liquidity limit (WL), the plasticity limit (WP) and the plasticity index (IP) according to the French norm (NF P 94-051, 1993).

➤ **Liquidity limit**

It corresponds to the water content necessary for the closure of a groove of one centimeter in length after about twenty-five shocks (Casagrande apparatus).

The material is washed with a mesh screen of 400 μm and then stored for 24 hours in water. After settling, it is spread on a plasterboard for drying and homogenization on the marble plate before being placed in the Casagrande apparatus where a groove is dug in the cup containing the sample. The crank is rotated at a speed of 2 shocks per second until the groove closes to one centimeter. Successive tests are carried out by allowing the water to evaporate gradually. The method is such that the number of impacts is between 15 and 35 for five attempts. The curve is constructed with ordinate the values of the water content and on the abscissa the logarithm of the number of hits and the line is drawn. The liquidity limit (WL) is given by the ordinate of the point corresponding to 25 strokes. It is also given by the formula (4) of the French standard

$$WL = \omega \left(\frac{N}{25}\right)^{0.121} \quad (6)$$

$\omega$  = water content

N = number of shots

➤ **Plasticity limit**

It is the water content for which a cylindrical roll of 10 to 15 cm breaks into segments varying from 3 to 10 mm. Thus, the paste of the material used for the last liquid limit test is used.

The kaolinitic clay paste from the last liquid limit test is lightly dried on the plaster. Then, a ball of about 12 mm in diameter was formed which was used to make a cylinder of about 10 to 15 cm with 3 mm in diameter rolling on a flat surface (marble plate), dry, clean and nonabsorbent.

➤ **Plasticity index**

It indicates the interval in which the clay material is workable. Its equation, (7) is given by the difference between the liquidity limit and the plasticity limit.

$$IP = WL - WP \quad (7)$$

**Table 2:** Classification of materials according to the plasticity index (NF P 94-051, 1993)

Plasticity index	State of the material
0-5	Not plastic
5-15	Little plastic
15-40	Plastic
>40	Very plastic

**b) Pores size distribution**

The pore size distribution is a quantitative description of the range of the pores size present in a given sample; it is the dependence of the quantity (volume, mass) of pores on their size in the material, as well as the curves (histogram) which describe this dependence. Size distribution reflect the dispersion of a system; when the distribution curve have the form of a sharp peak with a narrow base, it mean that pores has almost the same size, this is a monodisperse system; when the distribution curves have broad peaks with no well-defined maxima, we have polydisperse system. In the presence of two or more clearly defined peaks, the distribution is bimodal and polymodal respectively.

The Mercury Intrusion Porosimeter (MIP) used was an Autopore IV - 9500 which is a 33000 psia (228 MPa) MIP covering the pore diameter range from approximately 360 to 0.005 $\mu$ m having two low-pressure ports and one high-pressure chamber. Pieces collected from the mechanical test were used to prepare specimens of  $\sim 1 \text{ cm}^3$  of volume for the MIP. The sample is weighed and a file is created in which its characteristics are recorded together with the analysis conditions and other parameters for the analysis. The measurement include two steps: one with low-pressure done with a penetrometer from 0 to 50 psia (345 kpa), resolution 0.01psi, pore diameter 360 to 3.6  $\mu$ m and transducer accuracy of  $\pm 1$  of full scale and the second with high-pressure from atmospheric pressure to 33000 psia (228 MPa), resolution 0.2 psi from 3000 psia to 33000 psia and 0.1 psi from the atmospheric pressure to 3000 psia, pore diameter 6 to 0.005 $\mu$ m and transducer accuracy of  $\pm 1$  of full scale. When the sample information, analysis conditions, penetrometer properties, report options are set, the data portion of the sample file is created automatically by the Autopore software. Mercury porosimetry is based on the capillary law governing liquid penetration into small pores. This law, in the case of a non-wetting liquid like mercury and cylindrical pores, is expressed by the Washburn equation:



$$D = -\left(\frac{1}{p}\right) 4\gamma \cos\phi \quad (8)$$

Where,  $D$  is pore diameter,  $p$  the applied pressure,  $\gamma$  the surface tension, and  $\phi$  the contact angle, all in consistent units. The volume of mercury  $V$  penetrating the pores is measured directly as a function of applied pressure. This P-V information serves as a unique characterization of pore structure. Pores are rarely cylindrical, hence the above equation constitutes a special model. Such a model may not best represent pores in actual materials, but its use is generally accepted as the practical means for treating what, otherwise, would be a more complex problem. The surface tension of mercury varies with purity; it's usually accepted value and the value recommended here is 485 dynes/cm. The contact angle between mercury and the solid containing the pores varies somewhat with solid composition. A value of 130 degrees is recommended in the absence of specific information to the contrary.

Mercury extruding from pores upon reduction of pressure is in general accord with the above equation, but indicated pore diameters are always offset toward larger diameters. This result from equivalent volumes of mercury extruding at pressures lower than those at which the pores were intruded. It is also commonly observed that actual pores always trap mercury. The first phenomena is usually attributed to receding contact angles being less than advancing ones. The second is likely due to pore irregularities giving rise to enlarged chambers and “inkwell” structures. These phenomena give rise to hysteresis phenomena, i.e., distinct intrusion and extrusion P-V curves.

### c) Apparent density and open pores volumes

These experiments have been conducted based on Archimedes' method according to American Standard ASTM 373- 88. The principle, scope and procedure are same with water absorption; the calculation are as follow:

- The volumes of open pores  $V_{OP}$  and impervious portions  $V_{IP}$  in cubic centimeters were calculated as follows:  $V_{OP} = M - D$  (9)

$$V_{IP} = D - S \quad (10)$$

- The apparent porosity,  $P$ , expresses as a percent, the relationship of the volume of the open pores of the specimen to its exterior volume; it was calculated as follows:

$$P = [(M - D)/V] \times 100 \quad (11)$$

Where  $V$  is the exterior volume, in cubic centimeters:  $V = M - S$ ;  $M$  is the saturated mass;  $D$  is the dry mass and  $S$ , the impregnate mass of the specimen.

#### **d) Scanning Electron Microscopy**

Scanning electron Microscopy is a category of characterization techniques which probe and map the surface and sub-surface structure of a material. These techniques can use photons, electrons, ions or physical cantilever probes to gather data about a sample's structure on the range of length scales.

The microstructure of the fired samples was analyzed by Scanning Electron Microscopy (SEM). Fresh fractures surfaces from the mechanical test were used for the surface observation. Some of these pieces were polished using diamond paste after grinding with silicon carbide powders and water. The polished surfaces were etched for 1 min in 4% HF-1% HNO<sub>3</sub> solution and then gold coated after washing with acetone. The scanning electron microscope is equipped with EDS detector (operating at 20 kV) was used for microstructural examination of the specimens with secondary electron images (SEI) and back scattering images (BSI). Microanalysis for phase identification and distribution was performed using the embedded EDS digital controller and control software. The model, Jeol-JSM5500, available in the Laboratory of Ceramics and Glass of the University of Trento in Italy was used to analyze our fired samples.

#### **II-3-4: Methods of Thermal Behavior Analysis**

Thermal analysis of raw materials and sample's formulation have been studied through Differential Thermal Analysis (DTA), Thermal Gravimetry Analysis (TG), Differential Scanning Calorimetry (DSC) and Thermal Expansion Analysis.

##### **a) Differential Thermal Analysis**

The differential thermal analysis is a thermo-analytical technique used to detect changes in the samples during a thermal cycle (cooling or heating program). The DTA curve provides data on the transformation that have occurred such as: glass transition, crystallization, melting or sublimation. Differential Thermal and Thermo gravimetric analysis (DTA/TGA) of green samples were performed using a Standard thermal analysis instrument (model DTA409, NETZSCH, Germany) consisting of a sample holder, thermocouples, sample containers and a ceramic block; a furnace; a temperature programmer and a recording system. The analysis was carried out with a heating rate of 10 °C/min up to 1300 °C under nitrogen atmosphere. 100 mg of raw powder sample was used for each analysis in alumina crucible. The calibration of the DTA/TG is done with the Calcium Oxalate standard. Calcium oxalate Monohydrate (CaC<sub>2</sub>O<sub>4</sub>.H<sub>2</sub>O) undergoes three specific weight losses at precise temperature; those temperature are well separate from each other to easily identify each of the three decomposition products ;

these reactions are clearly identified true DTA by two endothermic peaks at ~ 200°C and ~ 800°C respectively and an exothermic peak at ~ 500°C.

#### ***b) Thermal Gravimetry Analysis (TG)***

Thermal Gravimetric Analysis (TG) is a thermo analytical technique used to measure the amount of weight change of a material, either as a function of increasing temperature, or isothermally as a function of time, in an atmosphere of nitrogen, helium, air and other gases or in vacuum.

##### **➤ *Other application of TG analysis***

- Determines temperature and weight change of decomposition reactions, which often allows quantitative composition analysis.
- May be used to determine water content or the residual solvents in a material.
- Allows analysis of reactions with air, oxygen, or other reactive gases
- Can be used to measure evaporation rates as a function of temperature, such as to measure the volatile emissions of liquid mixtures.
- Allows determination of Curie temperatures of magnetic transitions by measuring the temperature at which the force exerted by a nearby magnet disappears on heating or reappears on cooling.
- Helps to identify plastics and organic materials by measuring the temperature of bond scissions in inert atmospheres or of oxidation in air or oxygen.
- Used to measure the weight of fiberglass and inorganic fill materials in plastics, laminates, paints, primers, and composite materials by burning off the polymer resin. The fill material can then be identified by XPS and/or microscopy. The fill material may be carbon black, TiO<sub>2</sub>, CaCO<sub>3</sub>, MgCO<sub>3</sub>, Al<sub>2</sub>O<sub>3</sub>, Al(OH)<sub>3</sub>, Mg(OH)<sub>2</sub>, talc, Kaolin clay, or silica, for instance.
- Can measure the fill materials added to some foods, such as silica gels, cellulose, calcium carbonate, and titanium dioxide.
- Can determine the purity of a mineral, inorganic compound, or organic material.
- Distinguishes different mineral compositions from broad mineral types, such as borax, boric acid, and silica gels.

Standard thermal analysis instrument (model DTA409, NETZSCH-Germany) was used for carrying out the Differential Thermal and Thermo gravimetric analysis (DTA/TG) of samples. The analysis was carried out using a heating rate of 10 °C/min up to 1250°C.

### *c) Sintering measurement*

A hot stage microscope (Expert System Solutions, HSM; 20°-1600°C) was used to follow up the behavior of the pressed powers (finely ground to < 45 μm, in the form of cylinders with 2 mm diameter and 3 mm height) step by step during heating from room temperature up to fusion with an heating rate of 10°C/min. Samples were located on platinum plates as samples holders. The Camera coupled with hot stage microscope collects images of the sample under analysis with intervals of 2°C and the variation of the sample (height) is automatically stored by a software as measure of the sinterization.

### *d) Differential Scanning Calorimetry (DSC)*

Differential Scanning Calorimetry (DSC) is a thermoanalytical technique in which the difference in amount of heat required to increase the temperature of a sample and the reference is measured as function of temperature. The basic principle underlying this technique is that when the sample undergoes a physical transformation such as phases transitions, more or less heat will need to flow to it than the reference to maintain both at the same temperature. Whether less or more heat must flow to the sample depends on whether the process is exothermic or endothermic. For example, as a solid sample melts to a liquid, it will require more heat flowing to the sample to increase its temperature at the same rate as the reference. This is due to the absorption of heat by the sample as it undergoes the endothermic phase transition from solid to liquid. Likewise, as the sample undergoes exothermic processes (such as crystallization) less heat is required to raise the sample temperature. By observing the difference in heat flow between the sample and reference, differential scanning calorimeters are able to measure the amount of heat absorbed or released during such transitions. DSC may also be used to observe more subtle physical changes, such as glass transition. It is widely used in industrial settings as a quality control instrument due to its applicability in evaluating sample purity and for studying polymer curing (Dean, 1995 ; Pungor, 1995). Differential scanning calorimetry can be used to measure a number of characteristic properties of a sample as well as : fusion, crystallization, glass transition and oxidation (O'Neill, 1964)

### *e) Dilatometry test*

The Differential behavior of samples was measured using a dilatometer (L75HS 1600, Linseis, Germany) with a heating rate of 10 °C/min in the temperature range 30–1300 °C. The analysis was carried out on specimens with nominal dimensions of 5×5×15mm<sup>3</sup>, enough to allow

the alumina pushrod to exert some force on the top of the sample. While inserting the sample, clean the bottom surface of the furnace to ensure that, sample has a flat place to stand; lower the pushrod until it contacts the top of the sample, lower the tube back into the furnace and ensure that the sample did not shift during lowering by checking the displacement gauge. The experiment begin with powering the computer, equilibrating the sample temperature ensuring it is at room temperature and dilatometer on, making sure cooling system is running and nitrogen gas is flowing along with all other necessary systems with a pressure of 10 psi.

### **II-3-5: Methods of physicals analysis**

#### ***a) Water absorption***

Measurement of water absorption, density, porosity and specific gravity is a tool for determining the degree of maturation of a ceramic body or for determining structural properties that may be required for a given application. These experiments have been conducted based on Archimedes' method according to American Standard ASTM 373- 88. Archimedes principle states that the upward buoyant force that is exerted on a body immersed in a fluid, whether fully or partially immersed is equal to the weight of the fluid that the body displaces and acts in the upward direction at the center of mass of the displaced fluid (R. Wilson, 2012)

#### **(i) Apparatus and Materials**

To conduct the experiment, the following materials are needed: a Balance of adequate capacity, suitable to weigh accurately to 0.01 g; an Oven, capable of maintaining a temperature of 150 °C (302 °F); a Wire Loop, Halter, or Basket, capable of supporting specimens under water for making suspended mass measurements; a glass beaker or similar container of such size and shape that the sample, when suspended from the balance by the wire loop is completely immersed in water with the sample and the wire loop being completely free of contact with any part of the container and distilled water.

#### **(ii) Test Specimens**

At least five representative test specimens were considered; the specimens were unglazed and had as much of the surface freshly fractured as is practical and contain no cracks. The individual test specimens weighed at least 50g. Specimens were dried at constant mass by heating in an oven at 150°C (302°F), followed by cooling in a desicator; the dry mass, D were determined to the nearest 0.01 g. The specimens were then placed in a pan of distilled water; a setter pins were used to separate the specimens from the bottom and sides of the pan and from each other and

they were soaked for 24 h; the saturated mass,  $M$  is then determined. The suspended mass,  $S$ , were determined to the nearest 0.01 g by weighing the specimen placed in a wire loop or a basket suspended from one arm of the balance.

- **Calculation**

In the following calculations, the assumption is made that 1 cm<sup>3</sup> of water weighs 1 g.

- Calculate the exterior volume,  $V$ , in cubic centimeters, as follows:  $V = M - S$  (11)
- Calculate the volumes of open pores  $V_{OP}$  and impervious portions  $V_{IP}$  in cubic centimeters as follows:  
$$V_{OP} = M - D$$
 (8)  
$$V_{IP} = D - S$$
 (9)
- The apparent porosity,  $P$ , expresses, as a percent, the relationship of the volume of the open pores of the specimen to its exterior volume. The apparent porosity were calculated as follows:  
$$P = [(M - D)/V] \times 100$$
 (10)
- The water absorption,  $A$ , expresses as a percent, the relationship of the mass of water absorbed to the mass of the dry specimen. The water absorption were calculated as follows:  
$$A = [(M - D)/D] \times 100$$
 (12)
- The apparent specific gravity,  $T$ , of that portion of the test specimen that is impervious to water, were calculated as follows:  $T = D / (D - S)$  (13)
- The bulk density,  $B$ , in grams per cubic centimeter, of a specimen is the quotient of its dry mass divided by the exterior volume, including pores. The bulk density were  
Calculated as follows: 
$$B = D/V$$
 (14)

***b) Flexural strength***

Flexural strength is the ability of a material to withstand bending forces perpendicular to its longitudinal axis; the resulting stresses are a combination of compressive and tensile stresses. Mechanical load displaces the structure elements from their positions giving rise to strain-elastic or inelastic (Kingery, 1965). As a rule, elastic strain closely follows the applied stress is time dependent, reversible and varies proportionally with stress. Inelastic strain in a material under load varies with time, is irreversible and is accompanied by the flow of matter without discontinuities (plasticity or viscosity)

Bi-axial strength of the fired samples was measured by the piston-on-three balls method. The test was carried out according to ASTM standard F394-78 using a universal mechanical testing machine (MTS 810, USA, load cell 100 kN). The strength of each disk was calculated as (*ASTM F394-78, 1991*).

$$\sigma_{max} = \frac{3P(1-\nu)}{4\pi t^2} \left[ 1 + 2 \ln \left( \frac{a}{b} \right) + \left( \frac{1-\nu}{1+\nu} \right) \left( 1 - \frac{b^2}{a^2} \right) \frac{a^2}{R} \right] \quad (15)$$

where  $P$  is the failure load,  $t$  the thickness,  $a$  the radius of the circle of the support points,  $b$  the radius of the region of uniform loading at the centre,  $R$  the radius of the specimen and  $\nu$  Poisson's ratio (assumed equal to 0.23) for the semi-vitrified products. In our specific test configuration  $a = 17.45\text{mm}$  and  $b = 1.50\text{ mm}$ . Five specimens of each formulation were used to obtain average values and standard deviations.

### c) *Vicker hardness test/ Knoop hardness test for ceramics*

The Knoop hardness and Vicker hardness of a ceramic is the material's resistance to penetration by the Knoop indenter. In this test, a pointed rhombic-based, pyramidal diamond indenter of prescribed shape is pressed into the surface of a ceramic with a predetermined force to produce a relatively small, permanent indentation. The surface projection of the long diagonal of the permanent indentation is measured using light microscope. The length of the long diagonal and the applied force are used to calculate the Knoop hardness. This test method describes an indentation hardness test using a calibrated machine to force a pointed, rhombic-based, pyramidal diamond indenter having specified face angles, under a predetermined force, into the surface of the material under test and measures the surface projection of the long diagonal of the resulting impression after removal of the load.

#### (i) *Procedure*

Place the specimen on the stage of the machine so the specimen will not rock or shift during the measurement. The specimen shall be clean and free of any grease or film. The surface of the specimen being tested shall lie in a plane normal to the axis of the indenter. If one leg (one half) of the long diagonal is more than 10% longer than the other, or if the ends of the diagonal are not both in the field of focus, the surface of the specimen may not be normal to the axis of the indenter. Align the specimen surface properly, and make another indentation. Start the machine smoothly. The rate of indenter motion prior to contact with the specimen shall be 0.015 to 0.070 mm/s. If the machine is loaded by an electrical system or a dash-pot lever system, it should be mounted on shock absorbers which damp out all vibrations by the time the indenter touches the specimen. The time of application of the full test force shall be 10s to 15 s unless

otherwise specified. After the indenter has been in contact with the specimen for this required dwell time, raise it carefully off the sample to avoid a vibration impact. The operator shall not bump or inadvertently contact the test machine or the associated support (for example, the table) during the period of indenter contact with the specimen. Allow a distance of at least one-and-one-half indentation times the long diagonal between the indentations. If there is excessive cracking from the indent sides, the indent shall be rejected for measurement. If this occurs on most indentations, a lower indentation force shall be used. If one or both tips of an indentation fall in a pore, the indentation shall be rejected. If the indentation lies in or on a large pore, the indent shall be rejected. If the impression has an irregularity that indicates the indenter is chipped or cracked, the indent shall be rejected and the indenter shall be replaced.

**(ii) Calculation**

Knoop hardness may be calculated and reported either in units of GPa or as a Knoop hardness number.

The Knoop hardness reported with units of GPa is computed as follows:

$$HK = 0.014229 P/d^2 \quad (16)$$

Where P = force (N), d = length of the long diagonal of the indentation (mm)

The dimensionless Knoop hardness number may be computed as follows:

$$HK = 14.229 P/d^2 \quad (17)$$

Where P = force, kgf, and d = length of the long diagonal of the indentation (mm).

### **II-3-6: Resistance of Ceramic Tile to Chemical Substances**

This test method calls for one or more tests, each consisting of exposing flat pieces of ceramic tile to the action of a specific chemical substance for a definite period of time at a prescribed temperature. After exposure, the surfaces of the tile are rinsed with water and inspected for effect. It is intended for testing ceramic tile that are to be used for food counters, lavatories, and similar residential, medical and commercial installations, where they may come in contact with food, chemical and waste substances ; for tile in areas where they may be exposed to contact with strong cleaning agents.

**a) Scope**

This test method covers a procedure for determining whether and to what degree, ceramics tiles are affected by prolonged exposure to chemical substances that are commonly used in the household or for cleaning purposes as well as other more severe conditions. The values stated in SI units are to be regarded as standard. No other units of measurement are included in this



standard. The units used for concentration in this standard are v/v which refers to the volume of reagent/1 L of solution and g/L which refers to the weight of reagent, in g, to be dissolved in 1 L of water.

#### **b) Apparatus**

Plain-end flint glass test tubes with a diameter of 20 mm and a length of 150 mm; pipets, glass with a volume of at least 50 mL with gradations in 1mL increments; oven capable of maintaining a constant temperature of  $110 \pm 5^{\circ}\text{C}$ ; Pencil, HB hardness grade; absorbent cloths or paper towels; distilled or Deionized Water for preparation of the solutions; Light Source, standard, that supplies a 300 lux of illumination.

#### **c) Samples**

One defect-free test specimen that is representative of the entire surface for each test solution is to be used. Test specimens shall be representative of the sample, and where tiles have different colors of decorative effects, take care to include all distinctive parts and more test specimens as necessary to incorporate all surface features. The original tile for testing should be cut to 50 by 50 mm squares for testing with each cut piece labeled according to the testing solution to be applied. The sample surfaces should be cleaned thoroughly with a suitable solvent, such as acetone, and completely dried before testing. The test specimens can be glazed or unglazed tile. If the tile are glazed, then apply the testing solutions to the glazed surface.

#### **d) Procedure for test solution application**

Dry the test specimens thoroughly at  $110 \pm 5^{\circ}\text{C}$ ; transfer 20 mL of the testing solution to a test tube; place the surface of the tile to be tested face down on the open end of the test tube. While firmly holding the test tube and tile assembly together, invert the assembly so that the back of the tile is facing the table and the closed end of the test tube is facing up. Carefully place the assembly on the table and leave undisturbed for 24 h then, invert the assembly so that the test solution is contained in the test tube, and remove the test tube from the specimen and dispose of the testing solution properly; thoroughly rinse the specimens under running water for a period of 10 min to remove any residual testing solution. If needed, clean the surface with a soft bristle brush to remove test solutions. Dry the specimens thoroughly at  $110 \pm 5^{\circ}\text{C}$  and cool to room temperature before evaluation.

**e) Evaluation of results**

➤ ***Visual evaluation:***

Examine the surface at a standard distance of 25 cm and a standard illumination of approximately 300 lux. Rotate the sample to examine it for appearance color and texture from multiple angles. Examine for differences in appearance between the treated and untreated area. If the sample is attacked visibly by the test solution, then the results of that testing solution will be recorded as “affected.” If the sample passes the visual test, then use the pencil test in the following section to verify the results.

➤ ***Pencil test***

Draw several lines across the test specimen with the HB grade pencil, making sure to include treated and untreated areas. Attempt to remove the pencil lines with a damp cloth. If the pencil lines are removed from the treated surface, then the results for that test solution will be recorded as “not affected.” If the pencil lines are not removed from the treated surface, the results for that test solution will be recorded as “affected”. If the pencil mark is not removed from the untreated area, as well as the treated area, then the pencil test may not be applicable in this case.



## **CHAPTER III: RESULTS AND DISCUSSION**

## CHAPTER III : RESULTS AND DISCUSSION

This chapter present the physico-chemical properties of various raw materials used in this work so as properties of fire products from this study.

### III-1: PHASE EVOLUTION AND THERMAL BEHAVIOR OF RAW MATERIALS

#### III-1-1: Mineral phase

The table below outlined the minerals composition of the two first fluxing materials used in our study: Pegmatite of Boboyo 1 and nepheline syenite of Eboundja

**Table 3:** Mineral phases in the two minerals materials (Pegmatite of Boboyo (1) and Nepheline syenite

	Albite	microcline	plagioclase	pyroxene	muscovite	quartz	amphibole
Nepheline syenite (NPH)	46.4	24.0	3.5	15.0	/	/	11.3
Pegmatite Boboyo 1 (FBb1)	14.6	55.3	/	/	11.2	17	/

#### III-1-2: Phase evolution of raw materials

The XRD patterns of raw materials used for this study are shown in figure 18. Quartz exhibited only one phase ( $\text{SiO}_2$ , ICCD: 00-020-1045) meaning that the sample used was pure. The limestone sample exhibited calcite as main phase ( $\text{CaCO}_3$ , ICCD: 00-005-0586); the quantitative analysis shows that it contains 95% of  $\text{CaCO}_3$  and about 5% of dolomite ( $\text{CaMg}(\text{CO}_3)_2$ , ICDD: 00-036-0426). Figure 18c shows the main phases in two pegmatites; Boboyo pegmatite (2) has anorthite as the main phase ( $\text{CaAl}_2\text{Si}_2\text{O}_8$ , ICDD: 00-020-0528) followed with albite ( $\text{NaAlSi}_3\text{O}_8$ , ICDD: 00-009-0478) and quartz ( $\text{SiO}_2$ , ICCD: 00-020-1045) as secondary phases. Manjo pegmatite exhibits four minerals phases with phlogopite ( $\text{KMg}_3\text{Si}_3\text{AlO}_{10}(\text{OH})_2$ , ICDD: 00-010-0495) and anorthoclase ( $\text{KAlSi}_3\text{O}_8$ , ICDD: 00-0090478) as main phases, completed with albite and quartz as secondary phases. It is clear that Manjo pegmatite is a potash feldspar while Boboyo pegmatite (2) is a calco-potash pegmatite. The clay material shows kaolinite ( $\text{Al}_2\text{O}_3 \cdot 2\text{SiO}_2 \cdot 2\text{H}_2\text{O}$ , ICDD: 00-029-1488) as the main phase followed with quartz.

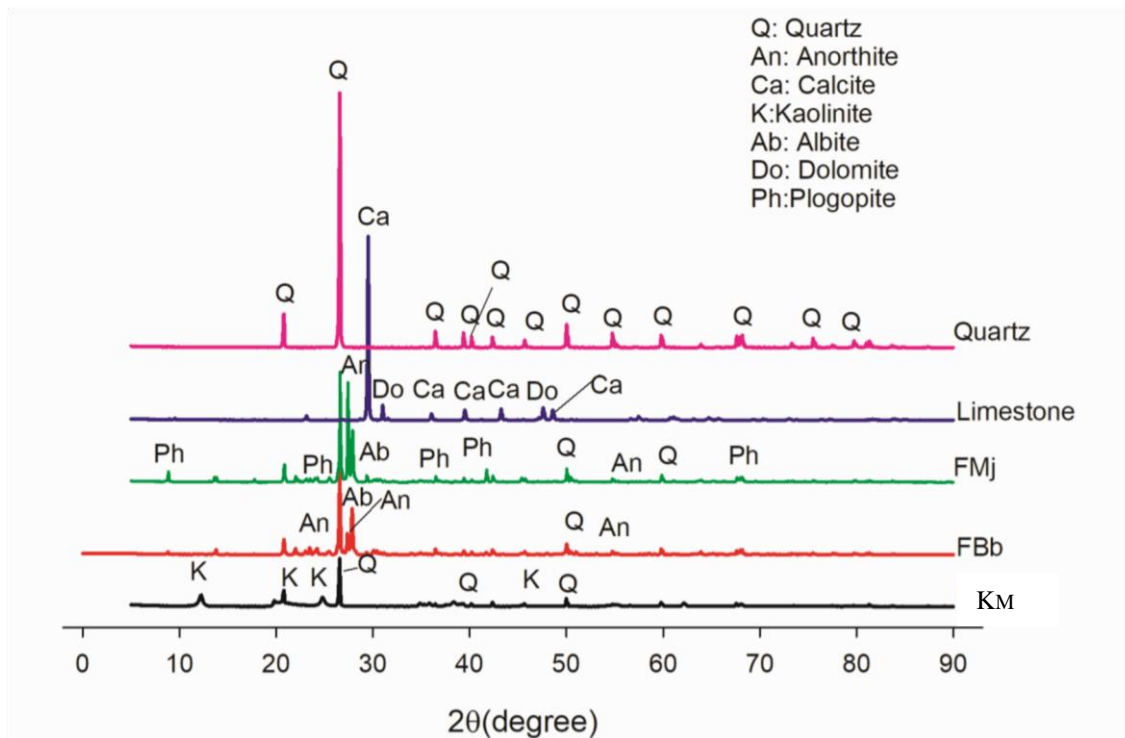


**Figure 17:** XRD of raw materials kaolin (KM), Boboyo pegmatite(FBb2) Manjo Pegmatite (FMj), limestone (Lst) and quartz

### III-1-3: Chemical composition of raw materials

The table below outline the chemical composition of various raw materials

**Table 4 :** Chemical composition of various raw materials (Boboyo pegmatite (FBb1 and FBb2), Manjo pegmatite (FM) and Mankon kaolinitic clay (KM), Quartz (Q) and limestone (Lst))

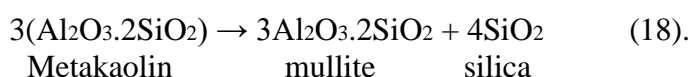
Oxides (%)	SiO <sub>2</sub>	Al <sub>2</sub> O <sub>3</sub>	K <sub>2</sub> O	Na <sub>2</sub> O	CaO	TiO <sub>2</sub>	P <sub>2</sub> O <sub>5</sub>	Fe <sub>2</sub> O <sub>3</sub>	MnO	MgO	LOI	Total (%)
<b>FBb(1)</b>	75.16	13.60	5.39	3.6	0.38	0.03	0.03	0.44	0.06	0.00	0.64	99.33
<b>FBb(2)</b>	76.12	13.40	4.13	4.77	0.34	0.03	0.04	0.51	0.06	0.00	0.65	100.04
<b>FM</b>	75.22	13.14	5.76	2.94	0.74	0.05	0.03	0.49	0.01	0.05	0.87	99.32
<b>KM</b>	61.84	24.88	0.06	0.04	0.00	0.58	0.0	0.69	0.0	0.08	11.8	99.97
<b>Q</b>	99.1	0.4	0.00	0.00	0.03	0.01	0.00	0.08	0.00	0.02	0.00	99.64
<b>Lst</b>	0.04	0.07	0.00	0.00	60.12	0.00	0.00	0.00	0.00	1.09	38.68	100

The Mankon kaolinitic clay has 61.84% of silica and a loss of ignition of 11.8%. This loss of ignition value is low compared to standard kaolins which have an average loss of ignition value of 13 to 14%; this can be explained by the high fraction of sand in the clay material (30%). The quartz sand has 99.1% of silica and no loss of ignition, these results are very indicative of

the level of purity of the raw material. The limestone present 60% of CaO and 39% of loss of ignition; it is clear that calcite is the main mineral of this material. The three feldspars materials (pegmatites) have almost the same silica and alumina content with an average content of 5% of potash oxide and 3% of soda oxide. These pegmatites presented less than a percent loss of ignition, these results confirm the XRD pattern. It can be noticed that our feldspar materials are rich in K<sub>2</sub>O; all the results confirm the XRD pattern.

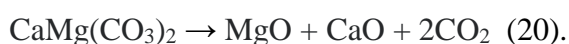
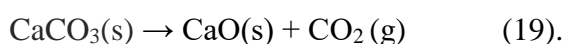
#### III-1-4: Thermal behavior of raw materials

The thermo-chemical transformation of raw materials under DTA/TG curve are shown in figure 18a and 18b. In the clay sample, the small endothermic peak at  $\approx 85^{\circ}\text{C}$  is attributed to the evaporation of physically adsorbed water, that's of  $547^{\circ}\text{C}$  can be attributed to the elimination of constituent water resulting from the loss of hydroxyl group from clay structure. The little exothermic peak around  $990^{\circ}\text{C}$  may be due to the conversion of metakaolin into spinel phase ( $2\text{Al}_2\text{O}_3 \cdot 3\text{SiO}_2$ ); the following exothermic peak above  $1045^{\circ}\text{C}$  is due to the formation of mullite (transformation of metakaolin into mullite) following the equation (18):



After the formation of primary mullite (mullite<sub>3/2</sub>), it is observe a progressive densification up to  $1300^{\circ}\text{C}$ . During this densification, the secondary mullite (mullite<sub>1/2</sub>) is formed, favored by the presence of alkaline and iron (even in low content, 0.69%). The thermal gravimetric (TG) curves confirm the interpretation of DTA with the two first transformation at about 100 and  $500^{\circ}\text{C}$  corresponding to the two deshydration phases; the formation of mullite occurs at about  $1033$  to  $1068^{\circ}\text{C}$ . During the densification, there is no weight loss due to the fact that the decomposition and the hydroxylation are generally completed after the formation of mullite.

The DTA curve of limestone shows a large endothermic peak around  $900^{\circ}\text{C}$  coupled in TG with a significant loss of mass (40%). These correspond to the decarbonation of CaCO<sub>3</sub> and CaMg(CO<sub>3</sub>)<sub>2</sub> as indicated into the equation (19) and (20):



The weight loss of forty percent (40%) is indicative of the level of purity of the limestone under study.

The quartz does not show any significant transformation through DTA but we can notice a little endothermic peak around  $530^{\circ}\text{C}$ , corresponding to transformation of quartz  $\alpha$  to quartz  $\beta$ .

(a)

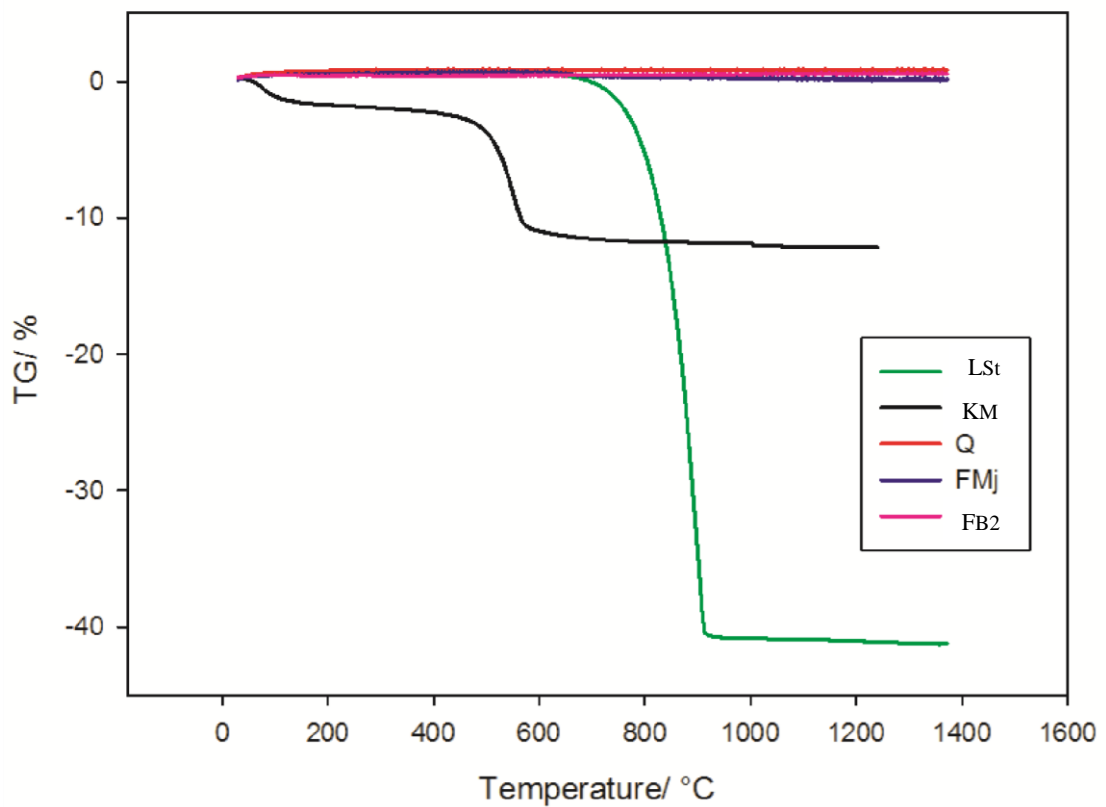
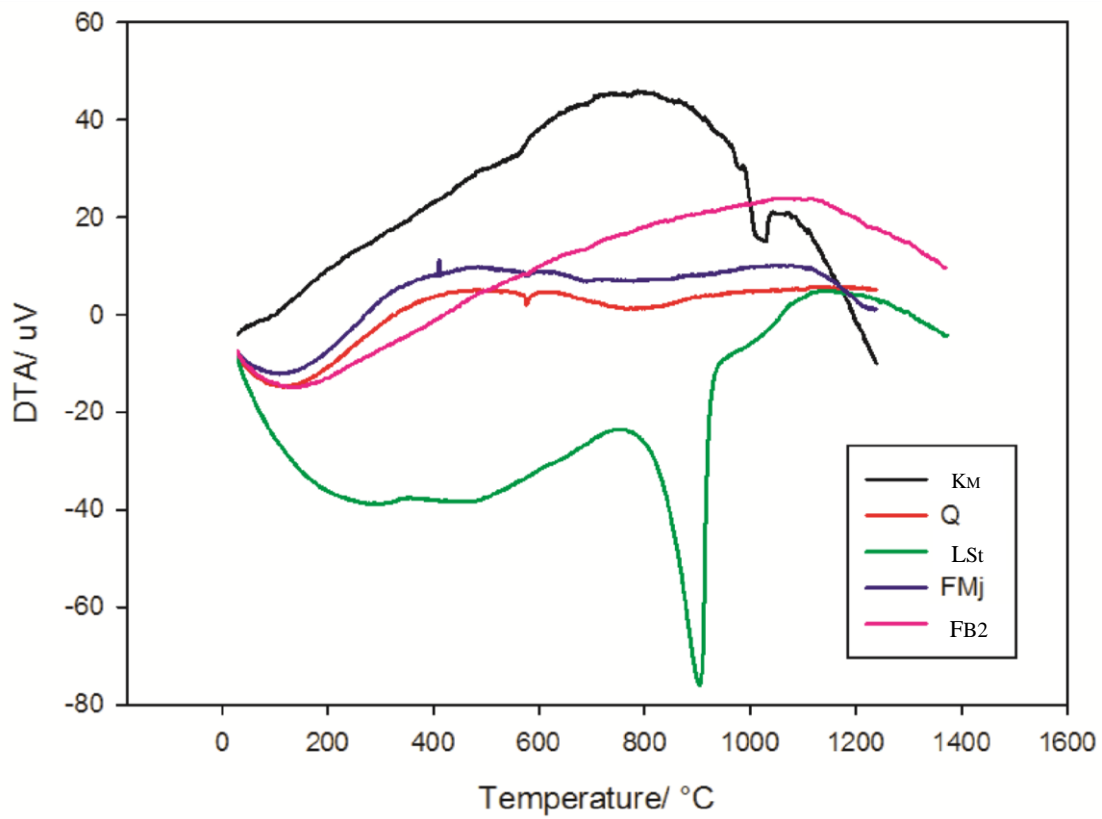


**Figure 18:** Thermo-chemical transformation of raw materials [(Limestone (Lst), Kaolin ( $K_M$ ), Quartz (Q), Manjo pegmatite (FMj) and Boboyo Pegmatite (FBb) under DTA (a) and TG (b)]



On submitting the raw pegmatite of Boboyo (1) and nepheline syenite to the differential thermal analysis and differential thermal gravimetry (DTA/TG), the two minerals do not present any significant transformation up to 575°C as observed in Figure 19: the DTA curves do not present any thermochemical reaction. The TG curve shows a slight decrease of less than 0.2 mass% for nepheline syenite at ~100°C. The loss of mass with the pegmatite reached 0.6 mass% at 400°C with a total loss of 0.6 mass%. This loss of mass is concluded at 575°C with an endothermic peak for the pegmatite as observed in Figure 19. The loss of mass alone with the small endothermic peak at 575°C can be ascribed to the decomposition of the structural water described in pegmatite. Solid solutions between potash and soda feldspars, with orthose or microcline as dominant mineral are metastable up to 600°C. In conditions of slow cooling, the solid solutions show alterations into oriented growth of subparallel lamellae which are alternatively rich in potash feldspar. The  $\alpha$ - $\beta$  quartz transformation also appears at 575°C but is not generally associated to weight loss. The high quartz fraction and water contained in the pegmatite in comparison with nepheline can explain the presence of the endothermic peak, since it is known that nepheline syenite does not have free quartz. Upon heat treatment, the nepheline syenite specimen showed a continue increase in mass up to 1 mass% above 1200°C, while the pegmatite specimen gains only 0.4 mass% at low temperature. These observations are linked to the oxidation of iron present in nepheline syenite but almost absent in pegmatite. The pegmatite presented melting with sluggishness at 1200°C and an exothermic peak at 1230°C because of the formation of leucite, the crystalline phase that appeared with the melt. This sluggishness was described to be due to leucite ( $\text{KAlSi}_2\text{O}_6$ ) and is justified by incongruent melting of orthose ( $\text{KAlSi}_3\text{O}_8$ ) which starts to decompose at 1200°C into leucite and a highly viscous silica-glass. The incongruent melting observed for microcline and orthoclase persists in the microcline albite series up to a mass of 53 % albite, although the temperature of complete liquidus falls with the increasing proportion of albite. This can explain the sluggishness observed with pegmatite solid solution and not with nepheline syenite. The molar ratio of  $\text{K}_2\text{O}/\text{Na}_2\text{O}$  (3.54) in pegmatite allows for good expression of the microcline contained in the solid solution. The nepheline syenite presents a continuous (congruent) melting with relatively low viscosity of the melt with respect to pegmatite (Figure 19).

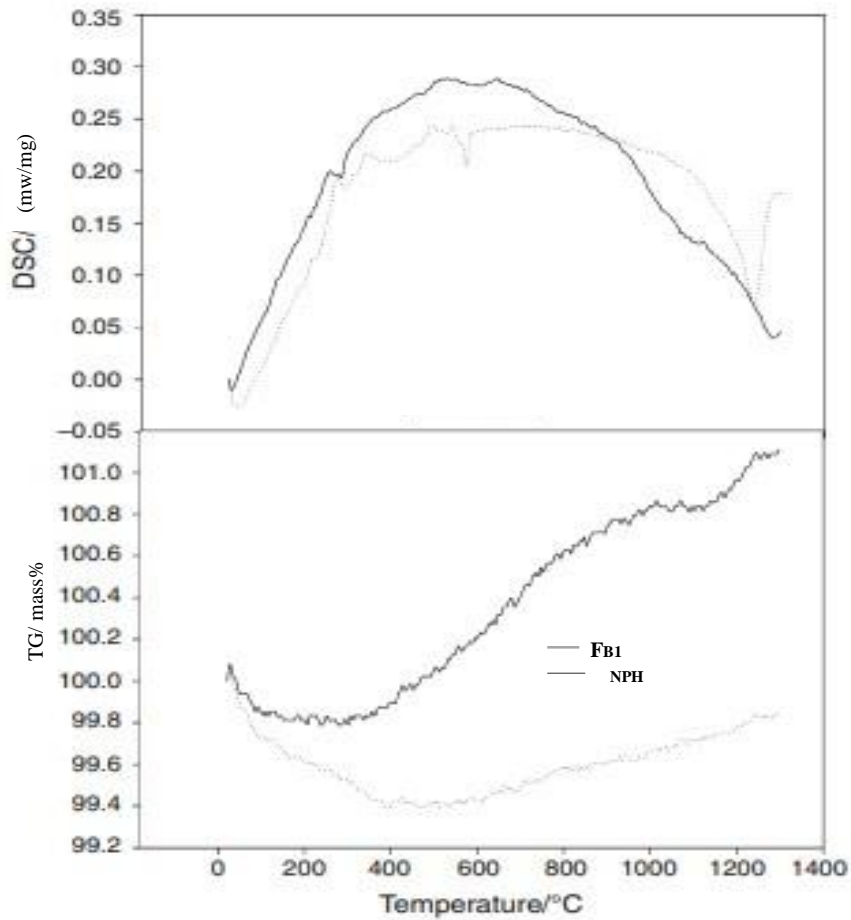


**Figure 19:** Thermo-chemical transformation of raw Boboyo pegmatite 1 (FBb1) and Nepheline syenite (NPH) under DSC

### III-1-5: Physical properties of Kaolinitic clay of Mankon

#### a) Particle size analysis

The results of particle size analysis obtained by wet sieving and sedimentometry are presented in Table 5 and Figure 20.

**Table 5:** Particle size distribution of the sample  $K_M$

Ref	Color	Aspect	% gravel $\Phi > 2$ mm	% sand $2 > \Phi > 0.02$ mm	% silt $0.02 > \Phi > 0.002$ mm	% Clay $\Phi < 0.002$ mm
$K_M$	White	Sandy clay	0.17	41.72	7.23	50.88

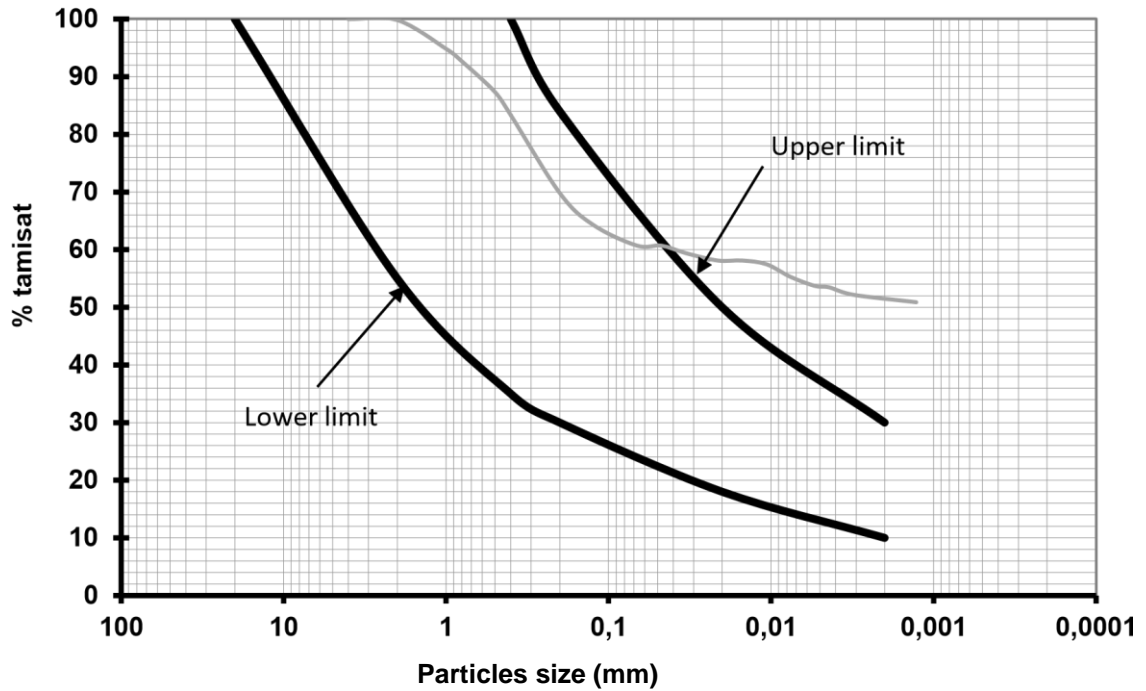


**Figure 20:** Particle size analysis of the Mankon clay sample (KM)

According to Figure 20, the finest particles are of the order of 1.5  $\mu\text{m}$  and represent about 60% of the grains. The silt is quite low (-10%) and about 30% sand; this clay is classified among siliceous clays

**b) Atterberg Limit**

The results of the plasticity tests are presented in Table 6.

**Table 6:** plasticity tests results

Sample	Liquidity limit (%)	Plasticity limit (%)	Plasticity index (%)
KM	<b>60.07</b>	<b>32.37</b>	<b>27.69</b>
Cameroonian Standard (NC 102-114, 20022006)	25 - 50	20 - 35	2 – 30

The plasticity limit and the plasticity index are respectively 32.37% and 27.69%; these values are in accordance with French standard (NF P 94-051, 1993) and with Cameroonian standard (NC 102-114, 2002-2006). Concerning the liquidity limit, the obtained value is out of range probably due to the high content of sand.

According to both the French Standard (NF P 94-051, 1993) and Cameroonian (NC 102-114, 2002-2006), the clay material is plastic.

## **III-2: INVESTIGATION OF THE PHYSICO-CHEMICAL PROPERTIES OF TWO PORCELAIN STONEWARE COMPOSITIONS BASED ON NEPHELINE SYENITE (G) AND BOBOYO PEGMATITE 1 (B)**

### **III-2-1: Thermal behavior of the two porcelain stoneware compositions based on Nepheline syenite and Boboyo pegmatite1**

When the two minerals (Boboyo pegmatite 1 and nepheline syenite) are added to clays and sand to form porcelain stoneware compositions B and G, respectively for pegmatite and nepheline syenite, it is observed during heating of the fine ground dried paste, an endothermic peak that appears at 100°C which can be ascribed to the dehydration of clay and the residual physic-absorbed water used for the processing of the pastes (Figure 21). At 575°C the second endothermic peak is attributed to the dehydroxylation of clay. The significance of the dehydroxylation of clay masks the slight endothermic peak observed in the Figure 21 with the pegmatite specimen. At 780°C, the third endothermic peak is completely ascribed to the decomposition of limestone added. The dehydration and the dehydroxylation of clays, the decomposition of the limestone, result to the weight loss as it can be observed in TGA curve. The combinaison of the phenomenon conducted to a total of 9.88 wt.% for the specimen G and 10.99 wt.% for the specimen B. After the two significant sequencies of decomposition, the structure of the two porcelain stoneware is disordered up to 850°C. The matrices contain Si-O, Al-O layers from the transformation of kaolinite to metakaolinite. Above this temperature, a small exothermic peak is observed at around 900°C ; exothermic ascribed to the crystallization of plagioclase or anorthite. The peak size is linked to the CaO content which is relatively low to allow the significant anorthite content. Significant crystallization peak appears at ~1000°C (Figure 21). The peak correspond to the development of mullite needles (primary mullite) as from the decomposition of clay and formation of disordered metakaolinite. After the crystallization at 1000°C, the two porcelain stoneware compositions continue with densification enhanced by the progressive flow of liquid phase. From the Figure 21, apart from the difference of 1 wt% in weight loss, from the thermal curves, the two compositions tend to show similar thermal behavior.

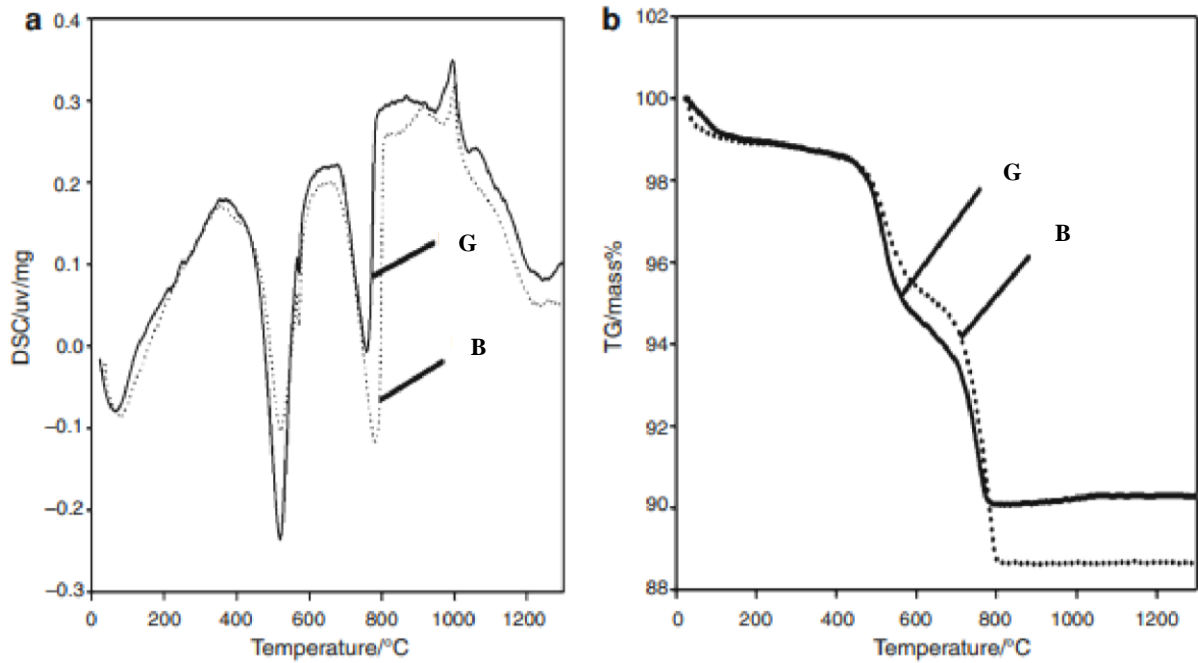


**Figure 21** : DSC/TG curves of porcelain stoneware composition **(B)** based on Boboyo pegmatite 1 and **(G)**-based nepheline syenite

### III-2-2: Sintering behavior of the two porcelain stoneware compositions based on nepheline syenite and Boboyo pegmatite 1

The addition of limestone has provided sufficient quantity of lime capable to affect the thermal behavior of the orthoclase in pegmatite ; the two formulae were :

$(\text{Na}_2\text{O}, \text{K}_2\text{O}) \text{CaO} \cdot 4.8\text{Al}_2\text{O}_3 \cdot 13.4 \text{SiO}_2$  for G and  $(\text{K}_2\text{O}, \text{Na}_2\text{O}) \text{CaO} \cdot 4.8\text{Al}_2\text{O}_3 \cdot 13.4 \text{SiO}_2$  for B. Figure 21a interprets in the form of curve, the sequences of images (variation of volume) collected from the hot stage microscope.

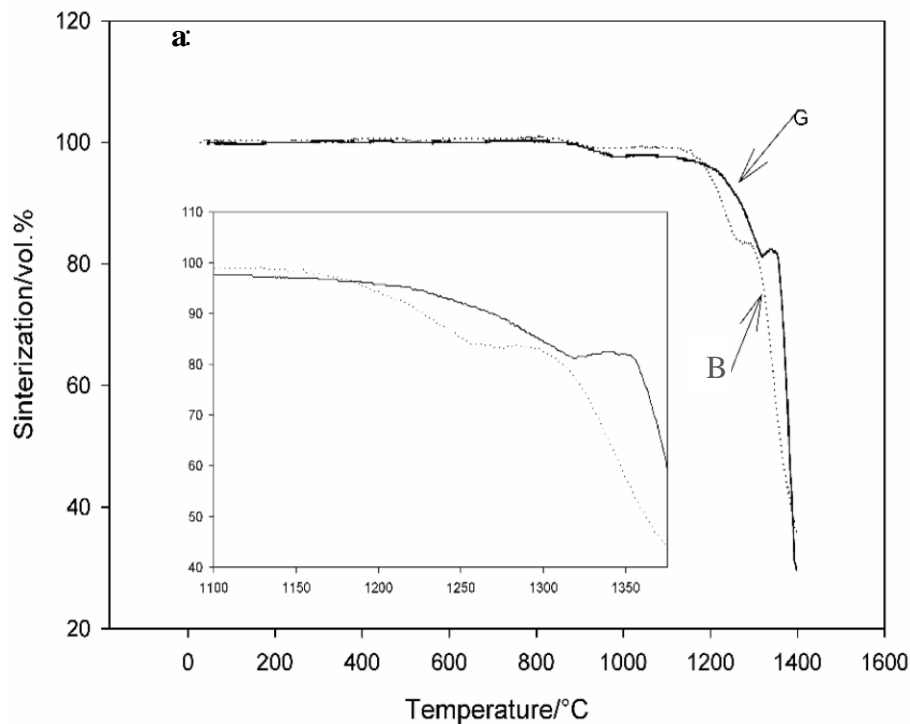


**Figure 22a :** Variation of the volumes of the two compositions of porcelain stoneware with temperature

The significant steps of the two compositions indicate 1194°C and 1220°C as temperatures at which the two compacts, B and G respectively, present maximum solid state sintering. Even though, the liquid film is described in the alkali fluxes as from 990°C ; the melting begins at the surfaces of crystals and proceeds so slowly that much of the crystal can exist in the presence of the melt. The first signs of deformation due to the increase in liquid content appears at 1312°C for B and 1349°C for G while the fusion is obtained at 1359°C (B) and 1386°C (G). The sintering behavior of the two compositions of porcelain stoneware can be summarized as:

- (i) Maximum solid densification with the shape of the pressed specimen that remain unchanged: this correspond in the Figure 22b to the sinterization.
- (ii) Starting vitrification (corners become round)
- (iii) Flow of the liquid phase (formation of the hemispherical shape)
- (iv) Melting (height lower than  $\frac{1}{2}$  of the initial value).

When the feldspathic materials initiate to vitrify, they approach equilibrium conditions very sluggishly. The melting that begins at the surface of crystals proceeds slowly with very high viscosity. Viscosity which is the basis of evaluating the thermal behavior of the flux. As the temperature or time increases, more liquid forms which begins to draw particles together by surface tension and progressive solution takes place. Crystals which were formed after the

decomposition of clay may diffuse into the melt or crystals may continue to grow. Above the normal vitrification range, air which has been entrapped into the pores will build up sufficient pressure to expand against the viscous glass and cause bloating.

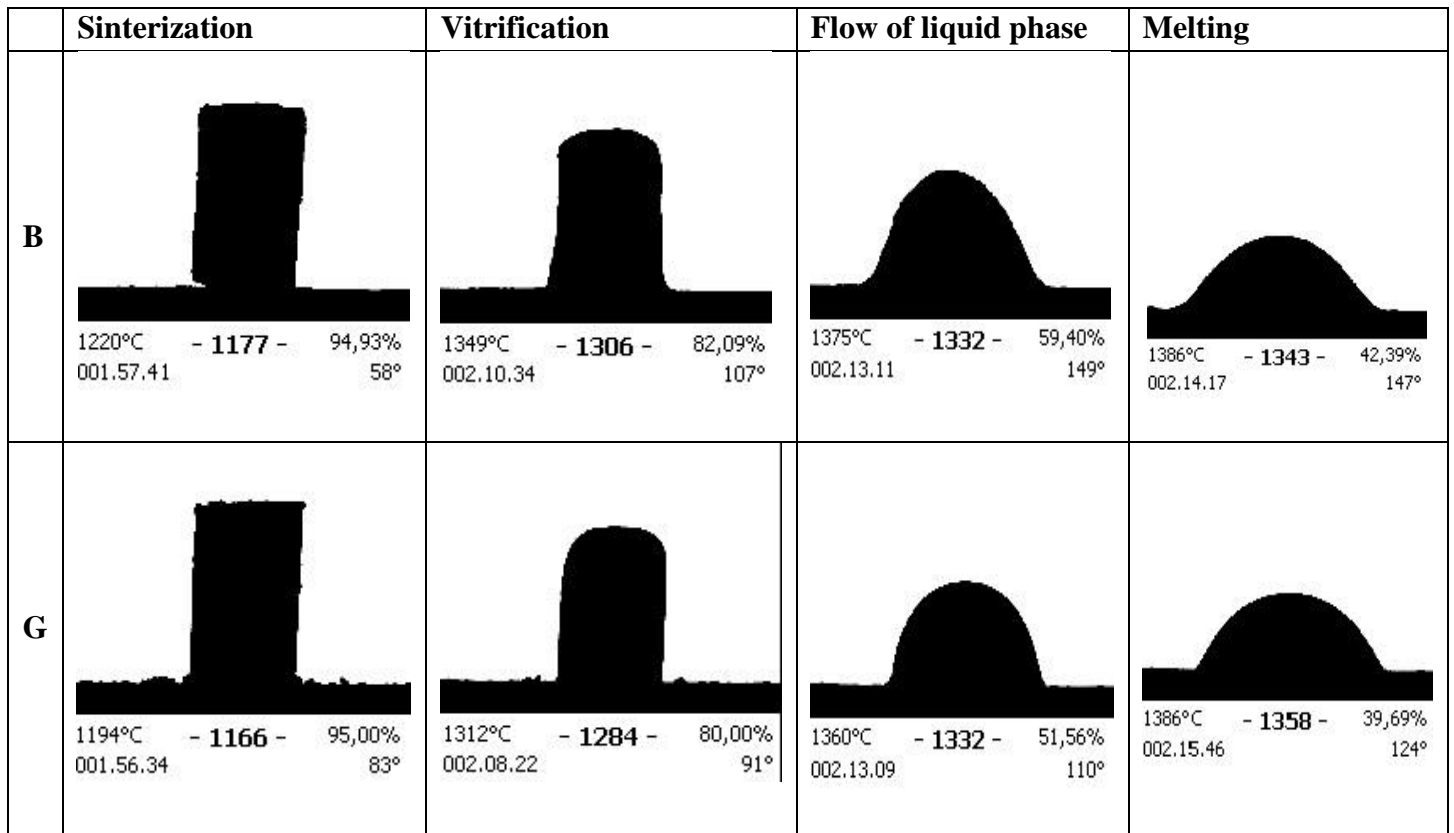


**Figure 22b** : sintering behavior of the two compositions of porcelain stoneware B and G

It was expected that nepheline syenite based composition will be the specimen with early vitrification and densification (Bowen N. L., Tuttle O. F., 1950). It has been demonstrated from the works of Martz J. A. (1933), Geller and Creamer (1931) that the presence of lime in the potash feldspar modifies significantly the thermal behavior. In fact studying the potash-lime and soda-lime systems as fluxes for ceramics bodies, they concluded that:

- (1) Semi-vitreous bodies designed without lime indicated the soda-feldspar body with earlier maturation with respect to potash-feldspar body;
- (2) Semi-vitreous bodies containing lime showed a reversed situation, the potash-feldspar body maturing ahead to the soda-feldspar.

These results have significant importance for the design of the pastes for fast firing. In the case of pegmatite, a recrystallization peak is clearly observed in the Figure 21 which completely

disappears in the formulation of porcelain stoneware with 5 wt% of lime. Moreover the sintering curve elaborated from the hot stage microscope shows the earlier flow of liquid (Figure 22).

### **III-2-3 : Variation of the physico-mechanical properties with firing temperature and rate.**

The bending strength of the two porcelain stoneware was affected by the temperature development and the firing rate (soaking time). From the sintering curves (DTA and curves from hot stage microscope), the two compositions presented similitude up to 800°C, temperature at which they present no significant volume shrinkage. Above 800°C, shrinkage began and G appears to shrink much more than B up to the temperature of maximum solid state sintering. With the formation of the liquid phase, B tends to shrink more than G (Figure 22a). To understand these differences, it should be noted that, the two compositions of porcelain stoneware were prepared using the chemical approach. However, the earlier vitrification of pegmatite based flux explains the densification and earlier melt of B. The effects on the mechanical properties are that G treated with 1 and 2 hours soaking time (Figure 23) see the values of flexural strength increase with the increase of temperature. Additionally, the change of soaking time from 1 to 2 hours also increases the flexural strength, this is valid up to 1200°C. From the Figure 23, the flexural strength value is 57 MPa and 59 MPa respectively at 1175°C and 1200°C when considering 1 hour soaking time. The strength increases to 60 MPa and 63 MPa for the thermal treatment using 2 hours soaking time. At 1225°C, the flexural strength remains at 63 MPa for 2 hours soaking and increases to 67 MPa with 1 hour soaking time. The flexural strength that remains constant at 1225°C for 2 hours soaking time and increases to 67 MPa for 1 hour soaking time is an indication of the action of liquid phase in this range of temperatures if we consider the sintering curves (Figures 21 and 22). It can be concluded that, between 1175°C and 1225°C, the amount of liquid phase progressively increases in G with temperature and soaking time, liquid phase that contributes to densify the matrix and close open porosity ; by the way, the mechanical properties are improved.

For the B serie, the maximum flexural strength was obtained as from 1175°C with 2 hours soaking time. As shown in the Figure 23, the specimen fired with this program showed 78 MPa as flexural strength. With the same temperature and only 1 hour of soaking time, the flexural strength were 72 MPa. Value that did not change significantly with the increase in temperature to 1200°C for the same soaking time of 1 hour. For the same temperature of 1200°C and 2 hours soaking time, the flexural strength decreases from 78 MPa to 72 Mpa. The decreases in flexural



strength continue and was very important at 1225°C where at 2 hours soaking time the flexural strength was under 65 MPa and 67 MPa for 1 hour.

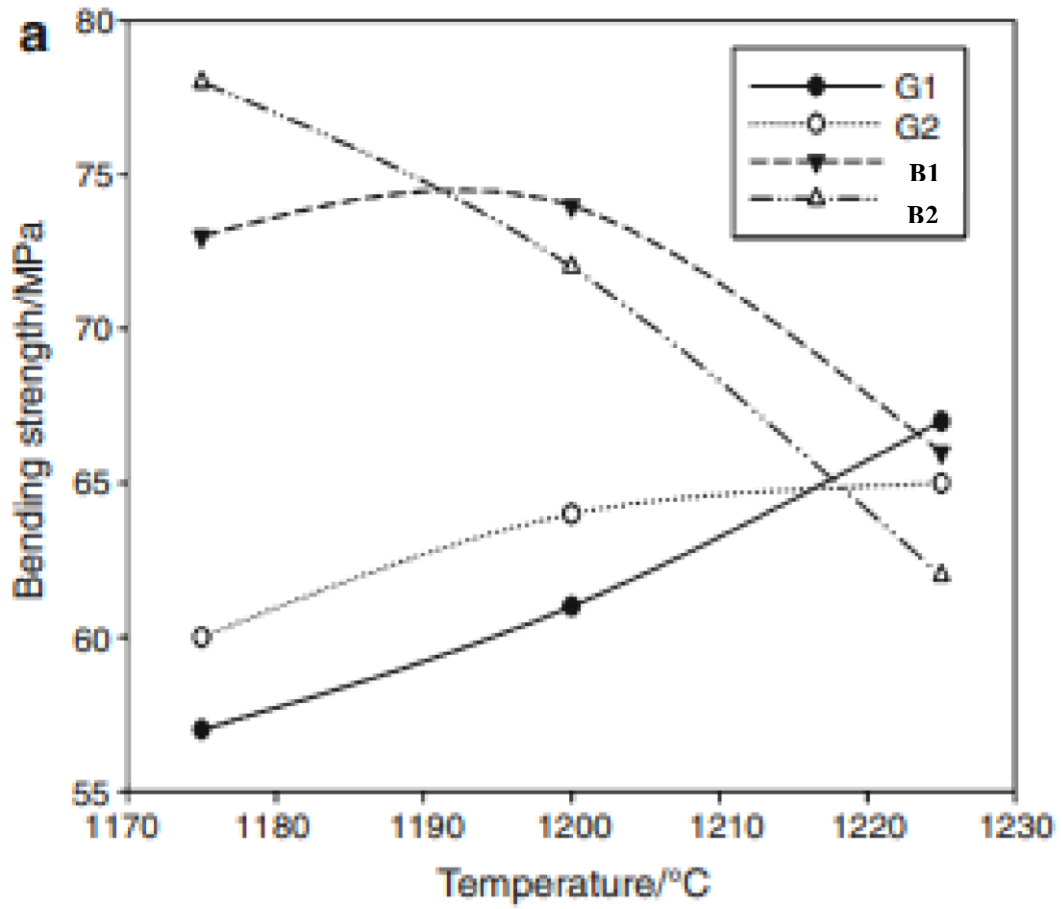


**Figure 23:** Variation of the flexural strength (MPa) of the two porcelain stoneware with temperature and soaking

### III-2-4: XRD patterns of the fired samples as function of temperature and soaking time

Figure 24 presents the XRD patterns of the fired composition G at 1200°C for 2h and 1225°C for 1 h. The specimen contains mullite, quartz and plagioclase. These three phases appeared as from 1175°C and the difference with the change in temperature and soaking time was the intensity of peaks. As from 1200°C, clay completely disappeared, the increase in temperature or the change in soaking time within a temperature has as effects the increase in liquid content and the reduction in intensity of the crystalline phases. For the composition B, the same crystalline phases were observed between 1175°C and 1225°C with only variation in intensities with the increase of the temperature or change in soaking time. When 1 hour soaking time were applied, there were no changes of the significant importance between 1175°C and 1200°C. At 1225°C, peaks of mullite decreases considerably while those of plagioclase increase. Correlating these results with the mechanical properties and the sintering curves, greatest warpage is expected from the pegmatite based flux system which allow to design dense and high strength bodies at relatively low temperature.

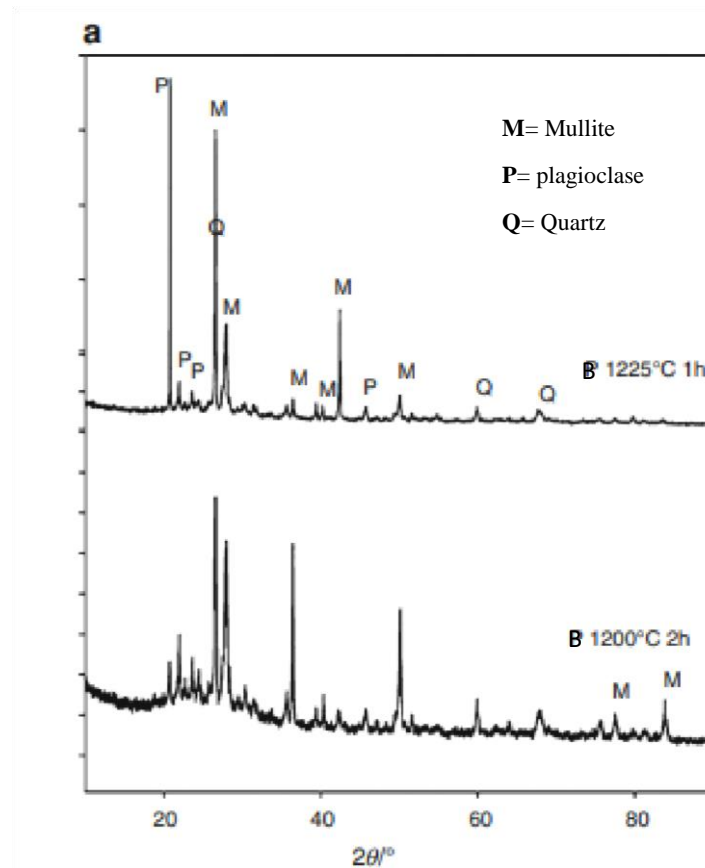


**Figure 24a:** XRD patterns of the fired samples of B at 1,200 C (2 h) and 1,225 C (1 h)

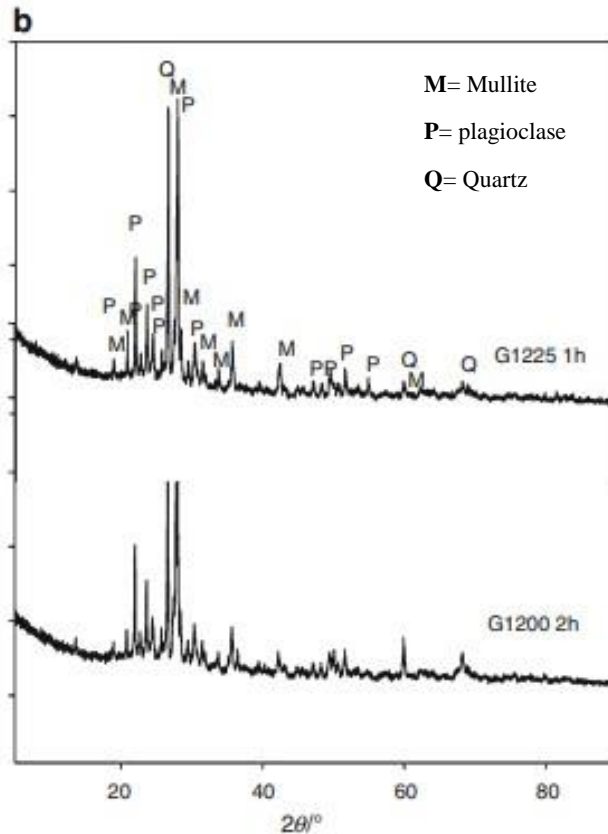


**Figure 24b:** XRD patterns of fired samples of G at 1,200 C (2 h) and 1,225 C (1 h)

### III-2-5: Water absorption and density of the fired specimen

Water absorption is generally used as one of the parameters to evaluate the maturation of porcelain, stoneware and others classes of traditional ceramics. The results of the water absorption are presented in the Figure 25 as function of the variation of the apparent (skeletal) density. The values of the density indicated in the Figure 25 correspond to the three range of density obtained with the three temperatures applied for this study. At 1175°C, the apparent density of the composition G is 2.04 g/cm<sup>3</sup> and 2.12 g/cm<sup>3</sup> respectively for 1 and 2 hours soaking time. The corresponding values of water absorption are 8.9% and 7.4%. At 1200°C, the density increases to 2.52 g/cm<sup>3</sup> and 2.54 g/cm<sup>3</sup> for 1 and 2 hours corresponding to 5.8% and 4.7% of water absorption. Up to 1225°C it appears that the density does not further increases significantly. Considering the sintering behavior of the specimen (Figure 24), this temperature correspond to the important flow of liquid phase. Hence it can be concluded on a final product of G with high porosity (2.5% water absorption) since 1225°C seem as the optimum temperature to apply. The fact that at 1225°C the flexural strength of the specimen G with 2 hours is lower than that with 1 hour soaking time is indicative on the maturation reached for the sintering of this composition. The sample B showed at 1175°C an apparent density of 2.24 and 2.42 g/cm<sup>3</sup> with 1 and 2 hours soaking respectively. These values correspond to the water absorption of 2.5 and 0.6%. The density increase to 2.61 and 2.59 g/cm<sup>3</sup> for 1 and 2 hours at 1200°C. These values correspond to

0.45% and 0.36% of water absorption. At 1225°C the water absorption of the composition B increases to 0.45 (1h) and 0.54 (2h). Firing at this temperature resulted in a drastic fall of the physical properties due to forced expulsion of gases resulting in blisters and bloating. Consequently the density fall under 2.46 g/cm<sup>3</sup> and the mechanical strength reach the minimum for the series considered (B).

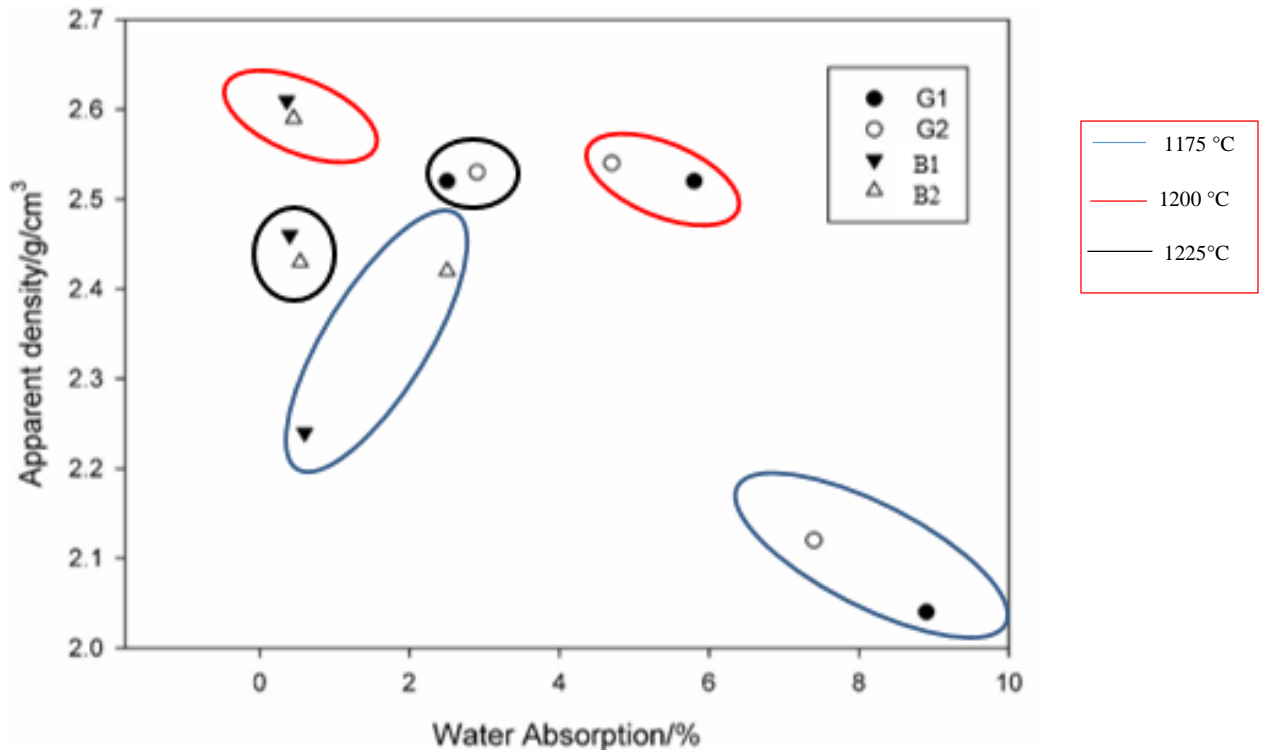


**Figure 25:** water absorption as function of the variation of apparent density

### III-2-6: Tortuosity

Figure 26 presents the variation of the tortuosity with the temperature and soaking time. It is observed that the tortuosity of the G series increases very slowly between 1175°C and 1225°C. The tortuosity of the series B increases significantly with temperature and for a giving temperature, the tortuosity at 1 hour soaking time is low with respect to that of 2 hours soaking time. From the variation of the cumulative pore volume, pore size distribution and water absorption, it can be suggested that the tortuosity is closely linked to the variation of the amount of liquid phase in the two formulations of the porcelain stoneware. The presence and amount of liquid phase determine both an increase of the tortuosity of the matrix as well as the effective decreases of the area of the cross section exposed to the diffusion of water. The poor liquid content of G explains the low value of the tortuosity and the high water absorption achieved. Meanwhile the extended fluid formed in B contributed to increase the tortuosity from the high compact of the matrix.

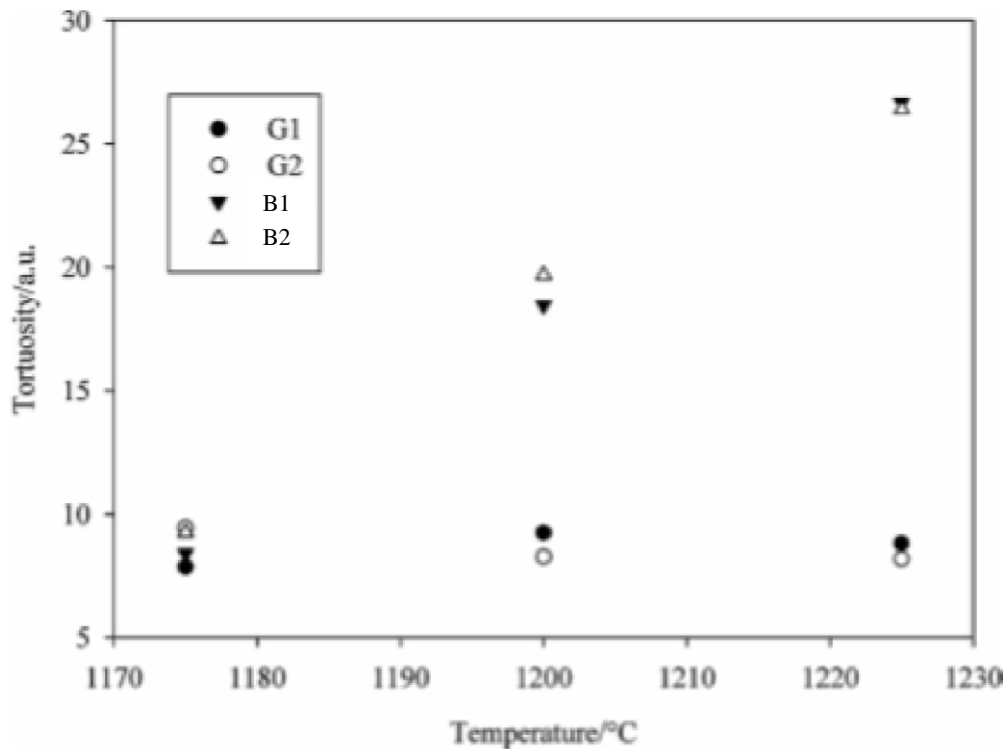


**Figure 26:** Variation of the tortuosity with temperature and soaking time for samples B and G.

### III-2-7: Cumulative pore volume and pore size distribution

#### a) *Cumulative pores volume*

The variation of the cumulative pore volume with size of pores presented in the Figure 27 (a) and (b) for the formulation B and Figure 27 (c) and (d) for the formulation G indicates the effects of the temperature, sintering rate (soaking time) and significantly the mineral nature of the fluxing agent used on the cumulative pore size as well as on the threshold of pores. The porcelain stoneware from the formulation B based on the first batch of Boboyo's pegmatite showed the highest value of the cumulative pore volume: 0.59 mL/g for the sample treated at 1175°C with 1 hour soaking time. This value decreased significantly to 0.058 mL/g when the soaking time was raised to 2 hours. Value not far from that of the applied temperature of 1200°C for 1 hour soaking time (0.054 mL/g). The cumulative pore volume is then reduced with the order of ten. Likewise, the increase in temperature to 1225°C with 1 hour soaking time reduces the cumulative pore volume to 0.050 mL/g. By applying the thermal cycle with 2 hours soaking time, the cumulative pore volume decreases from 1175°C (0.058 mL/g) to 1200°C (0.048 mL/g) then increases again to 0.050 mL/g when the temperature was 1225°C.

The sample G presented the cumulative pore volume of 0.09 mL/g for the specimen fired at 1175°C for 1 hour soaking time. This value is lower with respect to the 0.59 mL/g of the sample B treated with the same thermal cycle. Increasing the temperature to 1200°C, the cumulative pore

volume decrease to 0.12 mL/g and does not change significantly at 1225°C (1hour). Similar trend was observed when the thermal cycle is applied with 2 hours soaking time (Figure 29b)

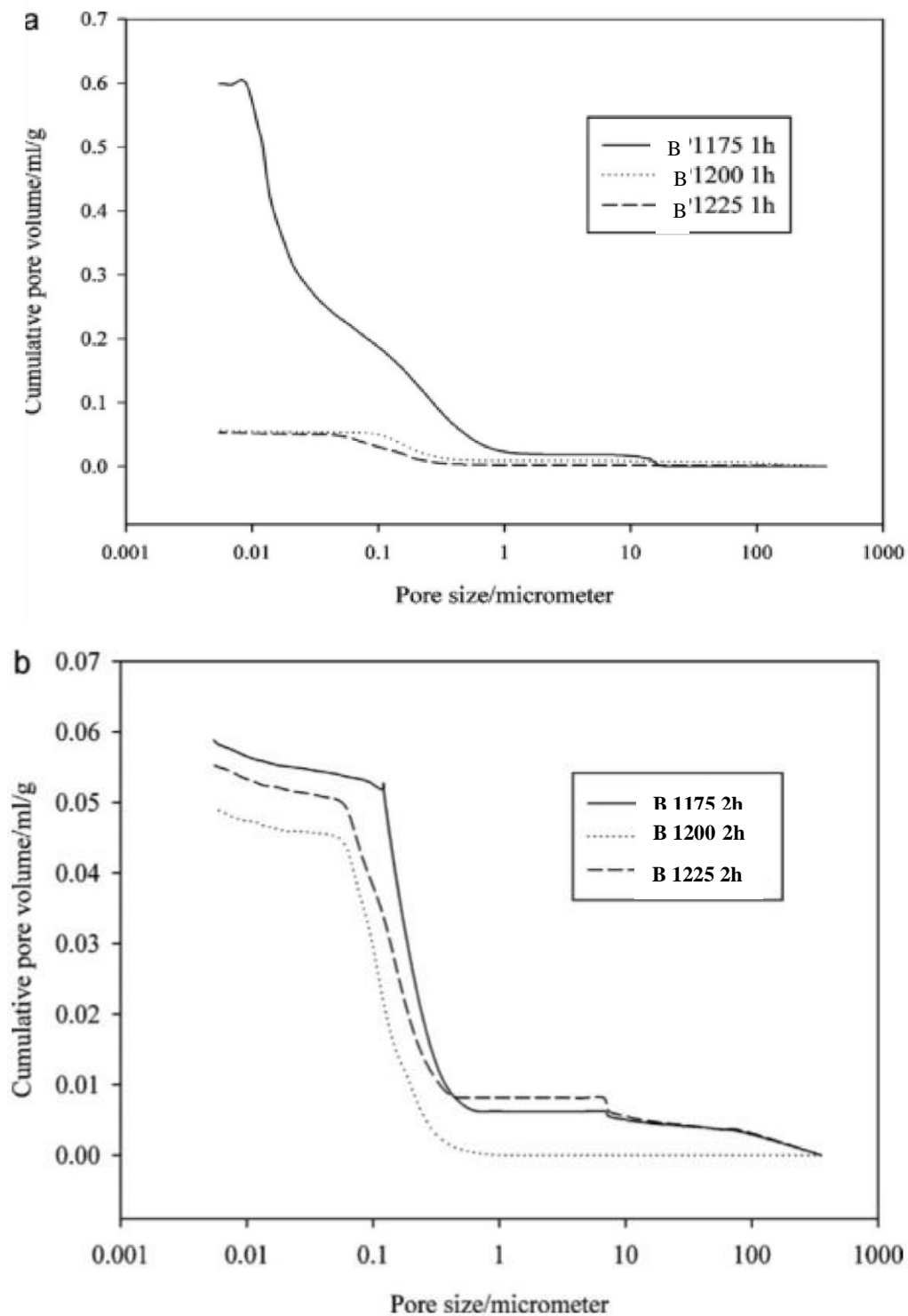


**Figure 27 :** variation of the cumulative pores volume (mL/g) with pores sizes (  $\mu\text{m}$ ) for sample B with 1h (a) and 2h (b) soaking time

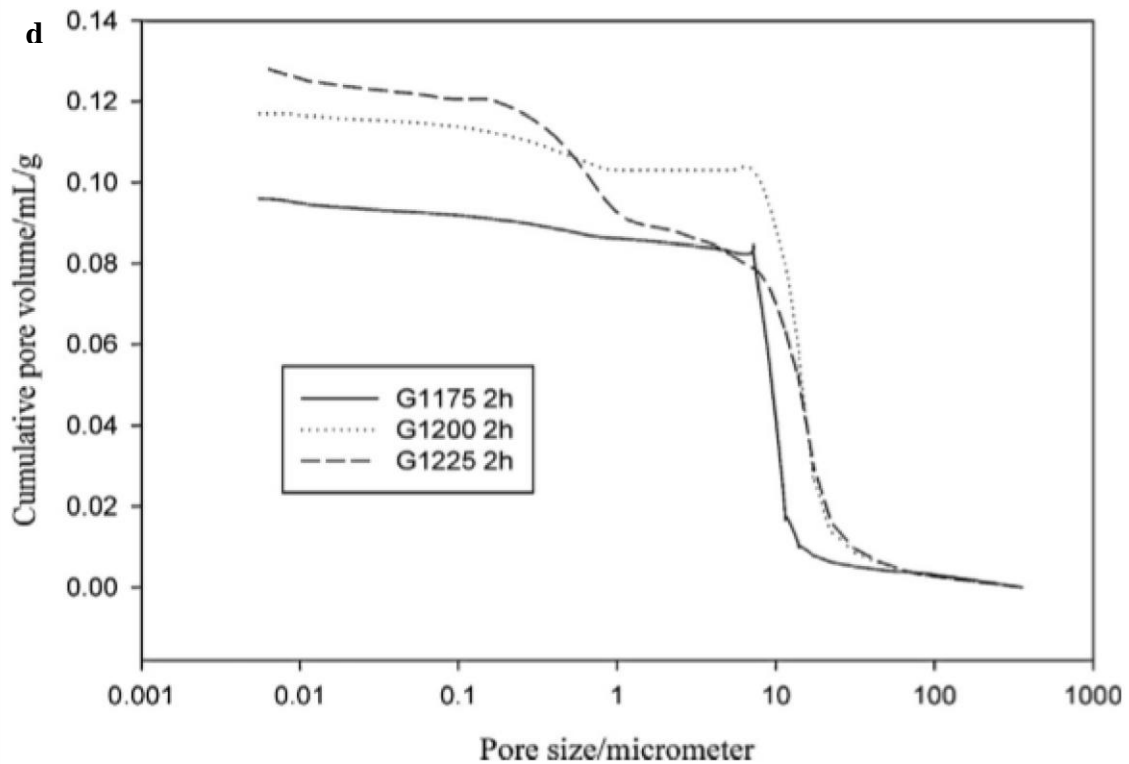
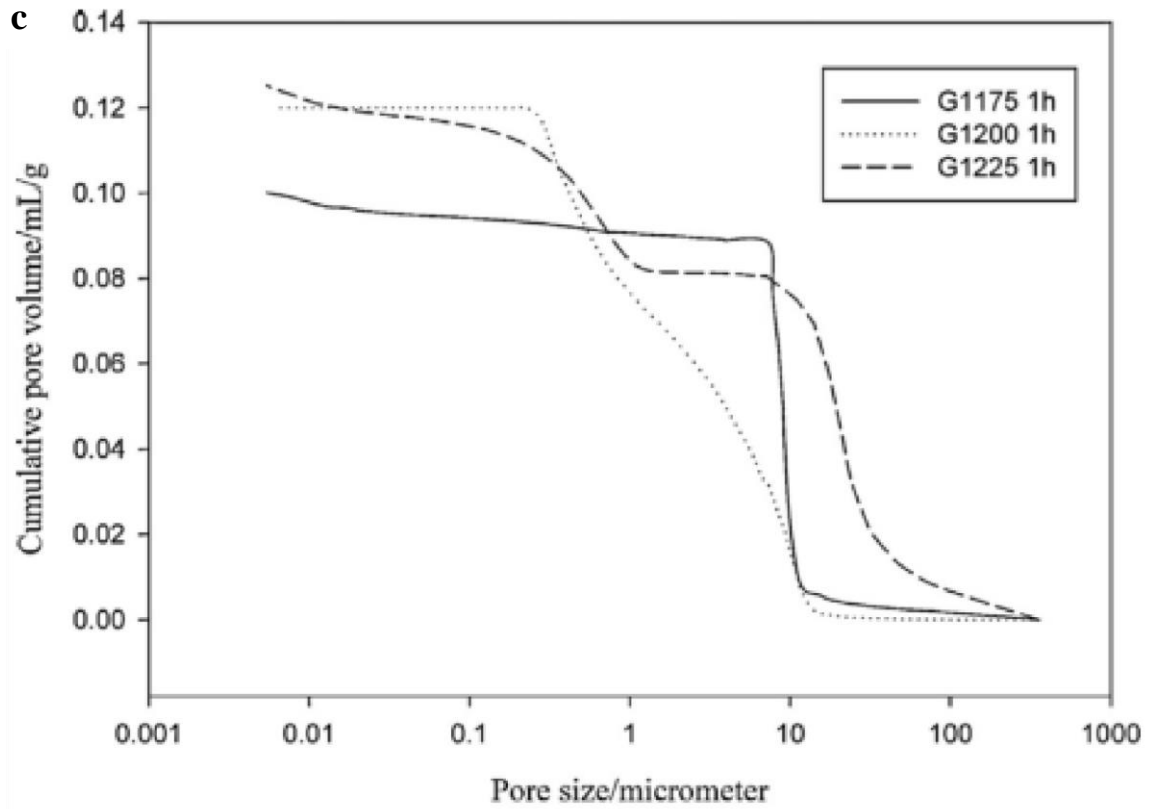
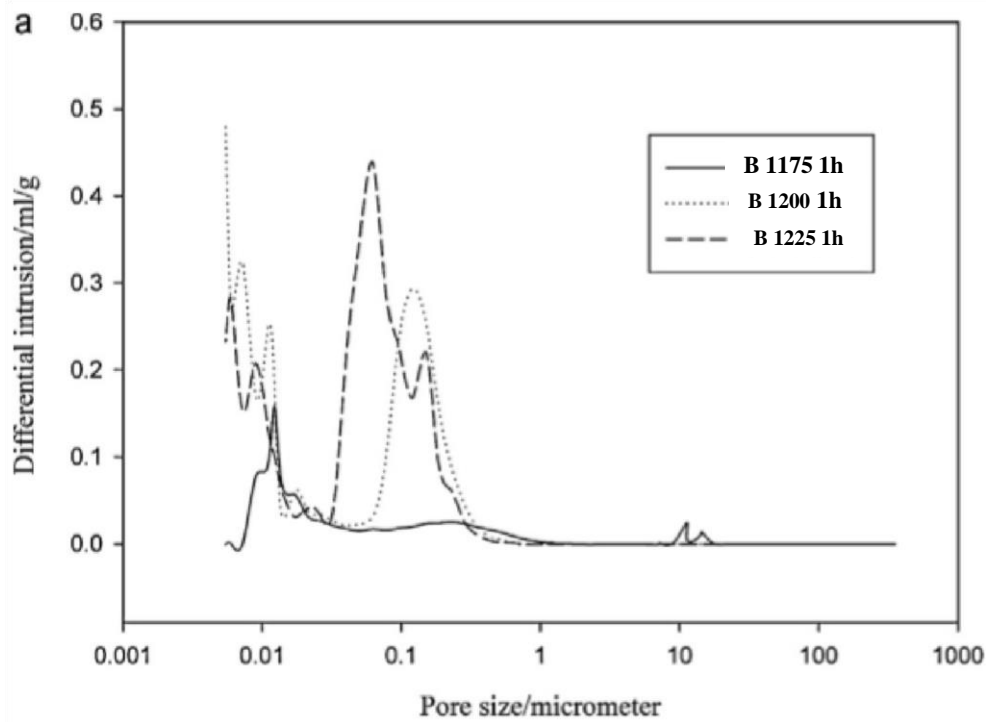


**Figure 27:** Variation of the cumulative pores volume (mL/g) with pores sizes ( $\mu\text{m}$ ) for sample G with 1h (c) and 2h (d) soaking time

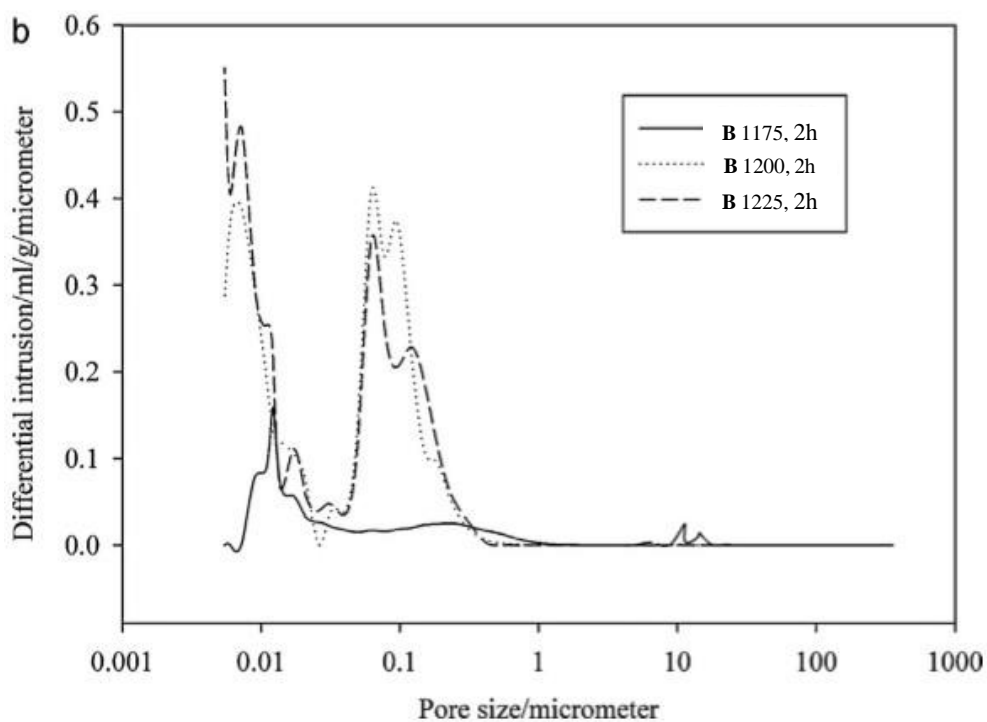
**b) Pores size distribution**

From the Figure 28, it is observed that when applies the thermal cycle with soaking time of 1 hour, coarsening pores appear at 1175°C with sizes concentrated at 11.23 and 14.58  $\mu\text{m}$ . The pores should be the residual open porosity from the sintering process. In fact when the ceramic paste is under sintering, dehydration, dehydroxylation and decomposition take place up to 800°C as in the present case with the development of open porosity due to gases resulting from the thermochemical transformations. With the increase of the temperature, the amount of the liquid phase formed increases and many of the open pores are closed (Figure 28a). Between the coarsening pores and the fine ones, 1175°C (1 hour), a larger band is observed between 0.08 and 0.93  $\mu\text{m}$ . The major part of pores of this specimen is concentrated between 0.001 and 0.007  $\mu\text{m}$ . At 1200°C, pores disappear and the band of pores concentrated between 0.08 and 0.93  $\mu\text{m}$  increases in intensity while the band of pores between 0.001 and 0.007  $\mu\text{m}$  moves through lower pore size with more dispersion suggesting the formation at this level of different groups of fine pores. The temperature 1225°C (1h) continue to move the fine pore bands to lower sizes. The band at 0.08-0.93  $\mu\text{m}$  tends to decrease in intensity giving access to a new band with lower size of pores (0.063  $\mu\text{m}$ ) as it can be observed in the Figure 28 (a) and (b). The variation of the pores size was similar when 2 hours soaking time was applied. Coarsening porosity concentrated to 10.88 and 14.61  $\mu\text{m}$  was identified in the specimen B fired at 1175°C (2h). This indicate that although the considerable reduction of the cumulative pore volume at this temperature with the change in soaking time, the class of pores remained. The increase of the soaking time here also moves the band from 0.08-0.93  $\mu\text{m}$  to 0.04-0.43  $\mu\text{m}$  but with higher intensity. At 1225°C, it is observed a reduction of the intensity of the band at 0.04-0.43  $\mu\text{m}$  and the increase of finer pores (< 0.009  $\mu\text{m}$ ). The pores with peaks at 0.018  $\mu\text{m}$  increased in intensity at 1200°C and do not change the intensity at 1225°C. A lower firing temperature determines the formation of open pores in the ceramic body, while a higher temperature leads to the increase of porosity, especially amount of closed pores, as result of oxygen release during the  $\text{Fe}_2\text{O}_3$  decomposition and gas expansion in the pores. The entrapment of gases forming bubbles explained the difference in the properties of the material.



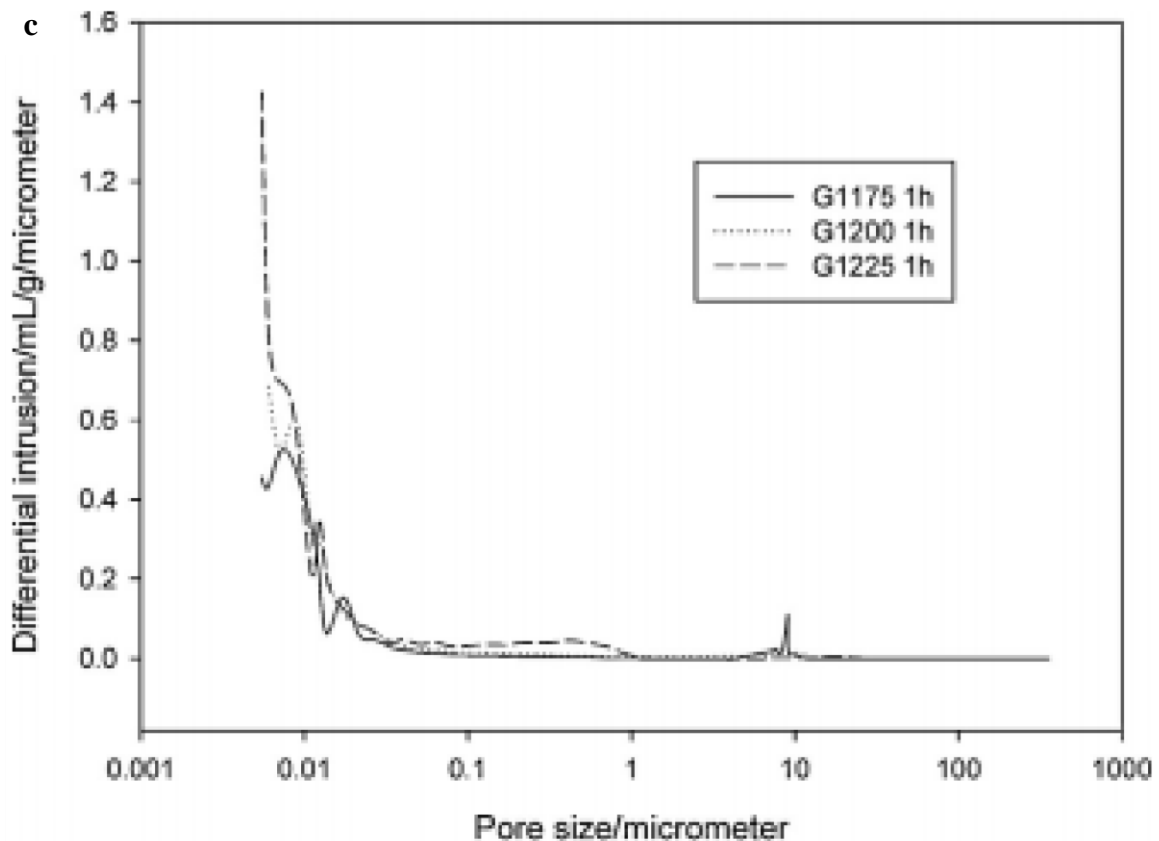


**Figure 28a:** Pore size distribution of sample B as function of temperature and 1 hour soaking time



**Figure 28b:** Pore size distribution of sample B as function of temperature and 2 hours soaking time

From the Figure 28 (c) and (d), the band of the coarsening pores is concentrated to 10  $\mu\text{m}$  for the specimen G fired at 1175°C for 1 hour and as in the case of the sample B with the increase in temperature. No band was observed at 0.08-0.93  $\mu\text{m}$  for the specimen treated at 1175°C for 1 or 2 hours. It seems that, this band is linked to the amount of the liquid phase developed in the matrix. The orthoclase catalyzed by the CaO presents liquid phase with low viscosity at temperature above 1190°C. The specimen of the sample G fired at 1175°C for 1 hour soaking time shows a band of pores centered at 0.007  $\mu\text{m}$ . The increase in temperature to 1200°C makes the band at 0.01-0.02  $\mu\text{m}$  move to lower values of the pore size. At 1225°C, the band at 0.08-0.93  $\mu\text{m}$  appeared and the fine pores continued to move to lower values in size. As it can be seen in the Figure 28a, the intensities of the bands of fine pores increase. The application of the soaking time of 2 hours makes observe the reduction of the band of pores at 10  $\mu\text{m}$ . The increase in temperature to 1200°C decreases the intensity of the band centered at 0.007  $\mu\text{m}$ . The band centered at 0.021  $\mu\text{m}$  disappeared and a new band of pores appears between 0.01-0.02  $\mu\text{m}$ . The increase in temperature to 1225°C (1 hour) make increase the peaks of the bands of fine pores (bands centered at 0.007 and 0.01  $\mu\text{m}$ ). The band of pores observed between 0.08-0.93  $\mu\text{m}$  appeared. The appearance of this band at 1225°C in both 1 and 2 hours soaking time can be correlated to those present in the sample B to suggest links between the band of pores and the formation of the liquid phase.



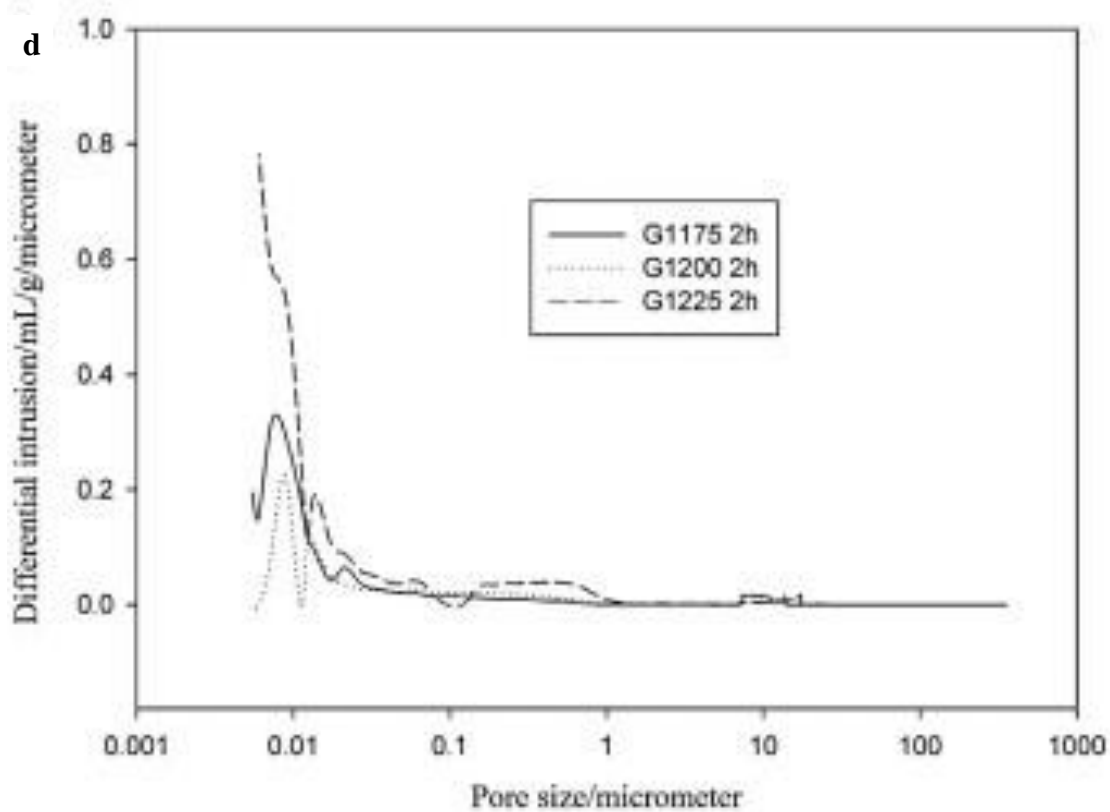


**Figure 28:** Pore size distribution of sample (G) as function of temperature and soaking time (c) for 1h and (d) for 2h soaking time

The frequencies of larger pores is significant in the sample G with the respect to the sample B even though the size of the coarsening pores are 10  $\mu\text{m}$  in B, and slightly larger in G (11  $\mu\text{m}$  and 14  $\mu\text{m}$ ). This explain the threshold of pores which is above 10  $\mu\text{m}$  in G series. In B series, the threshold is 0.69  $\mu\text{m}$  for the specimen fired at 1175°C (1h) and 0.35  $\mu\text{m}$  for the specimens fired at 1200°C and 1225°C. By applying the 2 hours soaking time, the threshold are 0.55, 0.41 and 0.32  $\mu\text{m}$  for 1175°C, 1200°C and 1225°C respectively. It appeared that during sintering, the pores in the sample B remain particularly concentrated in the range of larger size (diameter between 1 and 10  $\mu\text{m}$ ). Fraction of these larger pores are converted to small pores but the final product remains with closed pores.

### III-3: PARTIAL CONCLUSION

The phase evolution, water absorption and the results of the flexural strength demonstrated the temperature-time dependence of the characteristics of the compositions of porcelain stoneware under study. The pegmatite based composition presented earlier vitrification and densification with very high strength even with still relative high water absorption. By using a complex solid solution of orthoclase, albite, quartz and lime, the eutectic  $K_2O-Al_2O_3-SiO_2$  describes at  $990^\circ C$ , from the reaction of feldspar and amorphous silica of metakaolin, is affected by lime which contributes to enhance the liquid and lowering the viscosity. In the presence of these high viscous fluid, the mullite, plagioclase that still at this range of temperatures with fine size form a highly dense matrix with high flexural strength. The change in the firing rate (soaking time) affects the viscosity of the fluid and consequently the mechanical properties. This interpretation of the strength development in B and G in relation with the phase evolution falls with the theory of mullite generally used in the literature to explain the mechanical properties of porcelain and relative materials (Carty W. M., Senapati U., 1998). This is one of the oldest theory of the strength can justify the high strength at  $1175 - 1200^\circ C$  in the composition B and the decrease in flexural strength when important part of crystalline phases are dissolved by the flow of liquid. This is valid also for the composition G where the flow of liquid was more gradual and the crystalline phases progressively increase with the temperature and time up to  $1225^\circ C$ . Even in G the flow of liquid phase can explain the decrease in strength at  $1225^\circ C$  when 2 hours soaking time is considered. High temperatures have as effects the dissolve of mullite needles, dissolution that will conduct to the reduction of the densification and the decrease in strength. This gives right to consider the matrix strengthening effects which can be as complementary to the mullite theory. This theory referenced as the prestressed theory of strength improvement is discussed in regard to the difference in thermal expansion coefficients between the matrix and the dispersed particles and crystalline phases that produces strong compressive stresses on the glassy phase. These compressive stresses contribute to improve the strength. In semi-vitrified products as porcelain and stoneware, the nature of micro cracks depends on the expansion coefficients of the matrix and the particles. With reference to the works of Warshow and Seider (1967), it can be suggested that the drastic decreases in strength in B between  $1200$  and  $1225^\circ C$  is also linked to the quartz dissolution from the very fine particles used ( $\phi < 40\mu m$ ). The above results obtained demonstrated the role of the nature of the mineral phase in feldspars and the action of the mineralizers on the design of compositions for fast firing. The use of solid solutions instead of a specific mineral feldspar has the advantages that these solid solutions (nepheline syenite and

pegmatite) contain less free quartz, high alkali content and result in glassy matrix with thermal expansion closer to that of residual quartz.

The cumulative pore volume, the pore size distribution and the values of water absorption permitted to describe the composition (G) as essentially porous material compared to the composition B which showed more compacity.

Although their similar chemical compositions, the nephelinesyenite based body (G) saw its vitrification delayed with respect to the pegmatite based body (G). The recrystallisation of leucite that appeared in DTA curves of pegmatite was not found in the DTA curve of the porcelain stoneware B. These differences were ascribed to the action of CaO in enhancing the vitrification and reduce the viscosity of the fluid formed in orthoclase based systems compared to albite based systems

### III-4: INVESTIGATION ON THE ROLE AND PROPER PORTION OF LIMESTONE IN ENHANCING THE CRYSTALLIZATION PHENOMENA AND STRENGTH OF PORCELAIN STONEWARE

In this main part of the research work, Limestone was used to modify the fluxing action of two potash feldspars [a pure potash feldspar (Manjo feldspar) and a soda-potash feldspar (Boboyo feldspar 2)] labeled P and C, respectively, in the formulation of porcelain stoneware based on Cameroonian raw materials. The effect of limestone addition (0–10 weight %) was investigated in the range of sintering temperature between 1125 and 1300 °C. A basic formulation of porcelain stoneware comprising: 52.63% kaolin, 29.47% feldspar and 17.89% quartz was made. These compositions were named C0 for Boboyo feldspar-based porcelain stoneware and P0 for Manjo feldspar-based porcelain stoneware. The mass percent of limestone addition were varied inside the two reference compositions C0 and P0 according to Table 7.

**Table 7 : Porcelain stoneware formulations**

Base Formulations	Mass % of Limestone					
	0%	1%	3%	5%	7%	10%
<b>C</b>	C0	C1	C3	C5	C7	C10
<b>P</b>	P0	P1	P3	P5	P7	P10

#### III-4-1: Thermal behavior and phase evolution in formulations

##### a) *Thermal behavior of formulation*

The thermo-chemical transformations identified for two formulations without addition of limestone (C0 and P0) and two with addition (C10, P10) are shown in Figure 29a and 29b. Regarding the DTA (Fig.29a), all the four curves exhibited endothermic peaks between 99 and 128°C which can be ascribed to the dehydration of clay and the residual physic-absorbed water used for the processing of the pastes; the samples without addition of limestone (C0 and P0) showed endothermic peaks between 484 and 503°C corresponding to the progressive removing of the crystallization water. Significant crystallization peak appears at ~1110°C; the peak correspond to the development of mullite needles (primary mullite) as from the decomposition of clay and formation of disordered metakaolinite. After the crystallization at ~1110°C, the two porcelain stoneware compositions continue with densification enhanced by the progressive flow of liquid phase. The samples with addition of limestone (C10 and P10) exhibit almost the same peaks but

also demonstrate an exothermic peak observed around 850°C; exothermic ascribed to the crystallization of anorthite. The peak size is linked to the CaO content and is in accordance with XRD pattern observed in Figure 30.

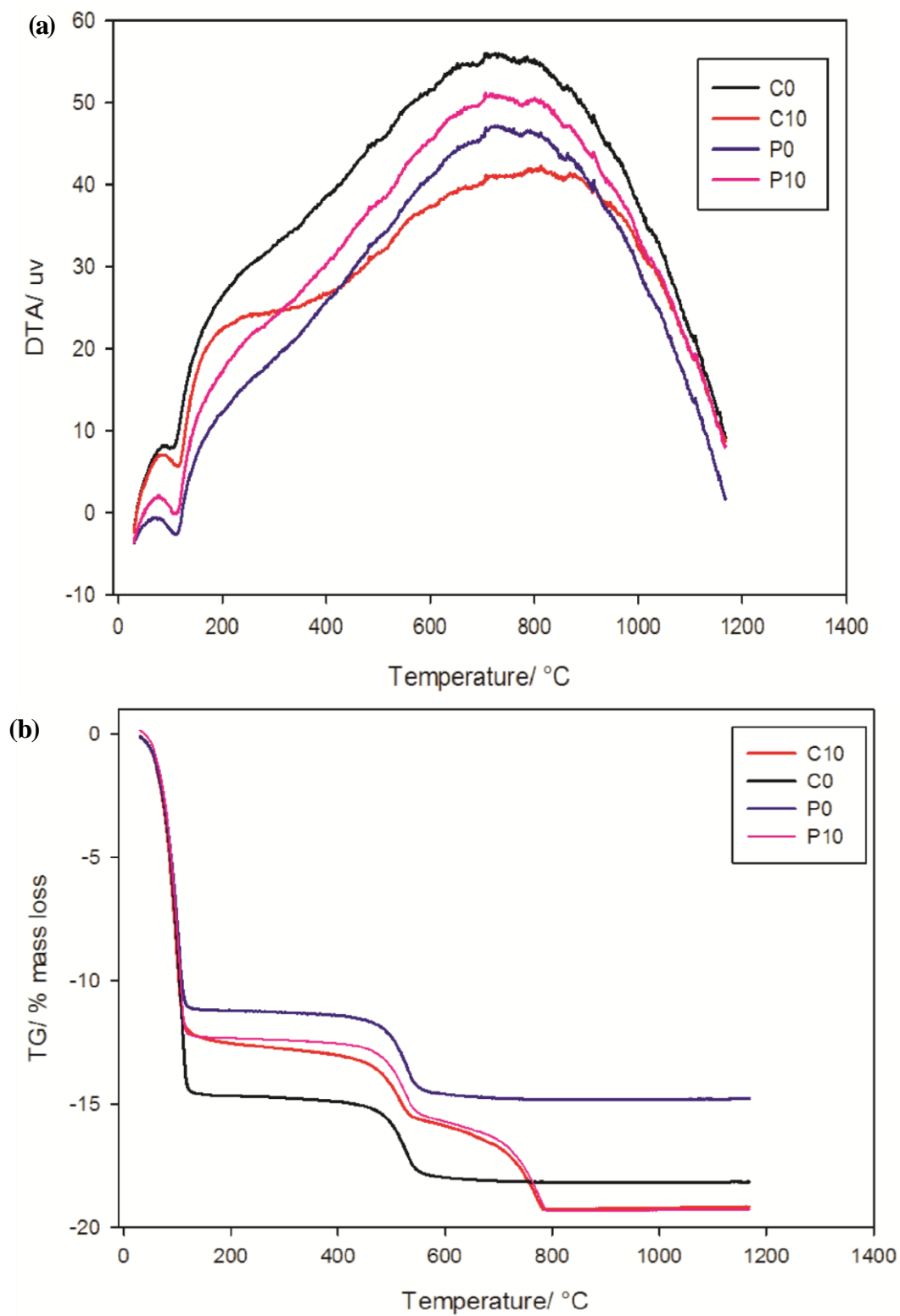


**Figure 29** :DTA (a)/ TG (b)curves of formulations (C0, C10, P0, P10)

As shown in Figure 29b, the Thermal gravimetric analysis of samples without addition of limestone (C0 and P0) showed the weight loss at two ranges whereas those with addition of limestone (C10 and P10) exhibited three ranges; the first range corresponds to the dehydration (50-127°C). The second range also common to all the samples (503-559°C) accompanied by weight loss, consistent with the evolution of the crystallization water that is progressively removed from the structure. The last one was observed only in samples with limestone addition around 780°C corresponding to the decomposition of calcite with a weight loss about 19%.

A focus on these curves permitted to have a good idea on the thermal behavior of various samples. At 1200°C, C0 seemed to shrink much more than P0, probably due to the presence of high Na<sub>2</sub>O content in its formulation. Both C10 and P10 presented similar trend of thermal behavior and were well densified compared to samples without addition of limestone (C0 and P0). The decomposition of calcite seemed to occur a bit earlier in samples (between 780 – 821°C) than in limestone raw material (~ 900°C) probably due to the formation of eutectics in samples during the sintering process.

**Figure 29c** let observe the variation of the thermal expansion of the porcelain specimens as function of the temperature up to 1300°C. From room temperature to 600 – 700°C, there is an expansion of the sintered matrices linked to the expansion phenomenon of the present phases. It is observed that in this range of temperature, P0 presented the highest value of expansion while C10 had the lower value. In fact, adding the limestone to the matrices, the overall expansion dropped. At ~ 595°C,  $\alpha$ ,  $\beta$  quartz transition occurred. The  $\alpha$ ,  $\beta$  quartz transition is significant in P0 and C0. The addition of limestone inhibited the  $\alpha$ ,  $\beta$  quartz transition surely due to the reduction of quartz content but also to the possible reaction between the silica available into the matrix and the CaO formed during the decomposition of limestone. All the dilatometric curves of the specimens showed a stability between 700 and ~980°C; in this range of temperature, there is no significant thermo-chemical transformation. As from 985°C, the formation of anorthite can justify the shrinkage observed in C10 and P10; the absence of mullite phase in these components can be explained by the fast formation of the liquid phase favoured by the addition of limestone which accelerated the formation of eutectics (Karamanov A., 2005). In the same time, P0 and C0 specimens show shrinkage at relatively high temperature due to the crystallization of mullite. Above 1150°C, the formation of high fraction of liquid phase contributed to the sintering of the matrices, closing porosity with consequent contraction of the matrices.



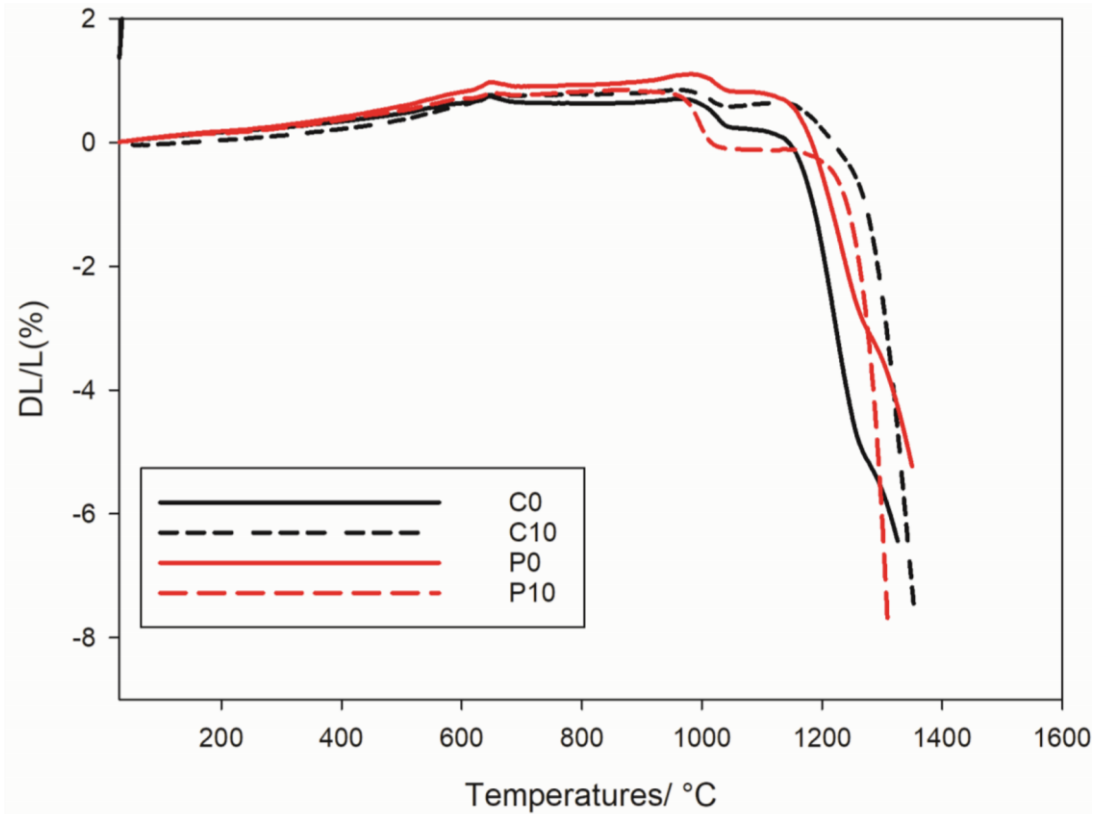


**Figure 29c:** Thermal expansion of formulation (C0, C10, P0, P10)

**b) Phase evolution of sintered samples**

The phase evolutions of sintered samples are presented in Figure 30. The common observation was that, during sintering process, the mixture of raw materials (composition) react and new crystalline phases were formed. These have been evidenced by many authors [M. Romero et al (2015), De la Torre et al (2009), Iqbal Y. (2000)]. In C0 and P0 samples, fired at 1200°C, the main phase observed is mullite, followed with quartz and amorphous silica. During the sintering of these samples, kaolinite ( $\text{Al}_2\text{O}_3 \cdot 2\text{SiO}_2 \cdot 2\text{H}_2\text{O}$ ), mica (phlogopite) and others feldspars minerals undergone different chemical reactions; as a result, part of quartz in the original raw materials mixtures is not present in the final composition and mullite ( $3\text{Al}_2\text{O}_3 \cdot 2\text{SiO}_2$ ) develops as an end product of the transformation of kaolin into metakaolinite and the metakaolinite into mullite ( $3\text{Al}_2\text{O}_3 \cdot 2\text{SiO}_2$ , ICDD: 00-015-0776). In fact, at 1200°C, metakaolin crystallised to mullite and amorphous silica following equation (20).

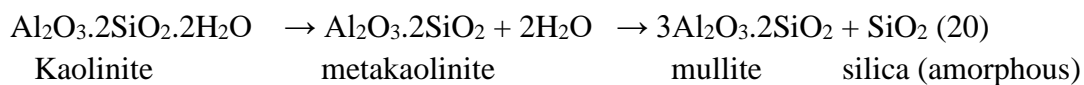
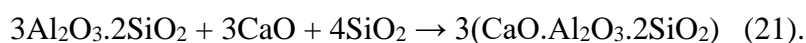
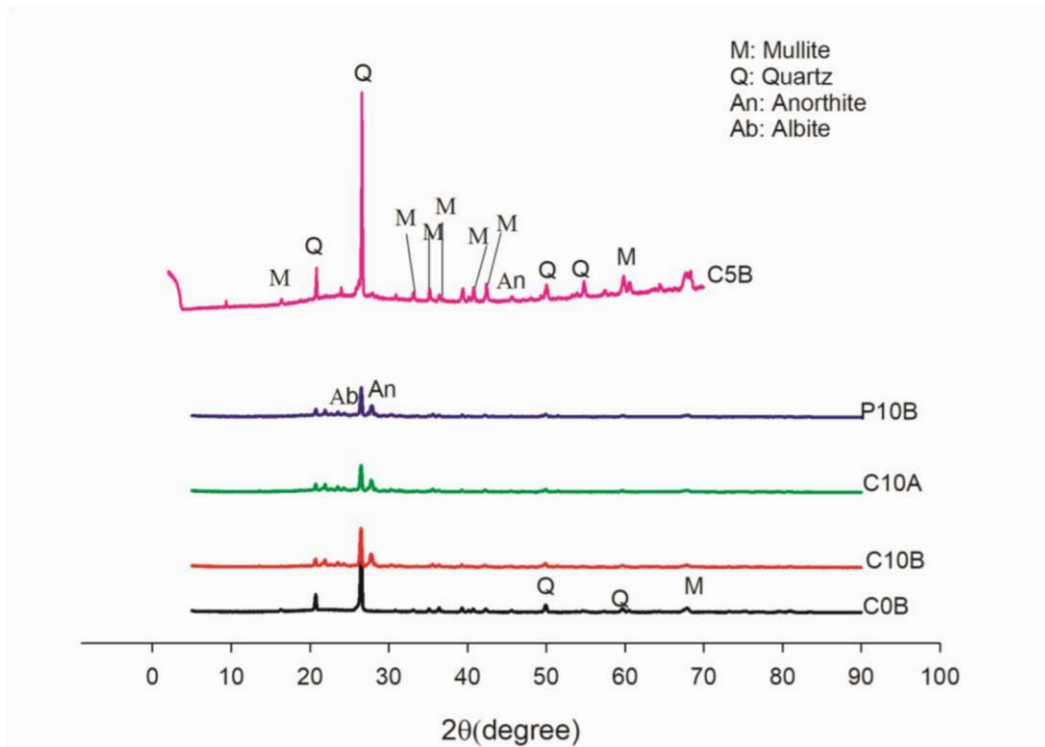


Figure 30 presents XRD analysis of sintered samples (C0, P0, C10 and P10) at 1175°C and 1200°C. In our reference samples (C0 and P0), up to 1175°C, the mullite phase was not found.

When the sintering temperature was raised up to 1200°C, mullite appeared as the main phase in reference samples. Anorthite (CaO.Al<sub>2</sub>O<sub>3</sub>.2H<sub>2</sub>O, ICDD: 00-020-0528) was found as the main phase in both series C10 and P10 (at 1200°C). Quartz, amorphous silica and albite were minor phases for P10 series and just quartz and amorphous silica in C10 series whereas, at 1175°C, albite appears as a phase in C10 sample; at this temperature, anorthite is still to be formed in quantity to appear. The fact that albite phase does not more appear in C10 sample at 1200°C can be explained by the excess quantity of limestone inside the bulk which formed more anorthite and inhibited albite as it can integrate in its matrix some quantities of sodium ions so, another form of anorthite (Na,Ca)(Al,Si)<sub>2</sub>Si<sub>2</sub>O<sub>8</sub> can be obtained. The absence of mullite phase in these component can be explained by the fast formation of the liquid phase favored by the addition of limestone which accelerated the formation of eutectics. This is in accordance with the work of Carty W. M. et al (1998) who concluded that: the eutectic temperature for potash feldspar with silica starts around 990°C and that, the lower liquid formation temperature in potash feldspar was beneficial for reducing the porcelain sintering temperature. In order to understand the transition from the mullite theory to the anorthite based porcelain stoneware, qualitative analysis was performed for P3 and C3 sintered at 1200°C; the two phases (mullite and anorthite) appeared. Both phases were influenced by limestone in all formulations. Thus, the increase of limestone amount favored the formation of the anorthite and conversely conducted to the disappearance of the mullite crystals in the matrix. In fact, the increase in the amount of limestone conducted to the formation of CaO which react faster with mullite to form anorthite (Rouabhia F., et al, 2018) according to equation (21):



All these phase transition and formation are directly linked and they influenced the physical properties and microstructure of the samples.



**Figure 30:** XRD pattern of fired samples

### III-4-2: Physical and mechanical properties: linear shrinkage, water absorption, density, flexural strength and hardness

The sintered bodies were further examined by measuring some of their physical properties such as linear shrinkage, water absorption, bulk density and flexural strength. The results of these physical test are presented in table 8a and 8b.

**Table 8a:** Physical properties values of C series

Sample	Temp (°C)	Water absorption(%)		Volume of op pores (%)		Apparent porosity (%)		Bulk density		Linear shrinkage Value(%)
		value	std	value	std	value	std	value	std	
C0	1150	7.56	0.83	6.12	0.04	18.16	0.75	2.03	0.015	3.03
COA	1175	6.55	0.19	5.82	0.05	14.4	0.67	2.19	0.01	6.99
COB	1200	4.33	0.50	3.17	0.01	9.61	0.01	2.22	0.09	8.02
COC	1225	2.91	0.31	2.13	0.01	8.10	0.013	2.7	0.11	8.85
COD	1250	1.42	0.34	1.748	0.01	0.39	0.01	2.83	0.08	9.12
C1	1150	3.67	0.32	4.60	0.05	10.31	0.61	2.13	0.02	3.67
C1A	1175	3.18	0.30	3.12	0.003	6.18	0.19	2.26	0.01	7.03
C1B	1200	2.38	0.25	1.17	0.01	1.123	0.03	2.31	0.01	8.22
C1C	1225	0.57	0.08	0.97	0.002	0.15	0.01	2.80	0.02	8.95
C3	1150	2.65	0.27	2.06	0.006	5.80	0.90	2.17	0.02	4.13
C3A	1175	0.89	0.14	1.66	0.003	2.35	0.77	2.33	0.02	8.88

C3B	1200	0.11	0.01	0.10	0.002	0.01	0.004	3.22	0.13	9.53
C3C	1225	0.2	0.01	0.09	0.001	0.03	0.002	2.78	0.12	6.56
C5	1150	2.31	0.20	2.02	0.001	4.83	0.9	2.25	0.01	6.28
C5A	1175	0.44	0.1	0.77	0.014	0.072	0.02	2.93	0.17	9.35
C5B	1200	0.09	0.030	0.17	0.002	0.209	0.072	2.79	0.16	7.42
C5C	1225	0.10	0.09	0.14	0.001	0.25	0.002	2.76	0.17	7.21
C7	1150	2.25	0.28	1.90	0.001	4.28	0.93	2.21	0.02	5.92
C7A	1175	0.34	0.09	0.24	0.001	1.17	0.008	2.53	0.02	8.59
C7B	1200	0.17	0.06	0.23	0.001	0.05	0.002	2.73	0.11	5.81
C7C	1225	0.12	0.07	0.20	0.003	0.32	0.002	2.5	0.14	5.58
C10	1150	2.23	0.28	1.82	0.005	4.15	0.73	2.18	0.03	6.13
C10A	1175	1.10	0.26	0.53	0.002	2.18	0.49	2.22	0.02	7.52
C10B	1200	0.18	0.08	0.25	0.007	0.05	0.002	2.67	0.06	4.80
C10C	1225	0.18	0.07	0.21	0.005	0.80	0.08	2.33	0.04	4.58

**Table 8b:** Physical properties values of P series

Sample	Temp (°C)	Water absorption (%)		Volume of open pores (%)		Apparent porosity (%)		Bulk density		Linear shrinkage Value (%)
		value	std	value	std	value	std	value	std	
P0	1150	7.28	0.8	6.08	0.002	16.82	0.88	2.08	0.02	2.80
POA	1175	6.76	0.57	5.46	0.002	14.51	1.25	2.142	0.03	4.94
POB	1200	4.53	0.56	4.18	0.012	10.04	0.015	2.214	0.02	5.61
POC	1225	2.89	0.45	2.716	0.018	8.136	0.014	2.78	0.10	7.14
POD	1250	1.38	0.17	1.92	0.01	0.36	0.004	2.81	0.07	7.43
P1	1150	3.75	0.34	4.3	0.052	12.8	0.57	2.18	0.04	3.20
P1A	1175	3.25	0.28	2.97	0.033	6.26	0.22	2.31	0.03	5.40
P1B	1200	2.05	0.15	1.12	0.038	0.97	0.10	2.74	0.01	6.35
P1C	1225	0.43	0.012	0.56	0.002	0.09	0.002	2.4	0.08	8.38
P3	1150	2.52	0.35	1.75	0.012	4.92	0.83	2.18	0.01	3.99
P3A	1175	0.25	0.08	0.322	0.001	0.78	0.028	2.85	0.02	8.59
P3B	1200	0.08	0.01	0.105	0.001	0.05	0.002	3.07	0.19	8.76
P3C	1225	0.16	0.06	0.09	0.002	0.10	0.04	2.75	0.13	8.85
P5	1150	2.47	0.33	1.7	0.022	4.85	0.83	2.19	0.02	6.05
P5A	1175	0.19	0.049	0.222	0.001	0.55	0.018	2.95	0.18	8.15
P5B	1200	0.1	0.064	0.33	0.015	0.034	0.002	3.09	0.19	8.54
P5C	1225	0.15	0.065	0.23	0.001	0.11	0.034	2.72	0.19	6.85
P7	1150	1.97	0.21	1.71	0.038	4.83	0.12	2.2	0.04	6.35
P7A	1175	0.37	0.1	0.28	0.001	1.57	0.37	2.52	0.03	8.13
P7B	1200	0.13	0.04	0.33	0.015	0.27	0.03	2.75	0.10	8.50
P7C	1225	0.34	0.10	0.23	0.001	0.79	0.003	2.43	0.05	4.57
P10	1150	2.12	0.23	1.68	0.043	3.88	0.17	2.18	0.04	4.07
P10A	1175	1.32	0.26	0.73	0.003	2.46	0.06	2.31	0.05	5.58
P10B	1200	0.17	0.08	0.20	0.001	0.29	0.002	2.75	0.10	6.97
P10C	1225	0.18	0.07	0.22	0.005	0.04	0.002	2.40	0.08	3.16

c) *Linear shrinkage*

Figure 31a and 31b highlighted the linear shrinkage true sintering at various temperature of C and P series respectively; the general observation were: the sample without addition (P0 and C0) shrinks continuously up to 1300°C; this is the normal behavior for common porcelain. When the amount of limestone increases, the linear shrinkage decreases. From 3% addition of limestone inside the compositions, the linear shrinkage increase up to a maximum and notice a common phenomenon of expansion without any deformation; this expansion phenomenon can be controlled up to 1225°C for these samples and contribute to reduce the linear shrinkage of anorthite based porcelain stoneware. These results corroborate with the investigation reported by Claudia Lira et al (1998). The authors studied the effect of calcium carbonate on the firing shrinkage of porous ceramics and then found that its addition reduced the firing shrinkage. The maximum shrinkage depends on the serie and the mass percent addition of limestone. This maximum shrinkage may be correspond to the maximum formation of liquid phase which induce the vitrification of the sample. For C serie, C3 achieved the maximum shrinkage at 1200°C whereas, P3 achieves at 1225°C. From C5 to C10, the maximum shrinkage was achieved at 1175°C whereas, from P5 to P10, maximum was achieved at 1200°C. After the decomposition of limestone, the carbon dioxide (CO<sub>2</sub>) gas remained in the specimens. Their evaporation was responsible to the increasing of level of porosities which consequently was responsible for the reduction of shrinkage.

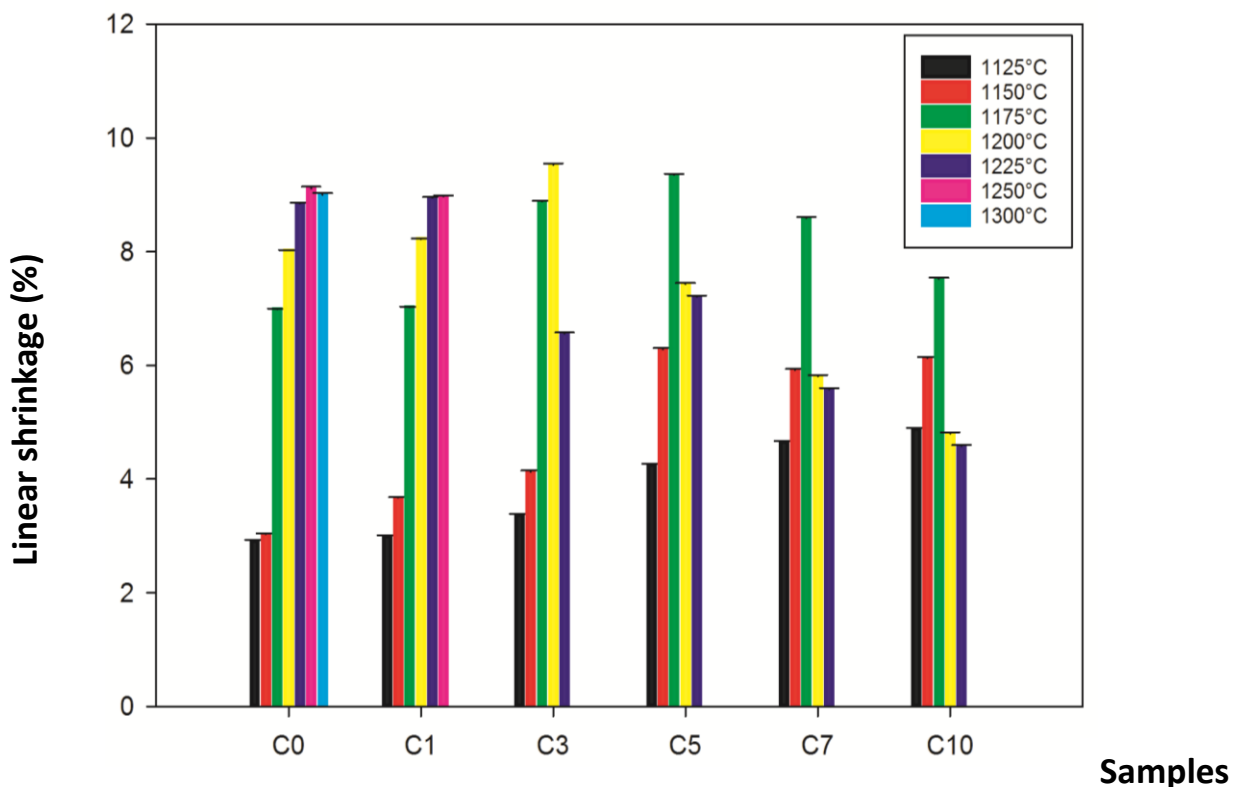


**Figure 31a:** Linear shrinkage true sintering at various temperature of C series

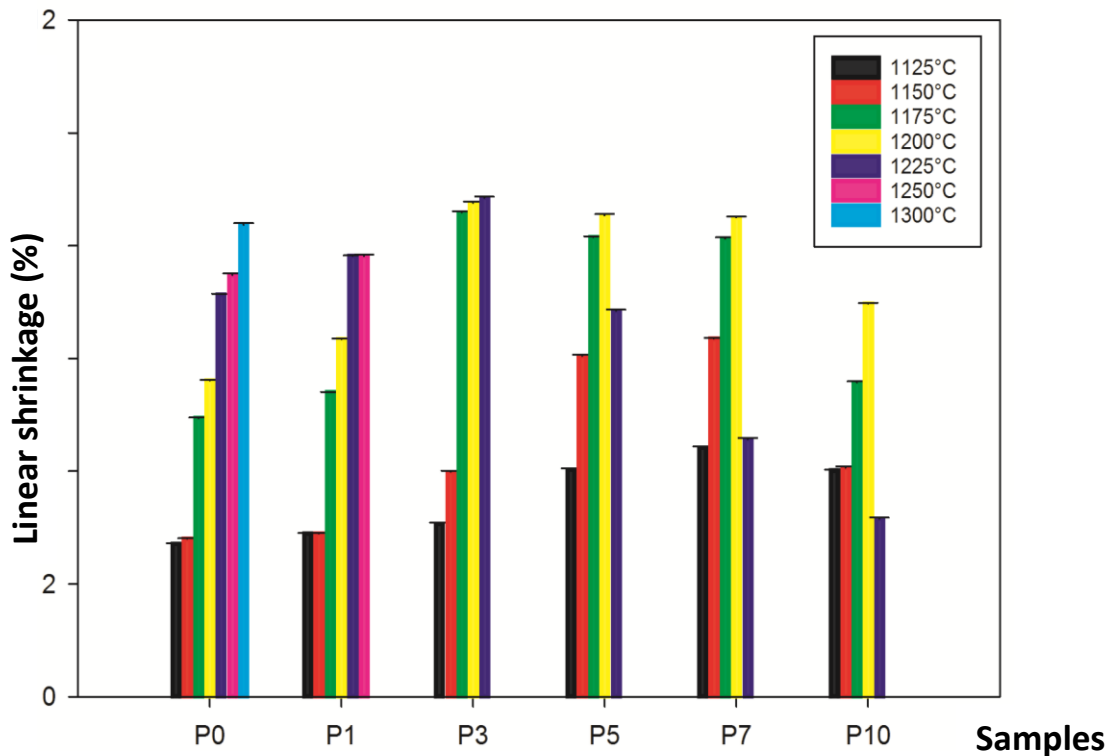


**Figure 31b:** Linear shrinkage true sintering at various temperature of P series

**d) Water absorption**

Water absorption is generally used as one of the parameter to evaluate the maturation in term of level of vitrification in porcelain, stoneware, and other classes of traditionally used ceramics (Tchakounte et al, 2013). The values of water absorption for all the samples are presented in Figure 31a and 31b for C and P series respectively. It was noticed that the water absorption of standard porcelain C0 and P0 decreased from 7.6% at 1125°C to 0.5% at 1300°C. According to the standard, it is only at this temperature (1300°C) that the standard porcelain presents the optimum vitrification. The addition of 1% limestone conducted to a decrease in the value of water absorption under 7% for both C and P series when the temperature of 1125°C is considered. This 1% of limestone reduced the optimum vitrification (Water absorption < 0.5%) at 1225°C for C and P series. As from 3% addition of limestone, the water absorption dropped considerably to below 4% at 1125°C for both C and P series and the temperature of maximum vitrification decreased again to 1180°C. It should be noted that above 7% of limestone, there is a tendency of an increase in the concentration of closed pores which induced the connectivity of some of these pores accessible to water. It was noticed that, for each sample, water absorption decreased with increasing temperature but for some samples with the addition of 3 to 10 percent of limestone, low water absorption values were obtained between 1175 and 1200°C. After the minima values, water absorption of those samples seemed to relatively increase. This

phenomenon is in agreement with that observed in linear shrinkage where it was observed an expansion phenomenon of those same samples after the maximum shrinkage between 1175°C and 1200°C. Sample C3 achieved a water absorption of 0.11% at 1200°C whereas P3 achieved 0.25% at 1175°C and 0.08% at 1200°C; progressively, C5 achieved a value of 0.4% at 1175°C and 0.09% at 1200°C where P5 achieved 0.19 and 0.09% water absorption at 1175 and 1200°C respectively: the series of 7 and 10% mass addition of limestone also performed very low water absorption at these temperatures. These results were in agreement with the work of Carty W.M. et al (1998). Tchakounte et al (2013) in their work reported that the use of orthoclase with CaO as mineralizer seems to offer a promising route with advantages including the energy saving. The two series exhibited lower water absorption but P series resulting from a more potash feldspar combined with albite performed better. This is in accordance with one of the conclusions of Carty W.M. et al (1998) who reported that the presence of albite in potash feldspar can reduce the liquid formation temperature by as much as 60°C.

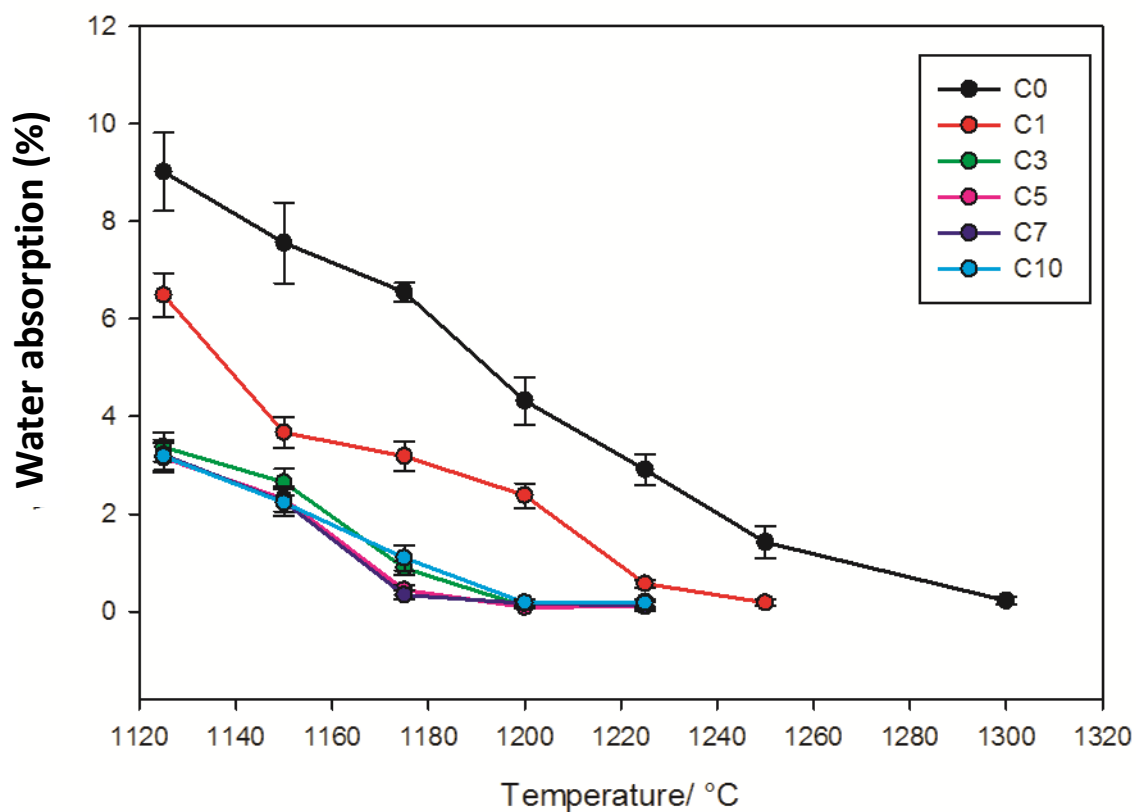


**Figure 32a:** Water Absorption true sintering at various temperature of C series

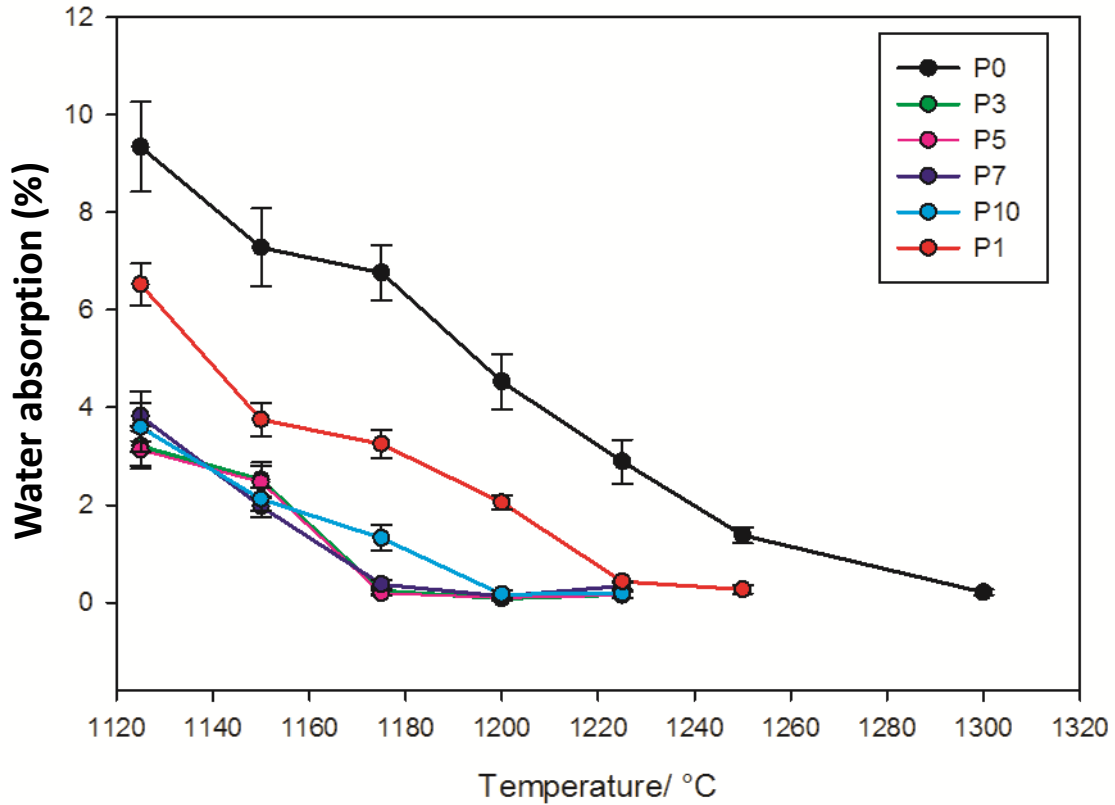


**Figure 32b:** Water Absorption true sintering at various temperature of P series

**e) Bulk Density**

As shown in Figure 33a and 33b, bulk densities of sintered reference samples (C0 and P0) increased continuously from  $2.02 \pm 0.08 \text{ g/cm}^3$  to  $2.81 \pm 0.07 \text{ g/cm}^3$  at  $1250^\circ\text{C}$ . When the sintered temperature was increased to  $1300^\circ\text{C}$ , the bulk density decreased to  $2.24 \pm 0.09 \text{ g/cm}^3$ . This may be due to the formation of many pores issued by melting and flowing of fluxing agent. With 1wt. % addition of limestone, the density of samples increased compared to reference sample at the same temperature; these samples achieved maximum densification of  $2.8 \pm 0.02 \text{ g/cm}^3$  at  $1200$  and  $1225^\circ\text{C}$  for P and C series, respectively. With 3wt. % addition of limestone, the samples showed good densification and achieved a maximum ( $3.22 \pm 0.13 \text{ g/cm}^3$  for C series and  $3.07 \pm 0.19 \text{ g/cm}^3$  for P) at  $1200^\circ\text{C}$ . In fact, at higher temperatures, limestone contributed more in crystallization and densification of the matrices. Samples with 5, 7 and 10 wt. % addition of limestone also achieved maximum densification at  $1200^\circ\text{C}$ . When the amount of limestone is above 5wt. % in both series (C and P), the specimen became less dense. These observations can be linked with the formation of more closed pores due to the elimination of  $\text{CO}_2$  as noticed previously. In general, it can be noted that the maximum densification corresponds to maximum vitrification (minimum water absorption) and the maximum shrinkage.



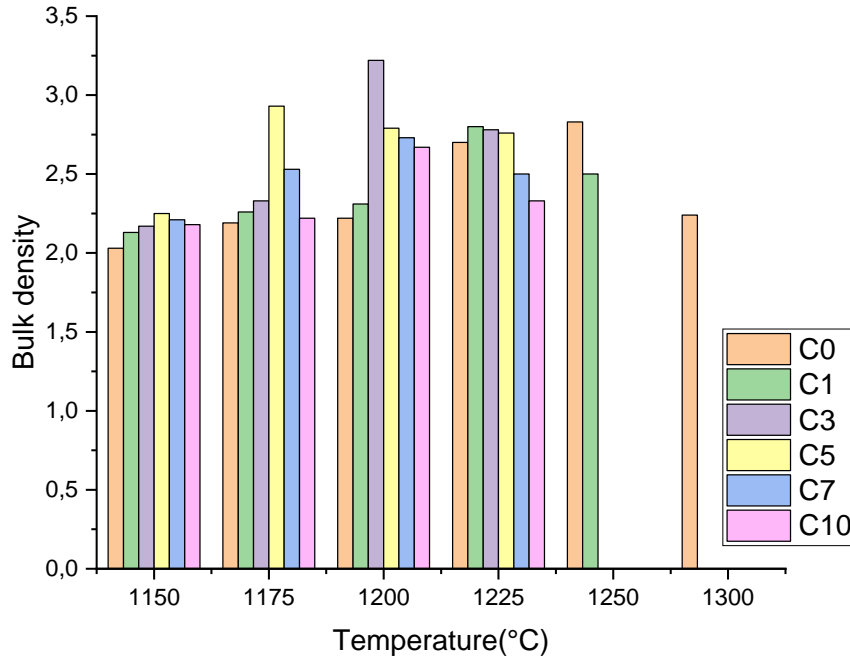


**Figure 33a:** Bulk density of sintered samples (C Series)

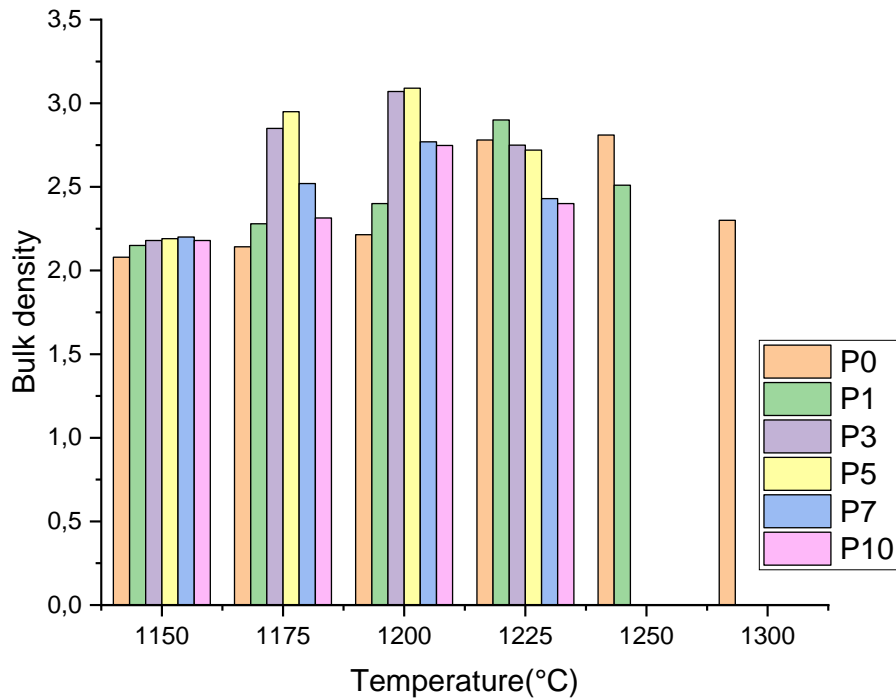


**Figure 33b:** Bulk density of sintered samples (P Serie)

*f) Open pores volume*

Open pores volume of sintered samples is presented in figure 34a and 34b. For references samples C0 and P0, when the sintering temperature increased from 1150°C to 1300°C, the open

pores volume decreased drastically from  $6.12 \pm 0.04\%$  to  $0.005 \pm 0.001\%$ . The behavior of the two references samples are quite similar; between 1250 and 1300°C, the decreasing is noticeable from  $1.91 \pm 0.01$  averagely to almost zero. This can be explained by melting of the fluxing agent and flowing of liquid phase which fill all the cavities connectivity. With 1wt% addition of limestone, it was observed that, starting from 1150°C, open pores volumes are smallest compared to reference samples at the same temperatures, meaning that, fluxing process began earlier. The minimum open pores volume of  $0.55 \pm 0.002\%$  was reached at 1250°C. With 3wt% addition of limestone, the minimum open pores volume ( $0.1 \pm 0.002\%$  for C and P series) is reached at 1200°C. Almost the same values were respectively repeated at 1225°C; P5 exhibited minimum open pores volume of 0.07% at low temperature (1175°C). This could be attributed to the crystallization phenomenon due to incongruent melting of the fluxing agent. Above this temperature, the normal melting process continued and a slight increase of open pores volumes was noticed. P7 and P10 presented the same behavior but their minimum open pores value (0.05%) was reached at 1200°C. Sample C5 acted differently and a continuous decrease of open pores volume was noticed with increasing temperature; the values varied from  $2.02 \pm 0.001$  to  $0.14 \pm 0.001\%$ . C7 and C10 had the same behavior as C5.

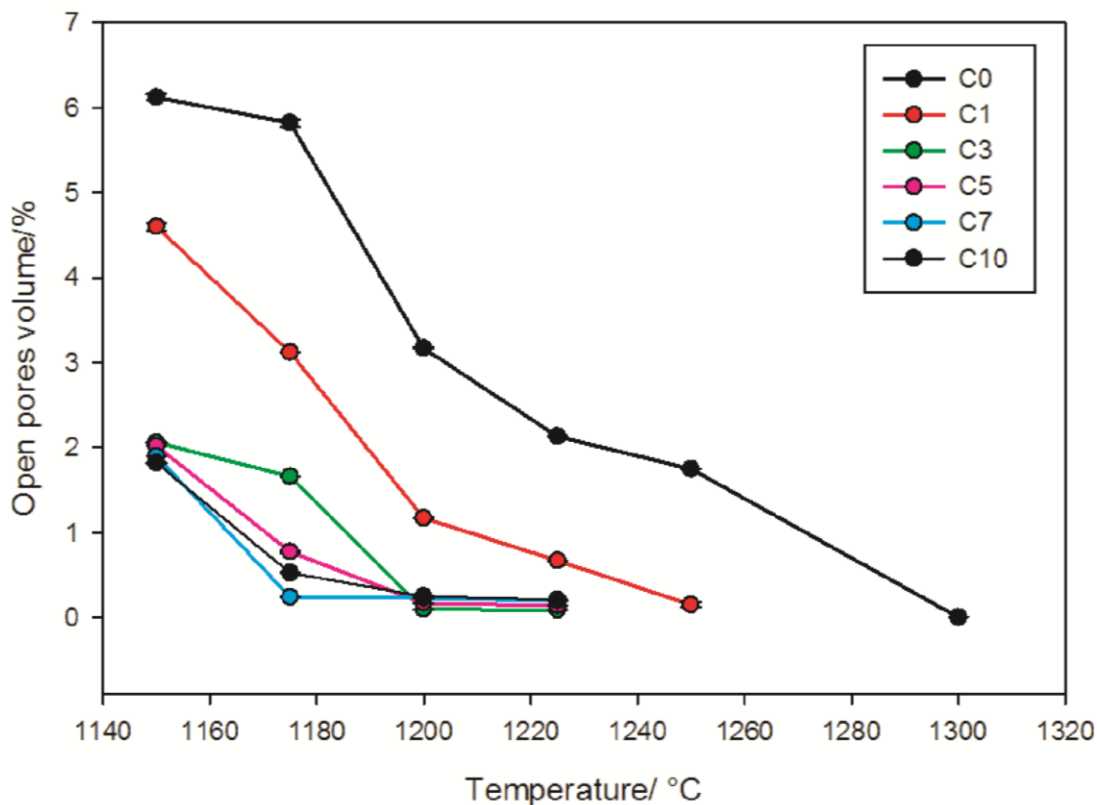


**Figure 34a:** Open pores volume of sintered samples (C serie)

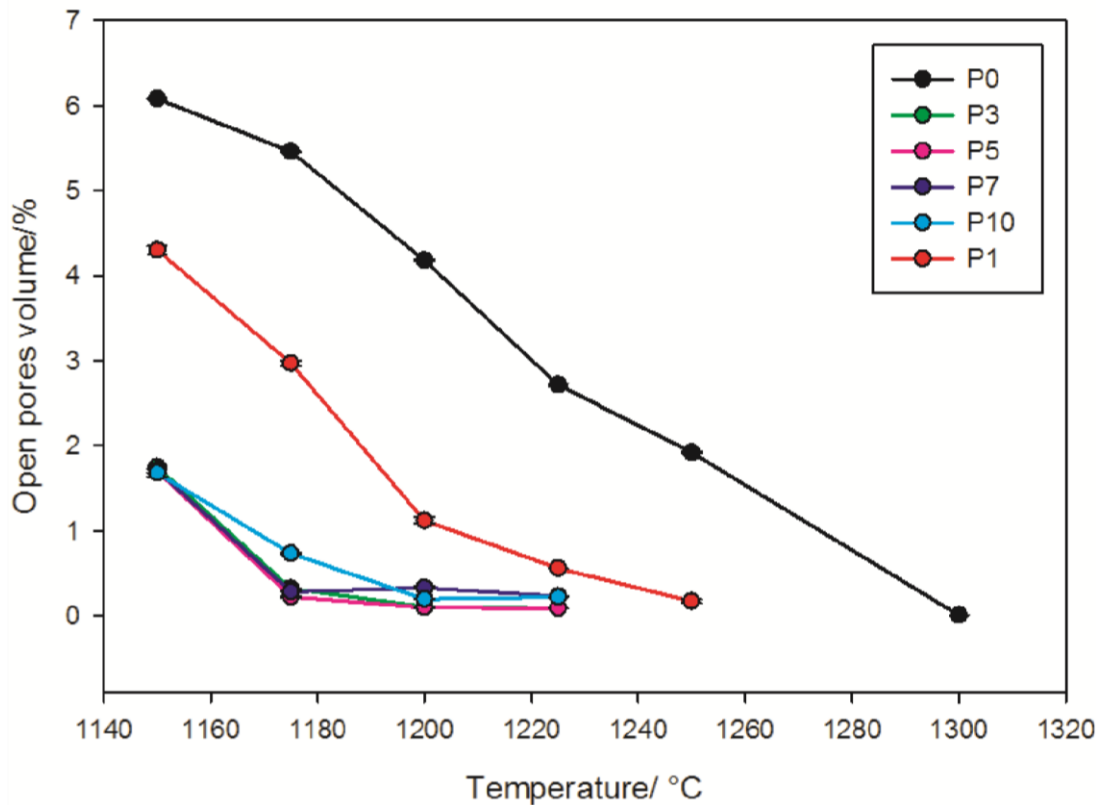


**Figure 34b:** Open pores volume of sintered samples (P series)

**g) Apparent porosity**

The apparent porosity of all the samples (figures 35a and 35b) was directly linked to their open pores volume and both presented similar behavior. With reference samples, these values were higher compared to those of open pore volume. With the addition of limestone to the formulation, the trend seemed to reverse. The evolution of these parameters was quiet the same for all compositions; generally, within these range of temperatures, the density increased with temperature as open pores volume and apparent porosity decreased. With 10 percent mass addition of limestone, there were; for C series,  $0.25 \pm 0.01$  % of open pores,  $0.3 \pm 0.001$ % of apparent porosity and a density of  $2.67 \pm 0.06$  g/cm<sup>3</sup>; for P series,  $0.20 \pm 0.001$ % of open pores volume,  $0.3\% \pm 0.002$  of apparent porosity and a density of  $2.75 \pm 0.11$ g/cm<sup>3</sup> at 1200°C. These values were still very good compared to international standard for porcelain and porcelain stoneware tiles (Dondi M. et al, 1999). Nevertheless, the porosity increased and the bulk density decreased in the samples containing the high amounts of limestone (> 7%) compared to those containing low amounts of limestone. This fact led to an assumption that it is possible to move from full dense matrix to porous matrix with other applications by increasing the mass percentage of limestone; further investigations will concern the field.

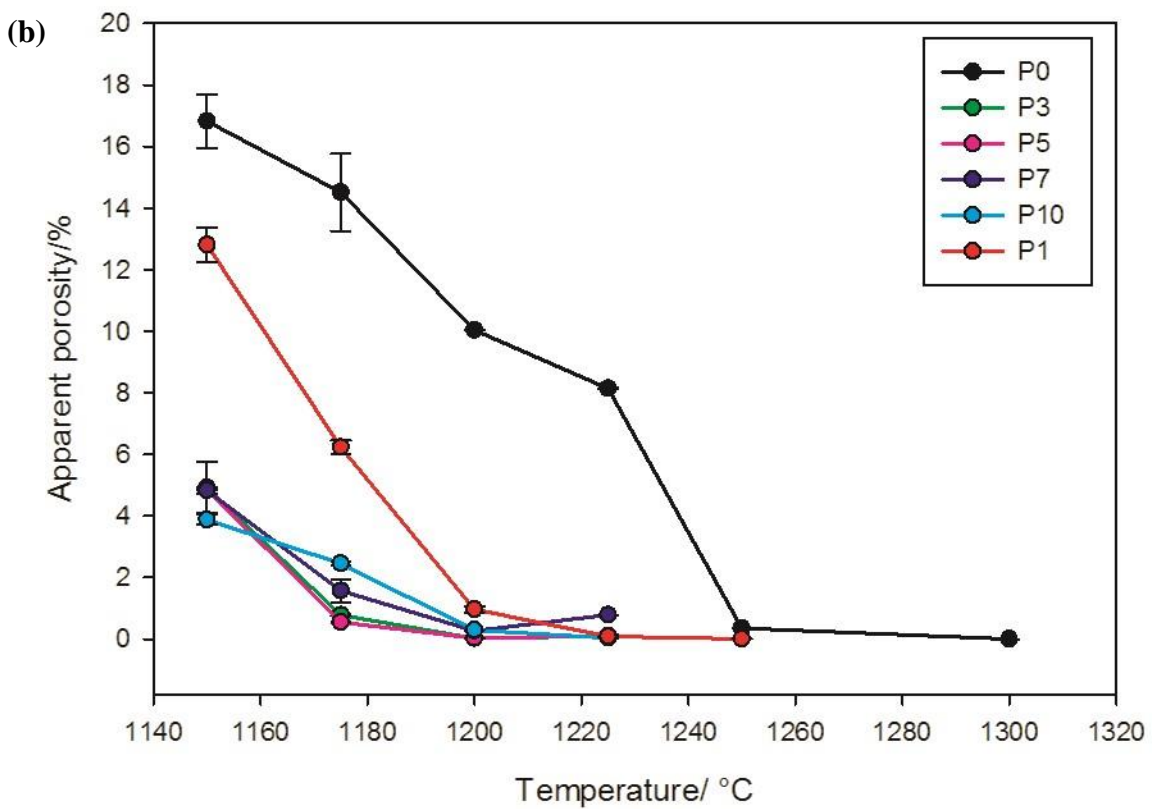
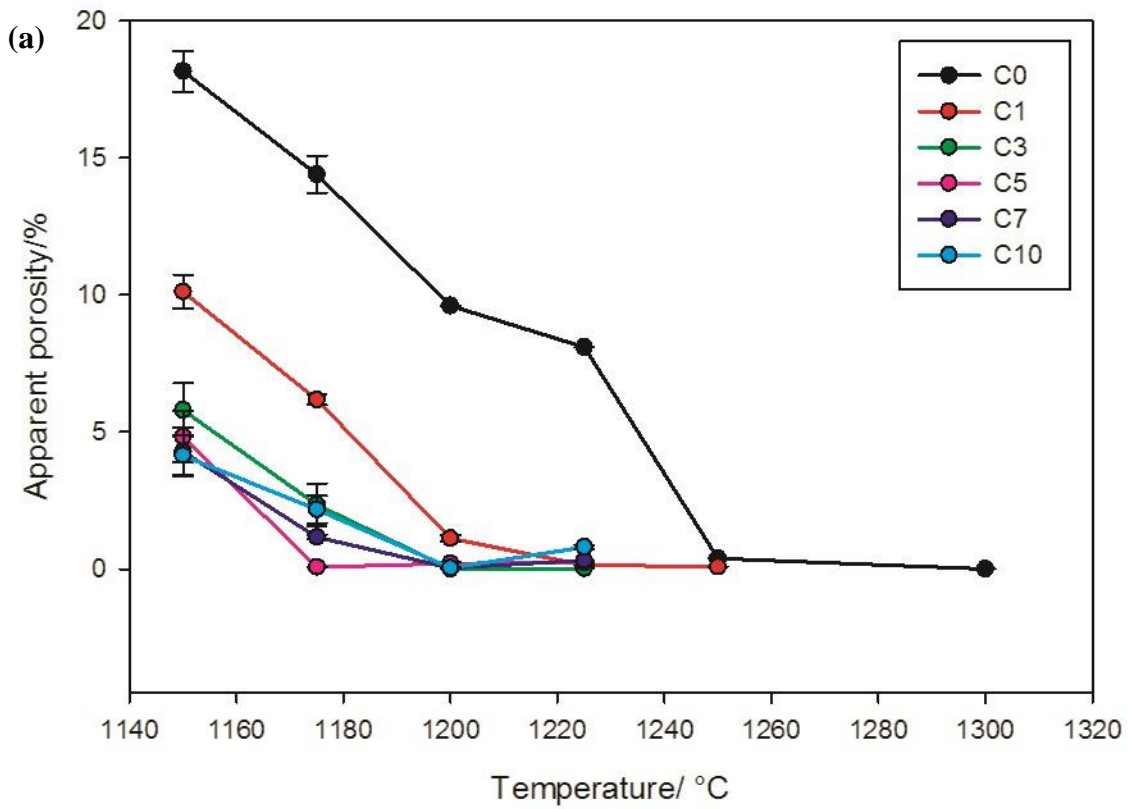


**Figure 35:** Apparent porosity of sintered samples (a) for C serie end (b) for P series)

### *h) Cumulative pores volume*

Figure 36a and 36b highlighted the cumulative pore volume of samples as function of radius. Formulations without addition of limestone showed high volume of porosity when sintered at 1175°C: cumulative pore volume  $> 50\text{mm}^3/\text{g}$  for C series and  $> 60\text{mm}^3/\text{g}$  for P series. The temperature of 1300°C made cumulative pore volume dropped down to  $2\text{mm}^3/\text{g}$  for C and P series (C0 and P0 at 1300°C 'C0E and P0E) confirming that high temperature is required for optimum vitrification of standard porcelain and to induce the closing of pores. However, the result showed that significant reduction of porosity can be achieved at low temperature with the addition of limestone. In general, formulations with limestone presented low porosity independent of the nature of the feldspar. P and C series showed similar trends with pores volume under  $2\text{mm}^3/\text{g}$  in agreement with the theory that presents porcelain as non-porous semi-vitrified matrix. Although the slight increase in the fraction of macro pores ( $> 1\mu\text{m}$ ), the overall behavior of the CaO based porcelain matrices is in agreement with the definition and requirements regarding porcelain and particularly porcelain stoneware. The significant reduction of cumulative pore volume from  $\approx 50\text{mm}^3/\text{g}$  to  $< 2\text{mm}^3/\text{g}$  is indicative of the efficiency of CaO to act in the  $\text{K}_2\text{O}$  based feldspathic semi-vitrified matrix for the reduction of the sintering temperature and the improvement of the sustainability of the final matrix.

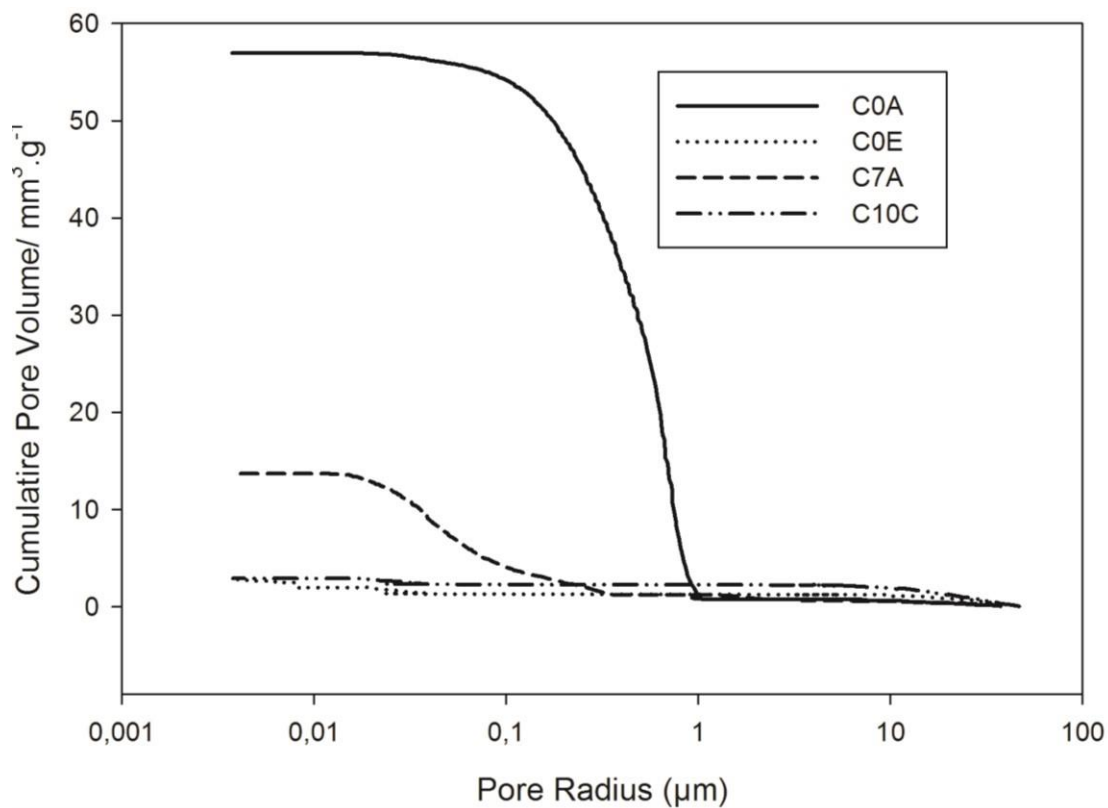


**Figure 36a:** Cumulative pore volume of samples (C series) as function of radius

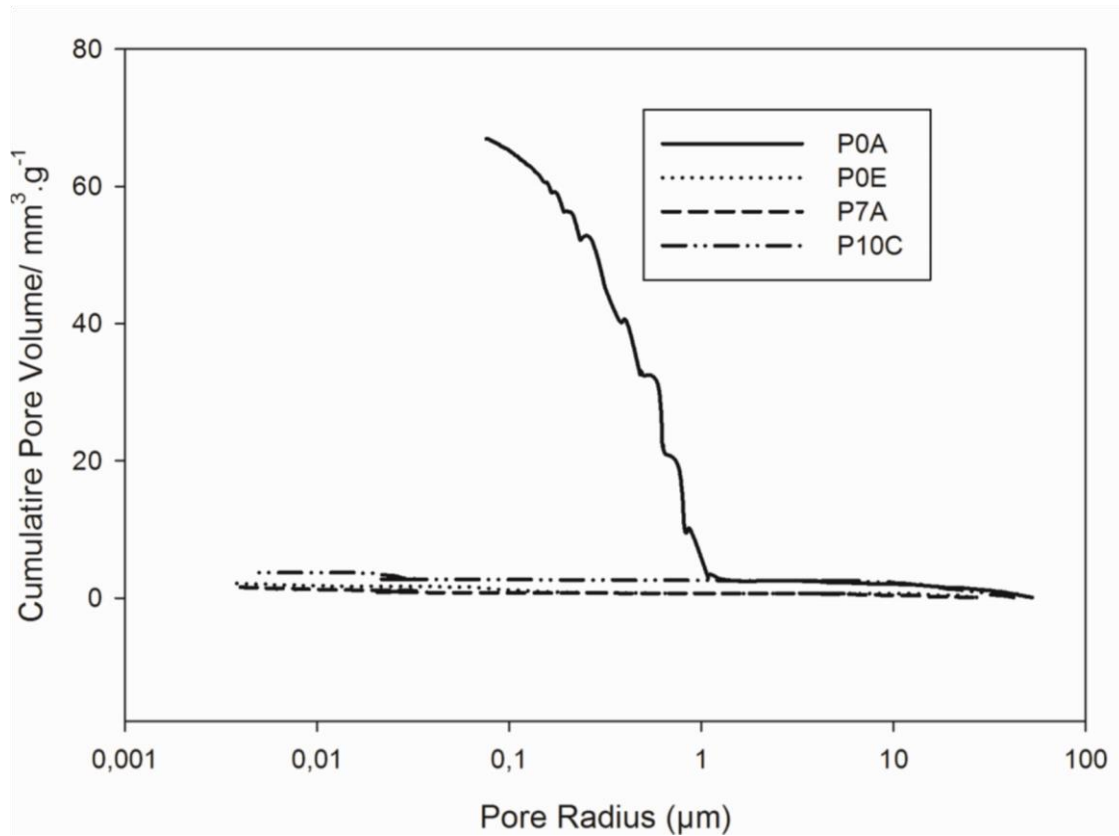


**Figure 36b:** Cumulative pore volume of samples (P series) as function of radius

*i) Flexural strength*

Flexural strength (Figures 37a and 37b) completed and confirmed the physical characteristics mentioned above. Generally, maximum flexural strength develops in porcelain stoneware body when apparent porosity decreases to zero (Oluseyi et al, 2013). Similar results were obtained in this study. For reference samples (without addition of limestone), a continuous increase in flexural strength with increasing of temperature up to 1300°C was noticed ( $109 \pm 1.20$  MPa for C series based on Boboyo feldspar and  $117 \pm 1.00$  MPa for P series based on Manjo feldspar). At 1250°C, P0 and C0 achieved  $96$  and  $86 \pm 2.04$  MPa, respectively whereas at 1225 and 1200°C, P0 and C0 achieved respectively  $86.8$  and  $78.7 \pm 0.90$  MPa. This is in accordance with the general behavior of clays feldspars based ceramics, where results in the increase of sintering temperature leads to high mullite formation and thereby resulted in the improvement of mechanical properties (Ke S. et al, 2013). With 1wt% addition of limestone, the flexural strength increased continuously up to a maximum ( $113 \pm 1.80$  and  $97 \pm 2.00$  MPa for C and P series) at 1250°C. Samples with 3wt% addition of limestone achieved their maximum flexural strengths at 1200°C ( $104 \pm 0.65$  and  $110 \pm 1.30$  MPa) for C and P series respectively. This was the same case of 5wt% addition where they achieved  $106.4 \pm 2.20$  and  $107.3 \pm 1.60$  MPa for C and P respectively. With 7wt% addition, the maximum flexural strength was achieved at low

temperature (1175°C) with  $110 \pm 0.90$  and  $138 \pm 2.0$  MPa for C and P series respectively. It was noticed that, the addition of limestone favors significant increase in the flexural strength, consequently, the crystallization phenomenon. These results corroborated the open pores volume behavior.

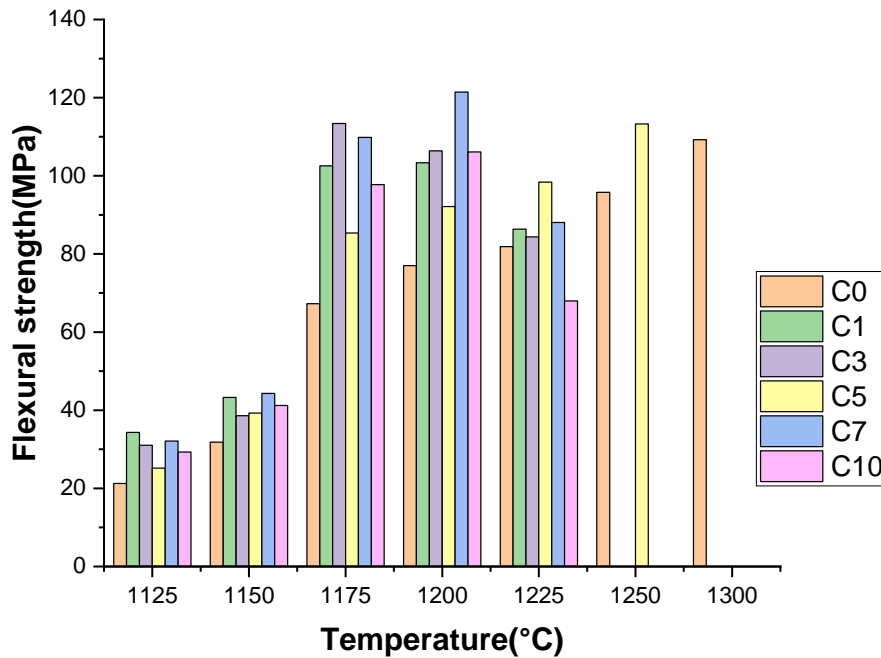


**Figure 37a:** Flexural strength of sintered samples (C series)

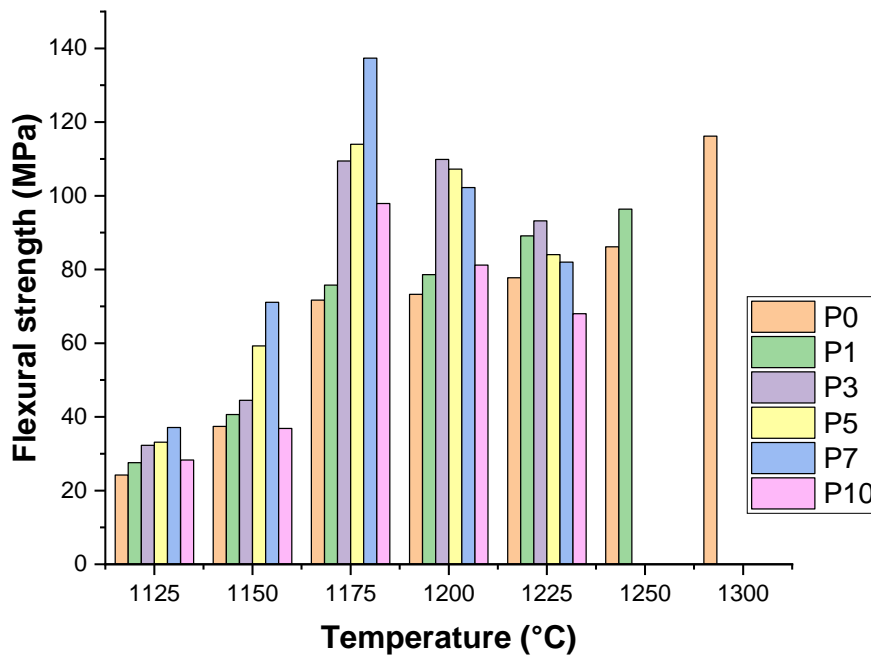


**Figure 37b:** Flexural strength of sintered samples (P series)

### III-5: Study of correlations between physical properties

#### III-5-1 : Study of the correlation between flexural strength and density

Figures 38a to 38d retrace the correlation between flexural strength and density for samples of C and P series at 1175 and 1200°C respectively; At first glance, the different curves taken in pairs do not look exactly the same. An analysis of the data of these curves shows that: at 1175 and 1200 °C, for the reference compositions C0 and P0, the low resistance values correspond to the low density values.

At 1175 °C, composition C3 shows a flexural strength of 114 MPa for a density of 2.33 g/cm<sup>3</sup>; this density increases to 3.22 g/cm<sup>3</sup> with the increase in temperature to 1200 °C. In compositions C7 and C10, a combined growth in flexural strength and density (from 2.53 to 2.73 g/cm<sup>3</sup> and from 110 to 123 MPa) is observed for composition C7. For composition C10, density of 2.22 to 2.5 g/cm<sup>3</sup> and a strength of 98 to 106 MPa when we go from 1175 to 1200 °C. Composition C5 exhibits the properties of an ideal ceramic at 1175 °C with high density (2.93 g/cm<sup>3</sup>) and high flexural strength (102.3 Mpa).

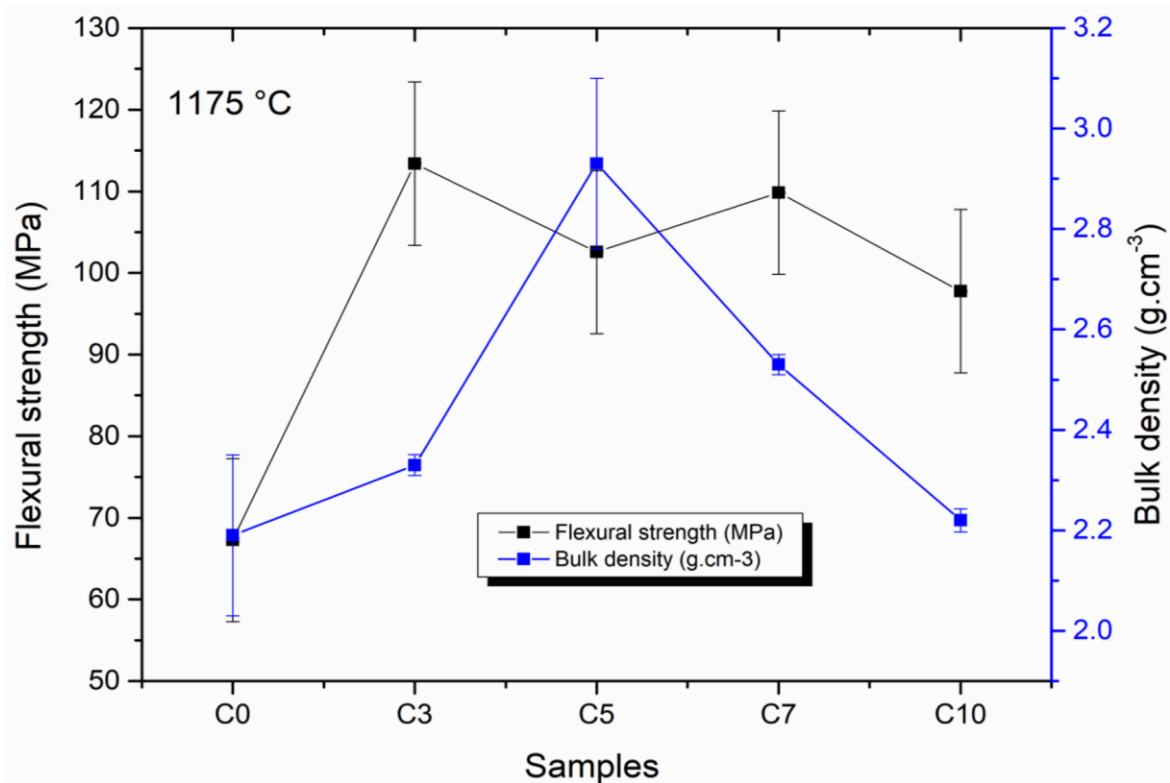


**Figure 38a:** Correlation between flexural strength and density for C serie at 1175°C



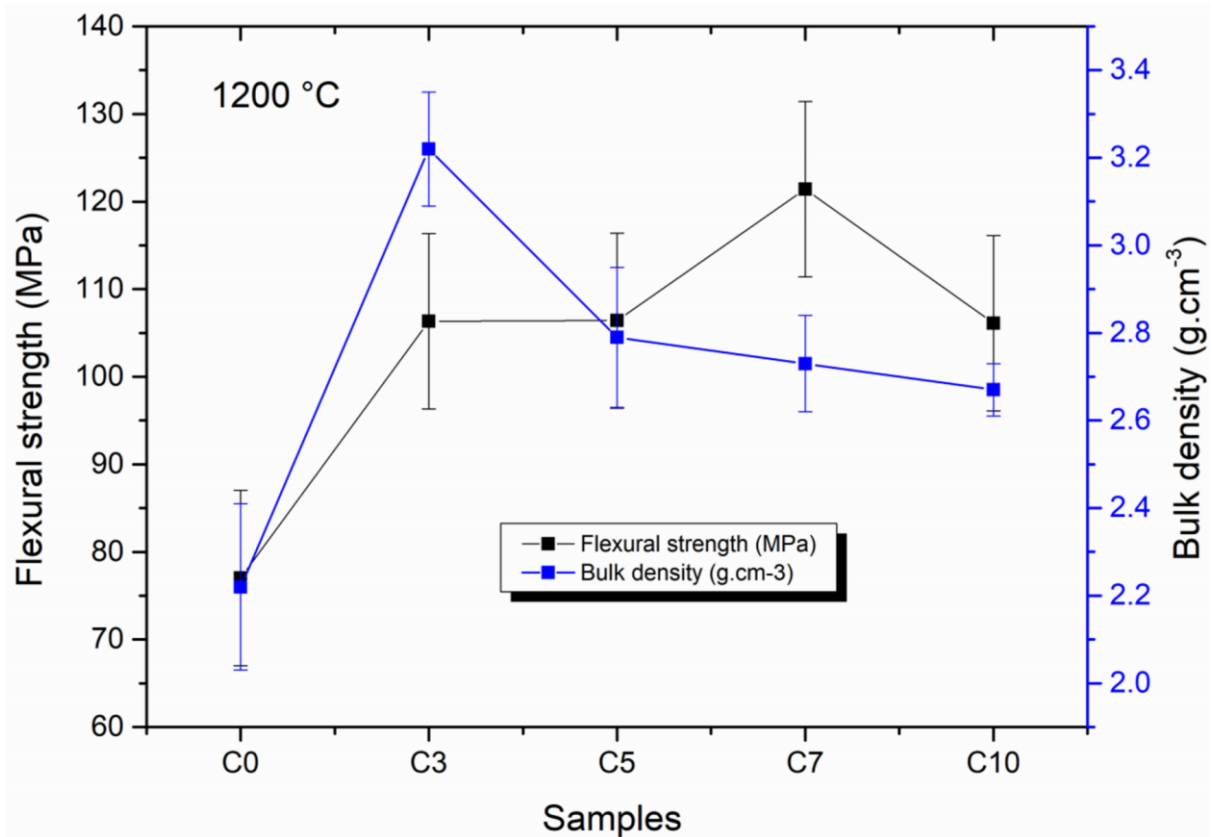


**Figure 38b:** Correlation between flexural strength and density for C serie at 1200°C

In the P series, at 1175 °C, a continuous increase in flexural strength and density is observed with increasing of limestone percentage from 0 to 5%. With composition P7 (7% addition of limestone), a large strength peak is observed at 1175 °C with a relatively low density (2.5 g/cm<sup>3</sup>); these data reflect the matrix crystallization phenomenon at this temperature, due to the formation of eutectics. The increase in temperature to 1200°C disrupts the structure of composition P7 with the melting of the crystallization points, the resistance peak observed at 1175 °C drops to 105 MPa but this time, the material gains in density (2.75 g/cm<sup>3</sup>). The same phenomenon is observed for the compositions P3 and P5 but with less pronounced intensities; the materials lose a bit in resistance and gain in density when going from 1175 to 1200°C [(from 110 MPa, 2.85 g / cm<sup>3</sup> to (108 MPa, 3.1 g/cm<sup>3</sup>) for composition P3 and from (113 MPa, 2.9 g / cm<sup>3</sup>) to (106 MPa, 3.05 g / cm<sup>3</sup>) for composition P5].

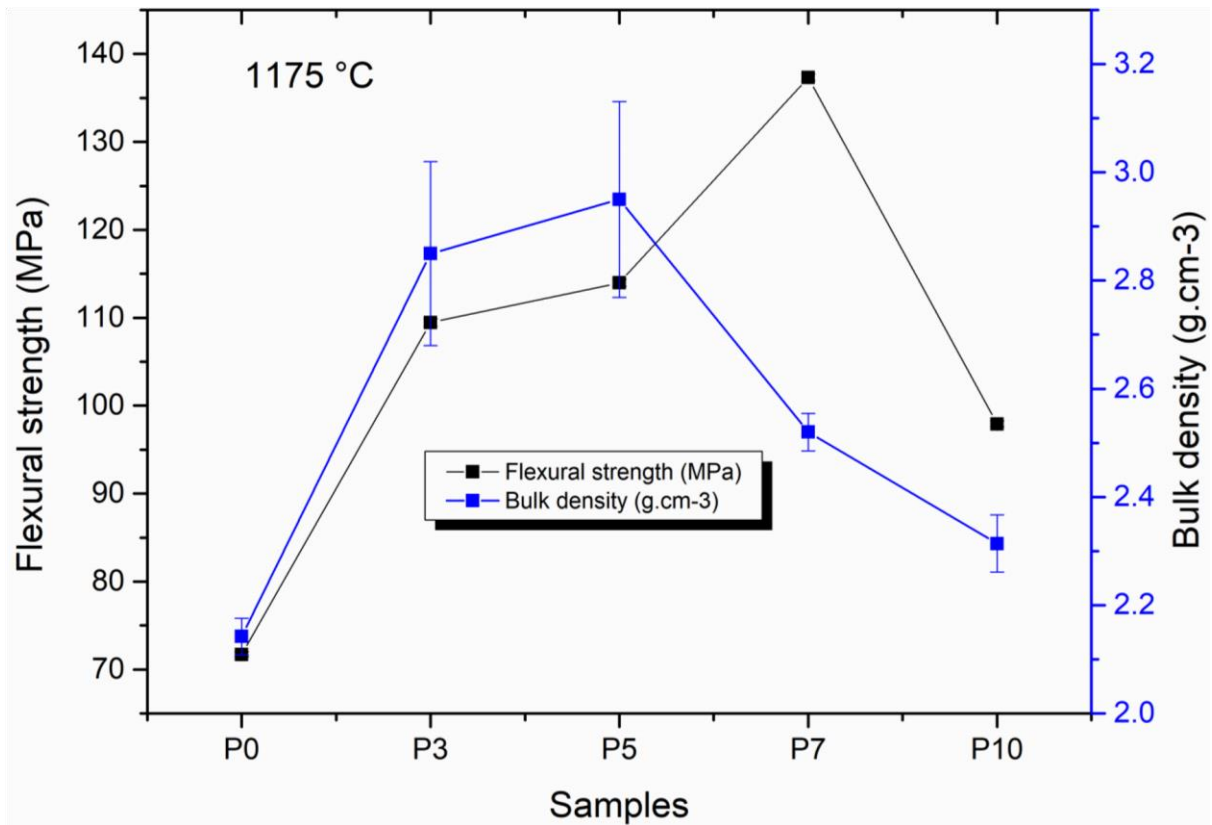


**Figure 38c:** Correlation between flexural strength and density for P series at 1175°C

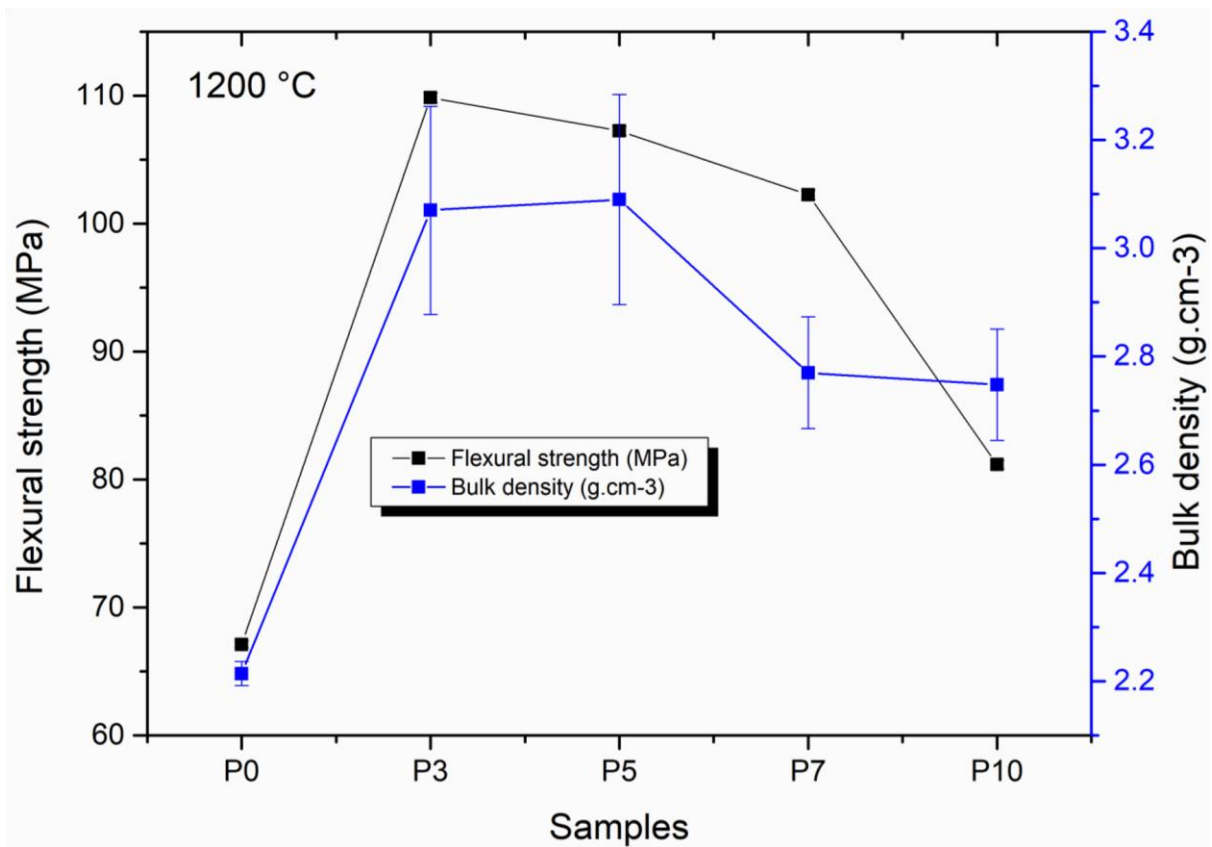


**Figure 38d:** Correlation between flexural strength and density for P series at 1200°C

From the interpretation of these data, it emerges that with the addition of limestone in variable and controlled proportion, the phenomenon highlighted at 1175 °C is that of the crystallization of the ceramic matrix.

### *III-5-2 : Study of the correlation between the evolution of water absorption and the volume of open pores*

Observations of the curves in figures 39a to 39c show an almost perfect correlation between water absorption and open porosity both at 1175°C and at 1200 °C for the compositions of the C and P series up to at 1200 ° C. The reference samples remain very porous with high open porosity values and high water absorption; samples with added limestone are less porous. Analysis of the data and curves shows that, the water absorption values are slightly higher than those for open pores for porous samples; this phenomenon is explained by the fact that when a material is soaked, water fills not only the interconnected pores, but also the closed pores. The values of the two parameters tend to balance or even invert as the material becomes denser; this could be explain by the fact that, as the material vitrifies, open pores disappear living small closes pores.

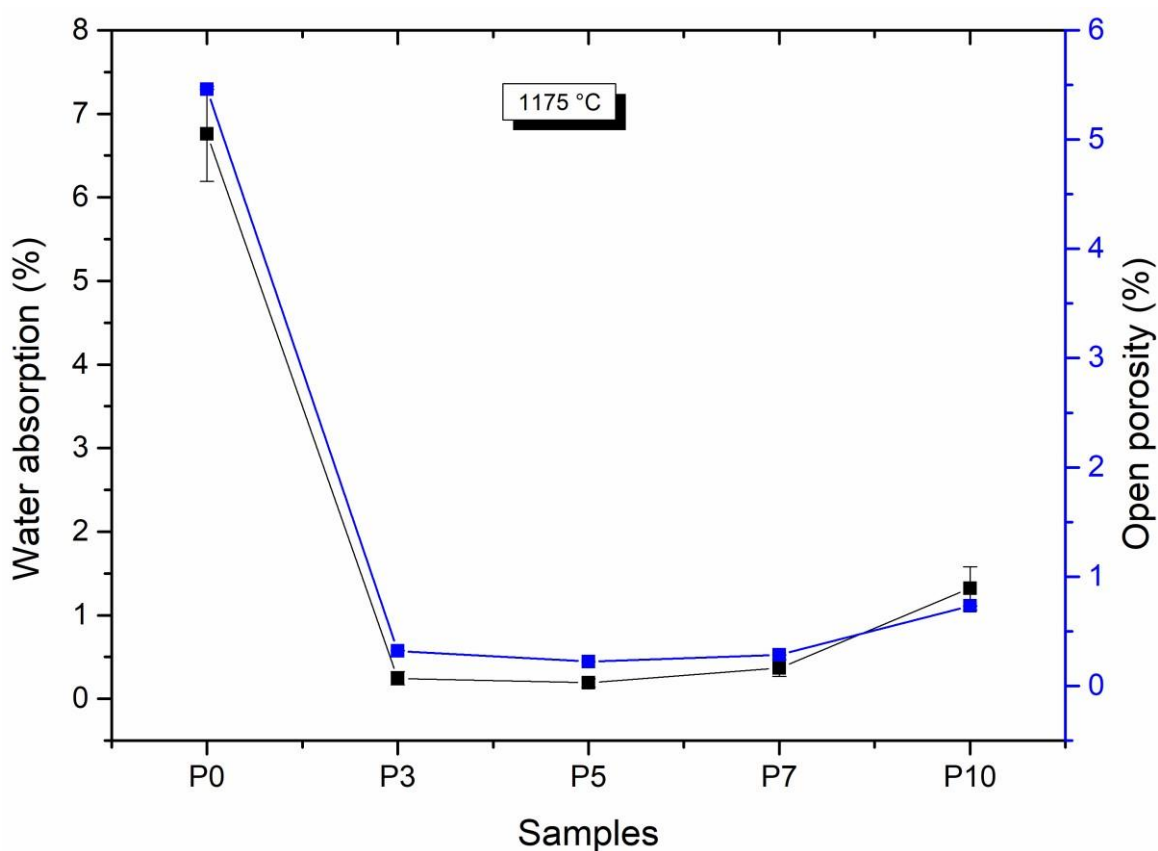


**Figure 39a:** Correlation between water absorption and open porosity for P serie at 1175°C

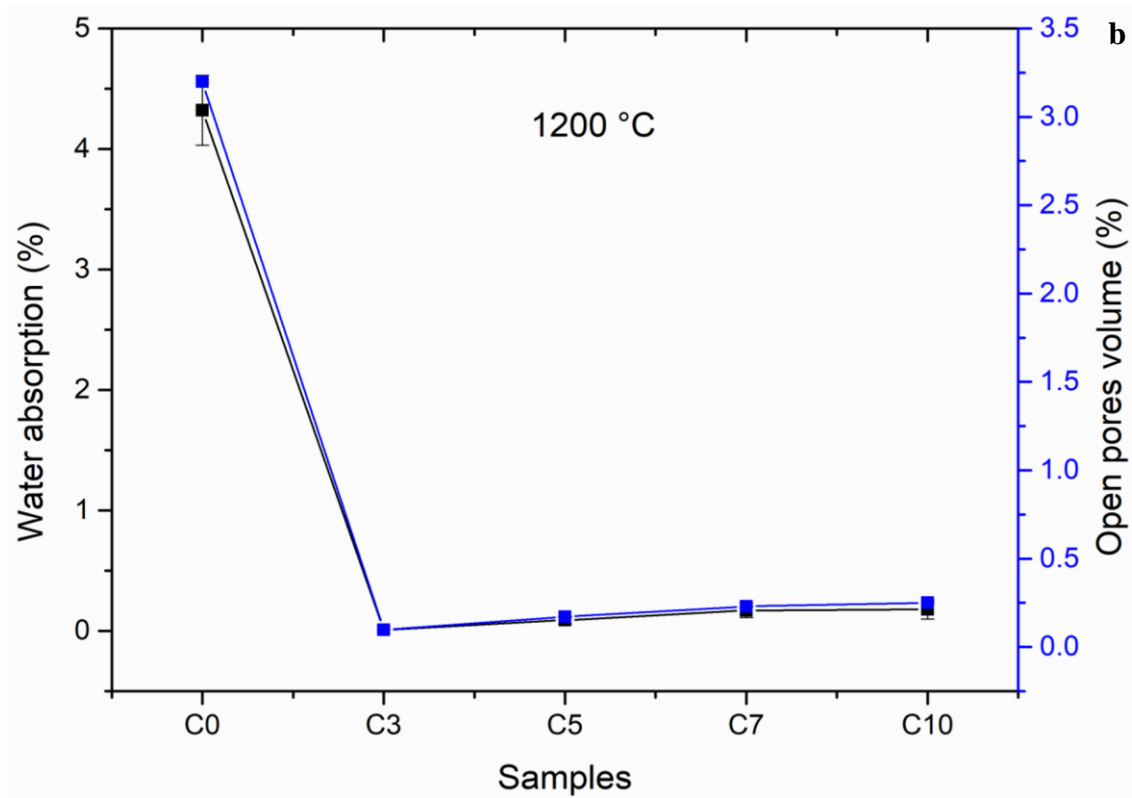
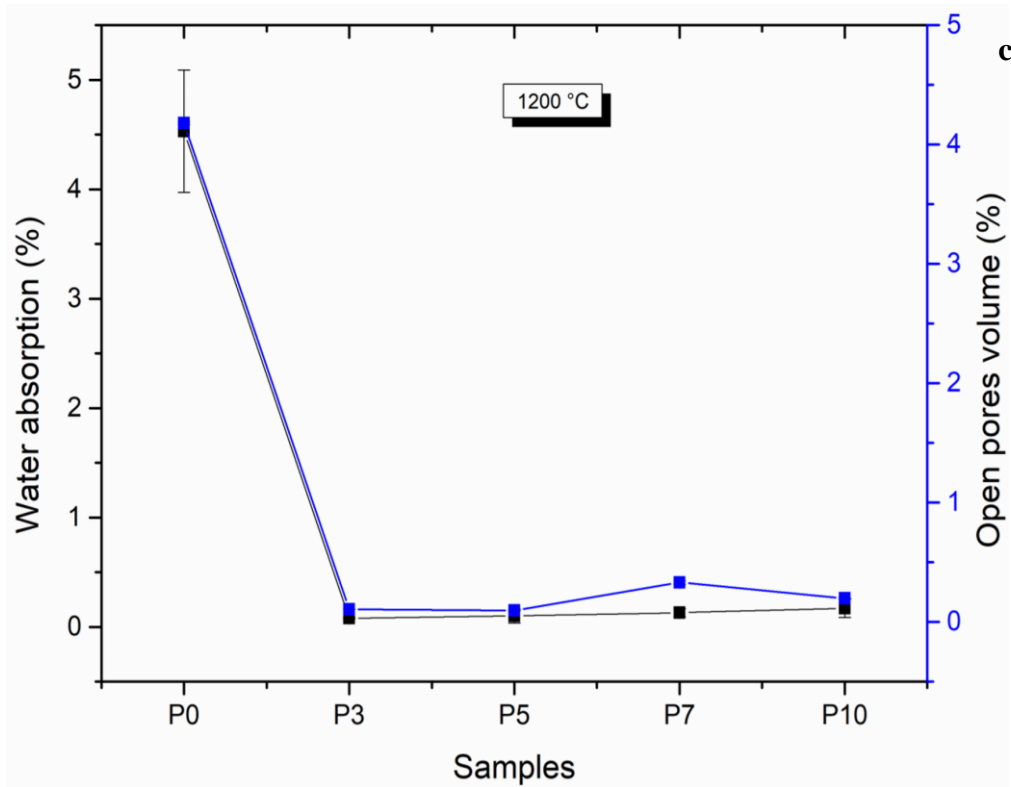


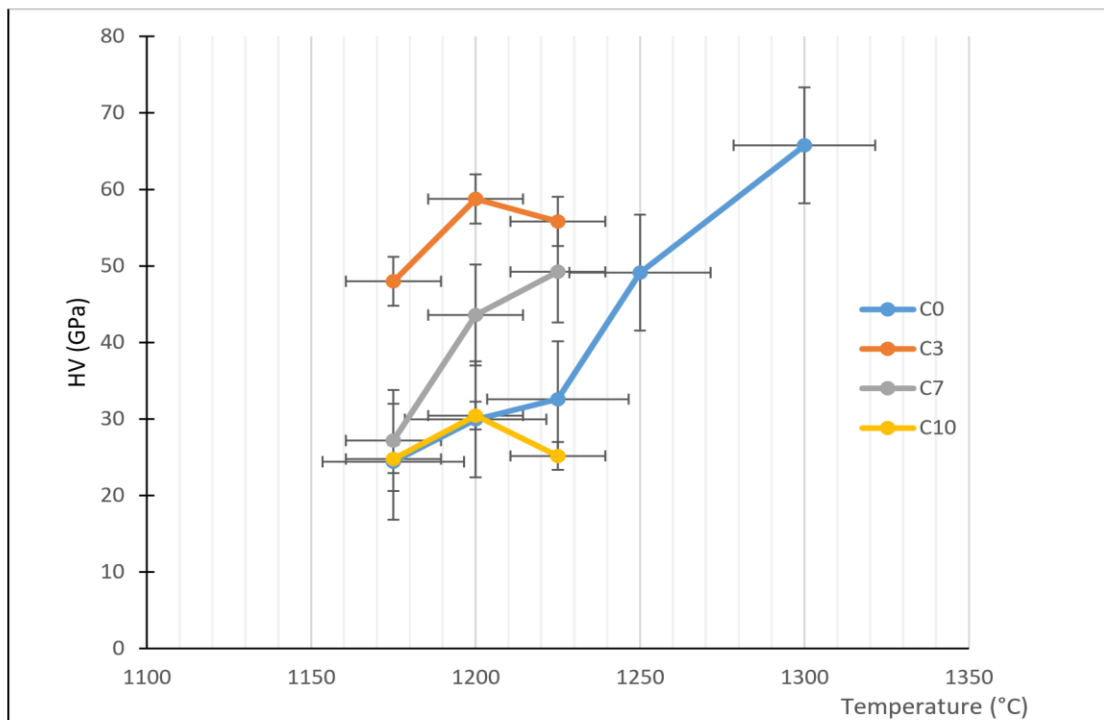
**Figure 39** : Correlation between water absorption and open porosity for C and P series at 1200°C

### III-6: Hardness of samples

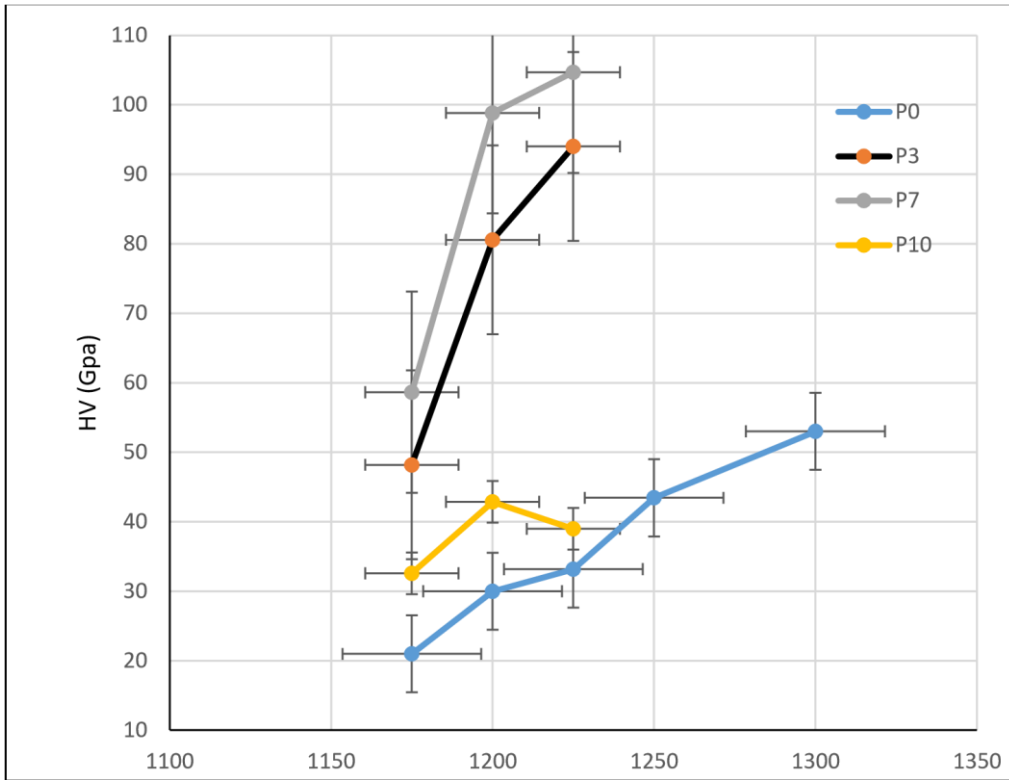
Hardness is a measure of resistance to penetration by a specified indenter under specified loading conditions. In ceramics, the process of forming a permanent impression is controlled not merely by classical plastic deformation, but also by densification, displacement and fracture. Densification is important since porosity is often present in sintered ceramics. Densification may also occur in some glasses and even nearly fully-dense ceramics with traces of microporosity.

Figure 40 (a) and (b) related the hardness of various samples of C and P series at different temperatures. For reference samples, a continuous increase in hardness with increasing of temperature up to 1300°C were noticed ( $65 \pm 1.2$  GPa for C series based on Boboyo feldspar and  $53 \pm 1$  GPa for P series based on Manjo feldspar). At 1250°C, P0 and C0 achieved  $49$  and  $43 \pm 2$  GPa, respectively whereas at 1225, P0 and C0 achieved respectively  $32.5$  and  $33 \pm 0.9$  GPa.

Samples with 3wt% addition of limestone achieved their maximum hardness at 1200°C for C series ( $58 \pm 1$  GPa) and at 1225 0C for P series ( $94$  GPa). With 7wt% addition, the maximum flexural strength was achieved at 1225°C) with  $59 \pm 0.9$  and  $104 \pm 2$  GPa for C and P series respectively. This is not the same behavior with flexural strength of these materials but these hardness values are largely above the standard value of ceramics comprise between 10 and 20 GPa



**Figure 40 (a):** Hardness of samples C at various temperatures



**Figure 40 (b):** Hardness of samples P at various temperatures

### **III-7: DESCRIPTIVE MICROSTRUCTURE**

The microstructure of porcelain stoneware is governed by the amount and viscosity of the vitreous phase formed during the sintering and the interaction between this major phase and the dispersed crystalline ones (mullite, anorthite, etc.) or remaining as non-transformed raw materials (quartz, amorphous silica, etc.). At equilibrium between the viscosity of the vitreous phase and the size of newly formed crystalline phases, optimum compactness is achieved and associated to minimum pores size (Kamseu et al, 2013). In these studies, the microstructure of various sintered samples were investigated through SEM/EDS and MIP.

#### **III-7-1: Descriptive microstructure of two porcelain stoneware based on nepheline syenite (G) and Boboyo's Pegmatite1 (B)**

From the XRD and SEM-EDS investigations, the two compositions consist of viscous and dense liquid phase in which mullite, quartz and plagioclase are dispersed forming a complex heterogeneous system. The composition B shows relatively low open porosity due to the presence of an extended liquid phase that embedded the crystalline phases and densify the matrix. This is due to the low viscosity of the liquid phase favored by the presence of the CaO in potassium-rich solid solution used as flux (Martz J. A., 1933). Figure 40 shows the micrographs of the specimen B (a) and G (b) fired at maximum densification. The micrograph (40a) illustrates the features of the formulation B at 1175°C with 2 hours soaking time. Similar micrograph was obtained at 1200°C with 1 hour soaking time. Etching surface of these specimens (Figure 40c) demonstrated that at these temperatures, the composition B has already developed dense matrix with crystalline phases. The micrographs (40b) and (40d) illustrate the sample G fired at 1200°C with 2 hours soaking time or 1225°C with 1 hour soaking time. Similar to P, the temperatures corresponded with high density of crystalline phases.

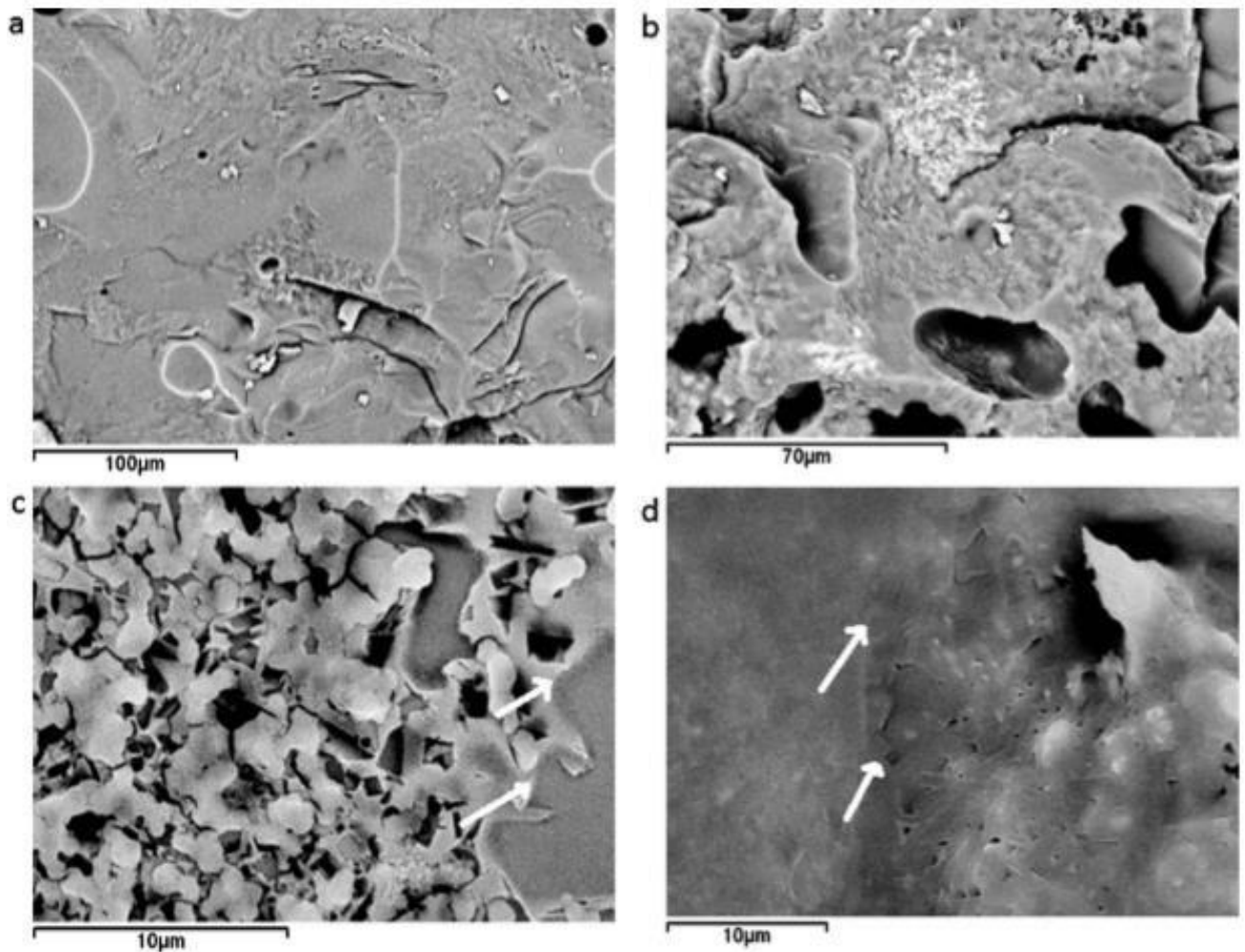


**Figure 41:** Micrographs of porcelain stoneware showing the semi-vitreous structure of B (a) and G (b) together with the interfaces matrix-crystalline phases for B (c) and G (d).

The Figure 41 shows the detailed distribution of the crystalline phases in the both formulations B (a and c) and G (b and d). It is observed that essentially small size of mullite and plagioclase are present indicating the limited grain growth in both cases due to the higher speed of heating. Examination of the micrographs of the composition B as their evolution with temperature indicates that, grains of crystalline completely surrounded by amorphous silica rich solution as from 1175°C with 2 hours soaking time. For the formulations G, the expression of crystalline phases is more important. The band of pores nucleated from the viscous phase is less significant in the G series even at 1225°C. The microstructural observations describe here can found explanation from the works of Martz (1933), Bowen and Tuttle (1950) which demonstrated that the presence of CaO in the matrix of orthoclase based porcelain compositions tend to decrease the fusibility temperature and increase the viscosity of the viscous phase obtained while with albite based compositions the situation is inversed. The addition of CaO to soda feldspar instead increase the viscosity of the melt and can explain the difference in the microstructural behavior of the two compositions G and B. We can here correlate the behavior of the two



compositions and say that the porosity of the bodies gives directly a measure of the quantity of the glassy phase formed. In their work on the microstructural variation in porcelain stoneware as a function of the flux system, Souza G. M., (2005) observed that, the use of soda lime-silica glass led to the crystallization of the plagioclase, wollastonite and sodium silicate. The formation of these phases directly affect the traditional mullite-glassy-quartz generally describe in the porcelain stoneware matrices. Furthermore, the increase in the viscosity of the  $\text{Na}_2\text{O}-\text{Al}_2\text{O}_3-\text{SiO}_2$  glass tend to favor the crystallization phenomena and by the way, the cumulative pore volume increases; this explain the porous properties of the composition G.

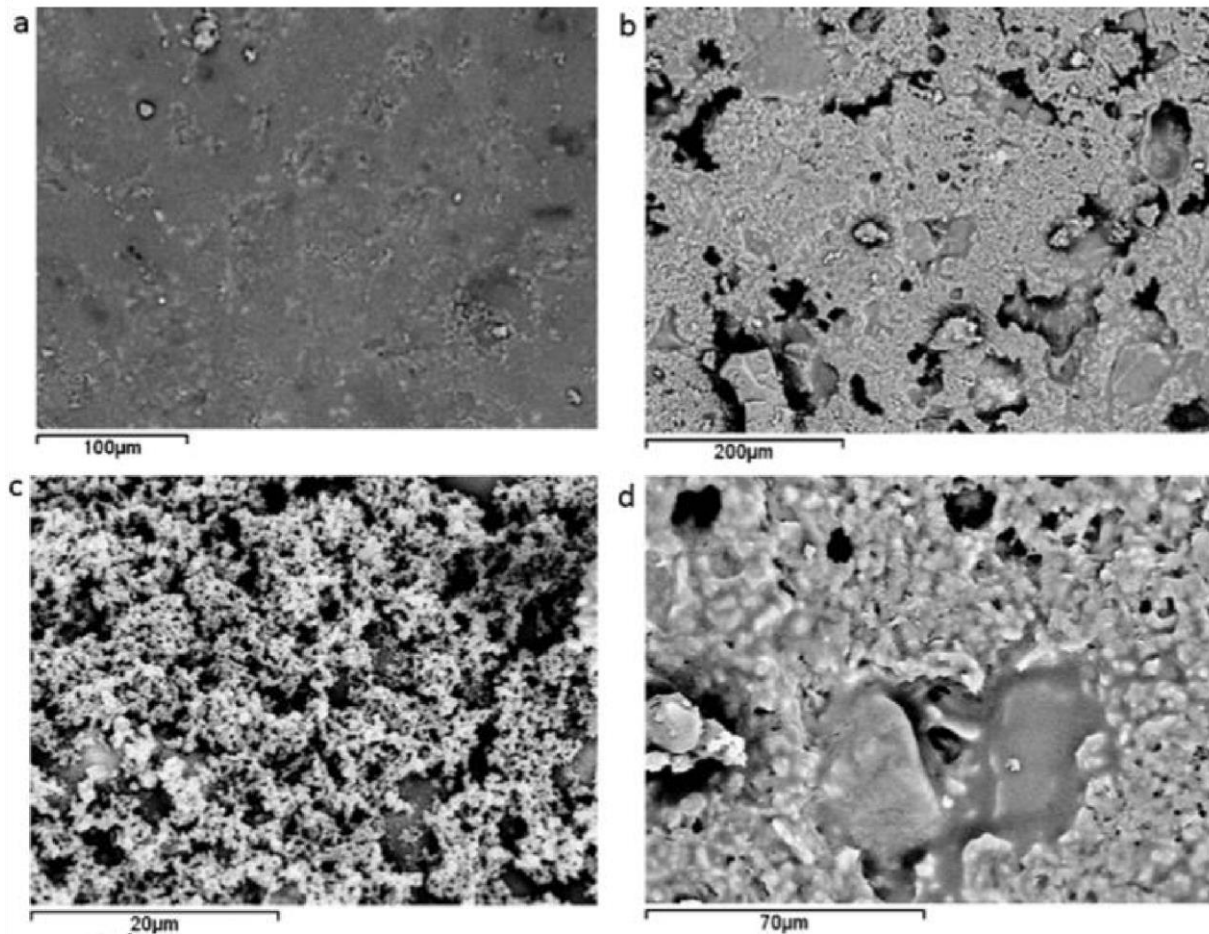


**Figure 42:** Micrographs of porcelain stoneware showing the optimum densification for B at 1200°C (a and c) and G at 1225°C (b and d)

**Figures 42 and 43** illustrate the action of CaO on the crystallization of the porcelain stoneware matrices. Evidence of the differential crystallization is reported and their contribution on the modification of the pore size distribution as well as cumulative pore volume. When the crystallization is the dominant mechanism of the strength development, some of the entrapped pores are unable to diffuse to the grain boundaries. Therefore the concentrated volume of crystalline phases remains with the pores. These crystalline phases enable the body to resist to high temperatures. The microstructural investigations have confirmed that, the strengthening mechanisms, the pore structure and shape into the two compositions are different. Round pores

are observed in the B series (Figure 43) while more complex geometry of pores are observed in the G series. These differences together with that of the tortuosity allow to suggest connections between some larger pores observed from the micrographs and those describe with MIP referring to the phenomenon of ink-bottle pores: some larger pores with small neck would have been evaluated during the porosimetry measurement as smaller pores.

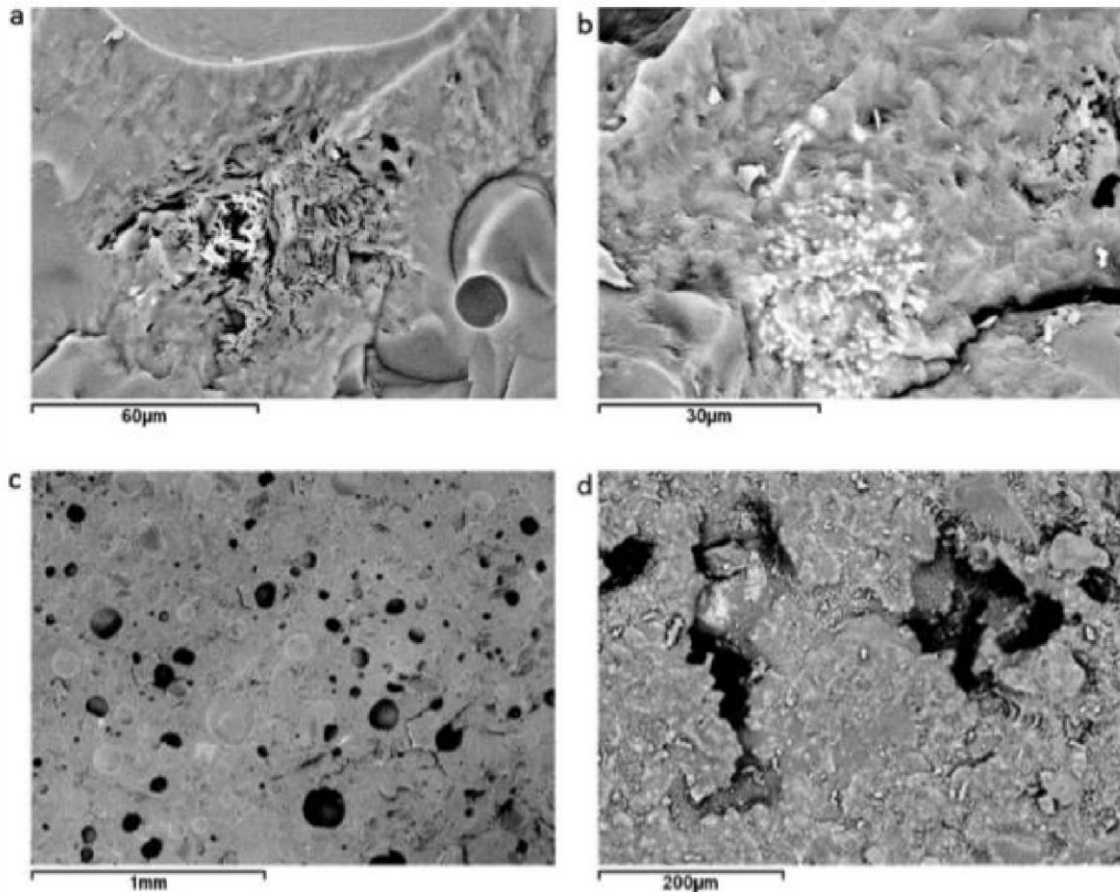


**Figure 43:** Inhomogeneity of crystallization (a and b) and difference in pores shape in porcelain stoneware (c and d)

The MIP technique is been considered as an invasion percolation and the pore size should be conceived as throats. Considering a pore with irregular geometry, with successively wide and narrow passages, wide chambers will only get filled with mercury at the kevenlaplace intrusion pressure of the finer pores (throats): misestimating the real value of the pores size. However, SEM techniques as many others alternative techniques cover a considerably smaller range of pores than MIP and no information about the 3D pore network nor about the connectivity can be observed directly (Roels S., 2001). By combining SEM and MIP technique, it was possible to describe the pores structure and estimate the cumulative pore volume. Results that was easily correlated to the tortuosity, water absorption and mechanical properties

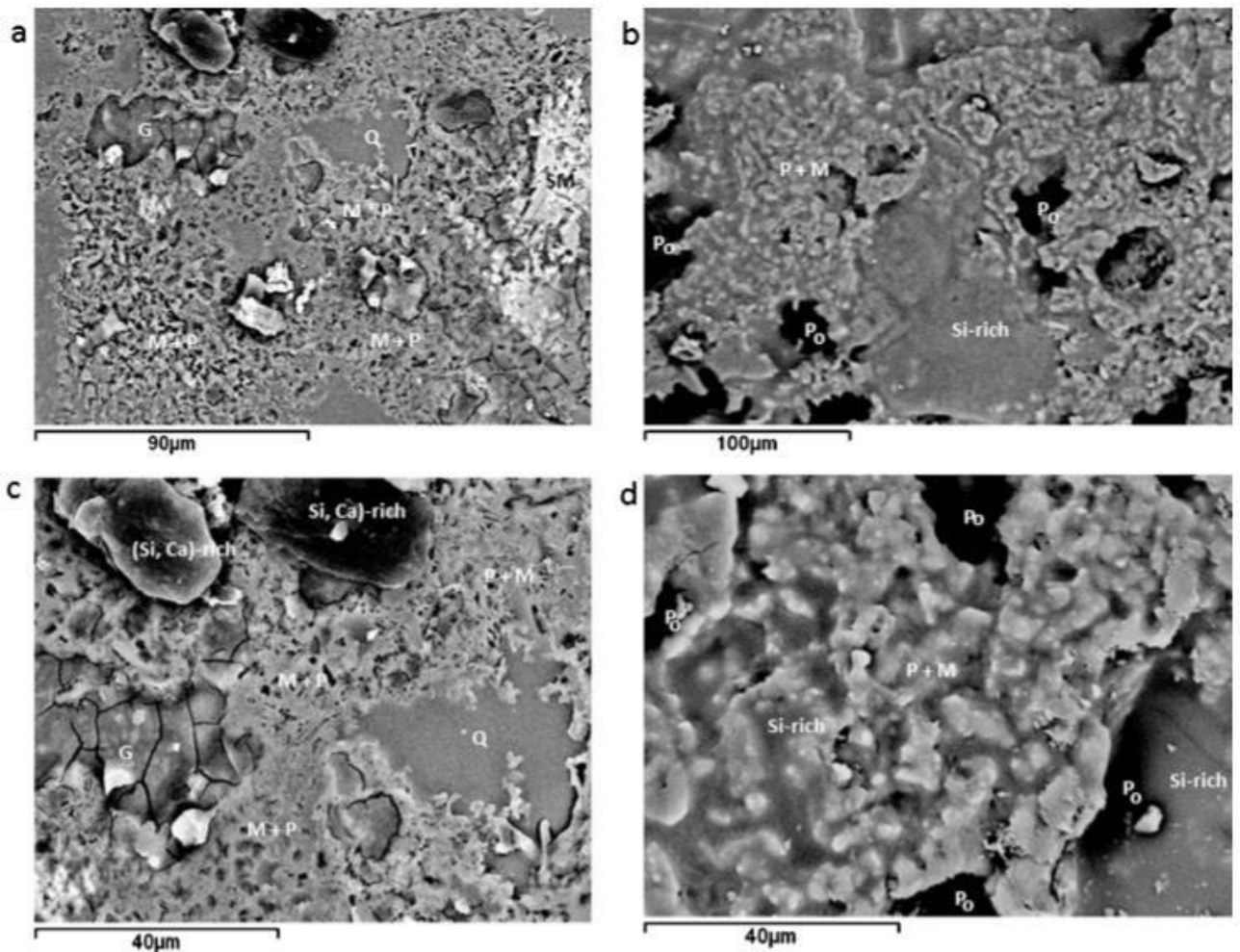


**Figure 44:** Phases distribution in the full dense (a and c) and relative porous (b and d) porcelain stoneware: M = mullite, P = plagioclase, Q = quartz, G = low viscosity glass with cracks from the contact with 4% HF–HNO<sub>3</sub> solution, Po = porosity.

### III-7-2: Descriptive microstructure of two porcelain stoneware based on Manjo (P) and Boboyo's Pegmatite2 (B)

In this study, the microstructure of various sintered samples was investigated. The observations were as follows: the microstructures of the bodies changed during firing. During the sintering process, the development of liquid phase progressively closed the capillaries that constituted the open porosity and the fine closed pores arise. This phenomenon influenced the microstructure. Figure 45 shows the evolution of the microstructure of porcelain stoneware at different sintering temperatures. In fig. 45a and 45b, samples without addition of limestone fired at 1175°C (C0A and P0A) show typical under firing ceramic microstructure with high interconnected pores. The pores size are distributed between 0.07 and 2.52 µm. This microstructure changes progressively and shows more and more liquid phases with less porosity when the sintering temperature increased from 1200 to 1225°C. The cumulative pores volume varies from

0.8 to 2.0 g/mm<sup>3</sup>. Then, the volume of smaller pores increased and those of larger pores reduced. With 10 percent mass addition of lime (figure 45c and 45d), at 1175°C, C10 shows a matrix with glassy process ongoing, the sintered matrices still present some interconnected pores; in this range of temperature, the morphology of P10 was similar to that of C10, but with less pores. When the firing temperature increased to 1200°C, both samples show vitrified matrices with closed pores not connected to each other. At 1200°C, P7 and C7 show a complete vitrified matrix (Figure 45b) with closed pores due to the low viscosity of the liquid phase favored by the presence of the CaO in potassium rich solid solution used as flux (Kamseu et al, 2013).

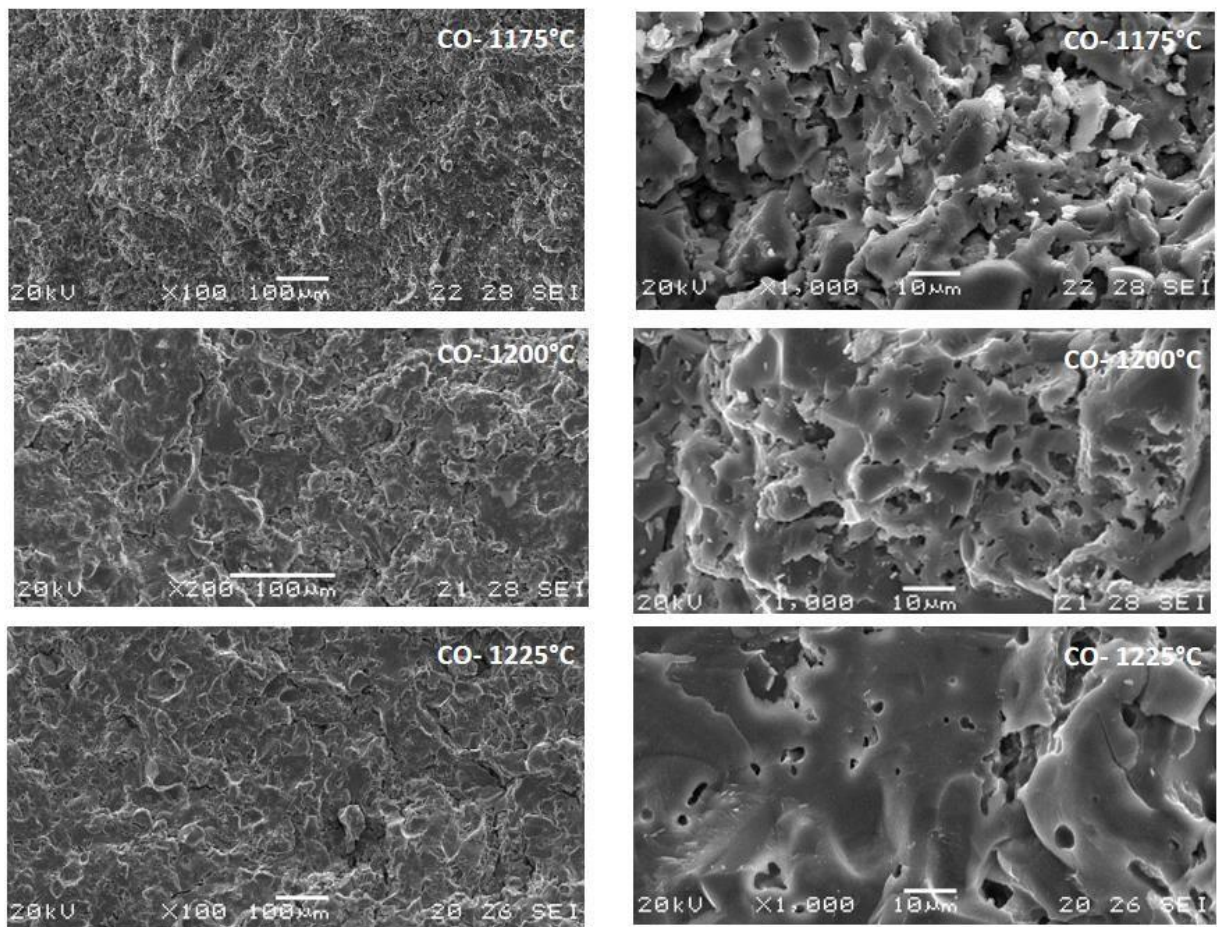


**Figure 45a:** Comparative microstructure of reference sample C0 at different temperature

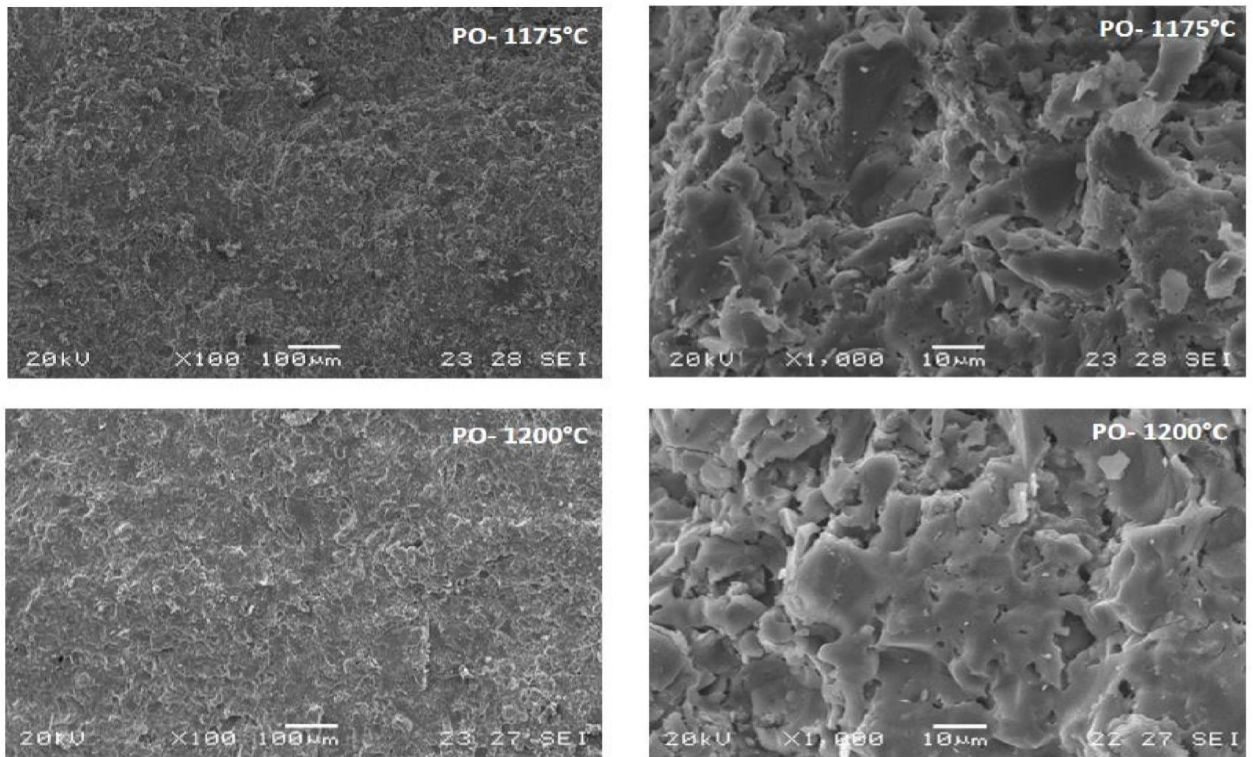


**Figure 45b:** Comparative microstructure of reference sample P0 at different temperature

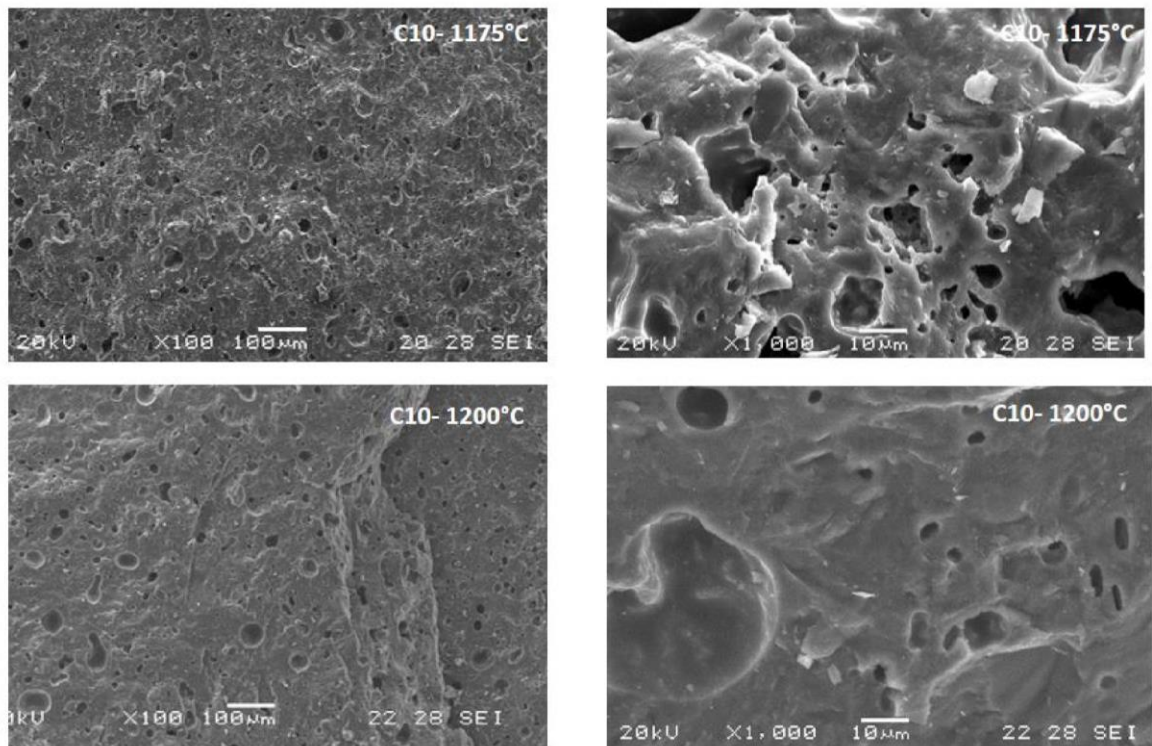


**Figure 45c:** Comparative microstructure of sample C10 at different temperature

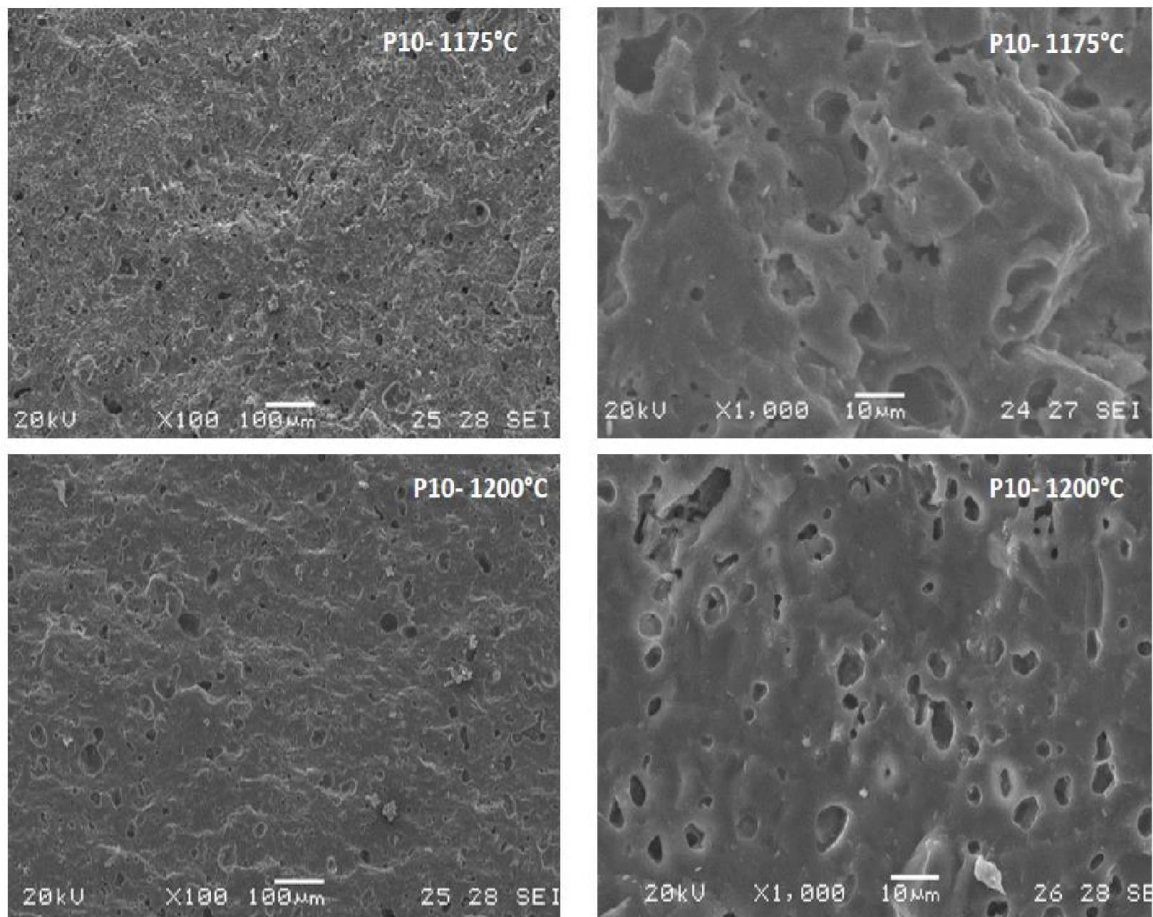


**Figure 45d:** Comparative microstructure of sample P10 at different temperature

Etching surfaces of reference samples C0 and P0, fired at 1175°C showed that primary mullite was effectively present as a mineral phase at this temperature, even though, it could not be found in XRD patterns probably because during etching process, the amorphous phases was removed by acid; crystalline phases are then liberated and can be appreciated in detail. As the temperature was raised to 1200°C, much mullite was formed and moved progressively from primary to secondary mullite. This mineral phase has also been found in XRD patterns at 1200°C (Figure 24a). As shown in Figures 24b, the micrographs illustrate the samples C7 and P7 fired at 1175 and 1200°C; at 1200°C, both of the formulation have already developed dense matrices with crystalline phases; anorthite was presented as the main phase for both formulations. At 1175°C, they present less expansion of the crystalline phase compared to micrographs at 1200°C.

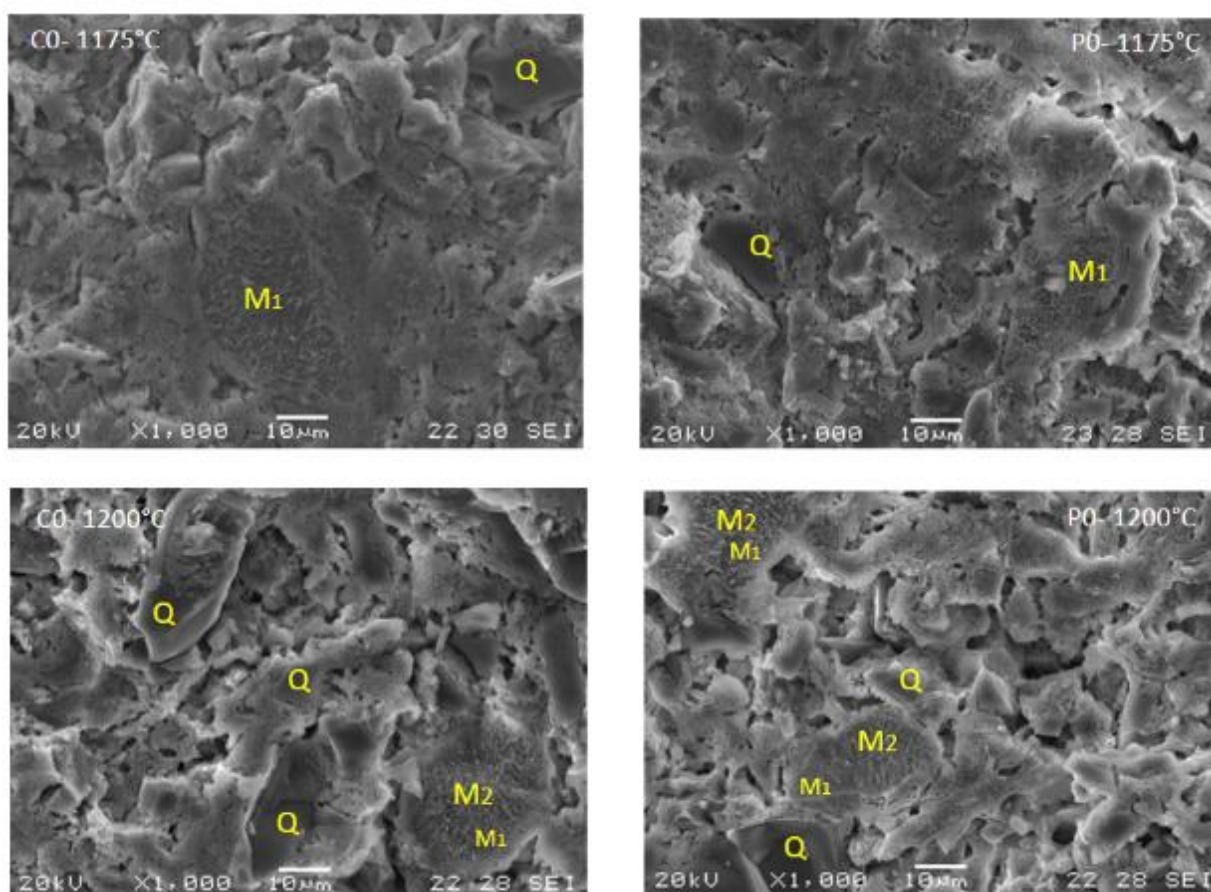


**Figure 46a** : comparative microstructures of etching surface of references samples at 1175 and 1200°C

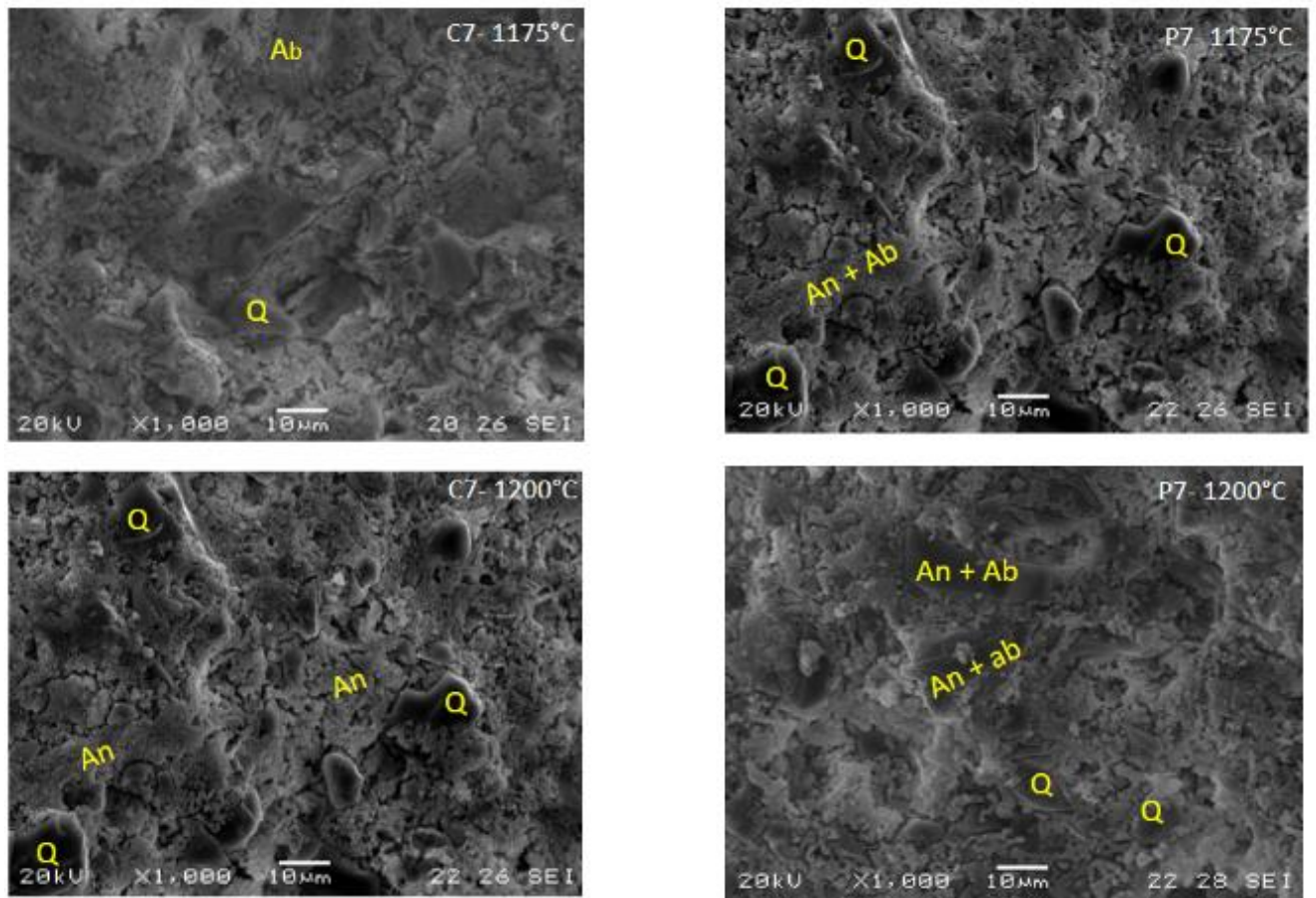


**Figure 46b** : comparative microstructures of etching surface of samples C7 and P7 at 1175 and 1200°C





## **GENERAL CONCLUSION**

## GENERAL CONCLUSION

The main objective of this research was to investigate and provide scientific and technological information on the production of low cost and high performance ceramics materials by relative low energy process, using locally available raw  $K_2O$  rich pegmatite combine with  $CaO$  rich materials. The aim of the research was to study the effects of the addition of portions of calcium oxide on potash feldspars and investigated their influence on the properties of semi-vitrified ceramics.

The mineral nature of the solid solutions affect the thermal behavior of porcelain stoneware under heat treatment. Although their similar chemical compositions, the nepheline syenite based body (G) saw its vitrification delayed with respect to the pegmatite of Boboyo1 based body (B). The recrystallisation of leucite that appeared in DTA curves of pegmatite was not found in the DTA curve of the porcelain stoneware (B). These differences were ascribed to the action of  $CaO$  in enhancing the vitrification and reduce the viscosity of the fluid formed in orthoclase based systems compared to albite based systems. The composition B showed high strength and relatively low porosity as from  $1175^\circ C$  with water absorption under 0.4% at  $1200^\circ C$ . However specimens of the (B) serie seem to be affected with the increase in soaking time at high temperature with the reduction of flexural strength and the increase in porosity. The composition G remained porous up to  $1225^\circ C$  (2.5% of water absorption) and have reached the flexural strength of the composition B only at  $1225^\circ C$ , showing the difference in thermal behavior between the two materials with similar chemical composition. The dominant strengthening mechanism could be described with the mullite theory for the composition G and matrix strengthening for the composition B when correlated the actual results with the mechanical properties.

The extended liquid phase of the body B allowed the complete reduction of open porosity and significant strength development at the early stage of densification ( $1175^\circ C$ ) with respect to the formulation G. In the range of the temperature of maturation, G presents more intergranular pores due to the high degree of crystallization in comparison with B which has more rounded closed porosity nucleated from the extended viscous liquid phase formed. The formulation G presented a range of cumulative pore volume between 0.09 mL/g and 0.12 mL/g while B presented cumulative pore volume concentrated at between 0.5 and 0.6 mL/g. Both compositions presented significant fraction of Nano size of pores under  $0.01 \mu m$ . The development of a band of pores with size between  $0.08$  and  $0.9 \mu m$  in the composition P and the absence in the composition G confirm the impact of the liquid phase on the nucleation of closed porosity.

With the necessity to use fast firing and achieve high strength at relative low temperature, the use of orthoclase with CaO as mineralizer seem to be promising solution which included the energy save, the sustainability and the low cost production. To set up this scientific opportunity, the effect of the addition of various mass percentages of limestone (from 0 to 10 wt.%) on the properties of fired ceramics porcelain stoneware tiles based on two potash feldspars from Manjo (P) and Boboyo2 have been investigated. Thermo-analytical techniques including DTA/TG as well as dilatometry test, mechanical properties and microstructure were used to evaluate the effectiveness of CaO to lowering the sintering temperature of porcelain stoneware while maintaining high mechanical properties and low porosity. At the end of the study, the following conclusion can be made:

- The addition of limestone to the mixture enhanced conveniently the physical and mechanical properties of porcelain stoneware tiles and decreased significantly the sintering temperature.
- Mullite was found to be the main phase on reference samples while mullite and anorthite were presented as main phases of samples based on limestone addition from 3 to 7%. Above 7% of limestone, excess of CaO favors the appearance of anorthite as the only phase. When anorthite was the unique crystalline phase, a decrease in viscosity was observed due to the reduction of the liquid phase formed; consequently, residual potash feldspar minerals were present in the finished product.
- The addition of limestone inhibits the  $\alpha$ ,  $\beta$  quartz transition due to the significant reduction of the quartz content and the possible reaction between residual silica and CaO;
- Samples with addition of limestone exhibited a controlled expansion phenomenon after the maximum shrinkage between 1175 and 1200°C; this contributed to reduce the firing shrinkage of the porcelain stoneware obtained in this work.
- Beginning from 1175°C, some samples with limestone addition exhibited very high flexural strength (up to 138 MPa), with good density (up to 3.2), low water absorption (close to zero) and low open pores.
- As from 1225°C, specimens with limestone addition (from 3%) showed a decrease in mechanical performance indicating that these formulations do not need firing temperature above 1200°C to achieve optimum porcelain stoneware tiles. This signifies an energy saving of almost 150°C by the limestone addition to the bulk composition and an optimum processing.

- The ceramics bodies based on mullite and anorthite simultaneously as main phases developed early vitrification, high flexural strength, low porosity and good density at relatively low temperature.
- The proper addition of limestone onto the two feldspars permitted to design very performant porcelain stoneware tiles formulations at relatively low temperature.
- P series which is based on a more potash feldspar performed better than C series based on potash and soda feldspar.
- In a decreasing order, the sintering behavior and properties of samples composed of 7wt%, 5wt% and 3wt% addition of limestone have been appreciated as more suitable for the designing of sustainable hard porcelain tiles based on a pure potash feldspar (P) and a soda-potash feldspar (C) but the progression is not strictly linear.

The chemical elements alone are not sufficient to design the suitable composition of semi-vitreous product with desired properties, the nature of the flux will play a significant role on the vitrification and change in viscosity of the matrix while the nature of clayey material will affect the crystallization of mullite and the nature of residual silica. Residual silica which is important for the fluctuation of the thermal expansion compatibility and promotion of compressive stresses. The flexural strength, the density, the water absorption obtained showed that the local available raw materials can be easily applied for the sustainable production of porcelain stoneware in Cameroon.

## RECOMMENDATIONS AND PROSPECTS

Several investigations have been made in order to develop semi-vitrified ceramics from materials rich in potassium oxide, sodium / potassium oxide and calcium oxide. We do not claim to have studied all the aspects of science; following the work,

- We will study the impact of variations in the percentages of addition of calcareous material in compounds based on nepheline syenite;
- Investigate the impact of adding high percentage limestone (> 10%) on the thermomechanical behavior of the matrix produced;
- Carry out comparative studies of the thermomechanical behavior of the compositions with variation in the percentage of limestone by fast firing;
- Complete the characterization study on the enamels produced;

In order to promote the valorisation of the results of this research, we will propose to the Local Materials Promotion Authority, a project of installation of a pilot unit of production of ceramic tiles.



# REFERENCES



## REFERENCES

- AFNOR. NF P 94-051; Soils: Investigation and testing – Determination of Atterberg's limits – Liquid limit test using Casagrande apparatus – Plastic limit test on rolled thread. AFNOR (1993)
- Ajakor, Anih, L.U, Ogwata C.M., Indigenous Production of Electrical Porcelain from Nigerian Mineral, International Journal of Scientific and Research Publications, Volume 5, Issue 6 (2015) 1 ISSN 2250-3153
- Alexander D. Harrison, Thomas F. Whale, Michael A. Carpenter, Mark A. Holden, Lesley Neve, Daniel O'Sullivan, Jesus Vergara Temprado, and Benjamin J. Murray. Not all feldspars are equal: a survey of ice nucleating properties across the
- Alves H. J., Melchiades F. G., Boschi A. O., Effect of feldspar particle size on the porous microstructure and stain resistance of polished porcelain tiles. J Eur Ceram Soc. (2012) 32: 2095–102.
- Alves H. J., Minussi F. B., Melchiades F. G., Boschi A. O., Characteristics of pores responsible for staining of polished porcelain tile. Ind Ceram (2011) 31: 21–6.
- Alves H. J., Melchiades FG, Boschi A. O., Effect of spray-dried powder granulometry on the porous microstructure of polished porcelain tile. J Eur Ceram Soc (2010) 30:1259 - 65.
- Amoros J. L., Orts M. J., Garcia-Ten J., Gozalbo A., Sanchez E., Effect of the green porous texture on porcelain tile properties. J Eur Ceram Soc. (2007) 27: 2295–301.
- Anderson Robert S., Anderson Suzanne P., Geomorphology: The Mechanic and Chemistry of Landscapes. Cambridge University Press (2010) P. 187. ISBN 978-1-13978870-0.
- Andreola F., Barbieri L., Corradi A., Lancellotti I., Manfredini T., Utilisation of municipal incinerator grate slag for manufacturing porcelainized stoneware tiles manufacturing, Journal of the European Ceramic Society Vol .22 (9-10), 1457-1462, (2002)
- Anthony John W., Bideaux Richard A., Bladh kenneth W., Nichols Monte C. 'Montmorillonite' Handbook of Mineralogy II (Silica, silicates). Chantilly. VA, USA : Mineralogical society of America (1995). ISBN 0962209716.
- Anthony John W., Bideaux Richard A.; Bladh, Kenneth W.; Nichols, Monte C. 'Calcite'. Handbook of Mineralogy. V (Borates, Carbonates, Sulfates). Chantilly, VA, US: Mineralogical Society of America (2003). ISBN : 978-0962209741.

- ASTM 373-88: Standard Test Method for Water Absorption, Bulk Density, Apparent Porosity, and Apparent Specific Gravity of Fired Whiteware Products, (2006).
- ASTM C1326-13: Standard Test Method for Knoop Indentation Hardness of Advanced Ceramics<sup>1</sup> (2018)
- ASTM C650 – 04: Standard Test Method for Resistance of Ceramic Tile to Chemical Substances (2014).
- B. Cicek, E. Karadagli, F. Dunan, Valorisation of boron mining waste in the production of wall and floor tiles. *Construction and Building Materials*, vol.179, pp.232-244, (2018)
- Bartusch R., Energy saving potentials in the ceramic industry. *Interceram*. 2004;53(5):312–6.
- Bertin E. P., Principle and practice of X-ray Spectrometric Analysis, Kluwer academic/ Plenum Publisher (1996) ISBN 0-306-30809-6
- Blum A.E., Determination of illite/smectite particle morphology using scanning force microscopy, in Nagy, K.L., and Blum, A.E. (eds.) *Clay Minerals Society Workshop Lectures*, v. 7, p. 171-202 (1994).
- Bragança and Bergmann. A view of whitewares mechanical strength and microstructure, *Ceramics International* 29 (2003), pp 801-806
- Brindley G.W., Brown G., *Crystal Structures of Clay Minerals and their X-ray identification* (3rd ed.). UK Mineralogical Society (1980). ISSN 0144-1485
- Buhrke V. E., Jenkins R., Smith D. K., *A practical guide for the preparation of specimens for XRF and XRD analysis*, Wiley, 1998, ISBN 0-471-29942-1
- Carty W. M., Senapati U., Porcelain-raw materials, processing, phase evolution, and mechanical behavior. *J Am Ceram Soc.* (1998);81(1):3–20. 2.
- C. Leonelli, F. Bondioli, P. Veronesi, M. Romagnoli, T. Manfredini, G. C. Pellaconi, V. Cannillo, Enhancing the mechanical properties of porcelain stoneware tiles: a microstructural approach, *Journal of European Ceramics Society*, (2001).
- Claussen N., Urquhart A. W., *Encyclopedia of Materials Science and Engineering*; Cahn, R. W. ed. Pergamon: Oxford, U.K., Vol. 2, 1111–1115, (2011)
- C.E.L. Franklin, A.J. Forrester, Development of bone china *Trans. J. Br. Ceram. Soc.* 74 – 4 P 141 – 154 (1975)
- C.G. Portillo, influence of type of melting on the properties of bone porcelain. *Bol. Ceram vidrio* 38 (5) P 397-402 (1998).
- C.M. Queiroz & S. Agatholous, The discovery of European Porcelain Technology, *Trabalhos de Arqueologia* (ISSN 0871-2581), 42 (2005), 211-215

- Cornelis Klein, Anthony Philpotts, Introduction to mineralogy and Petrology, Earth Materials, 2<sup>nd</sup> Edition. Cambridge University Press, ISBN : 97811071550404 (2017).
- Dana8. Illite Mineral data PHYS. PROP. (Eur. J. Min., Vol.9, p821-827,1997) OPTIC PROP.(Heinrich65).
- Das, K.S. & Dana, K., Differences in densification behaviour of K- and Na-Feldspar containing porcelain bodies. *Thermochimica Acta* 406 (2003), pp 199-206.
- Deer W. A., Howie R. A., and Zussman, J., An introduction to rock-forming minerals: Longman Group Ltd., London (1975), 528 p
- D. Grossin, «Développement du procédé de chauffage micro-ondes en vue de l'élaboration de céramiques à propriétés électriques particulières ». Doctorate Thesis, Caen University, (2006).
- D. Njoya, M. Hajjaji, C. Nkoumbou, A. Elimbi, M. Kwekam, A. Njoya, J. Yvon and D. Njopwouo, Chemical and mineralogical characterization and ceramic suitability of raw feldspathic materials from Dschang (Cameroon), *Bull. Chem. Soc. Ethiop.*, 24(1), (2010)39-46.
- D.U. Tulyaganov, S. Agathopoulos, H.R. Fernandes, J.M.F. Ferreira, «Influence of lithium oxide as auxiliary flux on the properties of triaxial porcelain bodies». *Journal of the European Ceramic Society*, 26, 1131–1139 (2005).
- Dunham, R. J., Classification of carbonate rocks according to depositional textures, In Ham, W. E. (ed.). *Classification of Carbonate Rocks*. American Association of Petroleum Geologists Memoirs. **1**. pp. 108–121 (1962).
- E. Kamseu, T. Bakop, Djangang, U.C. Melo, M. Hanuskova, C. Leoneli. Porcelain stoneware with pegmatite and nepheline syenite solid solutions: Pore size distribution and descriptive microstructure, *Journal of the European Ceramic Society* 33 (2013) 2775–2784
- E. Martini, D. Fortuna, A. Fortuna, G. Rubino, V. Tagliaferri. Sanitser, an innovative sanitary ware body, formulated with waste glass and recycled materials, *Cerâmica* 63 (2017) 542-548
- Ece, O. I. and Nakagawa, Z. Bending Strength of Porcelains, *Ceramics International* 28, (2002) pp 131-140.
- Elimbi, Njopwouo D., Lamilen D., Chinje Melo U., Caractérisation chimicominéralogique et comportement thermique de trois matériaux feldspathiques camerounais utilisables comme fondants en céramique. *Silic Ind.* (2005).
- Esposito, Salem A, Tucci A, Gualtieri A, Jazayeri SH. The use of nepheline syenite in a body mix for porcelain stoneware tiles. *Ceram Int.* 2005;31(2):233–40.

- F394-78: Standard Test Method for biaxial Flexural Strength (Modulus of Rupture) of Ceramics substrates ; American Society for Testing and Materials, 100 Barr, Harbor Dr., West Conshohoken, PA 19428 (1996)
- F. Koumetio, D. Njomo, C.T. Tahod, Tatchum C. Noutchogwe and E. Manguelle Dicoum; Structural interpretation of gravity anomalies from the Kribi-Edea zone, SouthCameroon: a case study, J. Geophys. Eng. 9 (2012) 664-673.
- Fleming John & Hugh Honour. The Penguin Dictionary of Decorative Arts. London : Allen Lane, P.622. ISBN 0713909412, (1977).
- Folk, R. L., Petrology of Sedimentary Rocks. Austin, Texas: Hemphill Publishing (1974).
- G. W. Morey and N. L. Bowen, "The Melting of Potash Feldspar," Am. Jour. Sci., 5th Ser., 4, p. 1 (1922).
- George Frederick Kunz, The Curious Lore of Precious Stone, New York : Dover Publication, 1971)
- Grim Ralph E., Bray R. H., Bradley, W. F. The Mica in Argillaceous Sediments, American Mineralogist, (1937) 22: 813-829
- H. Blatt, G. Middleton, and R. Murray, Origin of sedimentary rocks (Second edn.), Prentice\_Hall, Inc., 1980
- H. Boussak, 'Effet de la température sur les performances des céramiques contenant la bentonite de Maghnia', Doctorate Thesis, University of Bourmedes, 2010.
- Hildyard Robin. European Ceramics. London : V&A publications (1999), p.46. ISBN 185772596
- Hill Carol, Paolo Forti; Deposition and Stability of asd Silicate Minerals, Cave Minerals of the world (second ed.). National Speleological Society (1997). P.177. ISBN-1-8799607-5
- Hurlbut C.S., Klein C. Manual of Mineralogy (20th ed.). New York: Wiley & Sons (1985). ISBN 0471805807.
- Hurray, Traditionnal and new applications for kaolin, smectite and polygoskite: a general overview. Journal, appl-clay sci, vol 17, 207-221 (2000).
- Igor Štubňa, Anton Trník, František Chmelík and Libor Vozár, Advances in Ceramics-Characterization, raw materials, processing, properties, degradation and healing, Costas Sikadis, (2011); ISBN 978-307-504-4 (. P 229-242)
- Iqbal Y, Edward Lee W. Fired porcelain microstructures revisited. J Am Ceram Soc 1999;82(12):3584–90.
- ISO/FDIS 13006: Ceramics tiles. Definition, classification, characteristic, marking. ISO/TC 189 (1998)

- J. C. Kyonka, R. L. Cook, Properties of Feldspars and their use in white wares, University of Illinois, Large scale Digitization Project, (2007).
  - J. David, Weathering and sedimentary Rocks, Cal Poly Pomona. Archived from the original, (2007)
  - J. F. Schairer and N. L. Bowen, "Melting Relations in the Systems  $\text{Na}_2\text{O} \cdot \text{Al}_2\text{O}_3 \cdot \text{SiO}_2$  and  $\text{K}_2\text{O} \cdot \text{Al}_2\text{O}_3 \cdot 2\text{SiO}_2$ " Am. Jour. Sci., 245, p. 193 (1947).
  - J. W. Greig and B. T. W. Berth, "The System  $\text{Na}_2\text{O} \cdot \text{Al}_2\text{O}_3 \cdot 2\text{SiO}_2$  (Nephelite, Carnegieite) –  $\text{Na}_2\text{O} \cdot \text{Al}_2\text{O}_3 \cdot 6\text{SiO}_2$  (Albite)," Am. Jour. Sci., 35A, p. 93 (1938).
  - Nzeukou Nzeugang A., Minéralogie, géochimie et propriétés céramiques des argiles alluviales de la Sanaga entre Nanga-Eboko et Ebebda (Région du Centre-Cameroun), PhD Thesis, University Yaounde I (2014).
  - Jorge Martin Marquez, J. Ma. Rincon, M. Romero, Mullite development on firing in porcelain stoneware bodies, journal of *the European Ceramic Society* 30 (2010) 1599 – 1607.
  - Kamseu, E., Leonelli, C., Boccaccini, D. N., Veronesi, P., Miselli, P., Pellacani, G., & Melo, U. C. Characterisation of porcelain compositions using two china clays from Cameroon. *Ceramics international* (2007) 33(5), 851-857
  - Karamanov, A., Karamanova, E., Ferrari, A. M., Ferrante, F., & Pelino, M., The effect of fired scrap addition on the sintering behavior of hard porcelain. *Ceramics International*, 32(7), 727-732, (2006).
  - Ke S, Cheng X, Wang Y, Wang Q, Wang H. Dolomite, wollastonite and calcite as different sources in anorthite-based porcelain. *Ceram Int.* 2013;39:4953–60.
  - Kingery W. D., Introduction to Ceramics, New York: Wiley, Translated under the title *Vvedeniye keramiku*, Moscow: Stroiizdat, (1976).
  - Kivitz E., Palm B., Heinrich J.G., Blumm J., Kolb G., Reduction of the porcelain firing temperature by preparation of the raw materials. *J Eur Ceram Soc.* (2009)
  - Koenig C. J., Nepheline syenite in hotel chinaware bodies. *J Am Ceram Soc.* (1942);25(3):90–3.
- Kogel Jessica Elzea. *Industrial Minerals & Rocks: Commodities, Markets and Uses. SME.* ISBN 9780873352338 (2006). Archived from the original on 16 December 2017
- K. Krishnan, Indus Ceramic Industries: Complexities, Challenges and Prospects, *Indian Journal of History of Science*, 53.3 (2018) 263-270.
  - L. U. Anih, Indigenous Manufacture and Characterization of Electrical Porcelain Insulator, *Nigerian Journal of Technology*, Vol. 24, No. 1, (2005).

- Leonelli C., Kamseu E., Melo U. C., Corradi A., Pellacani G. C., Mullitisation behavior during thermal treatment of three kaolinitic clays from cameroon: densification, sintering kinetic and microstructure. *Interceram*. 2008;57(6):396–401.
- Leven E. M., Robbins C. R., Mc Murdie H. F., In: Reser M. K, editor. Fig. 407 (P.156, K<sub>2</sub>O–Al<sub>2</sub>O<sub>3</sub>–SiO<sub>2</sub>) and Fig. 501 (P.181, Na<sub>2</sub>O–Al<sub>2</sub>O<sub>3</sub>–SiO<sub>2</sub>) in phase diagrams for ceramics. Columbus, OH: American Ceramic Society; (1964).
- Lundin S. T., Studies on triaxial white ware bodies. Stockhom: Almqvist and Wiksell; (1959).
- M. Dondi, G. Ercoli, C, Mingazzini, M, Marsigli, The chemical composition of porcelain stoneware tiles and its influence in microstructural and mechanical properties, *International Ceramics Review*, (Jan 2009).
- M. Romero, J. M. Pérez, Relation between the microstructure and technological properties of porcelain stoneware. A review. *Mater. Construcc.* 65 [320] (2015).
- Maity S., Mukhopadhyay T. K., Sarkar B. K., Sillimanite sand-feldspar porcelains: I. Vitrification behavior and mechanical properties. *Interceram*. 1996; 45:305–12.
- Martin-Marques J., Rincon J., Ma Romero M., Effect of firing temperature on sintering of porcelain stoneware tiles. *Int Ceram* (2008);34 (8):1867–73.
- Martín-Márquez, J., Rincón, J. M., & Romero, M. Effect of microstructure on mechanical properties of porcelain stoneware. *Journal of the European Ceramic Society*, 30(15), 3063-3069, (2010).
- Martz., Potash–soda–lime feldspar eutectic study. *J Am Ceram Soc* 1933;16(7):299–304.
- Melo U. C., Tchuendem A., Nsifa N., Fusibility of nepheline syenite from south province, Cameroon. *Silic Ind.* 2004;69(3–4):35–41
- M. Kotal, A.K. Bhowmick, Polymer nano composites from modified clays: recent advances and challenges, *Prog. Polym. Sci.* 51 (2015) 127–187
- Motoki A., Araújo A. L., Sichel S. E., Motoki K. F., Silva S., Nepheline syenite magma differentiation process by continental crustal assimilation for the Cabo Frio Island intrusive complex, State of Rio de Janeiro, Brazil. *Geociências*, Rio Claro, (2011).
- Motoki A., Sichel S. E., Vargas T., Aires J. R., Iwanuch W., Mello S. L. M., Motoki K. F., Silva S., Balmant A., Gonçalves J., Geochemical evolution of the felsic alkaline rocks of Tanguá, Rio Bonito and Itaúna intrusive bodies, State of Rio de Janeiro, Brazil. *Geociências*, Rio Claro, 29-3, 291–310 (2010).
- M. U. Taskirana, N. Demirkola, A. Capoglua, A new porcelained stoneware material based on anorthite, *Journal of European Ceramic Society*, (2004).

- Mukhopadhyay, T. K., Das, M., Ghosh, S., Chakrabarti, S. and Ghatak, S., Microstructure and thermo mechanical properties of a talc doped stoneware composition containing illitic clay. *Ceram. Int.* (2003), 29, 587–597
- N. Editz, A. Yurdakal, Characterization of porcelain tiles bodies with Colemanite waste added as new sintering agent, *Journal of Ceramics Process Res.* 10 (4) (2009) 414-422
- N. Koumtoudji, «Transformations thermiques, organisation structural et frittage des composites kaolinite-muscovite». Doctorate Thesis, University of Limoges (2004).
- A. Njoya, C. Nkoumbou, C. Grosbois, D. Njopwouo, D. Njoya, Courtin-Nomade, J. Yvon, F. Martin. Genesis of Mayouom kaolin deposit (western Cameroon). *Appl Clay Sci.* 2006; 32(1–2):125–40.
- D. Njoya, M. Hajjaji, C. Nkoumbou, A. Elimbi, M. Kwekam, A. Njoya, J. Yvon J., Njopwouo D., Chemical and mineralogical characterization and ceramic suitability of raw feldspathic materials from Dschang (Cameroon). *Bull Chem Soc Ethiop.* (2010)-24(1): 39–46.
- C. Nkoumbou, A. Njoya, d. Njoya D., C. Grosbois, D. Njopwouo, J. Yvon, F. Martin, Kaolin from Mayouom (Western Cameroon): industrial suitability evaluation. *Appl Clay Sci.* 2009;43(1): 118–24.
- Norton, F.H. *Fine Ceramics, Technology and Applications.* McGraw-Hill Book Co. New York (1970).
- Nzenwa., Adebayo. Analysis of Insulators for Distribution and Transmission Networks, *American Journal of Engineering Research*, e-ISSN: 2320-0847 p-ISSN : 2320-0936, Volume-8, Issue-12, pp-138-145 (2020).
- Oberschmidt L. E., The use of nepheline syenite in electrical porcelain bodies. *J Am Ceram Soc Bull.* 1957;36(12):464–5.
- Oluseyi AK, Atul M, Das SK. Effect of substitution of sodalime scrap glass for K-feldspar in triaxial porcelain ceramic mix. *Refract Man.* 2013;1(2):299–303. 33 Raph W.G. Wyckoff, *Crystal Structures*, John Wiley, New York (1963).
- R. Calvet, «Le sol, propriétés et fonctions. Tome 1 : Constitution et structure, phénomènes aux interfaces », Dunod, Paris, (2003).
- Reed J. S., *Introduction to the principles of processing of ceramics.* 2nd ed. New York: Wiley; 1993. p. 40–474.
- Roeser Patricia, Franz Sven O., Litt Thomas. "Aragonite and calcite preservation in sediments from Lake Iznik related to bottom lake oxygenation and water column depth". *Sedimentology.* 63 (7): 2253–2277 (1996).

- R. J. Galán-Arboledas and S. Bueno, Production of ceramic materials using only waste as raw materials, *Key Engineering Materials* Vol. 663 (2016) pp 62-71
- R. Mark Wilson, Archimedes' principle get updated *Physics Today* 65(9), 15 (2012); doi: 10.1063/PT.3.1701
- R.V. Dietrich, Mica Mineral, *Encycloepedia britannica*, Encycloepedia Britannica.inc., (2020)
- Rickwood P.C., The largest crystals, *American Mineralogist*. 66: 885-907 (1981)
- Rincón, J. Ma., Principes of nucleation and controlled crystallization of glasses, *Polym. Plast. Technol. Eng.*, 31, 309-357, (1992)
- S. Akpinar, A. Evcin, O. Ozdemir, Effect of calcinated colemanite addition on the properties of hard porcelain stoneware tiles, *Ceramics International* 43 (2017) 83648371
- S. Chitwaree, J. Tiansuwan, N. Thavarungkula, L. Punsukumtanac, Energy saving in sintering of porcelain stoneware tile manufacturing by using recycled glass and pottery stone as substitute materials, *Case Studies in Thermal Engineering* 11 (2018) 81–88.
- Saleh. N Ahdiri., Elmugdad. A Ali., Adil. E. Ahmed., Naji. M. khalil, Salih A. Salih., Characterization and thermal analysis of raw clay for ceramic product design, *Journal of Sebha University-(Pure and Applied Sciences)-Vol.15 No.2* (2016)
- Sane S. C., Cook R. L.,. Effect of grinding and firing treatment on the crystalline and glass content and the physical properties of white ware bodies. *J Am Ceram Soc.* 1951;32:145.
- Schulle W., Trends and problems in the development of porcelain firing process. *Incerceram*, (2003);52(12):192–6.
- Singer, F. Singer, S.S. *Industrial Ceramics*, Chapman and Hall, London (1971).
- Sorensen H., *The alkaline rock*. 1st Edition. John Wiley & Sons Ltd. 634 p. ISBN 0471-81383-4 (1974).
- Stathis, G., Ekonomakou, A., Stournaras, C.J, and Ftikos, C. Effect of firing conditions, filler grain size and quartz content on bending strength and physical properties of sanitary ware porcelain *Journal of the European Ceramic Society* (2004) 24, pp 23572366.
- Tarvornpanich, T., Souza, G. P., & Lee, W. E., Microstructural Evolution in Clay based Ceramics II: Ternary and Quaternary Mixtures of Clay, Flux, and Quartz Filler. *Journal of the American Ceramic Society*, 91(7), 2272-2280 (2008).
- Tchakounte Bakop T., Tene Fongang R. T., Melo U. C., Kamseu E., Miselli P., Leonelli C., Sintering behavior of two porcelainized stoneware compositions using pegmatite and nepheline syenite minerals. *J Therm Anal Calorim.* 2013;114:113–23



- Tucci A., Esposito L., Malmusi L., Rambaldi E., New body mixes for porcelain stoneware tiles with improved mechanical characteristics. *J Eur Ceram Soc* (2007); 27:1875–81.
- Tomkeieff, S.I., On the Origin on the name Quartz, *Mineralogical Magazine* (1942). 26 (176) 172–178
- Trewin N. H.; Davidson, R. G., "Lake-level changes, sedimentation and faunas in a Middle Devonian basin-margin fish bed". *Journal of the Geological Society*. **156** (3): 535–548 (1999).
- V.C. Nwachukwu, S.A. Lawa, Investigating the Production Quality of Electrical Porcelain Insulators from Local Materials, *IOP Conf. Series: Material Science and Engineering* 413 (2018) 012076.
- W. A. Deer, R. A. Howie and J. Zussman, *An Introduction to the Rock Forming Minerals*, Longman, ISBN 0-582-44210-9 (1966).
- Dean JA. *The Analytical Chemistry Handbook*. *New York: McGraw Hill, Inc.* (1995) pp. 15.1–15.5. ISBN 0-07-016197-6
- Pungor E. *A Practical Guide to Instrumental Analysis*. *Florida: Boca Raton* (1995). pp. 181–191.
- O'Neill MJ. "The Analysis of a Temperature-Controlled Scanning Calorimeter". *Anal. Chem.* **36** (7) (1964).

# ANNEXES

**A- LIST OF PUBLICATIONS**

- 1- T. Tchakouteu Mbakop, Juvenal G. Nemaleu Deutou, Likiby Boubakar, Ndigui Billong, · U. Chinje Melo, Elie Kamseu, Vincenzo M. Sglavo; Enhancing the crystallization phenomena and strength of porcelain stoneware: the role of CaO. *J Therm Anal Calorim.*(2020)
- 2- Tchakounte Bakop T., Tene Fongang R. T., Melo U. C., Kamseu E., Miselli P., Leonelli C., Sintering behavior of two porcelainized stoneware compositions using pegmatite and nepheline syenite minerals. *J Therm Anal Calorim.* 2013;114:113–23
- 3- E. Kamseu, T. Bakop, Djangang, U.C. Melo, M. Hanuskova, C. Leoneli. Porcelain stoneware with pegmatite and nepheline syenite solid solutions: Pore size distribution and descriptive microstructure, *Journal of the European Ceramic Society* 33 (2013) 2775–2784

## B- Some Test Equipments for Materials Sciences



**Figure a:** Mercury Intrusion Porosimeter



**Figure b:** Scanning Electron Microscopy Apparatus (Model: Jeol – JSM 5500)



**Figure c:** Dilatometer (L75 HS-1600, Linsers, Germany)



**Figure d:** DTA/TG apparatus (Model DTA 409, Netzsch-Germany)

## C- Glossary of Common Ceramic Raw Materials

**Barium carbonate** ( $\text{BaCO}_3$ ): alkaline earth; active high temperature flux, but also promotes matt glaze surface. Unsafe for low-fire functional glazes. Often used as an additive in clay bodies in very small percentages to render sulfates insoluble, reducing scumming.

**Bentonite** ( $\text{Al}_2\text{O}_3 \cdot 5\text{SiO}_2 \cdot 7\text{H}_2\text{O}$ ): formed from decomposition of air borne volcanic ash; suspension agent used in quantities no more than 3% of dry materials weight.

**Bone ash** (calcium phosphate) ( $\text{Ca}_3(\text{PO}_4)_2$ ): high temperature flux; opacifier in low temperature glazes; translucence in high temperature glazes.

**Borax** (sodium tetraborate) ( $\text{Na}_2\text{O} \cdot 2\text{B}_2\text{O}_3 \cdot 10\text{H}_2\text{O}$ ): a major low temperature alkaline flux, available in granular or powdered form. Gives smooth finish, bright colors. Water soluble, so often used in fritted form.

**Chrome oxide** ( $\text{Cr}_2\text{O}_3$ ): standard vivid green colorant; often softened with a little iron or manganese. Very refractory. With tin produces pink.

**Cobalt carbonate** ( $\text{CoCO}_3$ ): standard blue colorant for slips and glazes. 5% will give dark blue in glaze or slip. Will cause crawling if used raw for underglaze brushwork.

**Copper carbonate** ( $\text{CuCO}_3$ ): a major glaze colorant to produce greens in low temperature and high temperature, copper reds in high temperature reduction, and greens and metallic effects in raku.

**Dolomite** ( $\text{MgCO}_3 \cdot \text{CaCO}_3$ ): high temperature alkaline earth flux, promotes hard, durable surfaces and recrystallization/matting in glazes.

**Feldspar**: High temperature alkaline fluxes—insoluble aluminum silicates of potassium, sodium, calcium, and/or lithium; inexpensive flux for glaze.

**Magnesium carbonate** ( $\text{MgCO}_3$ ): alkaline earth; high temperature flux, promotes mattness and opacity in low temperature glazes, smooth, hard, buttery surface in high temperature glazes. Promotes purples/pinks with cobalt. Used to promote controlled crawl glaze effects.

**Manganese dioxide** ( $\text{MnO}_2$ ): flexible colorant; with alkaline fluxes, gives purple and red colors. By itself, gives soft yellow-brown; with cobalt gives black. Used with iron to color basalt bodies. Concentrations of more than 5% may promote blistering.

**Nepheline syenite** ( $\text{K}_2\text{O} \cdot 3\text{Na}_2\text{O} \cdot 4\text{Al}_2\text{O}_3 \cdot 9\text{SiO}_2$ ): a common feldspathic flux, high in both soda and potash. Less silica than soda feldspars, and therefore more powerful. Increase firing range of low-fire and mid-range glazes.

**Rutile**: Source of titanium dioxide, contains iron, other trace minerals; gives tan color, promotes crystallization giving mottled multicolor effects in some high temperature glazes, or in over glaze stain.

**Silica** (silicon dioxide, flint, quartz) ( $\text{SiO}_2$ ): main ceramics-former—vitrification, fluidity, transparency/opacity controlled by adding fluxes and/or refractories.

**Spodumene** ( $\text{Li}_2\text{O} \cdot \text{Al}_2\text{O}_3 \cdot 4\text{SiO}_2$ ): lithium feldspar—powerful high temperature alkaline flux, promotes copper blues, good for thermal-shock bodies and matching glazes.

**Strontium Carbonate** ( $\text{SrCO}_3$ ): alkaline earth, high temperature flux, similar to barium, slightly more powerful; gives semi-matt surfaces. Nontoxic in balanced glaze.

**Talc** ( $3\text{MgO} \cdot 4\text{SiO}_2 \cdot \text{H}_2\text{O}$ ): high temperature alkaline earth flux in glaze, promotes smooth buttery surfaces, partial opacity - similar composition to clay

**Tin Oxide** ( $\text{SnO}_2$ ): most powerful opacifier, but expensive - inert dispersoid in glaze melt; 5- 7% produces opaque white in a clear glaze.

**Frit**: Fluxes that have been melted to a glass, cooled, and ground in order to stabilize soluble and/or toxic components during handling of unfired material.

**Ilmenite** An iron ore with significant titanium—most often used in granular form to produce dark specks in clay or glaze. Higher iron concentration than in rutile.

**Iron oxide**, red ferric oxide ( $\text{Fe}_2\text{O}_3$ ): refractory red in oxidation, converts to black iron (flux) in reduction and/or high-fire. Low quantities in clear glaze produces celadon green; high quantities produce temmoku black or saturated iron red powerful flux.

**Kaolin or china clay** ( $\text{Al}_2\text{O}_3 \cdot 2\text{SiO}_2 \cdot 2\text{H}_2\text{O}$ ): very refractory white primary clay. Source of alumina in glazes, porcelains and stonewares.

**Lithium carbonate**  $\text{Li}_2\text{CO}_3$ : powerful all temperature alkaline flux, especially with soda or potash feldspars. Promotes hardness and re- crystallization in low temperature glazes.

**Titanium dioxide** ( $\text{TiO}_2$ ): matting/opacifying agent. Promotes crystal growth, visual texture in glazes.

**Whiting** (calcium carbonate, limestone) ( $\text{CaCO}_3$ ): alkaline earth, contributing calcium oxide to glaze powerful all temperature flux; major high temperature flux for glazes, gives strong durable glass.

**Wollastonite** or Calcium silicate ( $\text{CaSiO}_3$ ): In some cases, it is used in place of whiting.

**Zinc oxide** ( $\text{ZnO}$ ): high temperature flux that promotes brilliant glossy surfaces. Can encourage opacity, with titanium in low-alumina glaze can encourage macrocrystalline growth.

**Zirconium silicate** ( $\text{ZrSiO}_4$ ) or Zircon: opacifier, low-cost substitute for tin oxide; use double the recipe weight of tin. Includes Zircopax, Opax, Superpax, Ultrox.

Excerpted from Clay: A Studio Handbook by Vince Pitelka.

**Biscuit or bisque firing**: initial firing usually to allow the ware to be decorated before the second firing

**Black pottery**: one of the most common forms of traditional pottery where the pots are turned black by cutting out the oxygen at the end of the firing. In an open firing this is done by smothering the fire with fine dung, or damp grass and then possibly pieces of metal sheeting. Sometimes the pots are taken out of the fire or kiln and plunged into grass, sawdust or dung.

Black pottery is to be found in many places in Africa, among Pueblo potters of the USA, in Mexico, Colombia, Denmark and Central Europe.

**Blanc-de-chine** (white of china): white glazed porcelain that was used to model small decorative ceramics and figurines. Such wares were widely imported into Europe from the East after 1700.

**Bone china**: ware to which bone ash has been added. It fires at a lower temperature than true porcelain and is used to make mass-produced fine white china.

**Burnishing**: one of the most common finishes on traditional pottery, especially that made by women. The surface polishing seals the outside of the vessel and makes it smooth to touch. This is usually achieved with a hard river pebble. The burnishing stone is the woman potter's most distinctive tool. Such stones are found in ancient burials and in modern times are frequently passed on from generation to generation.

**Celadon**: a pale grey-green to grey-blue glaze used for stoneware and porcelain. The glaze was first used in China and is especially associated with the Sung Dynasty. The colour is created by a small amount of iron oxide. It is translucent and is often combined with a carved decoration which shows through the glaze.

**Coiling**: coiling a system of forming used widely by potters in many parts of the world either to make the whole or part of a pot. The potter rolls sausages of clay which are then wound round and smoothed down to create the shape.



**Domestic ware:** ceramics produced for use in the home such as cups, saucers, bowls, casseroles and teapots.

**Earthenware:** a form of pottery fired at a low temperature 500- 1000 degrees C. It normally has a red or brown colour, is relatively porous and is used widely for domestic pottery. It is rendered non-porous by glazing in a second firing.

**Extrude:** a system used to create long pieces of shaped clay for handles, for example. Clay is fed into the top and pressed through a shaped tube

**Functional pottery:** pottery made for use rather than decoration. It includes domestic ware but also such things as water jars and cooking pots.

**Glaze:** fine ground solution of minerals that is used to cover pottery. Pieces are dipped in glaze or it can be sprayed or painted on. It fuses on to the surface during firing to create a matt or glossy non-porous surface.

**Grog:** crushed fired clay added to unfired clay to reduce shrinking and add stability during firing. It can also be used to create texture.

**Hand building:** general word for all forms of making pottery by simple forming systems such as thumb pots, coiling or pulling up from a mound of clay.

**Kiln:** a furnace or oven used to bake pottery. Most kilns separate the fuel from the pottery.

Modern kilns can be fuelled by electricity or gas but traditionally wood was used.

**Maker:** a word that is increasingly used for a person who works in the applied arts such as ceramics, textiles, metalwork etc. It attempts to distance itself from the more loaded designations of craftsman or artist.

**Modelling:** the plasticity of clay means that it is one of the most ancient materials used to model forms by hand.

**Mould:** system of making clay objects by pressing a sheet of clay over or into a shape usually made of fired clay or plaster. This may be a vessel form or a figurine.

**Porcelain:** a ceramic body which contains kaolin or china clay and must be fired to a high temperature (1300-1450 degrees C) giving a hard, white, translucent finish. First developed in China it is traditionally the most difficult body to work with although in recent years it has been used much more widely by studio potters.

**Press-mould:** a plaster or clay mould used to form ceramics especially figurines, bowls and plates. A slab of clay is pressed into or onto the mould. When the clay begins to dry out it takes on the form and can be removed easily from the mould. Complicated forms can involve several moulds.

**Roulette wheel:** a tool with a notched or carved wheel on the end of a handle. The wheel is pushed over the clay to make a line of relief pattern. It is used to give simple decorative effects especially at points where two different parts of the pot are joined such as the body and the neck.

**Salt glaze:** one of Germany's major contributions of ceramics. It was produced in Germany as early as the fifteenth century. In Britain its first use is recorded in the late seventeenth century. Salt Glaze is a thin glaze achieved by introducing common salt (NaCl) into the kiln at high temperature. The chlorine goes up the chimney as a gas and the sodium combines with the silica in the clay body to create a thin, glassy film on the surface of the ware. The texture is often finely dotted or mottled, not unlike orange peel. The technique has been very popular with studio potters.

**Slab building:** making a form from slabs of rolled out clay.

**Slip casting:** a system of making ceramics from a mould of clay or more commonly plaster. The casting slip is poured into the mould and as the water is absorbed by the plaster the clay dries out into the shape.

**Slip:** a system of making ceramics from a mould of clay or more commonly plaster. The casting slip is poured into the mould and as the water is absorbed by the plaster the clay dries out into the shape.

**Sponge decoration:** inexpensive system of decoration using small sponges, sometimes cut into simple shapes and dipped in coloured glaze or slip and then dabbed on the surface.

**Stoneware:** a strong hard body fired to around 1200 degrees C. It is usually brown or grey coloured and was used widely for functional pottery such as jars and drinking flasks. The subtle muted glaze effects have been much prized by studio potters in the 20th century.

**Studio pottery:** ceramics produced by individual makers usually trained in art school rather than learning as artisan potters in a family business. Studio pottery is a practice dating from the early 20th century and makers normally sign their work. Studio pottery often implies vessels of some kind but can extend to figurative pieces. Many practitioners now prefer to identify themselves as ceramist or ceramic artist or they use the more neutral word for craftsperson – maker.

**Temper:** material added to unfired clay to open up the body, reduce shrinkage and decrease the effect of thermal shock (stress due to sudden changes of temperature) during firing. Sand, shells, grog, grass or dung are all used depending on availability or tradition.

**Terracotta** (meaning cooked earth): once-fired earthenware which normally takes a red colour.

**Throwing:** a system of forming vessels using a potter's wheel which has a circular turning surface on which the clay is placed. The walls are formed by the centrifugal force of the spinning clay against the hands. The potter's wheel was developed in the Middle East over 5000 years ago.

**Transfer print or decal:** A form of ceramic decoration used especially for mass-produced china. The design in ceramic ink or underglaze colors is printed on paper and then applied to the surface of a glazed object and fired to a temperature where the glaze will begin to melt; this will give the appearance of lying beneath the glaze.

**Turning:** a process used to trim and finish off pottery, especially objects that have been thrown on a wheel. For example, a piece can be turned upside down on the wheel and the base is trimmed by holding a metal tool against the rim as the wheel revolves.

**Wood-firing:** most traditional kilns are fired with wood whereas modern kilns and factory production use coal, gas or electricity. Studio potters in the 20th century revived the art of wood-fired kilns which give interesting and lively surface effects.

**Yunomi:** Japanese word for a cup without a handle.

**Body:** The material from which ceramic is made, excluding the glaze.

**Impermeable:** Not porous; fluid does not pass through.

**Natural white ceramic body:** A colour value of 8.5 or greater on the Munsell Colour Chart and a Munsell chroma of 0.5 or less, not as a result of artificial colouring.

**Refractory ceramics:** Fired articles having the special property of resisting high temperatures as met in metallurgy, the glass industry, etc. (e.g. of the order of 1,500 °C and higher).

**Semi-vitreous:** Water absorption between 0.5% and 3% ; **Vitreous** (vitrified): Not porous;  $\leq 0.5\%$  of water absorption.

**Whiteware:** Can be white, off-white, ivory or light grey colour in the fired state. 2. This policy deals with the classification of various types of ceramic of Chapter 69 of the Customs Tariff (Tariff). In particular, it clarifies the distinction between “porcelain or china” and “other” ceramics. The latter include stoneware, vitreous china, semi-porcelain, white granite, earthenware, terra cotta, amongst other ceramics. 3. The General Explanatory Note to Chapter 69, Sub-chapter II, (I) Porcelain or china, and (II) Other ceramic products, relates to the classification of china, porcelain and other ceramic ware. It states that in order for goods to be classified as porcelain or china they must be almost completely vitrified, hard, essentially impermeable, white or artificially coloured, translucent and resonant. 4. The American Society for Testing and Material (ASTM) standard C242 defines “vitreous” as generally signifying that the ware has a water absorption rate below 0.5%, except for floor tiles, wall tiles and lowtension electrical porcelain which are considered to be vitreous provided that the water absorption does not exceed 3%. The vitrification is produced by heat and melting of the body material as opposed to simple sintering, which does not fuse the material. 5. For tariff classification purposes, all china and porcelain products must: (a) have a water absorption of less than or equal to 0.5%. (ASTM Specification C373 (except that the specimens may have a minimum weight of 10g and may be glazed) ; have a natural white colour value of 8.5 or greater on the Munsell colour chart and a Munsell chroma of 0.5 or less, unless it is artificially coloured. (Decisions Nos. 2914, 2928 and 2948 of the former Tariff Board of Canada) (c) be translucent through 4 mm thickness with glaze removed, when viewed against a 7W light. (British Standards Institute standard 5416) 6. Following is a description for standard permeability, colour, translucency and firing temperatures of porcelain or china, stoneware, vitreous china, semi-porcelain, white granite, earthenware and terra cotta:

(a) **Porcelain or China:** A glazed or unglazed vitreous ceramic whiteware that is translucent; generally made up of kaolin clay or China clay, quartz and feldspar; but can also contain ball clay, calcium carbonate, alumina, bone ash, steatites, etc. For example: bone china is a type of porcelain body in which calcined bone (bone ash / calcium phosphate) is a major component. Permeability: water absorption rate of less than or equal to 0.5% Colour: naturally white or naturally white, but artificially coloured Translucency: translucent through 4 mm thickness with glaze removed, when viewed against a 7W light Firing temperature: generally 1200° - 1400° C

(b) **Stoneware:** It may be vitreous or semi-vitreous; usually naturally coloured grey or brownish because of impurities in the clay used for its manufacture; normally glazed; made from non-refractory fireclay or a combination of clays, fluxes and silica. Permeability: water absorption rate of less than or equal to 3% Colour: naturally non-white Translucency: opaque through 4 mm

thickness with glaze removed, when viewed against a 7W light Firing temperature: generally 1150 - 1315°C

(c) **Vitreous China:** A vitrified, opaque ceramic composed of a mixture of kaolin clay or China clay, ball clay, quartz and feldspar; white or naturally coloured grey or brownish because of impurities in the clay used for its manufacture; normally glazed. Permeability: water absorption rate of less than or equal to 0.5% Colour: any; normally white or off-white Translucency: opaque through 4 mm thickness with glaze removed, when viewed against a 7W light Firing temperature: generally 1150° - 1315° C

(d) **Semi-porcelain** (Imitation Porcelain) or White Granite: commonly referred to as “ironstone”; semivitreous tableware having the commercial appearance of porcelain, without being as opaque as earthenware, or as translucent as porcelain; may be slightly translucent in thinner parts. Permeability: water absorption rate of more than 0.5% but no more than 3% Colour: naturally white or naturally white, but artificially coloured Translucency: opaque through 4 mm thickness with glaze removed, when viewed against a 7W light Firing temperature: generally 1150° - 1315° C

(e) **Earthenware:** mixture of quartz, kaolin, ball clay and feldspar; porous, opaque, and not as strong as other ceramic ware; must be glazed to be watertight. Permeability: water absorption rate of greater than 3.0% Colour: any Translucency: opaque through 4 mm thickness with glaze removed, when viewed against a 7W light Firing temperature: generally 1000° - 1150° C

(f) **Terra Cotta :** fired clay ceramic that is porous and usually unglazed; its uses include garden ware, vessels, water and waste pipes and surface embellishments in building construction and sculptures; the material is weak compared to stoneware, but can be glazed to increase its durability. Permeability: water absorption rate greater than 3.0% Colour: any; normally naturally red, orange or brown due to the iron content; other colours include yellow, grey and pink Translucency: opaque through 4 mm thickness with glaze removed, when viewed against a 7W light firing temperature: generally 850° - 1000° C.

